TREATMENT OF PETROLEUM REFINERY WASTEWATER BY ANOXIC-AEROBIC SEQUENTIAL MOVING BED REACTORS

Thesis

Submitted in Partial

Fulfillment of the Requirements for the Degree of

Doctor of Philosophy

By

Subrat Kumar Mallick

DEPARTMENT OF CIVIL ENGINEERING

INDIAN INSTITUTE OF TECHNOLOGY GUWAHATI

ASSAM, INDIA

SEPTEMBER 2019

TREATMENT OF PETROLEUM REFINERY WASTEWATER BY ANOXIC-AEROBIC SEQUENTIAL MOVING BED REACTORS

Thesis

Submitted in Partial

Fulfillment of the Requirements for the Degree of

Doctor of Philosophy

By

Subrat Kumar Mallick

DEPARTMENT OF CIVIL ENGINEERING

INDIAN INSTITUTE OF TECHNOLOGY GUWAHATI

ASSAM, INDIA

SEPTEMBER 2019

Dedicated

To

My Parents, Sister and Well Wishers

Department of Civil Engineering
Indian Institute of Technology Guwahati
Assam, India - 781039

CERTIFICATE

It is certified that the work contained in this thesis entitled "**Treatment of petroleum refinery wastewater by anoxic-aerobic sequential moving bed reactors"** by **Subrat Kumar Mallick** (Roll No. 136104021) has been carried out under my supervision in the Department of Civil Engineering, Indian Institute of Technology Guwahati. I forward his thesis to submit for the award of degree of Doctor of Philosophy from this institute. I certify that he has fulfilled all the requirements according to the rules of this institute regarding the investigations embodied in his thesis and this work has not been submitted elsewhere for a degree.

Date:

(**Dr. Saswati Chakraborty**)
Professor
Department of Civil Engineering
Indian Institute of Technology Guwahati,
Assam, India - 781039

Department of Civil Engineering
Indian Institute of Technology Guwahati
Assam, India - 781039

STATEMENT

I hereby declare that the work contained in this thesis entitled "**Treatment of petroleum refinery wastewater by anoxic-aerobic sequential moving bed reactors**" is carried out by me at the Department of Civil Engineering, Indian Institute of Technology Guwahati, under the supervision of Prof. S. Chakraborty.

(Subrat Kumar Mallick)
Department of Civil Engineering
Indian Institute of Technology Guwahati,
Assam, India - 781039
September 2019

ACKNOWLEDGEMENTS

I take this opportunity to thank the persons who made discernible contributions during my research work and completion of this thesis.

At first, I express my deepest thanks and most sincere gratitude to my thesis supervisor, **Prof. Saswati Chakraborty** for her excellent guidance throughout my research work. Her kindness, dedication, hard work, sacrifice, patience, attention to minute details have been a great inspiration to me. Her deep knowledge of the subjects is commendable and guidance on the moral principles of high quality research is exemplary. Her competence to deal with difficult situations is tremendous and always have helped me to tackle complicated situations. Her commitment and diligent encouragement during each phase of the research work have been truly admirable. She has always motivated me to be an independent thinker and contemplate the logics that lead to reasons, which is the biggest takeaway of her supervision.

I express deepest thanks to my doctoral committee members Prof. M. Jawed, Prof. C. Das and Prof. A. Kalamdhad for their valuable time, precious suggestions and right directions to improve the quality of my research work and to lead a professional life. I would like to thank the current head Prof. C. Mahanta and former heads Prof. S. Dutta and Prof. A. K. Sarma of Department of Civil Engineering, IITG for the facilities provided during my research. I sincerely thank Prof. S. Gokhale, Prof. P. K. Ghosh and Prof. S. K. Deb of Department of Civil Engineering, IITG for their encouraging and valuable advice.

I am thankful to Ms. Jonali Saikia (Scientific Officer, Department of Civil Engineering, IITG), Mr. Payodhar Pathak and Mr. Chittaranjan Medhi (Technical Superintendent, Environmental Engineering Laboratory, IITG) for their help with instrumental facilities and equipment. I am thankful to Center for Instrument Facility (CIF, IITG) for the allowance of sample analysis.

In the flow of my research life, I came across certain people who got adhered to my life as best mates with whom I could share my feelings, thoughts, ups, downs and research ideas. My acknowledgement would be incomplete without mentioning their contributions towards completion of my PhD journey. I am grateful to my seniors Dr. Praisy Terangpi and Mr. Sachin Kumar Tomar for their selfless love, care and support during my research work. I thank my seniors Dr. Ravindra Patil, Dr. Vihangraj Kulkarni, Dr. Biju Prava Sahariah, Dr. Arti Choudhary, Dr. Susant Padhi, Dr. Jayshree Dutta, Dr. Premanand Singh, Dr. Arvind Shakya,

Dr. Bharti Brahmacharimayum, Dr. Dhamodharan K., Dr. Sudharsan Varma and Dr. Jiwan Singh to teach me many aspects of continuous research work. I lay my deepest regards to my intimate friends Mitali, Dr. Rakhee Das, Dr. Geetimukta Mahapatra, Ardhendu, Abhradip, Dr. Anuma Singh, Dr. Rajkumar Das, Dr. Nibedita Behera and Dr. Rajendra Maity for their continuous affection, care and mental support during the rigors of my research. I appreciate the helps rendered by my juniors Rajneesh, Sayanti, Shweta and Jeenat during my research works.

I would like to thank my entire badminton group Dr. Shyam, Dr. Anand, Dr. Basant, Dr. Pankaj, Dr. Mukul, Shatrughan, Rajendra, Dr. Vinod, Uttam, Dr. Siddesh, Dr. Kishor, Subhasis, Tapaswini, Biswajit, Satya, Shrinu from various departments of IITG. Playing badminton with you all has been one of the most enriching experiences of my life. We went on to win Spardha tournament three times consecutively. I will always cherish those winning moments and countless match analysis that ensued those victories. I will also forever remember those cycling trips that we took on weekends, which were always rejuvenating and refreshing after tiring and exhaustive weekdays academic activities. I would like to acknowledge Dr. Anamika Barua mam from HSS department of IITG, Swapnali Bora mam and Tumpa deb mam for their love and support. I will forever cherish the dinner parties we had at your quarter.

Finally, I am very much indebted to my parents **Mr. Sudhakar Mallick**, **Mrs. Sumati Mallick** and my elder sister **Mrs. Sumitra Mallick Tibarewalla** for their selfless love, utmost care, patience and belief that made me stand up to the life I am living in. I thank the almighty god for giving me this life and blessings.

Subrat Kumar Mallick

September 2019

ABSTRACT

Produced water from petroleum refineries is a concoction of phenol, hydrocarbons, emulsifiers, ammonia-N, nitrate-N and volatile sulfide, which is characterized by high pH, dissolved and suspended solids, salinity and conductivity. Bio-treatment by microbial action is mostly adopted for the treatment of industrial wastewater due to their economy, ease of operation and much lesser generation of secondary pollutants compared to the physicochemical processes. Aerobic reactors are the most efficient biotransformation technique for the removal of industrial pollutants. However, abiotic loss of volatile sulfide is unavoidable due to continuous air purging. Hence, anaerobic/anoxic treatment becomes necessary as they are operated in a closed system and abiotic loss can be avoided. Anaerobic reactors are sensitive to the recalcitrant nature of the pollutants and require higher hydraulic retention time (HRT). Anoxic reactors are efficient in terms of organics removal by using nitrate-N/nitrite-N as electron acceptor. However, oxidation of ammonia-N is difficult in anoxic condition and requires aerobic treatment. Conversion of sulfide to elemental sulfur (S^0) is possible in anoxic condition and S^0 has monetary value. Therefore, Anoxic reactor can be employed for the removal of volatile sulfide and partial degradation of organics. Residual organics and ammonia-N can be oxidized in aerobic reactor. Hence, a combination of anoxic and aerobic treatment can be prudent for the treatment of petroleum refinery wastewater.

Anoxic and aerobic moving bed reactor systems were selected, as they provide the benefits of attached growth systems and less prone to clogging. Initially heterogeneous biomass was grown on polyurethane foam (PUF) cubes of $1cm^3$ dimension and acclimatized with gradual increase in feed concentrations in anoxic reactors operated in fed batch mode. Then concentrations of sulfide (0 - 1200 mg/L), phenol (0 - 1200 mg/L), diesel (0 - 700 mg/L), ammonia-N (0 - 450 mg/L) and nitrate-N (0 - 2000 mg/L) were varied to decide the optimum conditions for the maximum generation of S^0 from S^{2-}. Nitrate-N to sulfide molar ratio of 3.04 was found to be optimum for the maximum precipitation of sulfide as S^0, which correspond to influent concentrations of sulfide 750 mg/L, phenol 750 mg/L, diesel 300 mg/L, ammonia-N 350 mg/L and nitrate-N 1000 mg/L. At the optimum condition, maximum sulfur generation was 300 ± 12 mg/L.

Anoxic moving disc bed reactor (A1) with a conical bottom for the effective separation of S^0 was fabricated using PUF discs of 10 cm diameter and 1 cm thickness as biomass bed.

Heterogeneous biomass was grown on the PUF discs and acclimatized to the concentrations of the pollutants where maximum conversion of sulfide to S^0 was optimized. Agitation speed of 20 rpm was sufficient for the mass transfer of pollutants into the biomass bed and higher speed had no beneficial effect on the efficiency of A1. Complete removal of sulfide was obtained at 2.5d hydraulic retention time (HRT) in A1, removals of phenol and emulsified diesel were partial and ammonia-N removal was negligible. Effluent of A1 was supplied to the aerobic moving bed reactor (A2), which was fabricated with PUF cubes of 1 cm^3 dimension as biomass support. Aerobic biomass was acclimatized with phenol, emulsified diesel, thiosulfate and ammonia-N as per the effluent released from A1. HRT of 20h was sufficient for the oxidation of residual organics and ammonia-N. In the final effluent, sulfide was not detected, phenol, total hydrocarbon and ammonia-N were less than 5 mg/L and COD_T was 100 mg/L at overall HRT of 80h.

Effect of various hydrocarbons [kerosene (K), heavy engine oil (HO), mixtures of kerosene, heavy engine oil and diesel (K+HO and K+HO+D) and crude oil, 300 mg/L] with different density and viscosity were studied in the anoxic-aerobic system. Density and viscosity of the hydrocarbons decreased in the order of crude oil > HO > K+HO+D > K+HO > K. Organics degradation in A1 was hampered, sloughing of the biomass was triggered and decrease in solids retention time (SRT) was observed with increase in density and viscosity of the hydrocarbons. Effect of hydrocarbons was not observed in A2 and more than 99% removals of sulfide, organics and ammonia-N were achieved by the anoxic-aerobic sequential moving bed reactors at 80h HRT.

Identification of the dominant microbial species revealed the presence of *Pseudomonas aeruginosa* SKM2013 and *Pseudomonas aeruginosa* SC2013 in reactor A1. Pure culture analysis showed that, both the cultures were able to utilize organics and sulfide in denitrifying condition. *Pseudomonas aeruginosa* SC2013 was able to oxidize sulfide in anoxic condition in the absence of organics and showed chemolithotrophic characteristic. Aerobic culture was dominated by *Lysinibacillus sp.* **H200-510**, *Stenotrophomonas sp.* **LW-34**, *Pseudomonas aeruginosa* strain **ISB4** and *Pseudomonas aeruginosa* strain **LZS8436**. Pure culture analysis of the aerobic isolates showed that, *Lysinibacillus sp.* **H200-510**, *Stenotrophomonas sp.* **LW-34** and *Pseudomonas aeruginosa* strain **ISB4** were able to oxidize organics, ammonia-N and nitrite-N. *Pseudomonas aeruginosa* strain **LZS8436** could not utilize ammonia-N, but could oxidize organics and nitrite-N.

Complete oxidations of phenol, hydrocarbons and nitrate-N were achieved at 22.5h HRT in A1 and residual ammonia-N was oxidized at 7.5h HRT in A2, with an overall HRT of 30h during the treatment of real automobile service station wastewater by anoxic-aerobic sequential moving bed reactors. Metals analysis of the sludge released from A1 and A2 confirmed their suitability for utilization in agricultural lands.

Removal of organics deteriorated in A1 with increase in NaCl dose. More than 30 g/L of NaCl dose hampered the performance of A2 and decrease in the removals of organics and ammonia-N by the anoxic-aerobic system was observed. Both A1 and A2 recovered to their original performance after the withdrawal of NaCl dose. Organics removal and denitrification in A1 and ammonia-N nitrification in A2 were hampered with crude oil shock loads of 600 mg/L and 900 mg/L applied in two phases. Effect of shock load was more vulnerable to A1 as there was permanent decrease in performance after the second shock load. Recovery of A2 was achieved after each shock load, suggesting complete recovery of the anoxic-aerobic system.

Heterotrophic activity of both anoxic and aerobic biomass were higher whenever degradation of organics were higher. Similarly, chemolithotrophic activity of anoxic biomass was higher when sulfide oxidation and conversion of sulfide to sulfate were higher. Direct dependence of biomass activity with the removal of COD was observed. Hence, biomass activity test can be used as an indirect tool to predict bioreactor performance.

Keywords: petroleum refinery wastewater, anoxic-aerobic sequential moving bed reactors, sulfide, hydrocarbons, elemental sulfur, biomass activity, NaCl dose.

TABLE OF CONTENT

LIST OF TABLES

LIST OF FIGURES

ABBREVIATIONS

%	: Percentage
ΔG^0	: Gibbs free energy change
A1	: Anoxic disc-bed bed reactor
A2	: Aerobic moving bed reactor
AAS	: Atomic absorption spectroscopy
ABR	: Anaerobic baffled reactor
$Al_2(SO_4)_3$	: Aluminium sulfate
APHA	: American physical health association
API	: American petroleum institute
AOB	: Ammonia oxidizing bacteria
AOPs	: Advanced oxidation processes
ASBC	: Alkaliphilic sulfide oxidizing bacteria
ASFBR	: Aerobic submerged fixed-bed reactor
ASO	: Anoxic sulfide oxidizing reactor
ASP	: Activated sludge process
ATR	: Attenuated total reflection
BAC	: Biologically activated carbon
BAF	: Biological aerated filter
BOD	: Biochemical oxygen demand
BTCW	: Bio-treated coking wastewater
BTEX	: Benzene, Toluene, Ethylbenzene, Xylene
C_A	: Abiotic loss
C_f	: Final concentration
C_i	: Initial concentration
CA	: Chemolithotrophic activity
$CaCl_2$	: Calcium chloride
$CaCO_3$	: Calcium carbonate
CAS	: Conventional activated sludge
C_6H_5OH	: Phenol
CO	: Contact oxidation process
$CoCl_2$	: Cobalt chloride
CPCB	: Central pollution control board

COD : Chemical oxygen demand
COD_O : Chemical oxygen demand (organic)
COD_T : Chemical oxygen demand (total)
CO_2 : Carbon dioxide
CH_4 : Methane
CSTR : Continuously stirred tank reactor
$CuCl_2$: Cupric chloride
d : Day
D : Diesel
DAF : Dissolved air floatation
DO : Dissolved oxygen
DOC : Dissolved organic carbon
EC : Electrical conductivity
EDX : Energy dispersive x-ray
EPS : Extracellular polymeric substances
FA : Free ammonia
FCCU : Fluid condensate cracking unit
$FeCl_3$: Ferric chloride
FESEM : Field emission scanning electron microscope
$FeSO_4$: Ferrous sulfate
FTIR : Fourier transform infrared
g : Gram
GAC : Granular activated carbon
GCMS : Gas chromatography and mass spectroscopy
h : Hour
HA : Heterotrophic activity
HAIB : Horizontal flow anaerobic immobilized biomass
HC : Hydrodynamic cavitation
HCl : Hydrochloric acid
HO : Heavy oil
HOCl : Hypochlorous acid
HRT : Hydraulic retention time
HyVAB : Hybrid vertical anaerobic biofilm
H_2O : Water
H_2O_2 : Hydrogen peroxide

H_2S : Hydrogen sulfide
H_2SO_4 : Sulfuric acid
I-BAF : Immobilized biological aerated filter
IC : Ion chromatography
IOCL : Indian oil corporation limited
K : Kerosene
KCl : Potassium chloride
KNO_3 : Potassium nitrate
L : Liter
LDPE : Low density polyethylene
M : Molar
MABR : Membrane aerated biofilm reactor
MBR : Moving bed reactor
MBBR : Moving bed biofilm reactor
mg : Milligram
$MgSO_4$: Magnesium sulfate
mL : Milliliter
mM : Millimolar
MLSS : Mixed liquor suspended solids
MLVSS : Mixed liquor volatile suspended solids
MoEF : Ministry of Environment and Forests
n : Number of moles
NaCl : Sodium chloride
Na_2S : Sodium sulfide
NCBI : National center for biotechnology information
ND : Not detected
NH_3 : Ammonia
NH_4^+-N : Ammonia-N
NH_4Cl : Ammonium chloride
NH_4HS : Ammonium hydrosulfide
$NiCl_2$: Nickel chloride
NO_2-N : Nitrite-N
NO_3^--N : Nitrate-N
NOB : Nitrite oxidizing bacteria
NPAH : Nitrated poly aromatic hydrocarbons

NTU : Nephelometric turbidity unit
NZVI : Nanoscale zero valent iron
N_2 : Nitrogen gas
OLR : Organic loading rate
OS : Oil stream
O_3 : Ozone
P : Pressure
PAC : Poly aluminium chloride
PAH : Poly aromatic hydrocarbons
PBBR : Packed bed bioreactor
PCP : Porous ceramsite particles
PO_4^{3-}-P : Phosphate
PP : Polypropylene
PRR : Packed recycling reactor
PUF : Poly Urethane Foam
PW : Phenolic wastewater
R : Ideal gas constant
RABR : Rotating algae biofilm reactor
RBC : Rotating biological contactor
RFLR : Reverse fluidized bed reactor
rpm : Revolution per Minute
S^{2-} : Sulfide
S^0 : Elemental sulfur
SBR : Sequencing batch reactor
SBBR : Spouted bed bioreactor
$S_2O_3^{2-}$: Thiosulfate
SO_4^{2-} : Sulfate
SRT : Solids Retention Time
SS : Suspended solids
t : Temperature in ^oC
TCD : Thermal conductivity detector
TCP : Trichlorophenol
TDER : Three dimensional electrode reactor
TDS : Total dissolved solids
TH : Total hydrocarbon

TiO_2 : Titanium dioxide
TN : Total nitrogen
TOC : Total organic carbon
TP : Total phosphorous
TPH : Total petroleum hydrocarbon
TSS : Total suspended solids
UASB : Up-flow anaerobic sludge blanket
UFBR : Up-flow fixed bed bioreactors
USEPA : United states environment protection agency
UV : Ultraviolet
V : Volume
VS : Volatile solids
X : Biomass concentration
$ZnCl_2$: Zinc chloride
ZnO : Zinc oxide
ZnS : Zinc sulfide

1

CHAPTER

INTRODUCTION, LITERATURE REVIEW AND OBJECTIVES

CHAPTER 1

INTRODUCTION, LITERATURE REVIEW AND OBJECTIVES

1.1 INTRODUCTION

Requirement of sophisticated techniques and involvement of modernized accessories has led to the exigency of ample energy sources. The petroleum-derived products fulfil major part of this energy necessity. Although concerted efforts have been made to replace fossil fuels, crude oil remains an important raw material. The need to satisfy ever-increasing global energy demand, which is expected to be doubled by over the next two decades (Doggett and Rascoe, 2009), makes the processing of crude oil and the generation of petroleum refinery effluents globally important issues. Petroleum refineries are complex systems of multiple operations that depend on the type of crude refined and the desired products. For these reasons, no two refineries are alike.

The process of refining crude oil consumes large volume of water and significant wastewater is generated. Volume of wastewater generated during refining is 0.4−1.6 times the oil processed (Coelho et al., 2006). The undesirable crude oil constituents, introduction of new compounds and product finishing operations within a refinery (MoEF, 2010), cause contamination in the liquid effluent. Petroleum refineries can generate wastewater consisting of more than 2500 complex compounds varying in their chemical and physical properties (Razavi and Miri, 2015) such as oil, BTEX compounds, sulfides, dissolved solids, suspended solids, toxic metals and BOD exerting biodegradable organics. The prime compounds of petroleum refinery effluents are hydrocarbons in addition to considerable inorganic sulfide and nitrogen (ammonia-N and nitrate-N) (Diya'uddin et al., 2011). Pollutants released from petroleum refineries pose serious effects on the environment as well as can cause life-threatening diseases. Dissolved oxygen depletion in aquatic bodies, effect of sticky oily substances on aquatic animals, methemoglobinemia, cancer, infertility, heart disease and foul smell are some of the adverse effects caused by these pollutants.

Methods of petroleum refinery wastewater treatment include physicochemical processes like coagulation, adsorption, chemical oxidation, advance oxidation processes, membrane separation and biological techniques like suspended growth, attached growth and hybrid systems. Generation of high secondary sludge (Gonder et al., 2017), high cost (Ganiyu et al., 2018) and failure of membranes (Bhatti et al., 2011) limit the application of physicochemical processes. On the other hand, biological processes convert pollutants from toxic to nontoxic form by microbial action. Treatment of bio-sludge is comparatively simpler and can be recycled. However, bio-treatment of diverse types of immiscible oil, recalcitrant organics and inorganics becomes challenging considering the wide variety of pollutants.

Moderate efficiency, toxicity to sulfide and longer time requirement of anaerobic processes lead to their curtailment in the application of hydrocarbon biodegradation (Ghorbanian et al., 2014). Respiratory methods like anoxic processes that are operated in anaerobic condition using nitrate/nitrite as electron acceptor, can overcome the drawback of abiotic loss of sulfide and generate efficiency close to the aerobic reactors (Moussavi and Ghorbanian, 2015). Therefore, anoxic reactors can be a suitable apposite for the treatment of refinery hydrocarbons. Pertinence of the anoxic conditions and successful operation of anoxic reactors for the degradation of synthetic petroleum refinery hydrocarbons have been in study for quite a while. Assimilation of polycyclic aromatic hydrocarbons (Moussavi et al., 2016), alkanes (Zadelius et al., 2011) and volatile organic compounds (Munoz et al., 2013) in anoxic condition have been reported. Successful use of anoxic reactor systems such as biotrickling filter for toluene degradation (Munoz et al., 2013), membrane bioreactor for hydrocarbon degradation (Mannina et al., 2016), granular reactor (Ramos et al., 2016) are reported.

Real wastewater can be comprised of various complex compounds in addition to the target pollutants in lab scale synthetic wastewaters. Hence, exposure to the real-time scenario and reusability of the treated wastewater can give an idea of scaling up of the system for industrial purpose (Fakhru'l-Razi et al., 2009). Biological reactors are preferred due to their economic and environmental importance (Le-Clech et al., 2006) and reports on the treatment of real refinery wastewater are available (Ji et al., 2009; Alsalhy et al., 2016; Pajoumshariati et al., 2017). However, removal of volatile compounds are not discussed in the mentioned literatures.

Nevertheless, at higher loads of organics and inorganics, anoxic reactor alone is not sufficient to meet the discharge standards and a downstream supportive reactor like aerobic reactor is always necessary to increase the efficiency of the system (Nasirpour et al., 2015). In these systems, wastewater is first fed to the anaerobic/anoxic reactors for partial treatment and

rest of the pollutants are treated in a sequencing aerobic reactor. Complete removal of volatile compounds and partial oxidation of organics can be obtained in anoxic reactors and aerobic reactor can remove rest organics/inorganics. Two step sequential systems for the treatment of synthetic industrial wastewater containing hydrocarbons (Nasirpour et al., 2015), phenol and amines (Nguyn et al., 1995), organo-sulfide and organic nitrogen compounds (Lei et al., 2010) and three stage systems for the treatment of phenol, thiocyanate and ammonia (Sahariah and Chakraborty, 2013) has been reported in the literatures. Recently, sequential bioreactors for the treatment of real industrial wastewater has come into picture (Sahariah et al., 2016; Pajoumshariati et al., 2017). However, as of petroleum industry effluents, reports on sequential degradation of pollutants as a mixed entity are scarce. In addition, there are no literatures available for the treatment of real-time wastewater containing inorganics and complex hydrocarbons in anoxic-aerobic sequential bioreactors. Therefore, study of the two-step sequential systems for the treatment of petroleum refinery industrial effluents was considered.

Studies involved the performance evaluation of moving bed reactors for the biodegradation of petroleum refinery wastewater containing phenol, hydrocarbons, sulfide, ammonia-N and nitrate-N. An anoxic moving disc bed reactor and an aerobic moving bed reactor were operated sequential to each other in fed batch mode.

1.2 ORGANIZATION OF THE THESIS

The total work is furnished in form of seven separate chapters. The ongoing **Chapter 1** lays a foundation about the present work by supplying with a widespread introduction, scientific literatures, gaps in the literatures and objectives. **Chapter 2** includes optimization of sulfur (S^0) production in anoxic fed-batch reactors and their performance evaluation by varied loads of sulfide, phenol, total hydrocarbon, ammonia-N and nitrate-N. **Chapter 3** gives idea about the individual performance of anoxic disc bed and aerobic moving bed reactors at varied agitation speed in the anoxic reactor and hydraulic retention time in anoxic and aerobic reactors. Combined performance of anoxic-aerobic sequential system was also evaluated. **Chapter 4** comprises of the effects of various hydrocarbons on the performance of the anoxic-aerobic sequential reactors. **Chapter 5** includes isolation and identification of dominant microbial species of both anoxic and aerobic reactors and treatment of real automobile service station wastewater by the anoxic-aerobic sequential bioreactor system. Effect NaCl dose and crude oil shock loading on the performance of anoxic-aerobic reactors is covered in **Chapter 6**. Finally, conclusions of this study and scope for future research is presented in **Chapter 7**.

1.3 LITERATURE BACKGROUND

1.3.1 Wastewater generation in petroleum refinery

Wastewater is generated from multiple sources in a refinery premise and majority of petroleum products are derived from a refining industry. Hence, chemical constituents that are found in the petroleum products, appear in effluent as well (MoEF, 2010). Pollutants released from different units of a refinery are enlisted in Table 1.1 (MoEF, 2010). Petroleum refinery wastewater contains large quantities of oil both as free (floatable) and emulsified (mixed) form. In addition, water-soluble phenolic compounds are also present. Crude petroleum contains abundant sulfur compounds, which get removed during refining and effluent gets polluted with sulfur compounds and is mainly present as sulfide ion (S^{2-}) (Ishaq et al., 2012). Ammonia and organo-nitrogens like cyanide are the major contributors of nitrogen and therefore refinery wastewater is typically contaminated with appreciable amount of ammonia-nitrogen (Moreno et al., 2002). Presence of prolific amount of heavy metals such as chromium, lead, zinc, copper and nickel increases the complexity of refinery wastewater. The concoction of both inorganics and organics contribute to the chemical oxygen demand. A fraction of the organic compounds is biodegradable, exerting biochemical oxygen demand (Diya'Uddin et al., 2011). Typical characteristics of petroleum refinery wastewater are shown in Table 1.2.

Table 1.1: Pollutants and their sources in petroleum refineries (MoEF, 2010)

Pollutant	Source
BOD, COD, Oil	▪ Process wastewater ▪ Cooling tower blowdown ▪ Tanks drainage and runoff ▪ Ballast water ▪ Spent caustic from treating unit ▪ Organic waste
Phenolics and Sulfides	▪ Process wastewater from cracking unit ▪ Spent caustics from treatment unit ▪ Crude storage tank drains
Suspended Solids	▪ Process wastewater ▪ Cooling tower blowdown ▪ Ballast water ▪ Chemical treatment plants ▪ Tank bottom drainage
NH_3 and H_2S	▪ Process water from cracking units (FCCU, Coker, Hydrocracker etc.) ▪ Hydrodesulphurization and treating units
Heavy Metals	▪ Process wastewater ▪ Tanks drainage ▪ Residual oily sludge Catalytic process

Table 1.2: Reported constituents of petroleum refinery wastewater

Pollutant	Coelho et al. (2006)	El-Naas et al. (2009)	Ma et al. (2009)	Khaing et al. (2010)	El-Naas et al. (2010)	Chen et al. (2014)	Santo et al. (2012)	Wenyu et al. (2011)
pH	8.0 - 8.2	6.6	7 - 9	7.5 - 10.3	8.3 - 8.9	7.4	4.4 - 9.4	6.5 - 8.0
BOD	570	-	150 - 350	-	-	350	-	-
COD	850 -1200	596	300 - 600	330 - 556	3600 - 5300	3145	100 - 2900	3000 - 5000
Oil	12.7	-	50	40 - 91	-	70	1 - 2900	30 - 250
Phenol	98 - 128	-	-	-	160 - 185	105 - 200	0.5 - 71	50 - 420
Sulfide	15 - 23	887	-	-	-	1.5	0.1 - 46	70 - 750
Ammonia-N	5.1 - 21.1	-	10 - 30	4.1 - 33.4	-	130	3.4 - 490	-
SS*	100 - 250	120	150	130 - 250	30 - 40	70	44 - 1900	-

All units are in mg/L except pH

*SS: suspended solids

1.3.2 Toxic effects of petroleum refinery wastewater

1.3.2.1 Phenolic compounds

Phenolic compounds pose a significant threat to the environment due to their extreme toxicity, bioaccumulation and persistence, and depletion of dissolved oxygen in water bodies. The lethal dose of phenol is between 3 to 30g, but may be as little as 1g. Phenol is well absorbed by inhalation, dermal application, and ingestion (Todorovic, 2003). Phenols, chlorophenols and phenolic compounds are both acutely and chronically toxic to both land and aquatic animals. It is necessary to limit phenolic compounds in raw water used for drinking water supplies, as conventional treatment methods used by water supply facilities do not remove phenols (Anirudhan and Ramachandran, 2014).

1.3.2.2 Sulfur compounds

Sulfur compounds arise in the wastewater of petroleum refineries mainly from desulfurization units, first condensate corrosions (as NH_4HS) and from the spent caustic (as Na_2S and R-SH) and mostly remain as S^{2-} form (MoEF, 2010). These compounds are mostly volatile and lead to the formation of hydrogen sulfide, which has a strong characteristic smell. It is deleterious because of its corrosiveness and toxicity to both micro and macro size aquatic organisms. Sulfide (S^{2-}) increases the pH and reacts with metal ions to cause black precipitates. It is also associated with odor problems and can be toxic to aquatic life. S^{2-} also chemically reacts with dissolved oxygen present in water. S^{2-} predominantly released as spent caustic, which has pH more than 12 and certainly hazardous in nature at high alkaline pH (Townsend et al., 2003). Salinity of the produced water increases with increase in S^{2-}.

1.3.2.3 Nitrogenous compounds

Nitrogen components of the petroleum refinery effluents are mainly represented in the form of ammonia (NH_3) and organic nitrogen compounds. Ammonia is commonly found in combined form with sulfide as ammonium sulfide (NH_4HS) in overhead condensates from distillation units as well as cracking and desalting units in a petroleum refinery. The pH range (8 - 12) of the refinery wastewater is such that ammonium ions (NH_4^+) predominate. Marginal concentration (1 mg/L) of unionized ammonia restricts the ability of haemoglobin to combine with oxygen. Therefore, suffocation of the aquatic organisms is unavoidable if untreated petroleum refinery wastewater is released to water bodies (USEPA, 1985). Ammonia exerts a considerable toxic effect on all aquatic life within a range of 1 mg/L to 25 mg/L, depending on

the pH and dissolved oxygen levels (USEPA, 1985). Eutrophication can be a problem due to the breakdown products of ammonia (nitrate-N and nitrite-N). Excess nitrates (>500 mg/L) can cause damage to the intestines and symptoms like are diarrhea and diuresis may arise. Methemoglobinemia or more commonly known as blue baby disease can occur by the consumption of water having more than 10 mg/L of nitrate-N (USEPA, 1985).

1.3.2.4 Oil, grease and other hydrocarbons

The refining operations executed in a petroleum refinery premise primarily involve the separation and polishing of crude oil and its by-products. The generated hydrocarbons are sticky in nature and tend to agglomerate. These hydrocarbons (predominately oil and grease type compounds) contribute to the COD of the effluents. These compounds can be found in both floatable or mixed (emulsified) forms, which cause visibility effect in the water bodies, thus affecting the photosynthesis of aquatic plants and animals (Chavan and Mukherji, 2008). Water-soluble components of the hydrocarbons may exert toxic effects on aquatic life. The water insoluble hydrocarbons and free-floating emulsified oils in a wastewater will affect stream ecology by interfering with oxygen transfer, by damaging the plumage and coats of water animals (geese, fowls etc.), and by contributing taste and toxicity problems. Various hydrocarbons found in fuels can pose a wide range of human health problems, from affecting the liver, kidneys and blood to increasing the risk of cancer (Biswal et al., 2009).

Free hydrocarbons like paraffins, cycloparaffins and olefins (often found in kerosene) are highly volatile in nature and almost insoluble in water. However, aromatics, which include phenolics, benzene compounds, toluene and xylene are soluble in water and are easily transported to water bodies. Excessive exposure to aromatics may impair hearing, cause negative effects to the brain (neurological) and the foetus. Soluble aromatics are also potential hazard for the sensory as well as internal organs of humans. Free hydrocarbons categorized as volatile organic compounds (VOCs) that may contribute to the formation of ground level ozone and photochemical smog, which can cause damage to plants and materials as well as pose human health concerns (Mazzeo et al., 2010; Padhi and Gokhale, 2016). Benzene derived compounds are considered harmful to aquatic organisms (Sharma et al., 2014). Acceptable guidelines by Central Pollution Control Board (CPCB), India for industrial effluents, United States Environment and Protection Agency (USEPA) and Ministry of Environment and Forests (MoEF), India for petroleum refinery effluents are summarized in Table 1.3.

Table 1.3: Permissible limits of pollutants in the petroleum refinery effluents

Pollutants	CPCB, India (2019)	USEPA (2019)	MoEF, India (2008)
pH	5.5-9.0	6.0-9.0	6.0-8.5
BOD_5, mg/L	30	18	15
COD, mg/L	250	110	125
Oil and grease, mg/L	10	6	5
Phenolics, mg/L	0.35	0.12	0.35
BTEX, mg/L	0.1	-	0.1-0.2
Ammonia-N, mg/L	50	11	15
Nitrate-N, mg/L	10	10	10
Sulfides, mg/L	2.0	0.1	0.5
Heavy metals, mg/L	0.05-3	0.02-0.3	0.01-5
Suspended solids, mg/L	100	15	20

- CPCB: Central Pollution Control Board
- USEPA: United States Environment and Protection Agency
- MoEF: Ministry of Environment and Forests

1.3.3 Treatment options for petroleum refinery wastewater

There are two basic stages of treatment. The first stage consists of primary treatment followed by the advanced treatment of the pre-treated effluent. The heterogeneous components of the effluent, i.e. suspended solids, grit, immiscible liquids, and non-biodegradable solid particles are reduced significantly in the primary treatment process (Renault et al., 2009). The objective of the second stage is to reduce the effluent contamination level to allowable limits for discharge into water bodies by physicochemical or biological processes (Altas and Buyukgungor, 2008).

1.3.3.1 Physicochemical treatment

Physicochemical treatment consists of either physical separation of pollutants from one medium to another or chemical separation through either precipitation or change in subsequent ionic form. Physicochemical processes can include coagulation and flocculation, electrochemical methods, adsorption, chemical oxidation, membrane separation, advance oxidation processes. Volume of the pollutant wastewater, dose of chemical requirement,

separation of sludge and cost of the membranes are some of the common factors, which greatly affect these processes.

(A) Coagulation and flocculation

Coagulation involves curdling of particles in which destabilization of non-settling particles takes place. A coagulant is used for the particles to form clumps. On the other hand, flocs are formed during flocculation and are joined together to form masses to precipitate. Different coagulants, both inorganic and organic have been reported for treatment of refinery wastewater. Altaher et al. (2011) used ferric chloride ($FeCl_3$), aluminium sulfate ($Al_2(SO_4)_3$), lime and ferrous sulfate ($FeSO_4$) to treat real petroleum refinery wastewater. The wastewater had turbidity 200 NTU, total suspended solids (TSS) of 2217 mg/L and BOD 57.5 mg/L. $FeCl_3$ showed promising results at 800 mg/L dose and pH 8.6 with 99% turbidity removal. Farajnezhad and Gharbani (2012) used poly aluminium chloride (PAC) and $FeCl_3$ for the treatment of petroleum refinery wastewater with COD 1100 mg O_2/L and TSS 110 mg/L. The efficiency of both PAC and $FeCl_3$ were measured in terms of color, COD and TSS removal. PAC was found to be more effective compared to $FeCl_3$ in the removals of COD and TSS. COD removal of 80% and TSS removal of 90% were obtained at pH 7.5 at much lower dose of 20 mg/L. Santo et al. (2012) used different coagulants such as PAX-18 (17% Al_2O_3), aluminium sulfate ($Al_2(SO_4)_3$), ferric sulfate ($Fe_2(SO_4)_3$) and NALCO 71408 as flocculent for the treatment of petroleum refinery wastewater with COD 580 mg O_2/L, TOC 97 mg/L, total petroleum hydrocarbon 875 mg/L. S^{2-} was absent in the wastewater. Different blends of these coagulants and flocculants were used and efficiencies were measured in terms of COD and TOC removals. COD removal of 80%, TOC and turbidity (initial 76 NTU) removal of 77% were achieved by PAX-18 at pH 6-7. TPH removal was 95% by the combination of PAX-18 (28.6 mg/L) and NALCO 71408. The dose was similar to the previous literature (Farajnezhad and Gharbani, 2012) at lesser influent COD.

Coagulation and flocculation process can be effective for wastewaters of small volumes as released by small-scale industries. For large volume of wastewater, especially for oily wastewater having a mixture of many complex compounds, high chemical requirement becomes necessary. Hence both treatment and maintenance costs increase. Disposal of sludge generated in high amount also contributed to the problems associated with the coagulation and flocculation process of refinery wastewater treatment.

(B) Electrochemical methods

Electrochemical methods include the chemical reactions which take place in a solution at the interface of an electron conductor (the electrode: a metal or a semiconductor) and an ionic conductor (the electrolyte). In this process, an appropriate anode material gets oxidized and in situ generation of coagulants occur. Electrocoagulation is efficient in removing suspended solids as well as oil and grease (Xinhua and Xianfeng, 2004). This process is advantageous as it promotes flocculation (Canizares et al., 2006). In addition, the process does not require any dosing of coagulant and depends on the applied current density or cell potential.

Aluminum and iron electrodes have been mostly used for the treatment of petroleum refinery wastewater. El-Naas et al. (2009) performed batch coagulation experiments with aluminum, stainless steel and iron as electrodes for the removals of COD (596 mg/L and 4050 mg/L) and sulfate (SO_4^{2-}) (887 mg/L and 1222 mg/L) in two real petroleum refinery wastewaters (WW-A and WW-B). Efficiency was determined in terms of COD removal. Removals of COD were 60% and 40%, and removals of SO_4^{2-} were 100% and 50%, respectively, for WW-A and WWB at current density of 13 mA/cm^2 and contact time of 120 min when aluminum electrode was used. Wei et al. (2010) used a three-dimensional electrode reactor (TDER) with granular activated carbon (GAC) and porous ceramsite particles (PCP) for the treatment of heavy oil refinery wastewater having COD 3150 mg O_2/L and total organic carbon (TOC) 1550 mg/L. The treated wastewater under optimum conditions (GAC 75%, current density 30 mA/cm^2, retention time 100 min) presented 46% and 43% removals of COD and TOC, respectively. Hariz et al. (2013) used iron and aluminum electrodes for the treatment of synthetic petroleum spent caustic with S^{2-} (34517 mg/L) and COD (72450 mg/L) by electrocoagulation. The optimum time, initial pH and current density were found to be 30 min, 9 and 21.2 mA/cm^2, respectively, where more than 80% removal of S^{2-} and COD occurred. Furthermore, successive electrocoagulation (dual EC units) yielded 95% COD removal.

Keramati and Ayati (2019) used a combination of electrocoagulation and photocatalytic process with immobilized ZnO nanoparticles on concrete surface for the treatment of petroleum refinery wastewater. For the electrocoagulation process, COD removal (initial 900 mg/L) was 94% at 60 min at current density, pH and NaCl concentrations of 20 mA/cm^2, 8.5 and 0.5 g/L, respectively. For the photocatalytic process, COD removal (initial 600 mg/L) was 76% at 300 min at ZnO concentration, pH and irradiation power of 32W, respectively. In the combined process, initially the electrocoagulation process showed 47% COD removal (initial 1000 mg/L)

at 8.5 min. The partially treated effluent entered the concrete photo-reactor for 120 min, which led to 85% COD reduction and final effluent COD was 75 mg/L.

Different bioelectrochemical reactors were utilized by Mohanakrishna et al. (2019) for the removal of petroleum hydrocarbons (124-130 mg/L) and sulfate from wastewater at pH 7.0. Single and dual chamber microbial fuel cells were operated at similar HRT, electrode materials, inlet characteristics of petroleum wastewater and ambient temperature. Among both the configurations, dual chamber fuel cell showed higher efficiency with respect to bioelectrogenesis (single chamber - 789 mW/m2; dual chamber - 1089 mW/m^2), sulfates removal (single chamber - 80%; dual chamber - 94%), total petroleum hydrocarbon removal (single chamber - 48%; dual chamber 53%) and COD degradation (single chamber - 55%; dual chamber - 60%). Evaluated polarization behavior of both fuel cells evidenced the effective response of the electroactive anodic biofilm.

Electrocoagulation is more expensive in comparison to other processes due to the requirement of special kinds of equipment like electrode materials and conducting salts, which significantly affect the applicability of the treatment system. Effective for low volume of wastewater, but certainly not cost effective for the treatment of high volume. In addition, special maintenance is required for the smooth running of these processes including regular replacement of electrodes. Despite of the advantages, a larger power supply is required to run the whole operation, sole dependence of the process on anodic reactions, non-availability of electrodes and sludge production are the main limitations of this process.

(C) Adsorption

Adsorption is the process of extracting substances on a suitable interface from a solution. The main purpose in the treatment of petroleum refinery wastewater using adsorption technique is mostly to remove the organic compounds like phenol, BTEX, oil etc. Activated carbons, zero-valent iron, surface modified adsorbents have been used for the treatment of petroleum refinery wastewater. El-Naas et al. (2010) used date pit activated carbon and compared its performance with commercially available activated carbon for the removal of COD (influent 3490 mg O_2/L, 1662 mg O_2/L and 950 mg O_2/L). At each initial COD, more than 90% removal was achieved in 2h at adsorbent dose of 20 g/L. The results obtained from the date pit activated carbon were comparable with the efficiency obtained by commercially available activated carbon. Chen et al. (2014) compared the treatment of heavy oil refinery wastewater by adsorption with granular activated carbon (GAC) and GAC supported with manganese oxides

(MnO_x/GAC). MnO_x/GAC was utilized for the catalytic ozonation of the wastewater. MnO_x/GAC performed better than only GAC when COD (initial 3145 mg/L) and TOC (initial 1812 mg/L) removals were taken into account.

Nanoscale zero valent iron (NZVI) was used by Rasheed et al. (2011) for the treatment of refinery wastewater with high COD (40000 mg/L) and low pH (5.4). NZVI dose of 0.15 g/L was optimum and 40% reduction in COD occurred in 60 min. Adsorption assisted with ultra-sonication reduced 90% of COD in 50 min at pH 5.4. Performance of NZVI was better compared to activated carbon. Anirudhan and Ramachandran (2014) modified bentonite with surfactant for the removal of trichlorophenol (TCP) from petroleum refinery wastewater and found 99% removal from initial concentration of 20 mg/L at pH 3.0. Surface modified bentonite proved to be 2.3 times efficient than unmodified bentonite.

Adsorption is a polishing process and is costly. The process may lead to failure due to loss of regeneration capacity while treating wastewater with high concentrations of multiple pollutants. Hence, disposal of adsorbents becomes an issue. Cost, type and capacity of adsorbent are the considerable factors for the selection of adsorbents during treatment of petroleum refinery wastewater.

(D) Advanced oxidation processes

Advanced oxidation processes (AOPs) are characterized by the generation of hydroxyl radical ($^{\bullet}OH$), that can potentially destroy wide range of organic compounds. Most AOPs use various combinations of hydrogen peroxide, ozone and ultraviolet light to generate $^{\bullet}OH$, and thus are quite energy intensive. AOP is a good alternative for COD containing recalcitrant wastewater (Parilti and Akten, 2010).

Galvao et al. (2006) applied photo-Fenton process for the treatment of wastewaters contaminated with commercial diesel oil. Synthetic wastewater was prepared initially by dispersion of 200 mL diesel in 2L distilled water by stirring 1h in a magnetic stirrer. Then, separation of liquid phases was done by keeping the mixture stagnant for 1h. Aqueous phase was separated, filtered through filter paper (2 µm) and used as wastewater. At Fe^{2+} and H_2O_2 concentrations of 0.1 mM and 50 mM, respectively, 95% TOC (initial 120 mg /L) was removed within 180 min. Fenton process was used by Hasan et al. (2012) for the oxidative mineralization of petroleum refinery effluent. COD and TOC degradation were analyzed to evaluate the efficiency of the process. Under optimal conditions the COD (initial 1343 mg/L) and TOC

(initial 398 mg /L) reduction of 70% and 98.1% were achieved in 30 min at pH 7.0 and efficiencies were found to be better than the previous literature (Galvao et al., 2010).

Saien and Nejati (2007) used a circulating photocatalytic reactor for the removals of aliphatic and aromatic compounds from petroleum refinery wastewater with TiO_2 as catalyst. The efficiency of the process was measured through the removal of COD. Optimal catalyst concentration, pH and temperature were obtained to be 100 mg/L, 3 and 45°C. A maximum of 90% COD (initial 170-180 mg/L) was reduced in 4h. Shahrezai et al (2012) performed the photocatalytic oxidation and mineralization of petroleum refinery wastewater in aqueous catalyst suspensions of TiO_2 in a batch circulating photocatalytic reactor. A maximum reduction in COD (initial 220 mg/L) of more than 83% was achieved at the optimum conditions (pH 4, catalyst 100 mg/L, 45 °C and reaction time 120 min). Both the photocatalytic process obtained similar results. Chen et al. (2019) used catalytic ozonation process (COP) by using waste sludge derived biochar for the treatment of refinery wastewater. The biochar contained functional C groups, Si-O structures and metallic oxides which promoted the formation of $^{\bullet}OH$ radicals for the mineralization of petroleum contaminants. Catalytic ozonation using biochar achieved TOC removal of 54% compared to 27% efficiency shown by simple ozonation. Oxygen, nitrogen and sulfur containing contaminants were reduced by 33%, 58% and 13%, respectively.

Doltade et al. (2019) used hydrodynamic cavitation (HC) in an AOP for the treatment of petroleum refinery wastewater. The reactor configurations included the orifice (CN0) and venturi with different throat diameters (CN1 and CN5). Operating pressure and number of passes were considered as optimized for each individual reactor configurations through the cavitating zone. The maximum bacterial disinfection and COD reduction were obtained using CN5 reactor operated at 5 bar pump discharge pressure and the extent of reduction was found to be 59% and 52% respectively. It was reported in this study that, disinfection percentage can be further improved by increasing the number of passes and integrating it with other advsnced oxidation process.

The chemicals involved in AOP like O_3, H_2O_2, HOCl etc. themselves are very costly and continuous study is required to optimize different parameters for this process, which makes the total process very expensive and problematic for commercial application. UV assisted degradation and photo-Fenton processes require special attention and experienced operation, which increases the maintenance cost of the whole process. This process becomes costly while treating large volume of wastewater.

1.3.3.2 Biodegradation of petroleum pollutants

Biodegradation of phenol, sulfide, oil, hydrocarbons and nitrogen compounds are discussed in the following sections.

(A) Phenol biodegradation

Phenol is an aromatic compound and microorganisms are capable of degrading phenol through enzymatic action. Phenol is utilized as both carbon and energy source by the microbial population (both aerobic and anaerobic) due to its widespread occurrence in the environment.

In anaerobic degradation, phenol is carboxylated in the para position to form 4-hydroxybenzoate in the first step. Following para-carboxylation, thioesterification of 4-hydroxybenzoate to co-enzyme A allows subsequent ring reduction, hydration and fission (Schie and Young, 2007). The organisms capable of degrading phenol under anaerobic conditions were *Thauera aromatica*, *Desulphobacterium phenolicum* and *Clostridium* species. Degradation of phenol in denitrifying/anoxic conditions occurs through an enzyme activity from phenol to 4-hydroxybenzoate with nitrate as terminal electron acceptor. The enzyme is known as phenol carboxylase (Schie and Young, 2007). The phenol carboxylase activity is located in the cytosol, where it catalyses the reversible para-carboxylation of phenol to 4-hydroxybenzoate. An enzyme-bound phenolate anion is generated as the intermediate of 4-hydroxybenzoate decarboxylation, indicating phenolate could be the actual substrate for carboxylation (Lack and Fuchs, 1992). *Thauera aromatica* is a microorganism reported to degrade phenol in denitrifying condition. In the aerobic biodegradation of phenol, the first steps include oxygenation of phenol, by phenol hydroxylase enzymes to form catechol, followed by ring cleavage adjacent to or in between the two-hydroxyl groups of catechol. Molecular oxygen is used by the enzyme phenol hydroxylase to form 1,2- dihydroxybenzene which is degraded via two alternative pathways depending on the responsible microorganism by intradiol fission and extradiol fission to simpler intermediates (Harwood et al., 1996). The organisms, which utilize phenol by aerobic pathway, are *Acientobacter calcoceticus* and *Candida tropicalis*. Phenol degradation in anaerobic, anoxic and aerobic environment is given in equation 1.1, 1.2 and 1.3 (Chakraborty and Veeramani, 2006).

$$C_6H_5OH + 17H_2O \rightarrow 6HCO_3^- + 34H^+ \quad (\Delta G^0: \text{-2549 kJ.mol}^{-1}) \quad \ldots (1.1)$$

$$C_6H_5OH + 5.6NO_3^- + 0.2H_2O \rightarrow 6HCO_3^- + 4H^+ + 2.8N_2 \quad (\Delta G^0: \text{-2802 kJ.mol}^{-1}) \quad \ldots (1.2)$$

$$C_6H_5OH + 7O_2 \rightarrow 3H_2O + 6CO_2 \quad (\Delta G^0: \text{-2866 kJ.mol}^{-1}) \quad \ldots (1.3)$$

As per the ΔG^0 for reaction, phenol degradation in anaerobic, anoxic and aerobic environments are thermodynamically favorable and aerobic treatment of phenol is the most favorable one.

(B) Sulfide biodegradation

The biological sulfide removing studies employ either photoautotrophic or chemolithotrophic sulfide (S^{2-}) oxidizing bacteria. Kuenen (1975) has postulated the overall biochemical reactions occur during S^{2-} oxidation under different S^{2-}/O_2 ratio (Eq. 1.4, 1.5 and 1.6) , and it indicates that reactions producing SO_4^{2-} is thermodynamically more favored and energy yielding and hence preferred by the S^{2-} oxidizing bacteria in aerobic condition.

$$2HS^- + O_2 \rightarrow 2S^0 + OH^- \quad (\Delta G^0: \text{-169 kJ.mol}^{-1}) \quad \ldots (1.4)$$

$$2HS^- + 2O_2 \rightarrow H_2O + {S_2O_3}^{2-} \quad (\Delta G^0: \text{-387 kJ.mol}^{-1}) \quad \ldots (1.5)$$

$$2HS^- + 4O_2 \rightarrow 2{SO_4}^{2-} + 2H^+ \quad (\Delta G^0: \text{-733 kJ.mol}^{-1}) \quad \ldots (1.6)$$

Equation 1.6 is more favorable, while eq. 1.5 represents the chemical auto oxidation of S^{2-} resulting in the formation of thiosulfate ($S_2O_3^{2-}$).

Various forms of equations give biological oxidation of S^{2-} in anoxic conditions (Eq. 1.7 to 1.11), which involve both complete and partial denitrification coupled to complete and partial S^{2-} oxidation. The principal products are SO_4^{2-} and elemental sulfur (S^0) particles (Montabello et al., 2012).

$$15{NO_3}^- + 12H_2S \rightarrow 9H_2O + 6S^0 + 6{SO_4}^{2-} + 5{NO_2}^- + 5N_2 + 2OH^- + 4H^+ \quad \ldots (1.7)$$

$$HS^- + \frac{2}{5}{NO_3}^- + \frac{7}{5}H^+ \rightarrow S^0 + \frac{1}{5}N_2 + \frac{6}{5}H_2O \quad (\Delta G^0: \text{-253 kJ.mol}^{-1}) \quad \ldots (1.8)$$

$$HS^- + \frac{2}{3}{NO_2}^- + \frac{5}{3}H^+ \rightarrow S^0 + \frac{1}{3}N_2 + \frac{4}{3}H_2O \quad (\Delta G^0: \text{-306 kJ.mol}^{-1}) \quad \ldots (1.9)$$

$$5S^{2-} + 2NO_3^- + 12H^+ \rightarrow 5S^0 + N_2 + 6H_2O \quad (\Delta G^0: \text{-191 kJ.mol}^{-1}) \ldots (1.10)$$

$$5S^{2-} + 8NO_3^- + 8H^+ \rightarrow 5SO_4^{2-} + 4N_2 + 4H_2O \quad (\Delta G^0: \text{-744 kJ.mol}^{-1}) \ldots (1.11)$$

As per the ΔG^0 values, oxidation of S^{2-} occurs more easily in the presence of NO_3^- (Eq. 1.9) compared to NO_2^- (Eq. 1.8). It is also reported that, S^{2-} oxidation in anoxic environment is a two-step process with formation of S^0 in the first step (Eq. 1.10) and further oxidation of

S^0 to SO_4^{2-} (Eq. 1.11) (An et al., 2010). The ratio between the available electron acceptor and S^{2-}, i.e. NO_3^-/S^{2-} in anoxic condition is a key parameter to end up with a certain SO_4^{2-}/S^0 production ratio (Manconi et al., 2006). *Thiobacilus denitrificans* is reported to oxidize S^{2-} to S^0 simultaneously reducing NO_3^- or NO_2^- to nitrogen gas (N_2) (de Lomas et al., 2006).

(C) Hydrocarbons biodegradation

Hydrocarbon biodegradation is a slow process due to the hydrophobic nature of the contaminants, consequent bioavailability limitations and complexity of the hydrocarbons (Mohanty and Mukherji, 2008). Microorganisms that use hydrocarbons as the sole source of carbon and energy are able to overcome the bioavailability limitations. Degradation of these hydrocarbons is achieved through one or more of the following mechanisms: solubilization of hydrocarbons in bio surfactant micelles; emulsification of oil achieved by release of bio emulsifiers; and by adhering to the oil water interface, which promotes direct interfacial uptake of hydrocarbons (Abbasnezhad et al., 2008). Hydrocarbons, which are very soluble in water, can directly diffuse into the cell wall of bacteria. However, insoluble/partially soluble hydrocarbons first reach the bacterial cell wall as microscopic droplets, and then diffuse into them by groove formation (Vajrani and Upasani, 2017). Various microorganisms like cyanobacteria (Plohl et al., 2002), *E. aurantiacum* and *B. sepacia* (Mohanty and Mukherji, 2008) are reported to degrade oil and long chain hydrocarbons.

(D) Nitrogen compounds biodegradation

(i) Ammonia biodegradation

Conventional microbial nitrogen removal is based on autotrophic nitrification and heterotrophic denitrification. The removal involves (i) aerobic nitrification (i.e., the conversion of NH_4^+ to NO_2^- and further to NO_3^- by ammonia oxidizing bacteria (AOB) and nitrite oxidizing bacteria (NOB), respectively, with molecular oxygen as the electron acceptor and (ii) anoxic denitrification i.e., the reduction of nitrate or nitrite to N_2, mostly catalysed by heterotrophic bacteria. The relevant nitrification reactions are as shown in equation 1.12, 1.13 and 1.14.

$$NH_4^+ + 1.5O_2 \rightarrow NO_2^- + 2H^+ \quad \ldots (1.12)$$

$$NO_2^- + 0.5O_2 \rightarrow NO_3^- \quad \ldots (1.13)$$

$$NH_4^+ + 2O_2 \rightarrow NO_3^- + 2H^+ + H_2O \quad (\Delta G^0: \text{-205 kJ.mol}^{-1}) \quad \ldots (1.14)$$

(ii) Nitrate and nitrite biodegradation

The anoxic denitrification (i.e., the conversion of NO_3^- and NO_2^- to gaseous nitrogen) is accomplished with a variety of electron donors in presence of heterotrophic denitrifying bacteria using nitrate/nitrite as electron acceptor (Grabinska-Loniewska, 1991). This process results in simultaneous removal of nitrate/nitrite and organic/inorganic matter used as electron donor. The anoxic denitrification involves the following reactions,

$$2NO_3^- + 10H^+ + 10e^- \rightarrow N_2 + 2OH^- + 4H_2O \qquad (\Delta G^0 = -1040\ kJ.mol^{-1}) \quad \ldots (1.15)$$

$$2NO_2^- + 6H^+ + 6e^- \rightarrow N_2 + 2OH^- + 2H_2O \qquad (\Delta G^0 = -205\ kJ.mol^{-1}) \quad \ldots (1.16)$$

1.3.3.3 Bio-systems for the remedy of petroleum refinery wastewater

Biological treatment systems for the remediation of petroleum refinery wastewater can be categorized into suspended growth systems and attached growth systems. In suspended growth processes, microorganisms are maintained in suspension mode within the liquid of a reactor, which is allowed to operate by mixing with the feed organics under aerobic, anaerobic or anoxic conditions. In attached growth process, microorganisms are attached to an inert material (rocks, slag or plastic), which enables to generate biofilm containing extracellular polymeric substances produced by them. Attached growth systems can be broadly classified into fixed bed and moving bed bioreactors. A discussion on different biological reactors/systems used for treatment of petroleum refinery wastewater is presented in the following sections.

(A) Aerobic processes

Aerobic treatment of petroleum refinery wastewater is associated with the degradation of organics (phenols and its products), hydrocarbons (oil, grease) and inorganics (ammonia, sulfide). Conventional activated sludge treatment has been in use for quite some time. However, there have been other reactors described in the subsequent sections employed for aerobic treatment of petroleum refinery wastewater. The studied treatment options are categorized into suspended, attached and hybrid processes.

(i) Suspended processes

A continuously stirred tank reactor (CSTR, 5L) was operated in continuous mode for the treatment of petroleum refinery wastewater characterized by COD (1380 mg O_2/L), BOD (395 mg O_2/L), oil and grease (250 mg/L), suspended solids (168 mg/L), phenol (18.6 mg/L), NH_4^+-N (35.3 mg/L), S^{2-} (23.3 mg/L) and pH (9.29) (Mizzouri and Shaaban, 2013). Airflow rate and

temperature were 1 L/min and 27 ± 2 ºC, respectively. COD removal was 90% to 97% with organic loading rate (OLR) of 0.18-0.74 g COD/g MLVSS.day. Maximum COD removal was achieved at OLR of 0.74 g COD/g MLVSS.d at 25h HRT. The dominating microbes found to be *Pseudomonas Putida* and *Acidovoraz Delafieldii*. A full-scale activated sludge process (ASP) was converted to contact oxidation (CO) process (HRT 27d) through bio-augmentation for the treatment of petrochemical wastewater (Ma et al., 2009). Before bio-treatment, the wastewater had the following parameters: COD (300-600 mg O_2/L), BOD (150-350 mg O_2/L), NH_4^+-N (10-30 mg/L), suspended solids (150 mg/L), oil and grease (50 mg/L), pH (7-9). The bio augmentation process achieved final concentrations of COD and NH_4^+-N as 80 mg/L and 10 mg/L, respectively, in 20 days, which was 10 days faster than the conventional ASP subjected to upper mentioned concentrations. During the shock load application [two times increase in the OLR from 600 g/(m^3.d) to 1100 g/(m^3.d)], bio augmentation showed higher resistance than ASP.

Fed batch continuously stirred tank reactor was used for the oxidation of S^{2-} with a mixed culture. S^0 and SO_4^{2-} were the end products controlled by the amount of oxygen supplied (Janssen et al. 1995). It was found that up to S^{2-} loading of 1800 g/(m^3.d), both S^0 and SO_4^{2-} can be formed at oxygen concentration below 0.1 mg/L. Under highly oxygen limited circumstances, i.e. an O_2/S^{2-} consumption ratio below 0.7, $S_2O_3^{2-}$ was abundantly formed. The dominant microorganisms were identified to be *Thiobacillus neapolitanus* and *Thiobacilus O*. Roosta et al. (2011) also observed increase in conversion of S^{2-} (6 mg/L) to SO_4^{2-} from 10% to 60% when DO was increased from 0.5 to 4.5 mg/L in a fed batch reactor. Alcantara et al. (2004) studied the simultaneous biodegradation of phenolics (-o, -m, -p cresol) and S^{2-} in the presence of NH_4^+-N (160 mg/L) in synthetic wastewater at pH 7.0-7.5. A recirculation reactor system and a CSTR was used for the biodegradation study in oxygen limiting condition. The reactors consisted of 10L cylindrical section for S^{2-} oxidation and 2L conical section for S^0 recovery. To control the S^{2-} oxidation, O_2 to S^{2-} loading rate ratio (R_{mt}) was varied between 0.5 to 1.5. Recovery of S^0 was maximum (85%) at R_{mt} 0.5 and S^{2-} was completely oxidized to SO_4^{2-} at R_{mt} 2 or more even in the presence of phenolic compounds. Phenol was varied from 25 to 200 mg/L with constant cresols of 100 mg/L along with S^{2-} dose of 2000 g/(m^3.d), which didn't affect the S^{2-} oxidation rate. Growth of microorganisms increased with increase in phenol concentration, suggesting coexistence of S^{2-} and phenol oxidizing microorganisms.

Actual petroleum refinery wastewater with pH 8.3-8.9, COD 3600-5300 mg O_2/L, total phenol 160-185 mg/L, o-cresol 14-16.5 mg/L, m, p-cresol 72-75 mg/L, n-hexane 1.8-1.85 mg/L

was collected by El-Naas et al., 2014. The treatment was studied in a three step process consisting of an electro chemical (EC) cell, a spouted bed bioreactor (SBBR) immobilized with *Pseudomonas putida* and an adsorption column packed with granular activated carbon produced from agricultural waste. There was 46% decrease in COD (4190 to 2267 mg O_2/L) in the EC chamber, followed by SBBR chamber (HRT 1.8d) which removed overall 73% COD (2267 to 1116 mg O_2/L) and finally 96% COD (1116 to 110 mg O_2/L) was removed by adsorption column. Later in that study the authors used a pilot plant (El-Naas et al., 2016) with similar arrangement for the treatment of petroleum refinery wastewater and achieved 96% COD removal (initial 3970-4745 mg O_2/L) and 100% phenol (initial 107-138 mg/L) removal at 12h HRT.

Aerobic sequential batch reactor (SBR) was used for the treatment of petroleum refinery wastewater with COD 350 mg O_2/L, TOC 70 mg/L, phenol 10 mg/L and pH 8.0 (Thakur et al., 2014). Maximum COD and TOC removal efficiencies were found to be 80% and 84%, respectively, at 0.8d HRT. FTIR and UV analysis of the influent and effluent confirmed the biodegradation during the study. The study reported advantages of SBR operations such as flexibility in cycle time, resistance to shock loads and lesser area requirement for operation.

(ii) Attached process

Rotating biological contactor (RBC) has been mostly used for the treatment of petroleum refinery wastewater in attached aerobic systems. Studies are also conducted with packed bed/fixed bed reactors. An RBC with PUF as biomass support was used by Tyagi et al (1993) for the treatment of wastewater from the effluent of American Petroleum Institute (API) separator and dissolved air floatation (DAF) unit of a petroleum refinery. The RBC units were operated at different HRTs (30.4, 15.2, 10.1 and 7.6h) and 10 rpm rotational speed to investigate the removal efficiency of COD (235 - 925 mg O_2/L), NH_4^+-N (3 - 52 mg/L), phenol (6 - 88 mg/L), oil and grease (26 - 125 mg/L) and suspended solids (64 - 110 mg/L) at pH 7.3 -7.4. Efficiency of the system was measured at steady state of 23 - 40 days. COD removal was 85-90% irrespective of the loading rate. Maximum removals of phenol (94%), oil (90%) and NH_4^+-N (99%) were achieved at 30.4h HRT. A three stage RBC of 4L working volume was used for the degradation of phenolics, heterocyclics and polynuclear aromatic hydrocarbons in a synthetic gasifier wastewater with average COD 1388 mg O_2/L using *Exiguobacterium aurantiacum* and activated sludge consortia (Jeswani and Mukherji, 2012). Each stage of the RBC consisted of 27 discs of 14 cm diameter each and rotation of 10 rpm was fixed. Effect of

different HRT (48, 36, 24, 16, 12h) was studied and increase in removal was observed with increase in HRT. Maximum removal (94%) of COD was observed at highest HRT (48h). The OLR was varied from 3.3 to 14.0 g/(m^3.d) and the COD removal ranged from 63% to 93%. Complete removals of all the pollutants were observed at the lowest OLR of 3.3 g/m^3.day. At 24h HRT and OLR of 6.6 g/(m^3.d), complete removals of pyridine, quinoline, benzene and 85-96% removals of phenol, naphthalein, phenanthrene, fluoranthene and pyrene were observed. Treatment of hydrocarbon rich synthetic wastewater with COD 4513 mg O_2/L, total petroleum hydrocarbon (TPH) 4961 mg/L, alkalinity 58 mg/L as $CaCO_3$, PO_4^{3-}-P 7 mg/L and pH 7.5 was attempted in a three stage RBC with working volume 4L (Chavan and Mukherji, 2008). Each stage of the RBC consisted of 9 discs of 14 cm diameter with rotation of 10 rpm. The synthetic wastewater had 3-4 times more influent COD compared to the other above-mentioned literatures. An oil degrading bacteria *Burkholderia cepacia* and photoautotrophic organisms were used for the degradation study. TPH removal of 95-99% and COD removal of 78-97% were achieved at 21h HRT and OLR of 27.3 g TPH/(m^3.d). In an extension of this study, Mukherji and Chavan (2012) studied the degradation of diesel oil as sole carbon substrate and obtained 99% removal at TPH loading rate up to 31.8 g/m^3.day.

Jou and Huang (2003) constructed a fixed-film bioreactor system for the treatment of oil refinery wastewater. The reactor was equipped with a 4-chamber horizontal tank packed with PUF with an airflow rate of 2350 L/min. The reactor was operated at pH 6.5 to 7.5 and DO 2 mg/L. Performance data for fixed film bioreactor with 8h HRT demonstrated COD (initial 500 mg/L) removal of 85-90% and phenol (initial 30 mg/L) removal of 100%. The reactor in this study generated only one third of the sludge waste compared to the traditional ASP. Vendramel et al. (2015) operated an aerobic submerged fixed-bed reactor (ASFBR) for the treatment of petroleum refinery wastewater with COD 1183 mg O_2/L, dissolved organics carbon (DOC) 397 mg/L, TSS 101 mg/L and pH 7.9 at 12h HRT. The ASFBR showed COD, DOC and TSS removals up to 91%, 90% and 92%, respectively. NH_4^+-N removal of 90% was reported in this study but data was not shown. Biological S^{2-} removal was studied from wastewater caustic streams in a packed recycling reactor (PRR) in aerobic condition (Sanchez and Revah, 2009). The reactor consisted of a 3.4L up-flow cylindrical reactor column, 0.67L aerator and 1.9L conical settler. The study was operated at high alkaline condition (pH 10.0) and an alkaliphilic sulfide-oxidizing bacteria consortium (ASBC) was used. Nylon fiber was used as packing/biomass support material. The PRR reached a maximum S^{2-} oxidation rate of 0.0032 g/(m^3.d) with efficiency close to 100%. Increase in the S^{2-} from 1600 mg/L to 12800 mg/L

induced oxygen-limiting conditions and reduced the biological activity despite considerable biofilm attached to the nylon fiber.

A laboratory pilot scale reactor (550L) was used for the treatment of petroleum refinery wastewater with COD 1568 mg O_2/L, TPH 55.3 mg/L, NO_3^--N 1.5 mg/L, PO_4^{3-}-P 9 mg/L, turbidity 63 NTU, formaldehyde 372 mg/L, phenol 0.66 mg/L, total nitrogen (TN) 19 mg/L and NH_4^+-N 16 mg/L and pH 7.1 (Mahmoudkhani et al. 2012). The reactor was filled with 85% polyurethane elements, occupying 3% of the reactor's liquid volume and operated at 15 to 25 °C, DO 4 to 5 mg/L, MLSS 1400 to 1700 mg/L, HRT 4h and unlimited SRT. COD, NO_3^--N and PO_4^{3-}-P removal efficiencies were 99%. Formaldehyde, phenol and TPH were removed up to 96%, 79% and 94%, respectively.

(iii) Hybrid processes

Hybrid bioreactors are mostly the combinations of both suspended and attached type of reactors. They provide flexibility of the biomass bed to move around inside the reactor as well as separation of the undesired suspended particles. Efficiency is enhanced due to the movement of the biomass bed, which is more suitable for the treatment of wastewater containing colloidal organic matter like oil, grease and emulsifiers. Hybrid processes like moving bed reactors and membrane bioreactors have been adopted for the treatment of petroleum refinery wastewater in aerobic condition, which are discussed below.

Biodegradation of petroleum wastewater was studied in a fluidized bed reactor (170L) with PUF as biomass support at 24h HRT (Ochieng et al., 2003). The petroleum wastewater was characterized by phenol 600 mg/L, 2,4-dimethyl phenol 720 mg/L, total suspended solids (TSS) 1800 mg/L, benzene 500 mg/L, toluene 95 mg/L, xylene 15 mg/L, BOD 15600 mg O_2/L and COD 45000 mg O_2/L. The parameters were studied in terms of COD reduction. COD reduction of 36% occurred in a period of 24h with a biomass concentration of 78 mg/L due to deficiency in nutrients such as nitrogen and phosphate. In an extension of this study, performance of the reactor increased when operated with a mixture of brewery and petroleum refinery wastewater. Krishnakumar et al. (2005) used a reverse fluidized loop reactor (RFLR) in micro aerobic condition to recover S^0 from aqueous S^{2-}. The RFLR (0.48L) contained buoyant career particles made out of low-density polyethylene on which chemolithotrophic S^{2-} oxidizing bacteria (*Thiobacillus denitrificans*) formed a biofilm. The RFLR was operated at both uncontrolled and controlled (8.0, 9.0 and 9.5) pH with 1.5d HRT. The reactor was operated for the first 60 days at uncontrolled pH with influent S^{2-} of 250 mg/L and 95% of removed S^{2-}

was recovered as S^0. The maximum S^{2-} loading supplied to the reactor was 30 kg/(m^3.d) at pH 8.0, of which 90% was completely oxidized and 65% recovered as S^0.

Two moving bed biofilm reactors (MBBR) were operated by Borghei and Hosseini (2004) for the treatment of phenolic petroleum refinery wastewater in aerobic mode at different HRTs (24, 20, 16, 12 and 8h) and phenol concentrations (200, 400, 620 and 800 mg/L). During the experiments, the ratio of phenolic COD to total COD was varied from 0.2 to 1.0 and maximum COD removal efficiency (90-95%) was observed at ratio of 0.6, which was effective at all HRTs. The effects of hydraulic and toxic shocks (1000 mg/L COD) on the performance of the reactors were examined, and the results proved that the MBBR had good resistance to shock loads and return to steady state condition within two or three cycles of retention time. Microscopic examinations showed that the main bacteria culture attached to carrier elements and biofilms were of filamentous type.

A pilot scale three phase airlift loop bioreactor (170000L) was used for the treatment of petroleum refinery wastewater with pH 8.0-9.0, oil 30-55 mg/L, phenol 11-41 mg/L, COD 250-600 mg O_2/L, NH_4^+-N 55-125 mg/L (Xianling et al., 2005). Low height to diameter ratio was chosen to counteract the cost involved in high ratios in case of pilot scale reactors. The influences of pH, HRT, airflow rate on the removals of COD and NH_4^+-N were investigated and the optimum operational conditions of pH 7-8, airflow rate 9066 L/min and HRT 6.5h were found. Effluent COD and NH_4^+-N were less than 100 mg/L and 15 mg/L, respectively, at steady state period of 40 days, which were safe as per the local discharge limit of China.

Long-term feeding effect of oil refinery wastewater in a submerged membrane bioreactor was studied by Viero et al. (2008). The oil refinery wastewater consisted of oil stream (OS) and phenolic wastewater (PW). The HRT and airflow rate were kept constant at 10h and 2.5 L/min, respectively. The system was run in three phases i.e. day 1 to 33, 34 to 63 and 64 to 93 with only OS, OS+PW (OS: PW = 6:1) and OS+PW (OS: PW = 240:1), respectively. In the first phase COD, TOC and phenol removals were 67%, 60% and 99% with initial concentrations being 616 mg/L, 250 mg/L and 14 mg/L, respectively. In the second phase, COD, TOC and phenol removals were about 10-15% with initial concentrations being 1000 mg/L, 600 mg/L and 80 mg/L, respectively. The decrease in the efficiency was due to the increased OLR in the presence of NH_4^+-N (160 mg/L). In the third phase, COD, TOC and phenol removals was 40%, 70% and 99% with initial concentrations being 700 mg/L, 300 mg/L and 12 mg/L, respectively, due to increase in the biomass and membrane retention. The presence of high amount of chloride (1.7-3.0 g/L) did not have any effect in all the three phases.

Alsalhy et al. (2015) operated a hybrid hollow membrane bioreactor at much higher HRT of 5d for the treatment of oil refinery wastewater having COD 235 mg O_2/L, oil 14 mg/L, phenol 0.7 mg/L and pH 7.2. Removal of COD was 72% and 100% removals of phenol and oil were achieved. Effluent released from the reactor met the discharge standards of Baghdad city.

Mizzouri and Shaaban (2013) studied the toxic, hydraulic and organic shocks on the performance of a lab-scale sequencing batch reactor (5L) at 12.8h HRT. Petroleum refinery wastewater had COD 1290 mg O_2/L, oil and grease 235 mg/L, phenol 16 mg/L, TSS 171 mg/L, NH_4^+-N 37 mg/L, S^{2-} 21 mg/L and pH 8.9-9.0. A considerable variation in the COD removal was observed for organic, toxic, hydraulic and combined shock loads with minimum efficiencies 69%, 77%, 70% and 58%, respectively. The system was adversely affected by organic shock load with three times of the normal feed concentration.

B. Anaerobic processes

(i) Suspended processes

Bio-treatment of petroleum refinery wastewater by suspended anaerobic processes is chiefly reported for up flow anaerobic sludge blanket (UASB) reactors. Macarie et al. (1992) used two UASB reactors (T and U) of 3L for the treatment of wastewater from a petrochemical industry. After neutralization, the following parameters were exhibited by the wastewater: total COD 6477 mg O_2/L, soluble COD 5958 mg O_2/L, total suspended solids 704 mg/L, NH_4^+-N 93 mg/L and alkalinity 1777 mg/L as $CaCO_3$. UASB (T) was inoculated with sludge sampled from an anaerobic stabilization pond receiving waste activated sludge from a petrochemical industry treatment plant. UASB (U) was inoculated with anaerobically adapted activated sludge from a municipal plant. Both the UASB reactors were operated at different HRTs 7, 3 and 2d and organic load of 1.0, 2.4 and 3.0 kg COD/(m^3.d), respectively. The reactor pH was maintained at 7.1-7.2. UASB digesters presented comparable treatment efficiencies with rather low COD removals: the best results were 46% for UASB (T) at 2.6 kg COD/m^3.day and at HRT of 2.7d and 44% for UASB (U) at 2.2 kg COD/m^3.day and HRT of 3.2d. Rate of gas production was maximum at low HRT and decreased with increase in HRT. Gasim et al. (2012) operated two UASB reactors for the treatment of petroleum refinery wastewater with COD 7896 mg O_2/L, BOD_5 3378 mg O_2/L, NO_3^--N 2 mg/L, total Kjeldahl nitrogen 41 mg/L, total phosphorous 10 mg/L, NH_4^+-N 14 mg/L, alkalinity 990 mg/L as $CaCO_3$ and pH 8.5. During the study, alkalinity in the wastewater restricted the reduction of pH and acted as buffer. COD removal efficiency was 78-83% at 40h HRT, which was higher, compared to Macarie et al.,

1992. Wang et al. (2016) used a UASB reactor for the treatment of heavy oil refinery wastewater at different HRTs (45, 30, 22 and 18h). The wastewater had the following characteristics: total COD 1992 mg O_2/L, soluble COD 1780 mg O_2/L, oil 273 mg/L, hydrocarbons 55 mg/L, polar organics 218 mg/L and NH_4^+-N 186 mg/L. Average removal efficiencies of COD and total oil were 61-86% and decreased when HRT was reduced from 45 to 18h. Dominant microbial population comprised of *methanosaeta*, *cloacamonaceae*, *blvii28*, *methanolinea* and *methanosarcina*. The long-term operation of UASB exhibited excellent polar organic removal efficiency. However, NH_4^+-N removal was not reported in the study.

Degradation of petroleum hydrocarbon (initial 16000 mg/L) in 3L flasks in anaerobic condition is reported at pH 7 (Chan, 2011). During the study, pH of the system reduced to 5.8, but final hydrocarbon concentration was 14980 mg/L even after 64 days of operation. This indicates that some organic acids were generated due to anaerobic action but removal was quite less. *Bacilus* species was found to be dominating microbial species. Townsend et al. (2003) studied the biodegradation of two crude oils named ANS and Alba with heavy n-alkane fractionation in methanogenic and sulfate reducing conditions. Crude oil degradation was measured based on sulfate reduction and methane generation. In oil unamended methanogenic and sulfate reducing conditions, endogenous electron donors produced 314 µmol of methane and 621 µmol of sulfate was reduced over an incubation period of 475 days. Naphthalene, 2-methylnaphthalene and 2-ethylnaphthalele were degraded only in sulfate reducing condition. This study concluded that n-alkanes are labile and their biodegradation is not necessarily limited by the availability of electron acceptors. Sherry et al. (2012) obtained similar results during anaerobic biodegradation of crude oil (alkane) for a period of 686 days.

(ii) Attached processes

Attached anaerobic processes have been reported for the degradation of BTEX compounds simulating petroleum refinery effluents and application of both packed bed reactors have been reported. Saghafi et al. (2010) studied the degradation of toluene and xylene in an up-flow anaerobic packed bed reactor with 3L volume. Walnut shell was used as the packing material and *Pseudomonas putida* **PTCC 1694** was used as the microbial culture. Efficiency of the reactor was determined in terms of COD removal. Reactor was subjected to three sets of HRT (8, 16 and 24h) at constant COD of 3000 mg O_2/L for both xylene and toluene. Maximum COD removal (62%) was obtained at 24h HRT and reduced to 42% and 30% when HRT was reduced to 18 and 8h, respectively, when xylene was degraded. Similarly, COD removal of

68%, 40% and 30% occurred at HRTs of 24, 16 and 8h, respectively, when toluene was subjected to biotransformation. Increase in the organic load decreased production of biogas due to self-inhibition beyond 10000 mg/L COD. However, maximum gas of 787 and 834 mL were produced at 24h HRT when xylene and toluene were biodegraded, respectively. Two bench scale horizontal flow anaerobic immobilized biomass (HAIB) reactors were used by de Nardi et al. (2005) for the treatment of ground water contaminated with gasoline. The first reactor was fed initially with synthetic substrate containing protein, carbohydrates and benzene, toluene, ethylbenzene and xylene (BTEX) solubilized in ethanol. The BTEX concentration of each compound ranged from 3 to 15 mg/L with COD 573 mg O_2/L. HRT was 11.4h and the temperature was kept constant at 30 ºC. COD removal efficiencies of about 96% and BTEX removal efficiencies varying from 75% to 99% were achieved during this experimental period. The second reactor was operated to simulate actual field conditions. Thus, the HAIB reactor was fed with a mixture of water and commercial gasoline devoid of ethylbenzene. The concentration of each compound considered in BTX composition (benzene, toluene, and *m*-xylene) was gradually raised to 15 mg/L. The HRT was 20h and the temperature was kept at 25 ºC. The HRT was progressively lowered to 8h to investigate the reactor loading rate capacity. The best COD (influent 463 mg O_2/L) and BTX removal efficiencies achieved were about 99% and 95%, respectively, with HRT exceeding 12h. The results indicate the viability of using the HAIB reactor to treat wastewater and groundwater contaminated with BTEX and gasoline. HAIB reactor showed lesser HRT requirement compared to the anaerobic packed bed reactor reported by Saghafi et al. (2010). However, the influent COD was six times lower.

(iii) Hybrid processes

Anaerobic biofilm and baffled reactors have been operated for the treatment of petroleum refinery wastewater. Macarie et al. (1992) used a tubular fixed film reactor for the treatment of wastewater from a petrochemical industry. Wastewater exhibited the following parameters: total COD 6477 mg O_2/L, soluble COD 5958 mg O_2/L, total solids 6644 mg/L, NH_4^+-N 93 mg/L and Alkalinity 1777 mg/L as $CaCO_3$. The fixed film reactor was made out of 100 cm high plexiglas column with internal diameter of 9.6 cm. The column was packed using 67.0 cm high, 1.3 cm diameter PVC tubes that provided a surface area of 221 m^2/m^3. Three different HRTs (2.9, 3.2 and 5.8d) were applied to the reactor and removal of COD increased from 73% to 77%. However, gas production rate decreased from 670 to 470 L/(m^3.d). Mainly a higher VSS content and a better resistance explained the better efficiencies of this reactor to toxicity

caused by the aromatics present in the wastewater. Wang et al. (2017) studied the performance of a pilot scale hybrid vertical anaerobic biofilm (HyVAB) reactor for the treatment of petrochemical refinery wastewater with COD 6900 mg O_2/L. The reactor was an integration of a bottom anaerobic sludge bed and top aerobic stage. The HyVAB removed 86% COD at 55h HRT which was similar to the efficiency reported by Macarie et al. (1992). Methane (CH_4) production from the degradation of organics was reported in this study.

Anaerobic baffled reactor (ABR) with total volume 150L and available volume 75L was operated for 212 days (including start-up period of 164 days) for the treatment of heavy oil produced wastewater at poor nutrient condition (COD: TN: TP = 1200:15:1) and high salinity (11.5-14.6 g/L) (Ji et al., 2009). After a successful start-up, the ABR was able to achieve high average COD [influent 600 mg O_2/L, 200 g/(m^3.d)] and oil (influent 200 mg/L) removals of 65% and 88%, respectively, at 2d HRT. The system was stable during the shock load of 2.5 times of COD [500 g/(m^3.d)] for 4 days.

C. Anoxic processes

Anoxic processes are typically used for the removal of nitrate/nitrite from wastewater, which is commonly known as denitrification. The nitrified water is exposed to an oxygen free environment. Organisms in this anoxic systems use the nitrate and nitrite as an electron acceptor and release nitrogen in the form of nitrogen gas or nitrogen oxides. A readily biodegradable carbon source is also needed for efficient denitrification processes to occur (Fukui et al., 1999).

(i) Suspended processes

Treatment of petroleum refinery wastewater in anoxic suspended medium has been carried by granular and UASB reactors as well as batch processes. Sarfaraz et al. (2004) developed anoxic granules for phenol degradation after maintaining for a long time without loss of its phenol degradation activity at 6h cycle time in a sequencing batch reactor. They achieved more than 80% phenol and nitrate removal up to influent phenol of 1050 mg/L and COD/NO_3^- ratio observed to be 3.4. However, phenol removal efficiency steeply decreased to 56% at influent phenol concentration of 1150 mg/L. Moussavi et al. (2016) used anoxic bio granules for the assimilation of total petroleum hydrocarbon (TPH) at different feed concentrations (2000-10000 mg/L) in saline media at 7.5 pH. Kerosene was used as TPH source and feed was prepared with seawater to resemble saline media. Bio granules were mostly consisted of *Bacillus* sp. and were able to degrade 99% of TPH at influent of 2000 mg/L with 22h HRT.

Maximum biodegradation rate was obtained to be 2600 mg/(g biomass.d) at 10000 mg/L infeed and confirmed high rate of kerosene degradation (used as a sole carbon source) in anoxic environment.

Treatment of refinery effluent involving S^{2-} is reported in a laboratory scale anoxic sulfide-oxidizing reactor (ASO) (Mahmood et al., 2007). The reactor was operated for 135 days to evaluate the potential of the reactor at different volumetric loading rates, HRTs and substrate concentrations. The process could endure high S^{2-} concentrations, as the S^{2-} removal remained higher than 89% with influent concentration up to 1920 mg/L and was inhibited at NO_2^--N concentrations more than 2265 mg/L at 2.4h HRT. Stoichiometric analysis showed that major part of S^{2-} (89-90%) was removed by NO_2^--N and rest was auto oxidation. Accumulation of NH_4^+-N occurred beyond NO_2^--N concentrations of 2265 mg/L. High NH_4^+-N concentrations (200-550 mg/L) in the bioreactor contributed towards the overall process inhibition. *Thiobacilus denitrificans* was found to be the responsible microorganism for the oxidation of S^{2-}. Later in this study, Mahmood et al. (2008) found the optimum pH to be 7.0-9.0 and the ASO system could operate in a wider pH range of 5.0-11.0. Jing et al. (2010) evaluated the performance of an anoxic sulfide oxidizing UASB reactor using NO_3^--N and NO_2^--N as electron acceptors during the oxidation of S^{2-} at 4h HRT and pH 7.0. For NO_3^--N-ASO process, S^{2-} and NO_3^--N concentrations were 160-1000 mg/L and 30-170 mg/L, respectively. S^{2-} and NO_2^--N removals were 90% and 32%, respectively. For NO_2^--N-ASO process, S^{2-} and NO_2^--N concentrations were 160-880 mg/L and 43-158 mg/L, respectively. S^{2-} and NO_2^--N removals were 90% and 30%, respectively. Nitrate was found to be the better electron acceptor for the oxidation of S^{2-}. *Betaproteo bacterium*, *Alphaproteo bacteria* and *Epsilonproteo bacterium* were the isolated microorganisms from this study. *Thiobacilus denitrificans* could degrade higher influent S^{2-} at low HRT compared to other organisms.

Laboratory batch studies were conducted by Mukherji et al. (2004) to test the biodegradation of diesel oil by the culture isolated from the Arabian sea sediment (ES1) in nitrate reducing conditions. The study was performed with 100 mL sample volume with 1 mL diesel and 2 mL culture media. ES1 was able to use diesel as sole source of carbon and energy but only 18% degradation was achieved in a period of 50 days. Microorganisms were tolerant to salinity of 35 g/L. Under anoxic nitrate reducing conditions the rate and extent of degradation was significantly lower. During the study 39% of abiotic loss of diesel was reported. Out of the lost amount of diesel, 80% were of aliphatic nature.

(ii) Attached processes

Attached growth reactors operated for the treatment of petroleum refinery wastewater involved the operation of trickling filters and fixed bed reactors. Fernandez et al. (2013) used a biotrickling filter of 2.4L packed with polypropylene pall rings for the removal of hydrogen sulfide (H_2S) in anoxic conditions. The influence of the H_2S inlet concentration, NO_3^--N feeding regime and liquid flow rate (20-180 L/h) on the elimination capacity of the bio trickling filter was studied. NO_3^--N feeding was done in both manual and controlled mode. The results indicate that 99% of the H_2S was removed for H_2S inlet loads lower than 120 g $S^{2-}/(m^3.h)$ by using controlled nitrate feeding. Both nitrate feeding regimes (manual and controlled) studies showed high H_2S removal of more than 99%. The manual regime caused nitrite accumulation due to faster reduction of nitrate than nitrite. However, there was no accumulation in controlled condition, which allowed better performance of bio trickling filter. Munoz et al. (2013) used a bio trickling filter (packed bed volume 1.5L) with kaldnes rings as packing material for the degradation of toluene in anoxic condition. Different loads of toluene [72, 120, 288 and 816 $g/(m^3.d)$] were supplied to the reactor at pH 7.0 and complete toluene removal was achieved in the load range of 72 to 144 $g/(m^3.d)$. *Actinobacteria* and *Proteobacteria* were observed to be the dominant microbial species for the degradation of toluene.

Ghorbanian et al. (2014) used a tubular up flow anoxic fixed bed reactor for the degradation of oil extracted from contaminated soil at different inlet concentrations (950-2500 mg/L) at 24h HRT and observed decrease in efficiency from 99% to 94% with increase in influent oil concentration. Maximum degradation rate of 2340 $g/(m^3.d)$ was achieved at a loading rate of 2496 $g/(m^3.d)$. The fixed bed reactor was more efficient compared to a suspended sequencing anoxic batch reactor used in the same study in similar conditions for the treatment of hydrocarbon-laden streams.

Sun et al. (2019) used two up-flow fixed-bed bioreactors (UFBRs) as pretreatment unit for the removal of nitrate and refractory organic pollutants from bio-treated coking wastewater (BTCW). The UFBRs were separately filled with alkali-pretreated or no alkali-pretreated corncobs used as solid carbon sources as well as biofilm carriers. More than 90% removal of nitrate was achieved. Furthermore, GC-MS analysis confirmed that the typical refractory organic matters decreased significantly after UFBR treatment. Dominant denitrifiers, fermentative bacteria and refractory-organic-pollutants-degrading bacteria co-existed inside the UFBRs system. Compared with no alkali-pretreated corncobs, alkali-pretreated corncobs provided more porous structure and much stable release of carbon to guarantee the growth and

the quantity of the functional bacteria such as denitrifiers. This study indicated that the UFBRs filled with alkali-pretreated corncobs could be utilized as an effective alternative for the enhanced treatment of the BTCW.

(iii) Hybrid processes

Moussavi and Ghorbanian (2015) used a fixed film tubular hybrid bioreactor operated in nitrate reducing condition for the treatment of synthetic wastewater prepared by crude oil. The effects of different total petroleum hydrocarbon (TPH) concentrations (950-2500 mg/L) and HRT (9-24 h) were studied. Marginal reduction in removal efficiency from 99% to 94% was observed with increase in TPH from 950 to 2500 mg/L at 24h HRT. However, decrease in HRT from 24h to 9h caused reduction in efficiency from 99% to 84%. Drastic decrease in the removal of TPH in this study in the absence of NO_3^--N confirmed the suitability of anoxic conditions over anaerobic. Anoxic biomass tolerated up to 30 g/L of NaCl during the study.

D. Multiple bioreactors operated in series

In series operation of the bioreactors, two or more bioreactors are operated in sequence to each other where effluent of one reactor is fed as influent to the other reactor. These types of treatment systems can be a combination of different types of bioreactors operated in series. These types of reactors are effective for the remediation of effluents with high concentrations of recalcitrant compounds (Nasirpour et al., 2015). Series operation of multiple bioreactors are reported for the treatment of effluents such as coke plant wastewater (Zhang et al., 1998; Kim et al., 2008), landfill leachate (Canziani et al., 2006; Chen et al., 2008) and batch reactors (Kargi et al., 1996; Liu et al., 2005). Reported literature works on the bioreactors operated in series for the treatment of petroleum refinery wastewater are discussed below.

Vaiopoulou et al. (2005) used a combination of anoxic (DN1) and aerobic (Nif1) continuously stirred tank reactors of 45L volume each for the removals of S^{2-} and NO_3^--N from petrochemical wastewater at 0.45d HRT (Fig. 1.1). Denitrification was carried out in DN1 until the exhaustion of NO_3^--N and effluent of DN1 was supplied to Nif1 for the aerobic removal of residual S^{2-}. Influent to DN1 comprised of COD 495-630 mg/L, S^{2-} 110 mg/L, NO_3^--N 170 mg/L and pH 7.5. The effluent concentration of NO_3^--N from DN1 was almost zero and the S^{2-} concentration after the aerobic treatment was always lesser than 0.1 mg/L suggested 95% and 99% removals of S^{2-} and NO_3^--N throughout the process. Successful anoxic oxidation of S^{2-} to SO_4^{2-} was achieved and fluctuation of S^{2-} in the feed was tolerated by its aerobic oxidation in the subsequent downstream activated sludge plant.

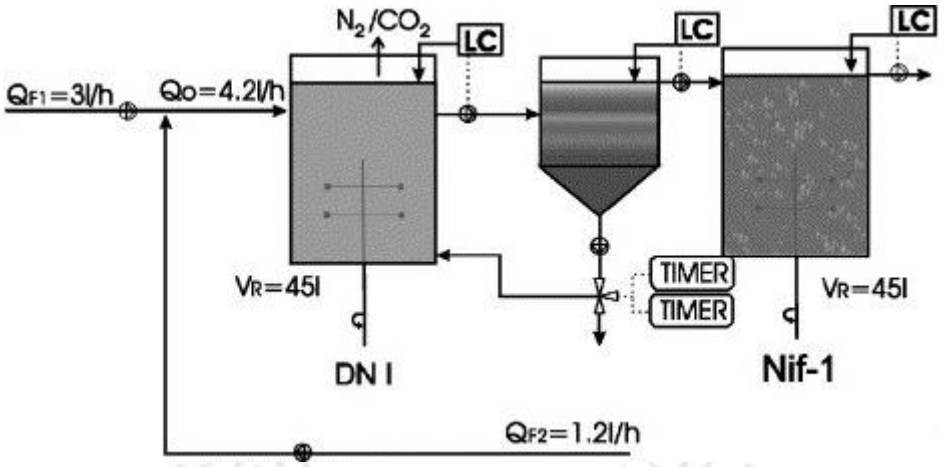

Fig. 1.1: Combination of anoxic (DN1) and aerobic (Nif1) for the removals of S^{2-} and NO_3^--N from petrochemical wastewater (Vaiopoulou et al., 2005)

A sequential anaerobic-aerobic moving bed biofilm reactor (MBBR) system was used by Lu et al. (2013) for the simultaneous removals of COD and NH_4^+-N from petroleum refinery wastewater. The HRT of the anaerobic-aerobic system was varied from 72 to 18h. The wastewater had COD 675-742 mg O_2/L, oil and grease 42-48 mg/L, NH_4^+-N 31-35 mg/L and pH 7.4-7.5. The anaerobic-aerobic system had a strong tolerance to shock loading. Compared with the professional emission standard of China, the effluent concentrations of COD and NH_4^+-N in the system could satisfy grade I criteria at HRTs of 72h and 36h. The average sludge yield of the anaerobic reactor was estimated to be 0.06 g suspended solid/g COD removed. This work demonstrated that the anaerobic-aerobic MBBR system (Fig. 1.2) using ceramsite as bio-carrier could be applied to achieve high wastewater treatment efficiency.

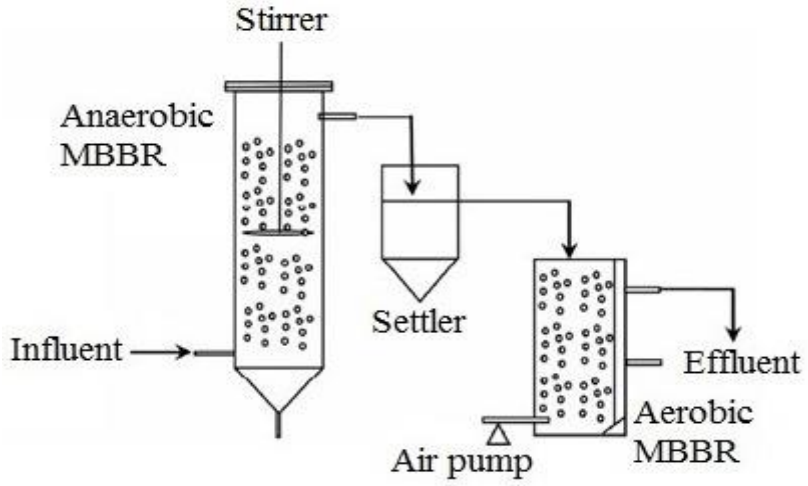

Fig. 1.2: Schematic diagram of the anaerobic-aerobic MBBR system used for the treatment of petroleum refinery wastewater (Lu et al., 2013)

Tong et al. (2013) operated a conventional activated sludge process (CAS) coupled with immobilized biological aerated filter (I-BAF) for the treatment of heavy oil wastewater with COD 209 mg O_2/L, oil 11 mg/L, NH_4^+-N 12 mg/L, S^{2-} 0.05 mg/L and pH 6.3 (Fig. 1.3). After the biological treatment, the COD was removed around 64% at overall HRT of 36h (18h each for CAS and I-BAF). The average effluent COD reached 75 mg O_2/L, which met the national discharge standard. The bacterial species in the CAS and I-BAF reactors belonged to the *Pseudomonas*, *Actinobacter*, *Bacillus* and *Actinobacteria* group.

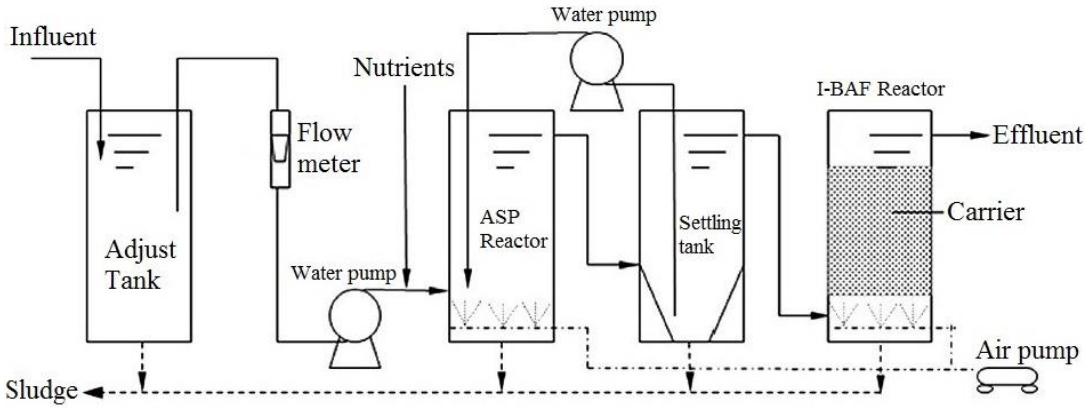

Fig. 1.3: Schematic diagram of the activated sludge process and immobilized biological aerated filter for the treatment of heavy oil wastewater (Tong et al., 2013)

Nasirpour et al. (2015) operated an upflow anaerobic sludge blanket (UASB) reactor and an aerobic packed-bed biofilm (PBBR) reactor in combination for the degradation of petroleum refinery wastewater (Fig. 1.4). The COD (influent 435 mg/L) removal efficiency of the reactors were 69% and 38%, respectively, for UASB and PBBR after 118 days of operation at pH 8.0. The overall COD removal was 81% by the combined treatment of the UASB-PBBR reactor system. The UASB reactor carried out major portion of the organics degradation at 72h HRT. A rise in the generation of biogas was observed with increase in reactor performance time during the study. Zou (2015) used a novel integrating UASB reactor and a two-stage biological aerated filter (BAF) system for the treatment of petroleum refinery wastewater characterized by COD (1008 mg O_2/L), oil (55 mg/L), hydrocarbons (43 mg/L), NH_4^+-N (68 mg/L) and SO_4^{2-} (41 mg/L) at 96h HRT (UASB: 48h, BAF1: 24h, BAF2: 24h). BAF reactors were inoculated with *Candida tropicalis* and *Rhodotorula dairenensis*. COD and hydrocarbons were partially removed in UASB reactor. Residual organics and NH_4^+-N were removed by the BAF units and effluent met with grade I discharge standards. During the study, COD, NH_4^+-N, oil and hydrocarbons were removed by 90%, 91%, 87% and 89%, respectively, at overall HRT of 96h.

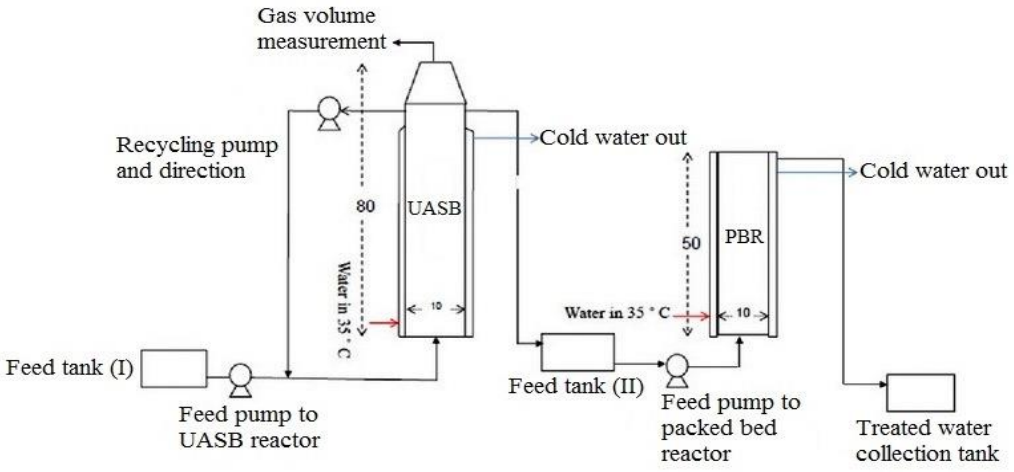

Fig. 1.4: Schematic diagram of UASB reactor and PBBR reactor for the treatment of petroleum refinery wastewater (Nasirpour et al., 2015)

Zica (2017) treated petroleum refinery wastewater using a combination of anaerobic and aerobic processes in an up-flow anaerobic sludge blanket (UASB) reactor paired with a rotating algae biofilm reactor (RABR) (24h HRT), respectively, to produce a treated effluent (Fig. 1.5). The wastewater contained COD (163 mg O_2/L), total nitrogen (25 mg/L), total phosphorous (1.8 mg/L) having pH 8.0. The reactor system was able to achieve the discharge limits for Utah State. Liu et al. (2013) constructed a field pilot study consisting of a UASB reactor and an integrated BAF for the treatment of heavy oil wastewater characterized by COD (130-1238 mg O_2/L), oil (25-316 mg/L), NH_4^+-N (38-84 mg/L) and pH 7.8-8.3. Removals of COD and NH_4^+-N were 74% and 94%, respectively, at overall HRT of 24h (12h each for UASB and BAF). Partial removal of organics and COD occurred in UASB reactor and BAF was responsible for the degradation of residual organics and NH_4^+-N. Dominant microbial species in the UASB reactor were *Bacillales* and *Rhodobacterales*.

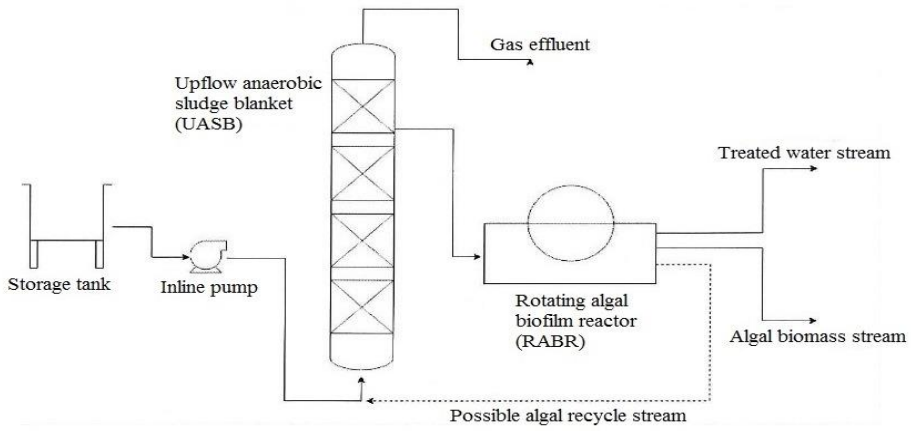

Fig. 1.5: Schematic diagram of UASB reactor and RABR reactor for the treatment of petroleum refinery wastewater (Zica, 2017)

Zheng (2016) developed a lab-scale hybrid system integrating a hybrid hydrolysis acidification (HA) reactor, a moving bed biofilm reactor (MBBR), an ozonation (O_3) reactor and biologically activated carbon (BAC) reactor for the treatment of heavy oil wastewater with COD (1130 mg O_2/L), oil (120 mg/L), NH_4^+-N (63 mg/L) and pH 7.5 (Fig. 1.6). The optimized HRT of the system was 41.33h (HA: 16h, MBBR: 16h, ozonation: 0.33h, BAC: 9h) where the effluent concentrations of COD, oil and NH_4^+-N were 48, 1 and 4 mg/L, respectively, corresponding to total removal efficiencies of 96%, 99% and 94%, respectively. The effluent could meet the grade I as required by the national discharge standard of China. The HA process remarkably improved the biodegradability of the wastewater, while the MBBR process played an important role in degrading COD. The ozonation process enhanced the biodegradability of the MBBR effluent, and finally, deep treatment was completed in the BAC reactor.

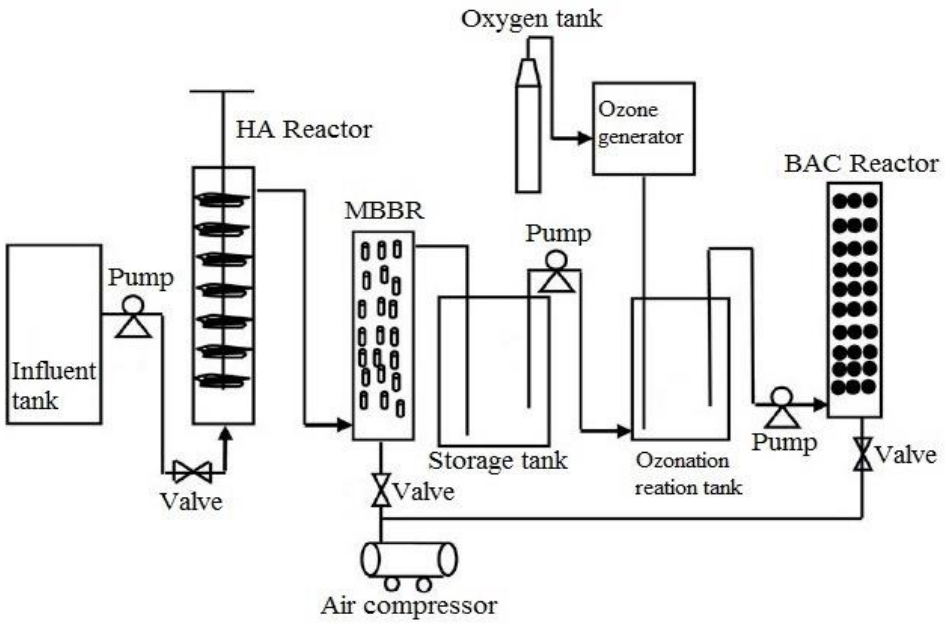

Fig. 1.6: Schematic diagram of HA reactor, MBBR reactor, O_3 reactor and BAC reactor for the treatment of heavy oil wastewater (Zheng, 2016)

Li et al. (2017) used anaerobic-aerobic biofilm reactor system for the treatment of petroleum refinery wastewater (Fig. 1.7). The total HRT of the system was kept at 108h (72h for anaerobic and 36h for aerobic reactors). COD (influent 650-1150 mg/L) and total nitrogen (influent 35-70 mg/L) removal efficiencies were obtained to be 93% and 83%, respectively, by combined action of the reactors with most of the removal (95-99%) carried out by the anaerobic reactor. Presence of different groups of bacteria like *Nitrosomonadaceae* for denitrification and *Chlorobiaceace* for oxidation of S^{2-} and S^0 in anaerobic reactor were reported in this study.

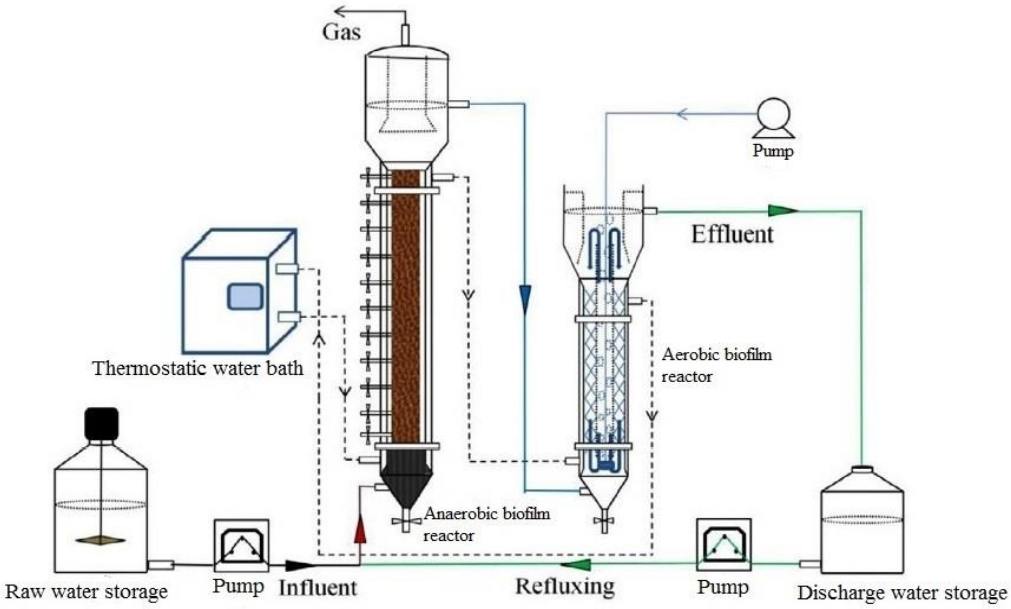

Fig. 1.7: Schematic diagram of anaerobic biofilm reactor and aerobic biofilm reactor for the treatment of petroleum refinery wastewater (Li et al., 2017)

Abass et al. (2018) operated anoxic and aerobic membrane reactors in series for the treatment of oil refinery wastewater (Fig. 1.8). Reactors were stable after two months of operation and the overall system showed 97% COD and oil removal efficiency. Increase in the influent oil concentration led to accumulation of non-biodegradable oil moieties, unsaturated extracellular polymers (101 mg/g VSS), aromatic compounds and metallic compounds. Major membrane colonizers were found to be *Commonas* and *Rhodobacter*.

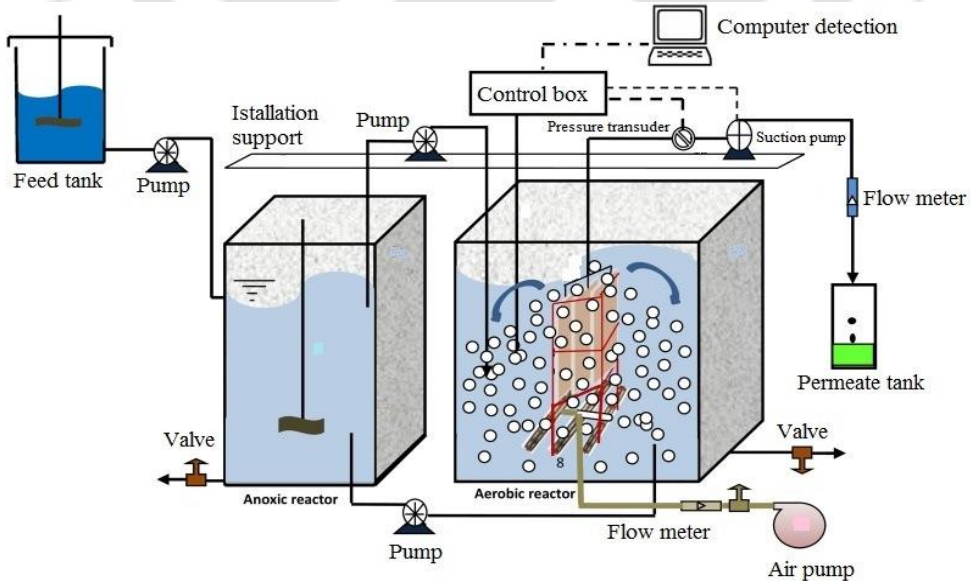

Fig. 1.8: Schematic diagram of anoxic and aerobic membrane reactors for the treatment of oil refinery wastewater (Abass et al., 2018)

Zhao et al. (2019) treated poly aromatic hydrocarbons (PAHs) (679–3818 ng/L) and nitrated polyaromatic hydrocarbons (NPAHs) (176–1392 ng/L) in wastewater. Anthracene and naphthalene were the predominant PAHs, and 2-nitrofluorene and 9-nitroanthracene were the predominant NPAHs by both the sequencing batch reactor/moving-bed biofilm (SBR/MBBR) and the anaerobic-anoxic-aerobic (A^2O) processes (Fig. 1.9). Low-molecular-weight PAHs were mainly removed through volatilization and biodegradation/biotransformation. Meanwhile, the removal of high-molecular-weight PAHs and NPAHs depended on adsorption and sedimentation. Overall, the removal capacity of the A^2O process for PAHs and NPAHs was better than that of the SBR/MBBR process. Tertiary treatment processes had little effect or even a negative effect on the removal of PAHs and NPAHs. The process diagram adopted in this study is shown in Fig. 1.9.

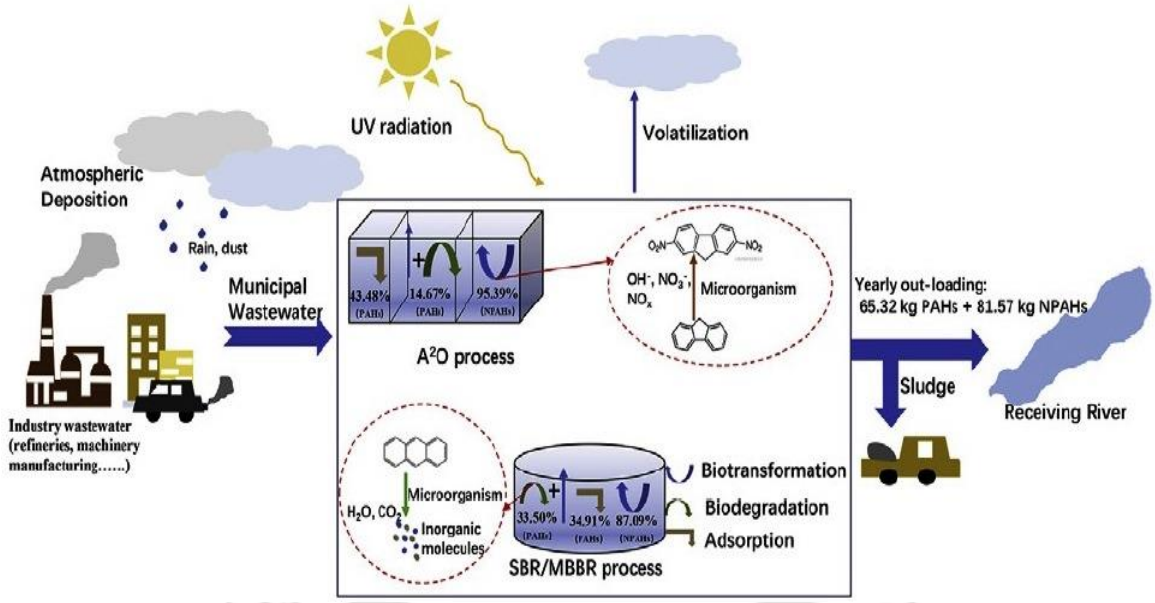

Fig. 1.9: Flow diagram of A^2O and MBBR processes for the treatment of polycyclic aromatic hydrocarbons (Zhao et al., 2019)

Sonwani et al. (2019) used three MBBR system (MBBR-1, MBBR-2 and MBBR-3) connected in series for the treatment of wastewater with naphthalene at different pH (5.0 to 9.0) and HRT (1.0 to 5.0d). Polypropylene (PP), low-density polyethylene (LDPE) and PUF were used as biomass support. At 7.0 pH and 5.0d HRT (Fig. 1.10). Maximum removal efficiencies were observed to be 72%, 84% and 90%, respectively, for PP, LDPE and PUF carrier materials. Gas chromatography and mass spectroscopy (GC-MS) analysis revealed catechol and 2-naphthol as intermediate metabolites for naphthalene degradation.

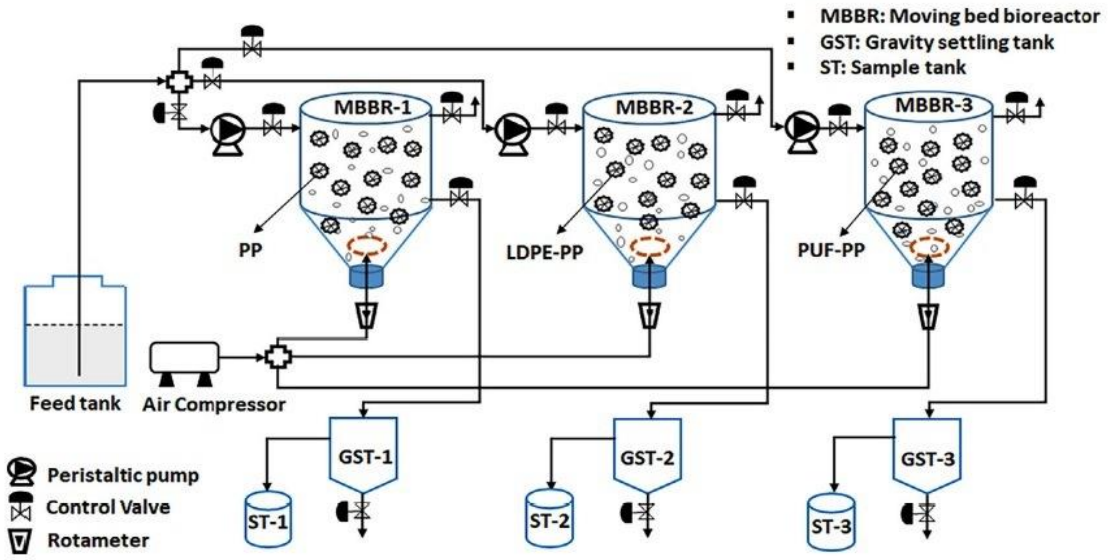

Fig. 1.10: Schematic diagram of MBBR reactors operated in series for the treatment of wastewater with naphthalene (Sonwani et al., 2019)

A two-stage bench-scale membrane-aerated biofilm reactor (MABR-1 and MABR-2) was developed by Tian et al. (2019) to treat wastewater containing high o-aminophenol (OAP) content (Fig. 1.11). MABR1 achieved removal rates of 17.6 g OAP/(m^2.d) and 29.4 g COD/(m^2.d). Total nitrogen removal of 90% was achieved after the addition of external glucose in MABR - 2. *Pseudomonas* and *Nitrosomonas* were the key functional genera in MABR-1 and MABR-2, respectively. The OAP-degrading species and functional contribution analysis indicated that OAP can be metabolized by a single *Pseudomonas* or by the synergistic effects of bacteria, mainly including *Cupriavidus*, *Thauera*, unclassified *Sphingomonadaceae*, *Lysobacter*, and *Azotobacter* or by the cooperation of all the bacteria above.

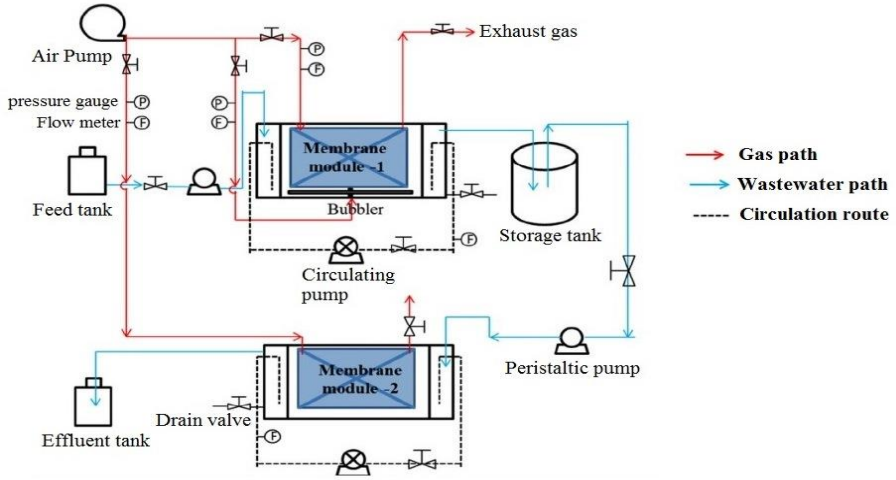

Fig. 1.11: Schematic diagram of membrane reactors operated in series for the treatment of wastewater with *o*-aminophenol (Tian et al., 2019)

1.4 SUMMARY OF THE LITERATURE REVIEW AND KNOWLEDGE GAP

The wastewater generated from petroleum refinery industry consists of toxic pollutants like phenol, S^{2-}, oil, hydrocarbons, NH_4^+-N, NO_3^--N, salts etc. Suspended systems like ASP, membrane reactor, sequencing batch reactors (SBR) and attached systems like trickling filter, rotating biological contractor (RBC), packed bed reactors in anaerobic, anoxic and aerobic conditions have been used by various researchers. The suspended systems contain less biomass and prone to high toxicity and wash out whereas fixed film system is prone to clogging. The membrane system and the fluidized process though very efficient, are reported to be expensive in terms of establishment and operating cost. Moving bed reactor (MBR) being a combination of conventional activated sludge process and fluidized bed system, where biomass is grown on inert carrier elements turn into an efficient and emerging technology for treatment of industrial wastewaters. MBR is less prone to clogging; uses the whole tank volume and possesses advantages of attached growth systems, biomass in the effluent is less than suspended growth system and is suitable for slow growing nitrifying bacteria (Chen et al., 2008).

Most of the reported systems used for the treatment of petroleum refinery wastewater are of aerobic type and less information is available for anaerobic and anoxic conditions. Phenolics, S^{2-}, oil and grease, NH_4^+-N removal studies have been carried out individually in anaerobic, anoxic and aerobic systems. However, the knowledge about interaction of multi substrates and energy sources during the treatment of multi-pollutants are scarce. Petroleum refinery wastewater often results in high concentration of salt and knowledge about the effect of saline conditions during its treatment is limited. Moving bed reactors used in the treatment of petroleum refinery wastewater are mostly of aerobic type and mixing was achieved through aeration. The information about the reactor operation in anaerobic and anoxic mode with different mixing systems are limited. Although adequate literatures are available on the biodegradation of phenol, S^{2-}, oil and grease and NH_4^+-N in single step ASP and sequencing batch rectors (SBRs), design data on application of anoxic-aerobic moving bed reactor system for removals of phenol, S^{2-}, oil and grease and NH_4^+-N containing wastewater are very limited.

Single reactor systems operated in anaerobic and anoxic conditions are not capable of simultaneous treatment of the above-mentioned pollutants. Degradation of nitrogen compounds by anaerobic and anoxic reactors alone doesn't meet the discharge limit (Chuang and Ouyang, 2000; Mosquera-Corral et al., 2003). In that case, a combination of anoxic-aerobic treatment for the removals of these pollutants frequently could achieve the desired results compared to single aerobic or anoxic reactor (Li et al. 2003).

Mode of biological reactor operation is an important parameter for influencing the reactor performance. In continuous feeding system, influent is added to the reactor and released as effluent continuously. Feed is diluted with large volume of liquid present in the reactor and thus helps in reduction of toxicity. In fed-batch operation, feed is added to the reactor for smaller duration and pumping time requirement is reduced, which makes the process simpler and economic. Cycle period of the reactor also play major role in the performance of the reactor controlling exposure of the organic load (Sahinkaya and Dilek, 2007; Damasceno et al. 2007).

1.5 OBJECTIVE OF THE STUDY AND RESEARCH PROTOCOL

The present study aimed for the treatment of petroleum refinery wastewater containing phenol, emulsified hydrocarbons, sulfide, ammonia and nitrate in anoxic-aerobic sequential system operated in fed batch mode. Anoxic disc bed reactor and aerobic moving bed reactor were developed and effects of agitation speed, HRT, hydrocarbon properties, salt concentrations and shock loads were analyzed. In addition, treatment of real hydrocarbon rich wastewater and identification of involved microbial species were done. Flow diagram of the research protocol is illustrated in Fig. 1.12. The following sequence of studies were carried out to achieve the objectives.

- Maximization of S^0 production by varying the concentrations of S^{2-}, phenol, diesel, NH_4^+-N and NO_3^--N in anoxic fed batch reactors.
- Optimization of agitation speed (rpm) and HRT in anoxic and aerobic reactors for the complete removals of S^{2-}, organics and NH_4^+-N.
- Effect of hydrocarbons of diverse properties on the combined performance of anoxic-aerobic sequential moving bed reactors.
- Identification of dominant microbial species in both anoxic and aerobic reactors and examine individual culture for their degradation ability by pure culture analysis.
- Treatment of real automobile service station wastewater and study the performance of anoxic-aerobic sequential moving bed reactors.
- Study of the effect of salt (NaCl) dose/ increased salinity and
- Crude oil shock loading on the performance of the anoxic-aerobic sequential reactor system.

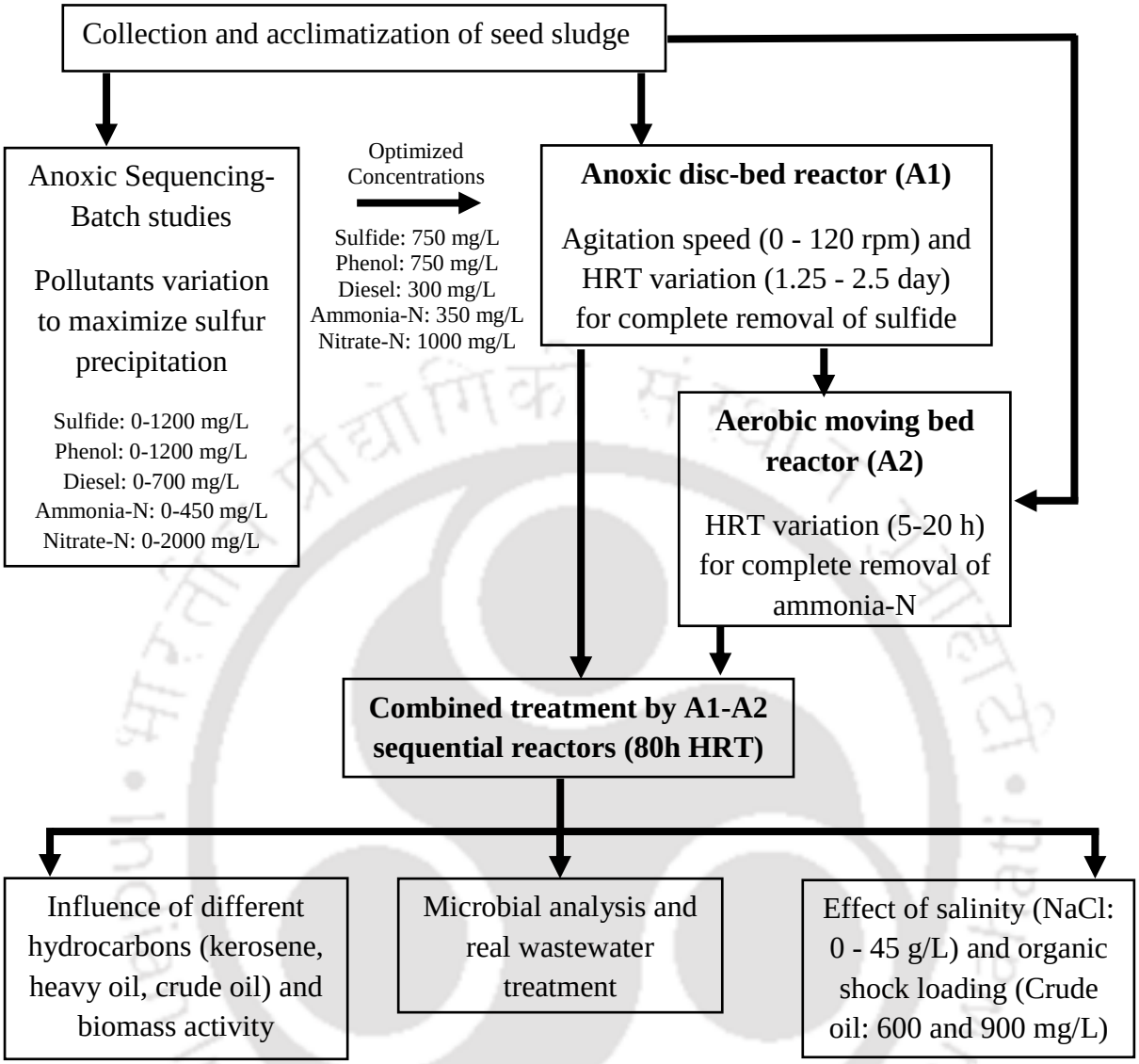

Fig. 1.12: Flow diagram of the research protocol

References

Abbas, O. K., Fang, F., Zhuo, M., Zhang, K. 2018. Integrated interrogation of causes of membrane fouling in pilot-scale anoxic-oxic membrane bioreactor treating oil refinery wastewater. Science of The Total Environment 642: 77-89.

Abbasnezhad, H., Gray, M., Foght, J. M. 2011. Influence of adhesion on aerobic biodegradation and bioremediation of liquid hydrocarbons. Applied Microbiology and Biotechnology 92(4): 653-675.

Alcantara, S., Velasco., A., Munoz, A., Cid, J., Revah, S., Razo-Flores, E. 2004. Hydrogen sulfide oxidation by a microbial consortium in a recirculation reactor system: sulfur formation under oxygen limitation and removal of phenols. Environmental Science and Technology 38: 918-923.

Alhater, H., Elqada, E., Omar, W. 2011. Pretreatment of wastewater stream from petroleum/petrochemical industries using coagulation. Advances in Chemical Engineering and Science 1: 245-251.

Alsalhy, Q. A., Almukhtar, R. S., Alani, H. A. 2016. Oil refinery wastewater treatment by using membrane bioreactor (MBR). Arabian Journal of Science and Engineering 41: 2439-2452.

Altas, L., Buyukgungor, H. 2008. Sulfide removal in petroleum refinery wastewater by chemical precipitation. Journal of Hazardous Materials 153: 462-469.

An, S., Tang, K., Nemat, M. 2010. Simultaneous bio desulphurization and denitrification using an oil reservoir microbial culture: Effects of sulphide loading rate and sulphide to nitrate loading ratio. Water Research 44(5): 1531-1541.

Aniruddhan, T. S., Ramachandran, A. 2014. Removal of 2,4,6-trichlorophenol from water and petroleum industry effluents by surfactant-modified bentonite. Journal of Water Process Engineering 1: 46-53.

Bhatti, Z. A., Mahmood, Q., Raja, I. A., Malik, A. H., Khan, M. S., Wu, D. 2011. Chemical oxidation of carwash industry wastewater as an effort to decrease water pollution. Physics and Chemistry of Earth 36: 465-469.

Biswal, B. K., Tiwari, S. N., Mukherji, S. 2009. Biodegradation of oil in oily sludges from steel mills. Bioresource Technology 100: 1700-1703.

Borghei, S. M., Hosseini, S. H. 2004. The treatment of phenolic wastewater using a moving bed biofilm reactor. Process Biochemistry 39: 1177-1181.

Canizares, P., Lobato, J., Paz, R., Rodrigo, M. A., Saez, C. 2007. Advanced oxidation processes for the treatment of olive-oil mills wastewater. Chemosphere 67: 832-838.

Canziani, R., Emondi, V., Garavaglia, M., Malpei, F., Pasinetti, E., Buttliglieri, G. 2006. Effect of oxygen concentration on biological nitrification and microbial kinetics in a cross-flow membrane bioreactor (MBR) and moving-bed biofilm reactor (MBBR) treating old landfill leachate. Journal of membrane Science 286(1-2): 202-212.

Central Pollution Control Board India 1986. The Environment (Protection) Rules. Schedule VI

Chakraborty, S., Veeramani, H. 2006. Effect of HRT and recycle ratio on removal of cyanide, phenol, thiocyanate and ammonia in an anaerobic–anoxic–aerobic continuous system. Process Biochemistry 41: 96–105.

Chan, H. 2011. Biodegradation of petroleum oil achieved by bacteria and nematodes in contaminated water. Separation and Purification Technology 80: 459-466.

Chavan, A., Mukherji, S. 2008. Treatment of hydrocarbon rich wastewater using oil degradation bacteria and phototrophic microorganisms in rotating biological contractor: Effect of N:P ratio. Journal of Hazardous Materials 154: 63-72.

Chen, C., Yan, X., Xu, Y., Yoza, B. A., Wang, X., Kou, Y., Ye, H., Wang, Q., Li, Q. X. 2019. Activated petroleum sludge biochar for efficient catalytic ozonation of refinery wastewater. Science of The Total Environment 651(2): 2631-2640.

Chen, C., Wei, L., Guo, X., Guo, S., Yan, G. 2014. Investigation of heavy oil refinery wastewater treatment by integrated ozone and activated carbon supported manganese oxides. Fuel Processing Technology 124: 165-173.

Chen, S., Sun, D., and Chung, J. 2008: Simultaneous removal of COD and ammonium from landfill leachate using an anaerobic-aerobic moving bed biofilm reactor system, Waste Management 28: 339-346.

Chuang, S. H., Ouyang, C. F. 2000. The biomass fractions of heterotrophs and phosphate-accumulating organisms in a nitrogen and phosphorus removal system. Water Research 34(8): 2283-2290.

Coelho, A., Castro, V. A., Dezotti, M., Sant'Anna Jr, G. L. 2006. Treatment of petroleum refinery wastewater by advanced oxidation processes. Journal of Hazardous Materials B137: 178-184.

Damasceno, L.H.S., Rodrigues, J.A.D., Ratusznei, S.M., Zaiat, M., Foresti, E. 2007. Effects of feeding time and organic loading in an anaerobic sequencing batch biofilm reactor (ASBBR) treating diluted whey. Journal of Environmental Management 85: 927-935.

de Lomas, J. G., Corzo, A., Gonzalez, J. M., Andrades, J. A., Iglesias, E., Montero, M. J. 2006. Nitrate promotes biological oxidation of sulfide in wastewaters: experiment at plant-scale. Biotechnology and Bioengineering 93(4): 801-811.

de Nardi, I. R., Ribeiro, R., Zaiat, M., Foresti, E. 2005. Anaerobic packed-bed reactor for bioremediation of gasoline-contaminated aquifers. Process Biochemistry 40(2): 587-592.

Diya'uddin, B. H., Daud, W. M. A. W., Aziz, A. R. A. 2011. Treatment technologies for petroleum refinery effluents: a review. Process Safety and Environmental Protection 89(2): 95-105.

Doggett, T., Rascoe, A. 2009. Global energy demand seen up 44 percent by 2030. DOI: http://www.reuters.com/articles/GCA-GreenBusiness/idUSN2719528620090527 (accessed 17.09.09)

Doltade, S. B., Dastane, G. G., Jadhav, N. L., Pandit, A. B., Pinjari, D. V., Somkuwar, N., Paswan, R. 2019. Hydrodynamic cavitation as an imperative technology for the treatment of petroleum refinery effluent. Journal of Water Process Engineering 29: 95-105.

El-Naas, M. H., Alhaija, M. A., Al-Zuhair, S. 2014. Evaluation of a three step process for the treatment of petroleum refinery wastewater. Journal of Environmental Chemical Engineering 2: 56-62.

El-Naas, M. H., Al-Zuhair, S., Alhaija, M. A. 2010. Reduction of COD in refinery wastewater through adsorption on date pit activated carbon. Journal of Hazardous Materials 173: 750-757.

El-Naas, M. H., Al-Zuhair, S., Al-Lobaney, A., Makhlouf, S. 2009. Assessment of electrocoagulation for the treatment of petroleum refinery wastewater. Journal of Environmental Management 91: 180-185.

El-Naas, M. H., Surkatti, R., Al-Zuhair, S. 2016. Petroleum refinery wastewater treatment: A pilot scale study. Journal of Water Process Engineering 14:71-76.

Fakhru'l-Razi, A., Pendashteh, A., Abdullah, L. C., Biak, D. R. Madaeni, S. S., Abidin, Z. Z. 2009. Review of technologies for oil and gas produced wastewater treatment. Journal of Hazardous Materials 170(2-3): 530-551.

Farajnezhad, H., Gharbani, P. 2012. Coagulation treatment of wastewater in petroleum industry using poly aluminum chloride and ferric chloride. International Journal of Research and Reviews in Applied Sciences 13(1): 306-310.

Fernandez, M., Ramirez, M., Perez, R. M., Gomez, J. M., Cantero, D. 2013. Hydrogen sulfide removal from biogas by an anoxic biotrickling filter packed with pall rings. Chemical Engineering Journal 225: 456-463.

Fukui, M., Harms, G., Rabus, R., Schramm, A., Widdel, F., Zengler, K., Boreham, C., Wilkes, H. 1999. Anaerobic degradation of oil hydrocarbons by sulfate-reducing and nitrate-reducing bacteria. 8th International Symposium on Microbial Ecology of Oil Fields.

Galvao, S. A. O., Mota, A. L. N., Silva, D. N., Moraes, J. E. F., Nascimento, C. A. O., Chiavone-Filho, O. 2006. Application of the photo-Fenton process to the treatment of wastewaters contaminated with diesel. Science of The Total Environment 367 (1): 42-49.

Ganiyu, S. O., dos Santos, E. V., de Araujo Costa, E. C. T., Martinez-Huitle, C. A. 2018. Electrochemical advanced oxidation processes (EAOPs) as alternative treatment techniques for carwash wastewater reclamation. Chemosphere 211: 998-1006.

Gasim, H. A., Kutty, S. R. M., Isa, M. P. M. 2012. Treatment of petroleum refinery wastewater by using UASB reactors. International Journal of Chemical and Biological Engineering 6: 174-177.

Ghorbanian, M., Moussavi, G., Farzadkia, M. 2014. Investigating the performance of an up-flow anoxic fixed-bed bioreactor and a sequencing anoxic batch reactor for the biodegradation of hydrocarbons in petroleum-contaminated saline water. International Biodeterioration and Biodegradation 90: 106-114.

Gonder, Z. B., Bacioglu, G., Vergili, I., Kaya, Y. 2017. Electrochemical treatment of carwash wastewater using Fe and Al electrode: Techno-economic analysis and sludge characterization. Journal of Environmental Management 200: 380-390.

Grabinska-Loniewska, A. 1991. Denitrification unit biocenosis. Water Research 25: 1565– 73.

Hariz, I. B., Halleb, A., Adhoum, N., Monser, L. 2013. Treatment of petroleum refinery sulfidic spent caustic wastes by electrocoagulation. Separation and Purification Technology 107: 150-157.

Harwood C. S., Parales R. E. 1996. The β-ketoadipate pathway and the biology of self-identity. Annual Review of Microbiology 50: 553–590.

Hasan, D. B., Aziz, A. R. A., Daud, W. M. A. W. 2012. Oxidative mineralization of petroleum refinery effluent using Fenton-like process. Chemical Engineering Research and Design 90: 298-307.

Ishaq, S., Malakahmad, A., Isa, M. H. 2012. Refinery wastewater biological treatment: A short review. Journal of Scientific and Industrial Research 71: 251-256.

Janssen, A. J. H., Sleyster, R., Van der kaa, C., Jochemsen, A., Bontsema, J., Lettinga, G. 1995. Biological sulfide oxidation in a fed-batch reactor. Biotechnology and Bioengineering 47: 327-333.

Jeswani, H., Mukherji, S. 2012. Degradation of phenolics, nitrogen-heterocyclics and polynuclear aromatic hydrocarbonsin a rotating biological contractor. Bioresource Technology 111: 12-20.

Ji, G. D., Sun, T. H., Ni, J. R., Tong, J. J. 2009. Anaerobic baffled reactor (ABR) for treating heavy oil produced water with high concentrations of salt and poor nutrient. Bioresource Technology 100: 1108-1114.

Jing, C., Ping, Z., Mahmood, Q. 2010. influence of various nitrogenous electron acceptors on the anaerobic sulfide oxidation. Bioresource Technology 101: 2931-2937.

Jou, C. G., Huang, G. C. 2003. A pilot study for oil refinery wastewater treatment using a fixed film bioreactor. Advances in Environmental Research 7: 463-469.

Keramati, M., Ayati, B. 2019. Petroleum wastewater treatment using a combination of electrocoagulation and photocatalytic process with immobilized ZnO nanoparticles on concrete surface. Process Safety and Environmental Protection 126: 356-365.

Kargi, F. 1996. Biological treatment of high strength wastewater by fed batch operation. Bioprocess and Biosystems Engineering 16: 35-38.

Khaing, T. H., Li, J., Li, Y., Wai, N., Wong, F. 2010. Feasibility study on petrochemical wastewater treatment and reuse using a novel submerged membrane distillation bioreactor. Separation and Purification Technology 74: 1738-1746.

Kim, Y. M., Park, D., Jeon, C., Lee, D. S., Park, J. M. 2008. Effect of HRT on the biological pre-denitrification process for the simultaneous removal of toxic pollutants from cokes wastewater. Bioresource Technology 99: 8824-8832.

Krishnakumar, B., Majumdar, S., Manilal, V.B., Haridas, A. 2005. Treatment of sulfide containing wastewater with sulfur recovery in a novel reverse fluidized loop reactor (RFLR). Water Research 39: 639-647.

Kuenen, J. G., Lesley, A., Robertson, A., Gemerden, H. V. 1975. Microbian interactions among aerobic and anaerobic sulfur oxidizing bacteria. TU Delft Institutional Repository.

Lack, A., Fuchs, G. 1992. Carboxylation of phenylphosphate by phenol carboxylase, an enzyme system of anaerobic phenol metabolism. Journal of Bacteriology 174(11): 3629-3636.

Le-Clech, P., Chen, V., Fane, T. A. G. 2006. Fouling in membrane bioreactors used in wastewater treatment. Journal of Membrane Science 284(1-2): 17-53.

Lei, C. N., Whang, L. M., Chen, P. C. 2010. Biological treatment of thin-film transistor liquid crystal display (TFT-LCD) wastewater using aerobic and anoxic/oxic sequencing batch reactors. Chemosphere 81: 57-64.

Li, J., Sun, S., Yan, P., Fang, L., Yu, Y., Xiang, Y., Wang, D., Gong, Y., Gong, Y., Zhang, Z. 2017. Microbial communities in the functional areas of a biofilm reactor with anaerobic-aerobic process for oily wastewater treatment. Bioresource Technology 238: 7-15.

Li, Y. M., Gu, G. W., Zhao, J. F., Yu, H. Q., Qiu, Y. L., Peng, Y. Z. 2003. Treatment of coke-plant wastewater by biofilm systems for removal of organic compounds and nitrogen. Chemosphere 52: 997-1005.

Liu, G. H., Ye, Z., Tong, K., Zhang, Y. H. 2013. Biotreatment of heavy oil wastewater by combined upflow anaerobic sludge blanket and immobilized biological aerated filter in a pilot-scale test. Biochemical Engineering Journal 72: 48-53.

Liu, Y. Q., Tay, J. H., Ivanou, V., Moy, B. Y. P., Yu, L., Tay, S. T. L. 2005. Influence of phenol on nitrification by microbial granules. Process Biochemistry 40: 3285–3289.

Lu, M., Gu, L. P., Xu, W. H. 2013. Treatment of petroleum refinery wastewater using a sequential anaerobic–aerobic moving-bed biofilm reactor system based on suspended ceramsite. Water Science and Technology 67(9): 1976-1983.

Ma, F., Guo, J. B., Zhao, L., Chang, C., Cui, D. 2009. Application of bioaugmentation to improve the activated sludge system into the contact oxidation system treating petrochemical wastewater. Bioresource Technology 100: 597-602.

Macarie, H., Noypla, A., Guyot, J. P. 1992. Anaerobic treatment of a petrochemical wastewater from a terephthalic acid plant. Water Science and Technology 25(7): 223-235.

Mahmood, Q., Zheng, P., Cai, J., Wu, D. L., Hu, B. L., Li, J. Y. 2007. Anoxic sulphide biooxidation using nitrite as electron acceptor. Journal of Hazardous Materials 147: 249-256.

Mahmood, Q., Zheng, P., Hayat, Y., Islam, E., Wu, D., Ren-Cun, J. 2008. Effect of pH on anoxic sulfide oxidizing reactor performance. Bioresource Technology 99: 3291-3296.

Mahmoudkhani, R., Azar, A. M., Dehghani, A., Ghoreishi, H. 2012. Treatment of contaminated waters with petroleum by moving bed biofilm reactor (MBBR). 2012 International Conference on Life Science and Engineering IPCBEE 45, Singapore.

Manconi, L., Carucci, A., Lens, P., Rossetti, S. 2006. Simultaneous biological removal of sulfide and nitrate by autotrophic denitrification in an activated sludge system. Water Science and Technology 53: 91-99.

Mannina, G., Cosenza, A., Di Trapani, D., Laudicina, V. A., Morici, C., Odegaard, H. 2016. Nitrous oxide emissions in a membrane bioreactor treating saline wastewater contaminated by hydrocarbons. Bioresource Technology 219: 289-297.

Mazzeo, D. E. C., Levy, C. E., de Angelis, D. F., Molares, M. A. M. 2010. BTEX biodegradation by bacteria from effluents of petroleum refinery. Science of The Total Environment 408: 4334-4340.

Mizzouri, N. S., Shaaban, M. G. 2013. Individual and combined effects of organic, toxic and hydraulic shock loads on sequenting batch reactor in treating petroleum refinery wastewater. Journal of Hazardous Materials 250-251: 333-344.

Mizzouri, N. S., Shaaban, M. G. 2013. Kinetic and hydrodynamic assessment of an aerobic purification system for petroleum refinery wastewater treatment in a continuous regime. International Biodeterioration and Biodegradation 83: 1-9.

Mohanakrishna, G., Al-Raoush, R. I., Abu-Reesh, I. M., Aljaml, K. 2019. Removal of petroleum hydrocarbons and sulfates from produced water using different bioelectrochemical reactor configurations. Science of The Total Environment 665: 820-827.

Mohanty, G., Mukherji, S. 2008. Biodegradation rate of diesel range n-alkanes by bacterial cultures Exiguobacterium aurantiacum and Burkholderia cepacia. International Biodeterioration and Biodegradation 61: 240-250.

Montabello, A. M., Fernandez, M., Almemglo, F., Ramirez, M., Cantero, D., Baeza, M., Gabriel, D. 2012. Simultaneous methylmercptan and hydrogen sulfide removal in the desulfurization of biogas in aerobic and anoxic biotrickling filters. Chemical Engineering Journal 200-202: 237-246.

Moreno, C., Farahbakhshazad, N., Morrison, G. M. 2002. Ammonia removal from oil refinery effluent in vertical upflow macrophyte column systems. Water, Air and Soil Pollution 135 (1-4): 237-247.

Mosquera-Corral, A., Campos, J. L., Sanchez, M., Mendez, R., Lema J. M. 2003. Combined system for biological removal of nitrogen and carbon from a fish cannery wastewater. Journal of Environmental Engineering-ASCE. 129 (9): 826-83.

Moussavi, G., Ghorbanian, M. 2015. The biodegradation of petroleum hydrocarbons in an upflow sludge blanket/fixed film hybrid bioreactor under nitrate-reducing conditions: Performance evaluation and microbial identification. Chemical Engineering Journal 280: 121-131.

Moussavi, G., Shekoohiyan, S., Naddafi, K. 2016. Anoxic biodegradation of petroleum hydrocarbons in saline media using denitrifier biogranules. Ecotoxicology and Environment Safety 129: 51-56.

Mukherji, S. Jagadevan, S., Mohapatra, G. Vijay, A. 2004. Biodegradation of diesel oil by an arabean sea sediment culture isolated from the vicinity of an oil field. Bioresource Technology 95: 281-286.

Mukherji, S., Chavan, A. 2012. Treatment of aqueous effluents containing non-aqueous phase liquids in rotating biological contractor with algal bacterial biofilm. Chemical Engineering Journal 200-202: 459-470.

Munoz, R., Souza, T. S. O., Glittmann, L., Perez, R., Quijano, G. 2013. Biological anoxic treatment of O_2 free VOC emissions from the petrochemical industry. Journal of Hazardous Materials 260: 442-450.

Nasirpour, N., Mousavi, S. M., Shojaosadati, S. A. 2015. Biodegradation potential of hydrocarbons in petroleum refinery effluents using a continuous anaerobic-aerobic hybrid system. Korean Journal of Chemical Engineering 32(5): 874-881.

Nguyen, V. T., Shieh, W. K. 1995. Anoxic and oxic biological fluidized bed treatment of amines and phenol. Water Science and Technology 31: 185-193.

Ochieng, A., Odiyo, J. O., Mustago, M. 2003. Biological treatment of mixed industrial wastewaters in a fluidised bed reactor. Journal of Hazardous Materials B96: 79-90.

Padhi, S. K., Gokhale, S. 2016. Benzene control from waste gas streams with a sponge-medium based rotating biological contactor. International Biodeterioration and Biodegradation 109: 96-103.

Pajoumshariati, S., Zare, N., Bonakdarpour, B. 2017. Considering membrane sequencing batch reactors for the biological treatment of petroleum refinery wastewaters. Journal of Membrane Science 523: 542-550.

Parilti, N. B., Akten, D. 2011. Response surface methodological approach and the kinetic study for the assessment of the photodegradation of pulp mill effluent with H_2O_2/Fe(III)/solar UV. Fresenium Environmental Bulletin 20: 1301-1400.

Plohl, K., Leskovsek, H., Bricelj, M. 2002. Biological degradation of motor oil in water. Acta Chimica Slovenica 49: 279-289.

Ramos, C., Suarez-Ojeda, M. E., Carrera, J. 2016. Denitrification in anoxic granular reactor using phenol as sole organics carbon source. Chemical Engineering Journal 288: 289-297.

Rasheed, Q. J., Pandian, K., Muthukumar, K. 2011. Treatment of petroleum refinery wastewater by ultrasound-dispersed nanoscale zero-valent iron particles. Ultrasonics Sonochemistry 18: 1138-1142.

Razavi, S. M. R., Miri, T. 2015. A real petroleum refinery wastewater treatment using hollow fiber membrane bioreactor (HF-MBR). Journal of Water Process Engineering 8: 136-141.

Renault, F., Sancey, B., Badot, P. M., Crini, G. 2009. Chitosan for coagulation/flocculation processes- An ecofriendly approach. European Polymer Journal 45(5): 1337-1348.

Roosta, A., Jahanmiri, A., Mowla, D., Niazi, A. 2011. Mathematical modeling of biological sulfide removal in a fed batch bioreactor. Biochemical Engineering Journal 58-59: 50-56.

Saghafi, S., Bakhshi, Z., Najafpour, G., Kariminezhad, E. 2010. Biodegradation of toluene and xylene in an UAPB bioreactor with fixed film of *Pseudomonas putida*. American-Eurasian Journal of Agriculture & Environment Science 9(1): 801-807.

Sahariah, B. P., Chakraborty, S. 2013. Performance of anaerobic-anoxic-aerobic batch fed moving-bed reactor at varying phenol feed concentrations and hydraulic retention time. Clean Technology and Environmental Policy 15: 225-233.

Sahariah, B. P., Kumar, J. A., Chakraborty, S. 2016. Treatment of coke oven wastewater in an anaerobic-anoxic-aerobic moving bed bioreactor system. Desalination and Water Treatment 57(31): 14396-14402.

Sahinkaya, E., Dilek, F.B. 2007. Effect of feeding time on the performance of a sequenting batch reactor treating a mixture of 4-CP and 2, 4-DCP. Journal of Environmental Management 83: 427-436.

Saien, J., Nejati, H. 2007. Enhanced photocatalytic degradation of pollutants in petroleum refinery wastewater under mild conditions. Journal of Hazardous Materials 148: 491-495.

Sanchez, A.G., Revah, S. 2009. Biological sulfide removal under alkaline and aerobic conditions in a packed recycling reactor. Water Science and Technology 59(7): 1415-1421.

Santo, C. E., Vilar, V. J. P., Botelho, C. M. S., Bhatnagar, A., Kumar, E., Boaventura, R. A. R. 2012. Optimization of coagulation-flocculation and floatation parameters for the treatment of a petroleum refinery effluent from a Portuguese plant. Chemical Engineering Journal 183: 117-123.

Sarfaraz S., Thomas S., Tewari U.K, Iyengar L. 2004: Anoxic treatment of phenolic wastewater in sequencing batch reactor. Water Research 38: 965–971.

Schie, P. M. V., Young, L. Y. 2007. Biodegradation of phenol: Mechanisms and applications. Bioremediation Journal 1: 1-18

Shahrezai, F., Mansouri,Y., Zinatizedah, A. K. L., Akhbari, A. 2012. Process modeling and kinetic evaluation of petroleum refinery wastewater treatment in a photocatalytic reactor using TiO_2 nanoparticles. Power Technology 221: 203-212.

Sharma, A., Kumar, P., Rehman, M. B. 2014. Biodegradation of diesel hydrocarbon in soil by bioaugmentation of Pseudomonas aeruginosa: A laboratory scale study. International Journal of Environmental Bioremediation and Biodegradation 2(4): 202-212.

Sherry, A., Gray, N. D., Ditchfield, A. K., Aitken, C. M., Jones, D. M., Roling, W. F. M., Hallman, C., Larter, S. R., Bowler, B. F. J., Head, I. M. 2012. Anaerobic biodegradation of crude oil under sulfate reducing conditions leads to only modest enrichment of recognized sulfate-reducing taxa. International Biodeterioration and Biodegradation 81: 105-113.

Sonwani, R. K., Swain, G., Giri, B. S., Singh, R. S., Rai, B. N. 2019. A novel comparative study of modified carriers in moving bed biofilm reactor for the treatment of wastewater: Process optimization and kinetic study. Bioresourse Technology 281: 335-342.

Sun, G., Wan, J., Sun, Y., Li, H., Chang, C., Wang, Y. 2019. Enhanced removal of nitrate and refractory organic pollutants from bio-treated coking wastewater using corncorbs as carbon sources and biofilm carriers. Chemosphere (In press)

Technical EIA guidance manual for petroleum refining industry 2010. The Ministry of Environment and Forests, Government of India

The Ministry of Environment and Forests Notification 2008. Environment (Protection) Amendment Rules.

Thakur, C., Srivastava, V. C., Mall, I. D. 2014. Aerobic degradation of petroleum refinery wastewater in sequential batch reactor. Journal of Environmental Science and Health Part A 49(12): 1436-1444.

Tian, H., Hu, Y., Xu, X., Hui, M., Hu, Y., Qi, W., Xu, H., Li, B. 2019. Enhanced wastewater treatment with high *o*-aminophenol concentration by two-stage MABR and its biodegradation mechanism. Bioresource Technology 289: 121649.

Todorovic, V. 2003. Acute phenol poisoning. Medicinski Pregled 56: 37-41.

Tong, K., Zhang, Y., Liu, G., Ye, Z., Chu, P. K. 2013. Treatment of heavy oil wastewater by a conventional activated sludge process coupled with an immobilized biological filter. International Biodeteriration and Biodegradation 84: 65-71.

Townsend, G. T., Prince, R. C., Suflita, J. M. 2003. Anaerobic oxidation of crude oil hydrocarbonsby the resistent microorganisms of a contaminated anoxic aquifer. Environmental Science and Technology 37: 5213-5218.

Tyagi, R. D., Tran, F. T., Chowdhury, A. K. M. M. 1993. A pilot study of biodegradation of petroleum refinery wastewater in a polyurethane attached RBC. Process Biochemistry 28, 75-82.

US EPA 1985. Ambient Water Quality Criteria for Ammonia, (EPA 440/5-85-001)

US EPA 1985. Petroleum Refining Effluent Guidelines (40-CFR, Part 419)

Vaiopoulou, E., Melidis, P., Aivasidis, A. 2005. Sulfide removal in wastewater from petrochemical industries by autotrophic denitrification. Water Research 39: 4101-4109.

Vajrani, S. J., Upasani, V. N. 2017. A new look on factors affecting microbial degradation of petroleum hydrocarbon pollutants. International Biodeterioration and Biodegradation 120: 71-83.

Vendramel, S., Bassin, J. P., Dezotti, M., Sant'Anna, G. L. jr. 2015. Treatment of petroleum refinery wastewater containing heavily polluting substances in an aerobic submerged fixed-bed reactor. Environmental Technology 36 (16): 2052-2059.

Viero, A. F., de Melo, T. M., Torres, A. P. R., Ferreira, N. R., Sant'Anna, G. L. jr., Borges, C. P., Santiago, V. M. J. 2008. The effects of long term feeding of high organic loading in a submerged membrane bioreactor treating oil refinery wastewater. Journal of Membrane Science 319: 223-230.

Wang, S., Ghimire, N., Xin, G., Janka, E., Bakke, R. 2017. Efficient high strength petrochemical wastewater treatment in a hybrid vertical anaerobic biofilm (HyVAB) reactor: A pilot study. Water Practice Technology 12: 501-513.

Wang, Y., Wang, Q., Li, M., Yang, Y., He, W., Yan, G., Guo, S. 2016. An alternative anaerobic treatment process for treatment of heavy oil refinery wastewater containing polar organics. Biochemical Engineering Journal 105: 44-51.

Wei, L., Guo, S., Yan, G., Chen, C., Jiang, X. 2010. Electrochemical pre-treatment of heavy oil refinery wastewater using a three-dimensional electrode reactor. Electrochimica Acta 55: 8615-8620.

Wenyu, X., Jianjun, C., Huawen, Z., Dehao, L., 2011. Treatment of alkaline wastewater from oil refinery using circulating biological aerated filter. International Conference on Distributed Control Intell. Environmental Monitoring, 2360-2365.

Xianling, L., Jianping, W., Qing, Y., Xueming, Z. 2005. The pilot study for oil refinery wastewater treatment using a gas-liquid-solid three-phase flow airlift loop bioreactor. Biochemical Engineering Journal 27: 40-44.

Xinhua, X., Xiangfeng, Z. 2004. Treatment of refectory oily wastewater by electro coagulation process. Chemosphere 56: 889-894.

Zadelius, J., Rabus, R., Grundmann, O., Werner, I., Brodkorb, D., Schreiber, F., Ehrenreich, P., Behrends, A., Wilkes, H., Kube, M., Reinhardt, R., Widdel, F. 2011. Alkane degradation under anoxic conditions by a nitrate-reducing bacterium with possible involvement of the electron acceptor in substrate activation. Environmental Microbiology Reports 3(1): 125-135.

Zhang, M., Tay, J. H., Qian, Y., Gu, X. S. 1998. Coke plant wastewater treatment by fixed biofilm system for COD and NH_3-N removal. Water Research 32: 519–27.

Zhao, J., Tian, W., Liu, S., Wang, Z., Du, Z., Xie, W. 2019. Existence, removal and transformation of parent and nitrated polycyclic aromatic hydrocarbons in two biological wastewater treatment processes. Chemosphere 224: 527-537.

Zheng, T. 2016. A compact process for treating oilfield wastewater by combining hydrolysis acidification, moving bed biofilm, ozonation and biologically activated carbon techniques. Environmental Technology 37(9): 1171-1178.

Zica, Z. 2017. Pairing of anaerobic and aerobic treatment of petroleum wastewater. All graduate thesis and Dissertations 6832. https://digitalcommons.usu.edu/etd/6832

Zou, X. L. 2015. Treatment of heavy oil wastewater by UASB-BAfs using the combination of yeast and bacteria. Environmental technology 36: 2381-2389.

2

CHAPTER

OPTIMIZATION OF MAXIMUM SULFUR (S^0) GENERATION IN ANOXIC FED-BATCH REACTORS

CHAPTER 2

OPTIMIZATION OF MAXIMUM SULFUR (S^0) GENERATION IN ANOXIC SEQUENCING-BATCH REACTORS

2.1 INTRODUCTION

Dilute alkali solution is used to capture H_2S from gas streams and hydrocarbons in petroleum refining industries. This process generates wastewater known as spent sulfidic caustic having high alkaline pH and large amount of S^{2-} (2-3% by weight) along with phenol, NH_4^+-N and several hydrocarbons (Hariz et al. 2013). Phenol, hydrocarbon and S^{2-} compounds are toxic and carcinogenic in nature (Graaff et al. 2011). Physicochemical processes like advanced oxidation, wet air oxidation are expensive due to high cost of chemicals and equipment. Electrocoagulation and membrane processes are restricted due to large amount of sludge generation and fouling of membranes (Diya'uddeen et al. 2011).

Biological treatment of spent caustic is reported in a five-stage bardenpho process at 8h HRT (Park et al., 2009). Simultaneous removals of S^{2-} and hydrocarbons in anoxic reactor is beneficial to handle sulfidic wastewater as abiotic loss is prevented. Liu et al. (2016a) used granular sludge bed reactor to treat phenol, S^{2-} and NO_3^- at 8h HRT. Cardoso et al. (2006) treated S^{2-}, acetate and NO_3^- in a UASB reactor at 24h HRT. However, discussion about the intermediate sulfur compounds during biodegradation is absent in the literature reports. Oxidation of S^{2-} in denitrifying condition occurs with the formation of S^0 in the first step (Eq. 1.10) and further oxidation to SO_4^{2-} in the second step (Eq. 1.11) (An et al., 2010). Formation of S^0 and SO_4^{2-} from the oxidation of S^{2-} depends upon the availability of NO_3^--N as electron acceptor. Oxidation tends towards the formation of SO_4^{2-} with more available NO_3^--N by generating intermediate $S_2O_3^{2-}$. Excessive SO_4^{2-} production is counterproductive. Hence, removal of S^{2-} through precipitation by biological conversion into S^0 can be prudent.

The prime objective of the current chapter was to maximize the formation of biological sulfur (S^0) by varying different concentrations of sulfide, hydrocarbons and nitrogen in anoxic fed-batch reactors. In addition, performance of the reactors was also evaluated in terms of pollutants degradation efficiency/rate.

2.2 MATERIALS AND METHODS

2.2.1 Chemicals and Reagents

Chemicals and reagents used in this work were either analytical grade (AR) or laboratory grade (LR). Phenol, potassium nitrate, ammonium chloride were purchased from Merck, India and sodium sulfide used in the feed was purchased from HiMedia. Dipotassium hydrogen phosphate and potassium dihydrogen phosphate used in phosphate buffer were purchased from Merck, India. $MgSO_4.7H_2O$, $CaCl_2.2H_2O$, $FeCl_3.6H_2O$, $CuCl_2$, $ZnCl_2$, $NiCl_2.6H_2O$ and $CoCl_2$ used for trace metal solution were procured from Merck, India. Yeast extract was purchased from CDH, India. Diesel was procured at the local Indian Oil petrol station.

Sodium nitrite, 4-aminoantipyrene, potassium ferricynate, ammonium hydroxide, sodium hypochlorite, tri-sodium citrate, sodium nitroprusside, ethanol, potassium dichromate, ferrous ammonium sulfate, mercuric sulfate, silver sulfate, anhydrous sodium sulfate, sodium thiosulfate, iodine, sodium hydroxide were of analytical grade and purchased either from Merck, India or CDH, India. Hydrochloric acid, sulfuric acid, nitric acid and n-hexane were bought from Merck, India. All the stock solutions were prepared by milli-Q water (Merck Millipore, USA, pH 7.0 ± 0.1).

2.2.2 Experimental set up and reactor operation

Eight reactors were fabricated using glass aspirator bottles (R1 to R8) with working volume of 5L and were operated in fed-batch mode. The top and bottom openings were closed with stopper cock with arrangements for adding feed and collection of gas. Polyurethane foam (PUF) sheets were bought from nearby shop and cut into cubes of 1cm × 1cm × 1cm dimension. The cubes were cleaned with Millipore water (pH 5.8 ± 0.2) and kept at 70 °C in a hot air oven (ICT, India) overnight for drying. The dried cubes were used as support for microbial growth. Sponge cubes had porosity 0.81, density 0.039 g/cm^3 and specific surface area 600 m^2/m^3 (Sahariah and Chakraborty, 2011). Fortuny et al. (2008) have used open pore PUF of specific surface area 600 m^2/m^3 in trickling filter. The total weight of the virgin biomass support was 60g in each reactor. Feed to the reactors was provided by a peristaltic pump (Miclins, PP 20x) through a feeding port 3 cm above from the bottom at 100 mL/min. Intermediate manual mixing was provided to the reactors every two hours for proper mixing of diesel and biomass along with release of trapped gas. Gas was collected by water displacement method connected to the top port of the reactors. Temperature of the reactors was maintained by a hot air blower (Bajaj, India) at 27 ± 3 ºC. Temperature was measured by digital thermometer (Fisher

Scientific, USA). Schematic diagram of the reactors and operating conditions are illustrated in Fig. 2.1 and summarized in Table 2.1, respectively. Efficiency of the reactors was determined by hydraulic retention time (HRT, day), loading rate [g/(m^3.d)], removal (%) and removal rate [g/(m^3.d)] which were calculated by equations (2.1), (2.2), (2.3) and (2.4), respectively.

$$\text{HRT (day)} = \frac{\text{Reactor volume (L)}}{(\text{Volume decanted per cycle,L}) \times (\text{No.of cycles per day})} \quad \ldots (2.1)$$

$$\text{Loading rate} = \frac{S_0}{\text{HRT}} \quad \ldots (2.2)$$

$$\text{Removal (\%)} = \frac{(S_0 - S_e) \times 100}{S_0} \quad \ldots (2.3)$$

$$\text{Removal rate} = \frac{S_0 - S_e}{\text{HRT}} \quad \ldots (2.4)$$

where,

S_0 = Influent concentration (mg/L); S_e = Effluent concentration (mg/L).

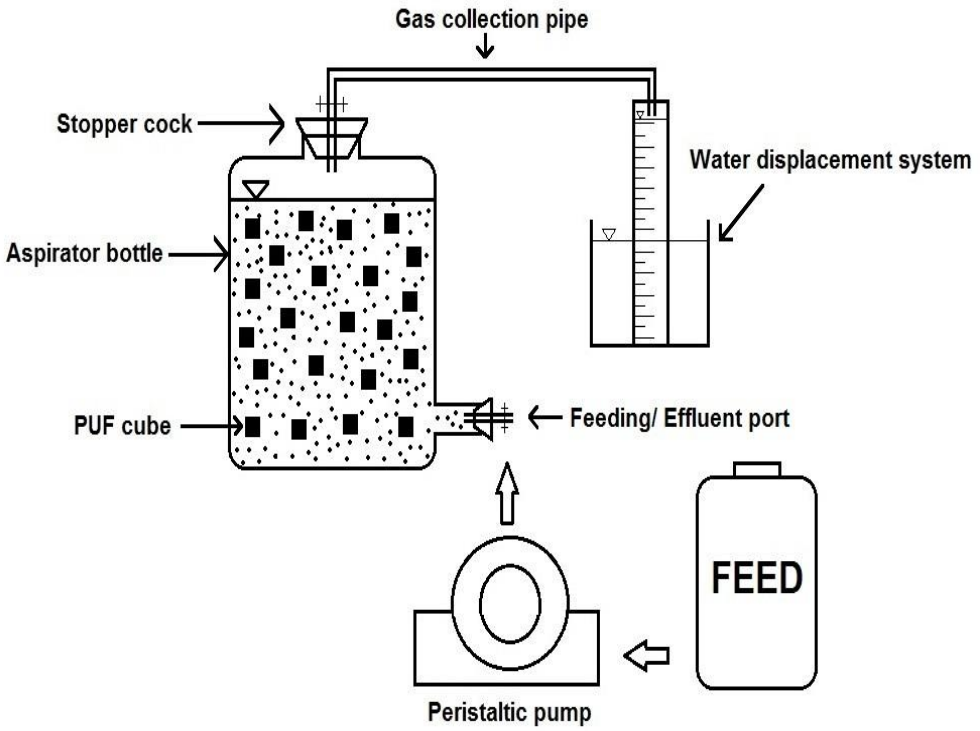

Fig. 2.1: Schematic diagram of the anoxic fed-batch reactors

Table 2.1: Operational conditions of anoxic fed-batch reactors at varied pollutants feed

Study	Conc. Range (mg/L)	Period (day)	Decant volume (L)	HRT (d)	Fill time (min)	Settle time (min)	Decant time (min)	React time (min)	Cycle time (h)
Acclimatization	-	0-145	4	1.25	40	20	15	1365	24
S^{2-} variation	0-1200	146-220							
Phenol variation	0-1200	221-290							
Diesel variation	0-700	291-360							
NH_4^+-N variation	0-450	361-430							
NO_3^--N variation	0-2000	431-500							

Concentration of any particular pollutant was varied at eight levels in eight reactors, while concentration of other pollutants were kept constant. Once a concentration variation study got over, reactors were gradually brought to the conditions for the next concentration variation study, which consumed a change over time of 7-10 days. After each change over, transient period of 10-15 days was observed and steady state of the reactors was confirmed by consistency of effluent quality. Steady state data was collected for 15 days and average was considered to analyze the performance of each reactor.

2.2.3 Seed Sludge

Biomass was collected from the anaerobic storage tank of Indian Oil Corporation Limited (IOCL), Noonmati, Assam, India and was used as inoculum for the anoxic fed-batch reactors. Three-litre sludge was used as bacterial biomass and remaining volume (2L) was filled with synthetic feed. Total solids and volatile solids of the sludge samples were measured by ignition method as per APHA (2005) and found to be 7.5 ± 0.2 g/L and 5.0 ± 0.2 g/L, respectively.

2.2.4 Synthetic feed

Feed was prepared by adding required amounts of phenol (as C_6H_5OH), S^{2-} (as $Na_2S.xH_2O$), diesel, NH_4^+-N (as NH_4Cl) and NO_3^--N (as KNO_3) in tap water (pH 8.0 ± 0.1). Characteristics of tap water is enlisted in Appendix A. Elimination of dissolved oxygen (DO) was done by purging the feed (without S^{2-} and diesel) by nitrogen gas (N_2). Required S^{2-} and diesel were added later to avoid abiotic loss by purging. Synthetic feed also contained phosphate buffer (1 mL/L), yeast extract (10 mg/L) and trace metal solutions (1 mL/L) as

nutrients. Phosphate buffer contained KH_2PO_4 (72.3 g/L) and K_2HPO_4 (104.5 g/L) and had initial pH 6.8, which acted as source of phosphorous to the microorganisms. Stock trace metal solution was comprised of the following: $MgSO_4.7H_2O$: 10,000 mg/L, $CaCl_2.2H_2O$: 10,000 mg/L, $FeCl_3.6H_2O$: 5,000 mg/L, $CuCl_2$: 1000 mg/L, $ZnCl_2$: 1000 mg/L, $NiCl_2.6H_2O$: 500 mg/L, $CoCl_2$: 500 mg/L (Chakraborty and Veeramani, 2006).

2.2.5 Properties of diesel

Density of diesel was determined by weighing 50 mL of the sample in a dry specimen tube and dividing the weight to the volume and obtained to be 800 kg/m^3. Absolute/dynamic viscosity ($m^2.s^{-1}$) of diesel was measured by U-Tube viscometer/glass capillary viscometer (JSGW, India) at room temperature (27 ± 3 ºC).

2.2.6 Analysis of wastewater parameters

Collected samples were centrifuged at 8500 rpm for by a research centrifuge (REMI CM-8 Plus, India) for 5 minutes prior to any analysis. pH was measured by a digital pH meter (Systronics, India) with 0.01 sensitivity and temperature correction facility. pH meter was calibrated using standard buffer solutions (pH 4.0, 7.0 and 9.2) periodically. Conductivity, salinity and total dissolved solids were measured by Microprocessor COND-TDS-SAL meter (Labtronics, India) with 0.01 sensitivity. Salinity meter was calibrated using 0.1N KCl solution at room temperature before any measurement was done. A digital thermometer (Fisher Scientific, USA) measured temperature.

Measurement of phenol was done by colorimetric method by using 4-aminoantipyrene and potassium ferricyanide and measuring absorbance at 500 nm (APHA, 2005). Ammonia-N (NH_4^+-N) was measured by phenate method by using sodium nitroprusside and sodium hypochlorite and absorbance was measured at 640 nm (APHA, 2005). Standard calibration curves were prepared for both phenol and NH_4^+-N, are illustrated in Appendix B. Sulfide (S^{2-}) was measured by iodometric method by precipitating S^{2-} as ZnS by zinc acetate solution, starch solution as indicator and titration by sodium thiosulfate (APHA, 2005).

Concentrations of NO_3^--N, NO_2^--N and SO_4^{2-} were determined through ion chromatography (Metrohm Basic IC) with an ion suppressor column (Metrosep A Supp 5-250/4.0). Mobile phase for the analysis consisted of 3.2 mM of sodium carbonate, 1 mM of sodium bicarbonate and 50 mM sufuric acid (APHA, 2005). Linear calibration curves were plotted for each of the anion by putting different concentrations (0, 1, 5 and 10 mg/L) in X-axis

and peak area of chromatogram in Y-axis (Appendix B). Concentrations in the samples were determined from the peak area of the generated chromatogram and standard calibration curve.

For the analysis of thiosulfate ($S_2O_3^{2-}$), the S^{2-} in the samples was precipitated by the addition of four drops of 1M zinc acetate solution. The solution was filtered and used as a titrant for titrating standard iodine solution using starch indicator as per APHA (2005). Standard iodine was prepared by drawing 10 mL each of potassium dichromate solution of known normality, 10% potassium iodide and 1M H_2SO_4 into a glass bottle and kept in dark for 5 minutes in closed condition for reaction to occur. The normality (molarity) of thiosulfate was measured as follows,

$$N_P \times V_P = N_T \times V_T \quad \ldots (2.5)$$

where,

N_P = normality of potassium dichromate, V_P = volume of potassium dichromate (mL), N_T = normality of sodium thiosulfate, V_T = volume of thiosulfate (mL)

Diesel was measured as total hydrocarbon (TH) by partition gravimetric method (APHA, 2005). Samples were first centrifuged at 8500 rpm for 5 minutes and supernatant was acidified with 1:1 HCl (5 mL/L of sample) to pH 2 with proper mixing to disperse the diesel equivalently. Ten millilitres of the acidified sample was then subjected to be extracted with 30 mL n-hexane in a separating funnel and shaken vigorously for 2 min. The funnel was kept unmoved for the separation of distinct aqueous and n-hexane layers. The aqueous layer was carefully separated and extracted again with the procedure mentioned above. Then the n-hexane (which dissolved hydrocarbons) was filtered through anhydrous sodium sulfate to eliminate moisture and collected in a distillation flask. To determine the total hydrocarbon (TH: phenol + diesel), the solution was transferred to a closed container and mixed with silica gel (3 g/100 mg of diesel) for 5 minutes by a magnetic stirrer to absorb the polar compounds. The remaining solution was filtered with Whatman 42 filter paper pre-moistened with n-hexane. n-hexane was evaporated at 85 ºC and total hydrocarbon (TH) was estimated by the following equation,

$$TH\left(\frac{g}{L}\right) = \frac{W_{Total} - W_{Empty}}{V_s} \quad \ldots (2.6)$$

where,

W_{Total} = total weight of the distillation flask and residue (g), W_{Empty} = Empty weight of the distillation flask (g), V_s = volume of the sample (L)

Chemical oxygen demand (COD) was analyzed by closed reflux titrimetric method mentioned by APHA (2005) with a slight modification. As diesel/oil is insoluble in water, 2h of digestion time was not sufficient for oxidation of diesel completely by $K_2Cr_2O_7$ (Chavan and Mukherji, 2008). Therefore, different concentrations of diesel (100, 200 and 300 mg/L) were digested with an increase in the digestion period (2, 4, 6, 8, 10 and 12h). Constant measurement of COD was obtained after 8h of digestion period (Fig. 2.2). Therefore, 8h digestion was selected for the measurement of COD. Sulfide (S^{2-}) is an inorganic compound, but it contributes to the total COD of the system. COD of different concentrations of S^{2-} were determined and observed that 1 mg/L S^{2-} (as $Na_2S.xH_2O$) was equal to 3.43 mg O_2/L (Appendix C). Nitrite-N exerts 1.1 mg/L of COD at 1 mg/L of its own concentration (APHA, 2005). Similarly, COD of 1 mg/L of thiosulfate ($S_2O_3^{2-}$) as 0.82 mg/L was experimentally determined (Appendix C). Organic fraction of the COD was calculated as follows,

$$COD_O = COD_T - (3.43 \times C_S) - (1.1 \times C_n) - (0.82 \times C_T) \quad \ldots (2.7)$$

where,

COD_O = COD due to organics (mg O_2/L), COD_T = Measured COD as per APHA (2005), C_S = residual concentration of S^{2-} (mg/L), C_n = concentration of NO_2^--N (mg/L), C_T = concentration of thiosulfate (mg/L)

List of all instruments used during the study are summarized in Appendix D.

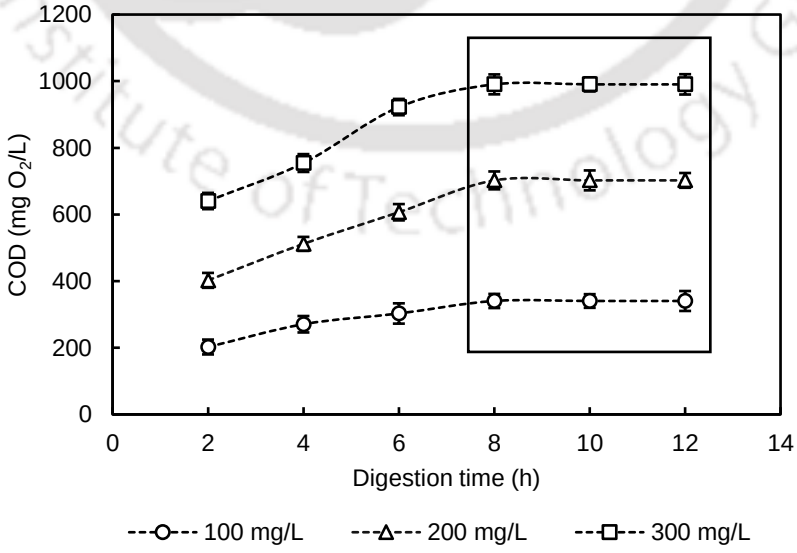

Fig. 2.2: Effect of digestion time on the COD of diesel at different concentrations

2.2.7 Microscopic images

Virgin PUF cube and biomass loaded PUF cube were collected and fragmented into thin pieces. Aluminum stubs were cleaned with acetone and carbon tape was adhered on it. Fragments of the PUF cubes were mounted on the stubs and coated with gold by sputter coater (Edward, USA). Stubs with mounted samples were placed in the specimen chamber of a field emission scanning electron microscope (FESEM) (Zeiss, Model: Gemini) for imaging.

2.3 ACCLIMATIZATION OF THE ANOXIC CULTURE

Acclimatization was initialized with phenol (5 ± 1 mg/L) as only carbon source, NO_3^--N (50 ± 2 mg/L) as electron acceptor and NH_4^+-N (10 ± 1 mg/L) as nitrogen source. Reactors were fed for a steady period of five days, then gradually the concentrations were increased. Phenol was the sole carbon source up to day 45 with feed containing phenol 250 ± 3 mg/L, NO_3^--N 550 ± 4 mg/L and NH_4^+-N 125 ± 2 mg/L. Acclimatization figures are given in Fig. 2.3. Degradation of phenol (Fig. 2.3a) and NO_3^--N (Fig. 2.3f) was confirmed by reduction in their concentrations. Decrease in the concentrations of COD_T (Fig. 2.3d) and COD_O (Fig. 2.3e) were observed each day. S^{2-} (10 ± 2 mg/L) was introduced in feed on day 46 (Fig. 2.3b). Feed diesel oil (50 mg/L) was instigated on day 71 (Fig. 2.3c). Gradually the concentrations were increased up to acclimatization period of 145 days having feed of phenol 1200 ± 6 mg/L, S^{2-} 1200 ± 10 mg/L, diesel 700 mg/L, TH 1700 ± 14 mg/L, NH_4^+-N 200 ± 4 mg/L and NO_3^--N 1000 ± 10 mg/L. Occurrence of NO_2^--N in the effluents and gas generation confirmed degradation of NO_3^--N in the reactors. Ghorbanian et al. (2014) acclimatized anoxic culture for 139 days up to total petroleum hydrocarbon and NO_3^--N concentration of 800 mg/L and 320 mg/L, respectively. Sahariah and Chakraborty (2012) reported acclimatization period of 100 days for anoxic biomass up to phenol, thiocyanate and NO_3^--N concentrations of 200, 40 and 200 mg/L, respectively. Both photographic and FESEM images of the virgin and biomass grown PUF cubes are illustrated in Appendix E.

During acclimatization, white (Fig. 2.4a) and yellow (Fig. 2.4d) solid precipitates were observed. FESEM images revealed irregular shape of both white (Fig. 2.4b) and yellow (Fig. 2.4e) solids. The precipitates were a possible mixture of elemental sulfur (S^0), metal sulfides and metal hydroxides. Metals in the feed was 0.16 mM, which was many-folds lower than the maximum S^{2-} in feed (23.5 mM). Therefore, the remaining solids had a high possibility to be elemental S^0. The solids were analyzed by EDX. Metals (Zn, Na) were detected in the white solids (Fig. 2.4c) and higher sulfur was detected in the yellow solids (Fig. 2.4f). Elemental

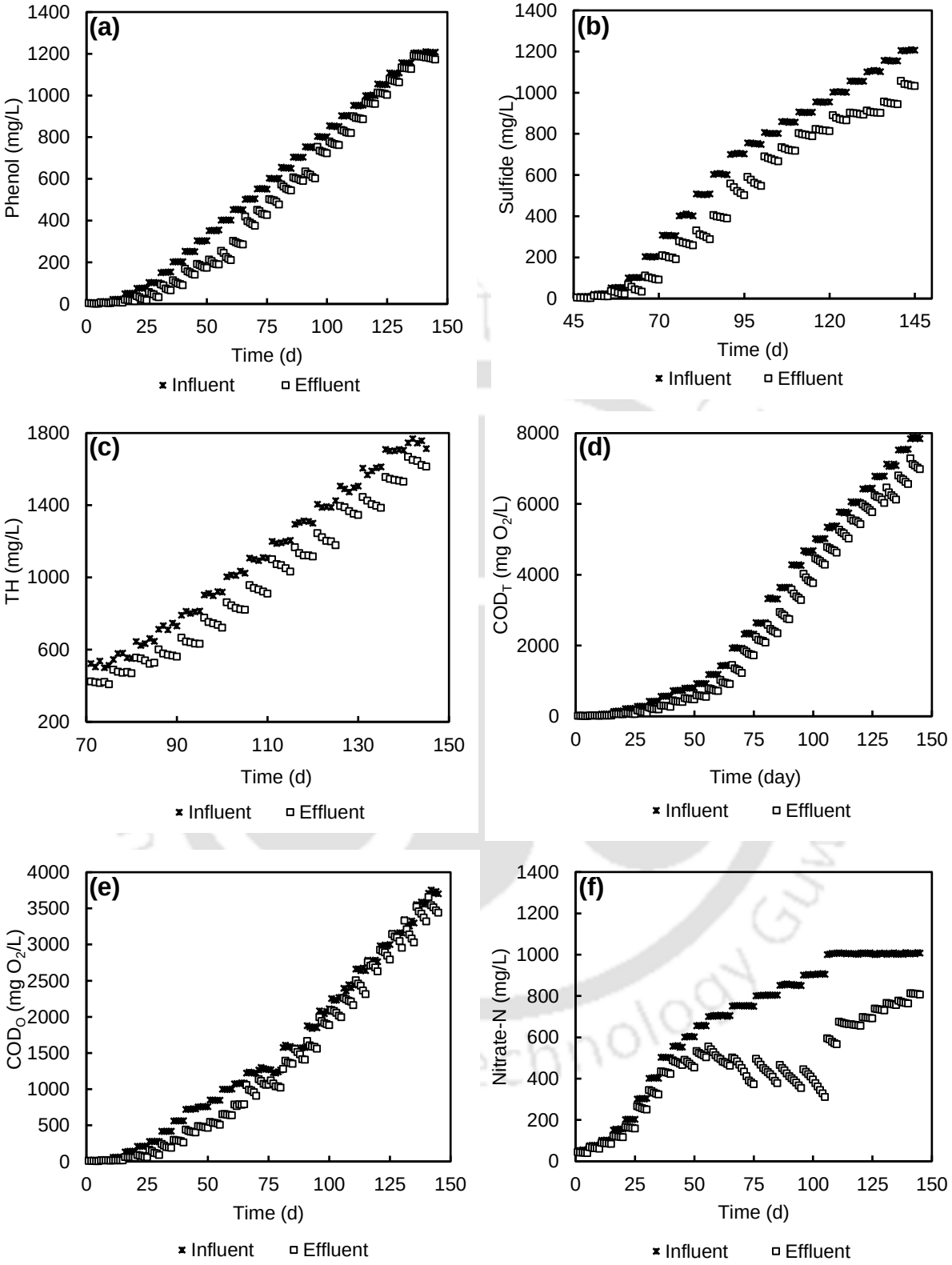

Fig. 2.3: Acclimatization of the anoxic culture with (a) phenol, (b) sulfide, (c) TH, (d) COD_T, (e) COD_O and (f) nitrate-N

analysis (CHNS elemental analyzer, Eurovactor, EA3000) of both types of solids showed higher sulfur content in the yellow solids and C, H and N were due to impurities caused by biomass (Table 2.2). Yellow solids were heated under flame and were instantly burnt and vaporized (Fig. 2.5). Thus, the yellow solids were confirmed as S^0 generated by biomass.

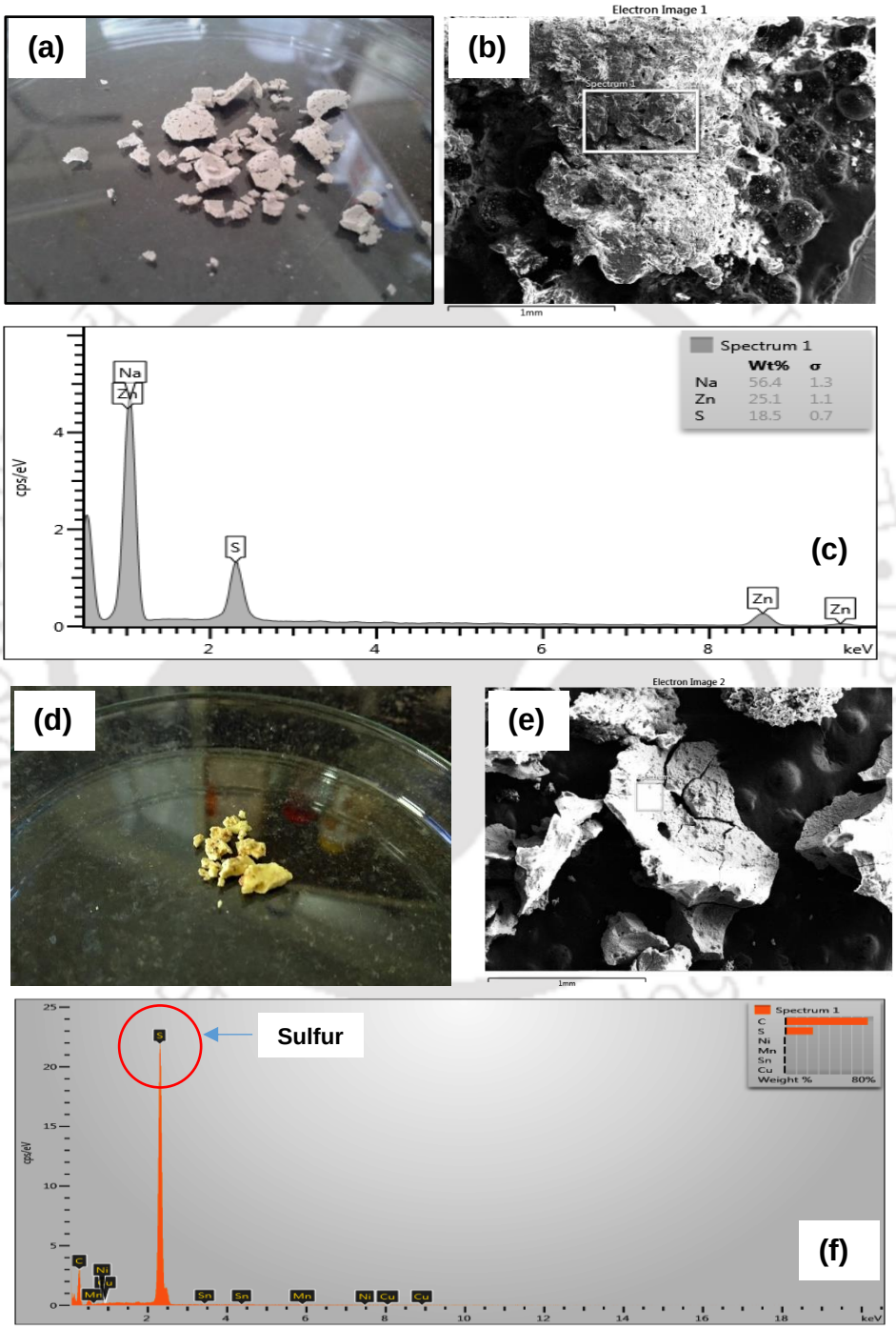

Fig. 2.4: (a) Image of the white precipitated solid, (b) FESEM image of the white solid, (c) EDX spectra of the white solid, (d) image of yellow precipitated solid, (e) FESEM image of yellow solid, (f) EDX spectra of the yellow solid

Table 2.2: Elemental C, H, N, S analysis of the white and yellow precipitates

Solid	C (%)	H (%)	N (%)	S (%)	Unaccounted (%)
White	3 ± 1	4 ± 1	2 ± 1	32 ± 2	59 ± 2
Yellow	2 ± 1	3 ± 1	3 ± 1	86 ± 2	6 ± 1

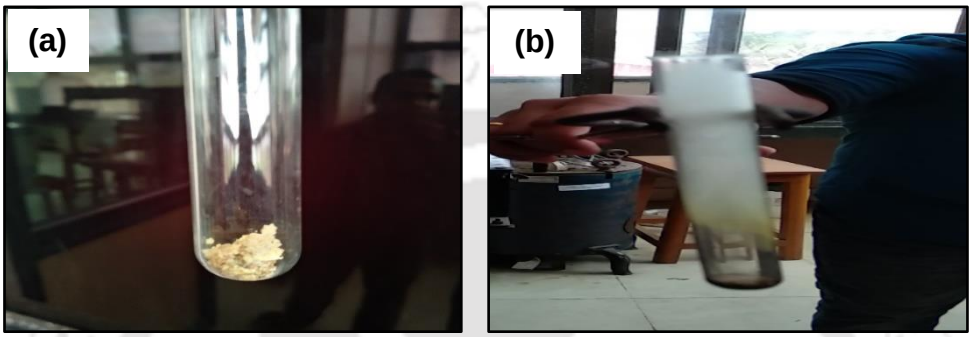

Fig. 2.5: Precipitated yellow solid (a) before and (b) after instant ignition

2.4 FED-BATCH OPERATION FOR THE OPTIMIZATION OF S^0 GENERATION

Anoxic fed-batch reactors were operated at varied concentrations of pollutants to determine the combination where maximum generation of sulfur (S^0) could be achieved. Pollutants were varied in the following order: S^{2-}, phenol, diesel (TH), NH_4^+-N and NO_3^--N. Possible polysulfide generation could occur during the oxidation of S^{2-} (Janssen et al., 1999; Kleinjan et al., 2005a). Kleinjan et al (2005a) reported that at pH ≤ 9, polysulfide was oxidized to $S_2O_3^{2-}$ and S^{2-}. Buisman et al. (1989) also observed polysulfide formation in the aerobic reactor when reactor pH was < 8. pH of reactors was more than 8 during the study, suggesting absence of polysulfide ions. Hence, generated sulfur (S^0) in the reactors was determined from the mass balance of the sulfur compounds and calculated as follows,

$$S^0 = \left[S_{inf}^{2-} - S_{eff}^{2-}\right] - \left[0.57 \times {S_2O_3}^{2-}\right] - \left[\frac{1}{3} \times (SO_4^{2-})\right] \quad \ldots (2.8)$$

$$S^0(\%) = \frac{S^0}{\left[S_{inf}^{2-} - S_{eff}^{2-}\right]} \times 100 \quad \ldots (2.9)$$

where,

S^0 = generated sulfur, mg/L, S^{2-}_{inf} = influent sulfide, mg/L, S^{2-}_{eff} = effluent sulfide, mg/L, $S_2O_3^{2-}$ = effluent thiosulfate, mg/L, SO_4^{2-} = generated sulfate, mg/L = (influent SO_4^{2-}) – (Effluent SO_4^{2-}), S^0 (%) = sulfur generation percentage from removed sulfide

2.4.1 Effect of initial sulfide (S^{2-}) feed

Feed S^{2-} was varied from 0 to 1222 ± 9 mg/L in R1 to R8, while the concentrations of phenol (750 ± 5 mg/L), diesel (300 mg/L), TH (1000 ± 10 mg/L), COD_O (2650 ± 16 mg O_2/L), NH_4^+-N (200 ± 5 mg/L), NO_3^--N (1000 ± 10 mg/L) and HRT (1.25d) were kept constant (Table 2.3). Increase in influent S^{2-} led to the increase of COD_T (2634 ± 16 to 6806 ± 24 mg O_2/L) , pH (7.7 to 9.9), conductivity (4.4 ± 0.2 to 7.1 ± 0.2 mS/cm), total dissolved solids (2.89 ± 0.07 to 4.69 ± 0.04 g/L) and salinity (3.3 ± 0.1 to 5.6 ± 0.1 g/L). The whole study was performed for 75 days (day 146-220).

Removal rate of S^2 increased linearly with increase in S^{2-} loading (Fig. 2.6a). Removal efficiency decreased from 82% to 52% with increase in loading from 87 ± 2 to 973 ± 6 g/(m^3.d). Mahmood et al. (2008) observed more than 90% removal of S^{2-} in the absence of organics at 48h HRT and pH 7.0-7.5 in an anoxic sulfide oxidizing (ASO) reactor and reported successful operation pH range of 5.0-11.0 at constant S^{2-} [576 g/(m^3.d)] and NO_2^- [680 g/(m^3.d)]. Can-Dogan et al. (2010) obtained more than 90% removal of S^{2-} within loading of 55-2004 g/(m^3.d) in denitrifying condition without organics. Removal of S^{2-} was 67% at S^{2-} and NO_3^--N loading of 604 ± 7 and 800 ± 9 g/(m^3.d) in the present study due to the presence of phenol and hydrocarbons.

When S^{2-} loading was lowest 87 ± 3 g/(m^3.d), SO_4^{2-} was the main product of S^{2-} oxidation (Table 2.3). S^0 generation increased with increase in S^{2-} loading and maximum S^0 generation (54% of removed S^{2-}) was observed at feed S^{2-} loading of 604 ± 7 g/(m^3.d) (750 ± 7 mg/L) at pH 9.0-9.5 (Fig. 2.6b). Beyond S^{2-} load of 604 ± 7 g/(m^3.d), $S_2O_3^{2-}$ generation started increasing (Table 2.3). Cardoso et al. (2009) observed complete conversion of S^{2-} to SO_4^{2-} during the simultaneous degradation of phenol and S^{2-} at lower S^{2-} load [37 g/(m^3.d)] in anoxic conditions. Conversion (%) of SO_4^{2-} decreased with increase in S^{2-} load up to 604 ± 7 g/(m^3.d), and then slightly increased in the present study. Oxidation of S^{2-} in denitrifying condition is a two-step process and described by the following equations (An et al. 2010),

$$5S^{2-} + 2NO_3^- + 12H^+ \rightarrow 5S^0 + N_2 + 6H_2O \qquad (\Delta G^0 = -191 \text{ kJ/mol}) \qquad \ldots (2.10)$$

$$5S^{2-} + 8NO_3^- + 8H^+ \rightarrow 5SO_4^{2-} + 4N_2 + 4H_2O \qquad (\Delta G^0 = -744 \text{ kJ/mol}) \qquad \ldots (2.11)$$

Formation of S^0 and SO_4^{2-} from the oxidation of S^{2-} depends upon the availability of NO_3^--N. Reaction tends towards the formation of SO_4^{2-} with more available NO_3^--N. Excessive SO_4^{2-} concentration in the effluent is undesirable. Hence, removal of S^{2-} through precipitation by biological conversion into S^0 can be prudent. Xu et al. (2016) observed that maximum S^0 was

Table 2.3: Effluent concentrations of the pollutants at feed sulfide (S^{2-}) variation

S^{2-} variation feed: S^{2-} 0 - 1222 ± 9 mg/L, Phenol 750 ± 5 mg/L, TH: 1000 ± 10 mg/L, NO_3^--N: 1000 ± 10 mg/L, NH_4^+-N: 200 ± 5 mg/L, COD_O: 2650 ± 16 mg O_2/L, SO_4^{2-}: 44 ± 3 mg/L															
Reactor	S^{2-} (mg/L)		SO_4^{2-} (mg/L)	$S_2O_3^{2-}$ (mg/L)	S^0 (mg/L)	Phenol (mg/L)	TH (mg/L)	COD_T (mg O_2/L)		COD_O (mg O_2/L)	NO_3^--N (mg/L)	NO_2^--N (mg/L)	NH_4^+-N (mg/L)	pH	
	Inf	Eff	Eff	Eff	Eff	Eff	Eff	Inf	Eff	Eff	Eff	Eff	Eff	Inf	Eff
R1	Absent	Absent	50 ± 2	ND	ND	417 ± 7	532 ± 17	2634 ± 16	1494 ± 19	1494 ± 19	246 ± 2	44 ± 3	222 ± 4	7.7 ± 0.1	8.1 ± 0.1
R2	106 ± 9	19 ± 3	311 ± 9	5 ± 1	5 ± 1	453 ± 5	609 ± 14	2998 ± 28	1720 ± 23	1594 ± 18	224 ± 7	56 ± 2	224 ± 4	8.3 ± 0.1	8.4 ± 0.1
R3	216 ± 3	58 ± 6	408 ± 17	4 ± 1	37 ± 2	502 ± 11	655 ± 16	3369 ± 27	2024 ± 33	1750 ± 31	199 ± 5	69 ± 2	222 ± 7	8.5 ± 0.1	8.6 ± 0.1
R4	304 ± 8	84 ± 4	512 ± 18	5 ± 1	64 ± 11	556 ± 23	688 ± 11	3669 ± 37	2284 ± 28	1907 ± 28	171 ± 6	80 ± 2	221 ± 3	8.7 ± 0.1	8.6 ± 0.1
R5	507 ± 11	152 ± 11	674 ± 22	7 ± 1	145 ± 9	597 ± 19	761 ± 20	4366 ± 46	2700 ± 19	2068 ± 25	148 ± 5	103 ± 1	223 ± 4	9.0 ± 0.1	8.6 ± 0.1
R6	755 ± 7	251 ± 16	743 ± 24	23 ± 1	269 ± 9	624 ± 21	796 ± 16	5214 ± 38	3151 ± 43	2162 ± 47	126 ± 4	114 ± 2	225 ± 5	9.5 ± 0.1	9.0 ± 0.1
R7	1034 ± 9	435 ± 25	942 ± 22	125 ± 12	208 ± 5	646 ± 20	862 ± 22	6173 ± 36	3959 ± 34	2269 ± 15	96 ± 3	144 ± 7	245 ± 4	9.7 ± 0.1	9.1 ± 0.1
R8	1222 ± 9	585 ± 28	1067 ± 44	185 ± 22	185 ± 7	664 ± 18	909 ± 12	6806 ± 24	4585 ± 55	2353 ± 25	68 ± 1	171 ± 5	254 ± 4	9.9 ± 0.1	9.2 ± 0.1

Inf: Influent, Eff: Effluent
ND: Not detectable
TH: Total hydrocarbon
COD_T: Total COD
COD_O: Organic COD

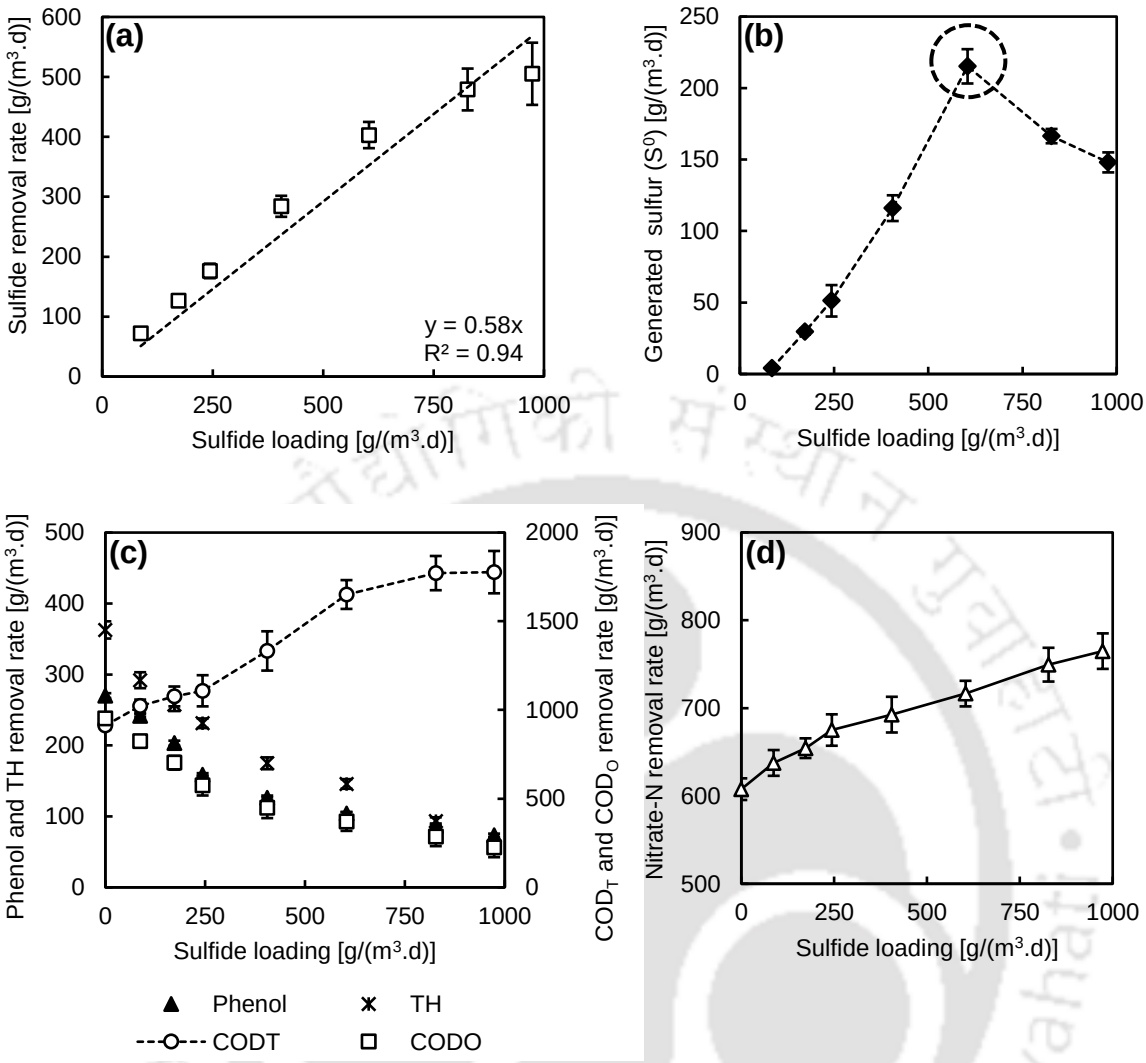

Fig. 2.6: Effect of sulfide loading on (a) sulfide removal rate, (b) sulfur production, (c) removal rate of organics, (d) nitrate-N removal rate

only 10% of the removed S^{2-} at pH 9.0 with influent NO_3^--N:S^{2-} molar ratio of 2.0. In the present study, at influent NO_3^--N: S^{2-} molar ratio of 1.9, S^0 generation was 47% of removed S^{2-}, which was higher compared to the reported literature. Eq. 2.10 and 2.11 show that influent molar ratio of NO_3^--N:S^{2-} of 0.4 and 1.6 are necessary for complete generation of S^0 and SO_4^{2-}. In the present study, maximum S^0 was obtained at influent NO_3^--N: S^{2-} molar ratio of 3.04 (Table 2.3), since besides S^{2-}, phenol and hydrocarbon were also oxidized using NO_3^--N in anoxic reactors.

With increase in feed S^{2-}, effluent phenol, TH and COD increased (Table 2.3), suggesting decrease in removal efficiency (phenol: 44 to 12%; TH: 46 to 7%; COD_T: 53 to 26%; COD_O: 45 to 12%) and removal rates (Fig. 3c). Lora and Flores (2004) observed complete inhibition

on phenol (influent 120 mg/L) removal at 480 mg/L of S^{2-}. Present study showed higher phenol removal even in the presence of other competing pollutants. Eq. 2.12 (Chakraborty and Veeramani, 2006) gives oxidation of phenol in denitrifying condition.

$$C_6H_5OH + 5.6NO_3^- + 0.2H_2O \rightarrow 6HCO_3^- + 4H^+ + 2.8N_2 \quad (\Delta G^0 = -2802 \text{ kJ/mol}) \quad \ldots (2.12)$$

Phenol and hydrocarbons degradation is favored at near neutral pH range (Margesin and Schinner, 2001; Ghaima et al., 2017). Hence, degradation of hydrocarbons reduced due to high alkaline pH. Organic COD (COD_O) removal rate decreased with increase in S^{2-} loading (Fig. 2.6c), since COD_O mainly composed of phenol and hydrocarbons and their removals inhibited at higher S^{2-} loading.

Effluent NO_3^--N decreased with increase in S^{2-} loading (Table 2.3) and increase in removal efficiency (75% to 93%) and removal rate (Fig. 2.6d) along with increase in effluent NO_2^--N was observed (Table 3). NO_2^--N was 4.4% of influent NO_3^--N in absence of S^{2-} and increased to 17% at S^{2-} loading of 978 ± 9 g/(m^3.d). Increase in NO_2^--N (%) (18% in absence of S^{2-} and 43% in presence of 20 mg/L S^{2-}) from the partial degradation of NO_3^--N with increase in S^{2-} has been reported elsewhere (Escalante et al., 2008; Moraes et al., 2013). At higher S^{2-} loading, organics degradation was inhibited and S^{2-} was the only electron donor. Due to less availability of electron donor, NO_3^--N reduction was partial to NO_2^--N.

2.4.2 Effect of initial phenol feed

Phenol was varied from 0 to 1214 ± 3 mg/L in R1 to R8. Increase in feed phenol resulted in increase in influent TH (TH comprises of both phenol and diesel), COD_T and COD_O (Table 2.4). Maximum S^0 generation occurred at 750 mg/L influent S^{2-} (section 2.4.1). Hence, feed S^{2-} was kept at 750 mg/L along with constant diesel (300 mg/L), NH_4^+-N (200 ± 5 mg/L), NO_3^--N (1000 ± 10 mg/L) and pH (9.5 ± 0.1). However, slight increase in salinity (4.15 ± 0.02 - 4.32 ± 0.03 g/L), conductivity (5.01 ± 0.04 - 6.54 ± 0.02 mS/cm) and total dissolved solids (3.99 ± 0.09 - 5.12 ± 0.07 g/L) was observed during the study conducted in 70 days (day 221 to 290).

With increase in phenol load, effluent S^{2-} decreased (Table 2.4), resulting into increment in both removal efficiency (51% to 74%) and rate (Fig. 2.7a). Generation of S^0 from the oxidation of S^{2-} increased (maximum 59%) up to phenol load of 606 ± 6 g/(m^3.d) (750 ± 6 mg/L) (Fig. 2.7b). $S_2O_3^{2-}$ generation remained within 12-20 mg/L and reached a maximum 2% of removed S^{2-}. Oxidation of S^{2-} to SO_4^{2-} decreased up to phenol loading of 606 ± 6 g/(m^3.d), and eventually increased (Table 2.4).

Table 2.4: Effluent concentrations of the pollutants at feed phenol variation

Phenol variation feed: phenol: 0 - 1214 ± 3 mg/L, Sulfide: 750 ± 7 mg/L, NO_3^--N 1000 ± 10 mg/L, NH_4^+-N 200 ± 5 mg/L, SO_4^{2-} 44 ± 3 mg/L, pH: 9.5 ± 0.1																
Reactor	Phenol (mg/L)		TH (mg/L)		COD_T (mg O_2/L)		COD_O (mg O_2/L)		S^{2-} (mg/L)	SO_4^{2-} (mg/L)	$S_2O_3^{2-}$ (mg/L)	S^0 (mg/L)	NO_3^--N (mg/L)	NO_2^--N (mg/L)	NH_4^+-N (mg/L)	pH
	Inf	Eff	Inf	Eff	Inf	Eff	Inf	Eff	Eff	Eff	Eff	Eff	Eff	Inf	Eff	Eff
R1	Absent	Absent	248 ± 5	96 ± 3	2799 ± 18	1500 ± 11	211 ± 6	81 ± 3	369 ± 9	871 ± 9	18 ± 1	108 ± 4	608 ± 9	135 ± 2	220 ± 5	9.2 ± 0.1
R2	103 ± 4	16 ± 2	356 ± 4	157 ± 8	3140 ± 11	1518 ± 19	549 ± 9	271 ± 8	321 ± 6	820 ± 7	18 ± 2	170 ± 3	505 ± 9	125 ± 6	224 ± 6	9.2 ± 0.1
R3	203 ± 4	59 ± 3	458 ± 9	245 ± 3	3452 ± 22	1546 ± 22	873 ± 7	348 ± 5	306 ± 6	818 ± 4	16 ± 2	178 ± 4	417 ± 7	122 ± 9	222 ± 5	9.2 ± 0.1
R4	304 ± 2	121 ± 6	559 ± 11	286 ± 9	3784 ± 24	1624 ± 11	1199 ± 8	532 ± 8	278 ± 9	790 ± 8	12 ± 2	222 ± 9	315 ± 8	120 ± 4	230 ± 2	9.1 ± 0.1
R5	507 ± 9	255 ± 9	757 ± 3	469 ± 12	4435 ± 27	2024 ± 19	1851 ± 13	1026 ± 16	258 ± 3	717 ± 2	17 ± 1	267 ± 4	228 ± 5	117 ± 3	221 ± 3	9.0 ± 0.1
R6	750 ± 6	571 ± 8	991 ± 18	728 ± 9	5229 ± 11	2710 ± 16	2644 ± 23	1822 ± 20	212 ± 9	711 ± 5	14 ± 1	317 ± 6	125 ± 3	116 ± 4	218 ± 5	9.0 ± 0.1
R7	1014 ± 8	873 ± 9	1268 ± 9	1036 ± 9	6068 ± 26	3775 ± 19	3491 ± 16	2960 ± 14	201 ± 5	765 ± 6	18 ± 2	290 ± 9	76 ± 3	154 ± 2	224 ± 2	8.9 ± 0.1
R8	1214 ± 3	1096 ± 9	1468 ± 9	1266 ± 6	6724 ± 19	4520 ± 25	4137 ± 14	3684 ± 12	200 ± 2	789 ± 4	20 ± 2	270 ± 9	66 ± 2	181 ± 2	219 ± 6	8.9 ± 0.1

Inf: Influent, Eff: Effluent
TH: Total hydrocarbon
COD_T: Total COD
COD_O: Organic COD

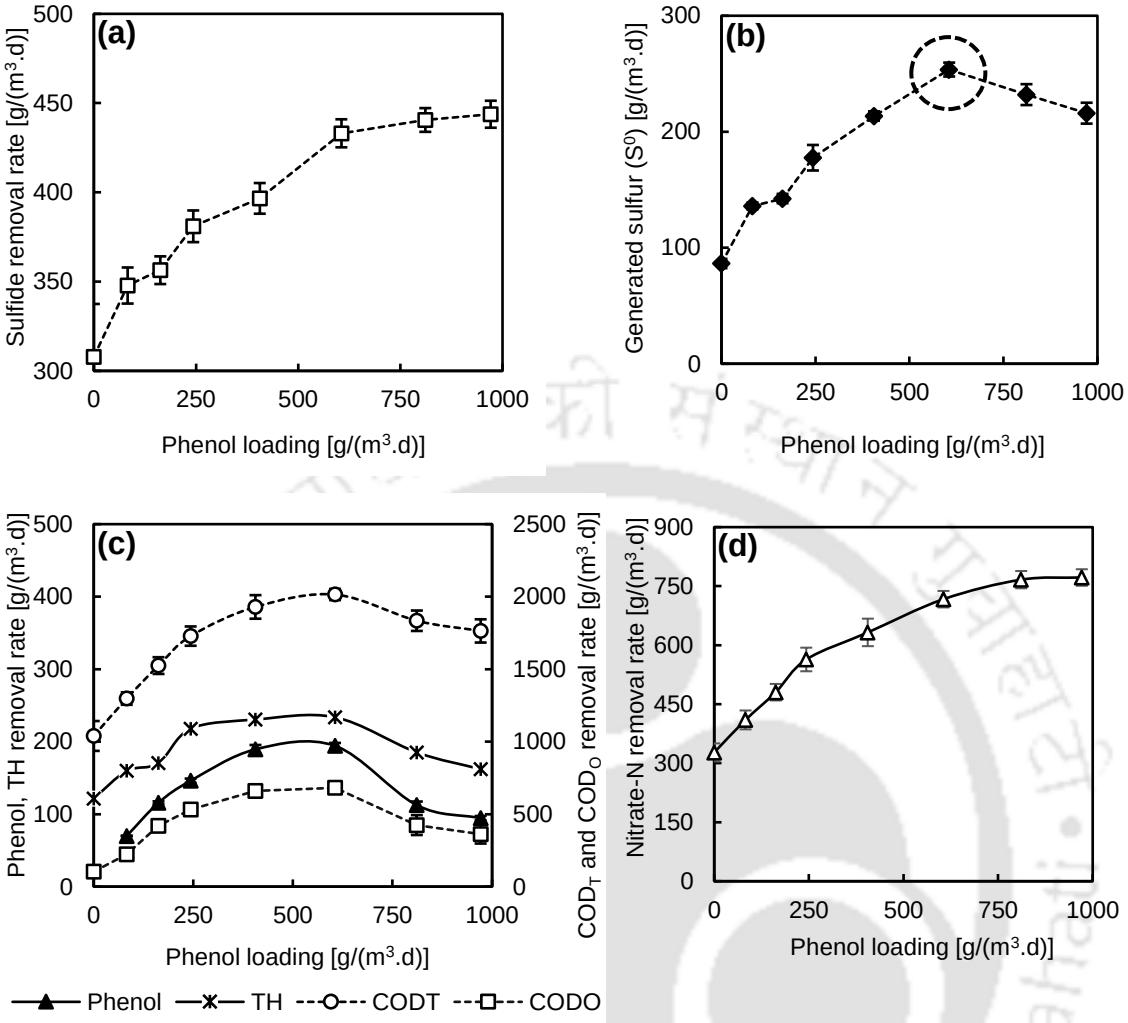

Fig. 2.7: Effect of phenol loading on (a) sulfide removal rate, (b) sulfur production, (c) removal rate of organics, (d) nitrate-N removal rate

Effluent phenol, TH, COD_T and COD_O increased with increase in phenol load (Table 2.4) and drop in the removal efficiency (phenol: 85% to 10%, TH: 61% to 14%, COD_T: 46% to 33%; COD_O: 62% to 11%) occurred. However, degradation rates increased up to phenol loading of 606 ± 6 g/(m^3.d) (750 mg/L) and decreased at higher loads (Fig. 2.7c). Phenol and TH being the contributor of COD, decrease in their degradation led to drop in the degradation of COD at high phenol load. Decrease in the degradation of phenol at higher loads advocates self-inhibition. Sharma and Philip (2014) reported no self-inhibition on phenol degradation at lower concentrations (50-200 mg/L) and Thomas et al. (2002) reported no self-inhibition on phenol degradation up to 600 mg/L in single substrate anoxic medium in anoxic batch reactors. However, Alcantara et al. (2004) reported inhibition in phenol removal at 250 mg/L during simultaneous removals of S^{2-} and phenol in anoxic condition. Above mentioned findings were

observed in moderate alkaline pH (7.5 ± 0.1). Present study was conducted at high alkaline pH (9.5 ± 0.1) and inhibition was observed in the presence of diesel, S^{2-} and NH_4^+-N.

More electron acceptor (NO_3^--N) was consumed with increase in phenol as decrease in the effluent NO_3^--N was observed (Table 2.4) along with increase in NO_3^--N removal efficiency (40% to 94%) and removal rate (Fig. 2.7d). Inhibition on NO_3^--N removal at phenol load of 561 g/(m^3.d) in anoxic UASB has been reported (Eiroa et al., 2005). However, such scenario was not observed in the present case. Effluent NO_2^--N marginally decreased up to phenol loading of 606 ± 6 g/(m^3.d), and then increased beyond that load. Generated NO_2^--N was 11-13% of the influent NO_3^--N.

Self-inhibition of phenol and decrease in organics removal led to more availability of NO_3^--N for the oxidation of S^{2-}. Hence, there was increase in SO_4^{2-} and decrease in S^0 generation beyond phenol loading of 606 ± 6 g/(m^3.d). S^0 generation was 58% of removed S^{2-} at phenol loading of 606 g/(m^3.d) (750 mg/L feed phenol). At higher phenol loadings [> 606 ± 6 g/(m^3.d)], electrons are mostly released from the oxidation of S^{2-} as degradation rate of organics reduced. Less available electrons led to partial degradation of NO_3^--N and increase in the formation of NO_2^--N (Table 2.4).

2.4.3 Effect of initial diesel feed

Diesel was varied from 0 to 700 mg/L in R1 to R8. Increase in diesel resulted in increase in influent TH, COD_T and COD_O (Table 2.5). Maximum S^0 generation occurred at influent S^{2-} and phenol of 750 mg/L (section 2.4.2). Hence, infeed S^{2-} and phenol were kept at 750 mg/L at constant NH_4^+-N (200 ± 5 mg/L) and NO_3^--N (1000 ± 10 mg/L). Reactor pH (9.5 ± 0.1) and salinity (4.27 ± 0.07 g/L) were constant and slight increase in conductivity (5.44 ± 0.04 - 5.90 ± 0.06 mS/cm) and TDS (4.63 ± 0.02 - 4.75 ± 0.02 g/L) was observed. The study was conducted for 70 days (day 291 to 360).

Effluent S^{2-} decreased with increase in diesel load (Table 2.5) and increase in removal efficiency (56% to 76%) and removal rate (Fig. 2.8a) was observed. Maximum production of S^0 occurred (62% of the removed S^{2-}) at diesel loading of 240 g/(m^3.d) (feed diesel of 300 mg/L) (Fig. 2.8b). Generation of $S_2O_3^{2-}$ marginally increased at higher influent diesel and maximum 3% of the removed S^{2-} was converted to $S_2O_3^{2-}$ (Table 2.5). Oxidation of S^{2-} to SO_4^{2-} decreased up to diesel load of 240 g/(m^3.d) and increased at higher diesel loading in feed (Table 2.5).

Table 2.5: Effluent concentrations of the pollutants at feed diesel variation

Diesel variation feed: Diesel: 0 - 700 mg/L, Phenol: 750 ± 5, Sulfide: 750 ± 7 mg/L, NO_3^--N: 1000 ± 10 mg/L, NH_4^+-N: 200 ± 5 mg/L, SO_4^{2-}: 44 ± 3 mg/L, pH: 9.5 ± 0.1															
Reactor	TH (mg/L)		COD_T (mg/L)		COD_O (mg O_2/L)		Phenol (mg /L)	S^{2-} (mg/L)	SO_4^{2-} (mg/L)	$S_2O_3^{2-}$ (mg/L)	S^0 (mg/L)	NO_3^--N (mg/L)	NO_2^--N (mg/L)	NH_4^+-N (mg/L)	pH
	Inf	Eff	Inf	Eff	Inf	Eff	Eff	Eff	Eff	Eff	Eff	Eff	Eff		
R1	708 ± 7	402 ± 9	4987 ± 15	2675 ± 18	2396 ± 12	1416 ± 10	452 ± 9	335 ± 4	776 ± 9	14 ± 1	174 ± 4	185 ± 5	97 ± 2	219 ± 6	9.3 ± 0.1
R2	805 ± 3	487 ± 6	5062 ± 24	2690 ± 11	2471 ± 20	1578 ± 13	489 ± 6	291 ± 9	748 ± 8	14 ± 1	227 ± 9	155 ± 7	100 ± 4	220 ± 3	9.1 ± 0.1
R3	932 ± 8	610 ± 3	5184 ± 19	2816 ± 13	2590 ± 10	1698 ± 17	524 ± 8	272 ± 6	729 ± 7	15 ± 1	254 ± 6	138 ± 6	100 ± 3	219 ± 8	9.1 ± 0.1
R4	1010 ± 9	650 ± 8	5241 ± 21	2824 ± 12	2656 ± 11	1908 ± 12	570 ± 9	210 ± 9	652 ± 8	17 ± 1	337 ± 9	116 ± 7	105 ± 6	222 ± 4	9.0 ± 0.1
R5	1111 ± 5	829 ± 9	5321 ± 18	2931 ± 17	2742 ± 13	2118 ± 14	594 ± 8	201 ± 4	723 ± 3	17 ± 1	320 ± 4	123 ± 3	140 ± 3	229 ± 9	8.8 ± 0.1
R6	1212 ± 8	1039 ± 5	5419 ± 12	3188 ± 22	2829 ± 14	2398 ± 10	636 ± 9	191 ± 7	783 ± 5	22 ± 2	311 ± 7	135 ± 7	150 ± 2	238 ± 4	8.8 ± 0.1
R7	1310 ± 3	1197 ± 6	5491 ± 16	3408 ± 14	2909 ± 10	2628 ± 12	677 ± 7	186 ± 9	802 ± 6	29 ± 2	303 ± 9	150 ± 5	161 ± 3	227 ± 4	8.8 ± 0.1
R8	1411 ± 9	1321 ± 6	5578 ± 19	3531 ± 16	2998 ± 12	2770 ± 14	692 ± 5	179 ± 9	812 ± 4	38 ± 3	301 ± 9	163 ± 6	171 ± 2	228 ± 6	8.7 ± 0.1

Inf: Influent, Eff: Effluent
TH: Total hydrocarbon
COD_T: Total COD
COD_O: Organic COD

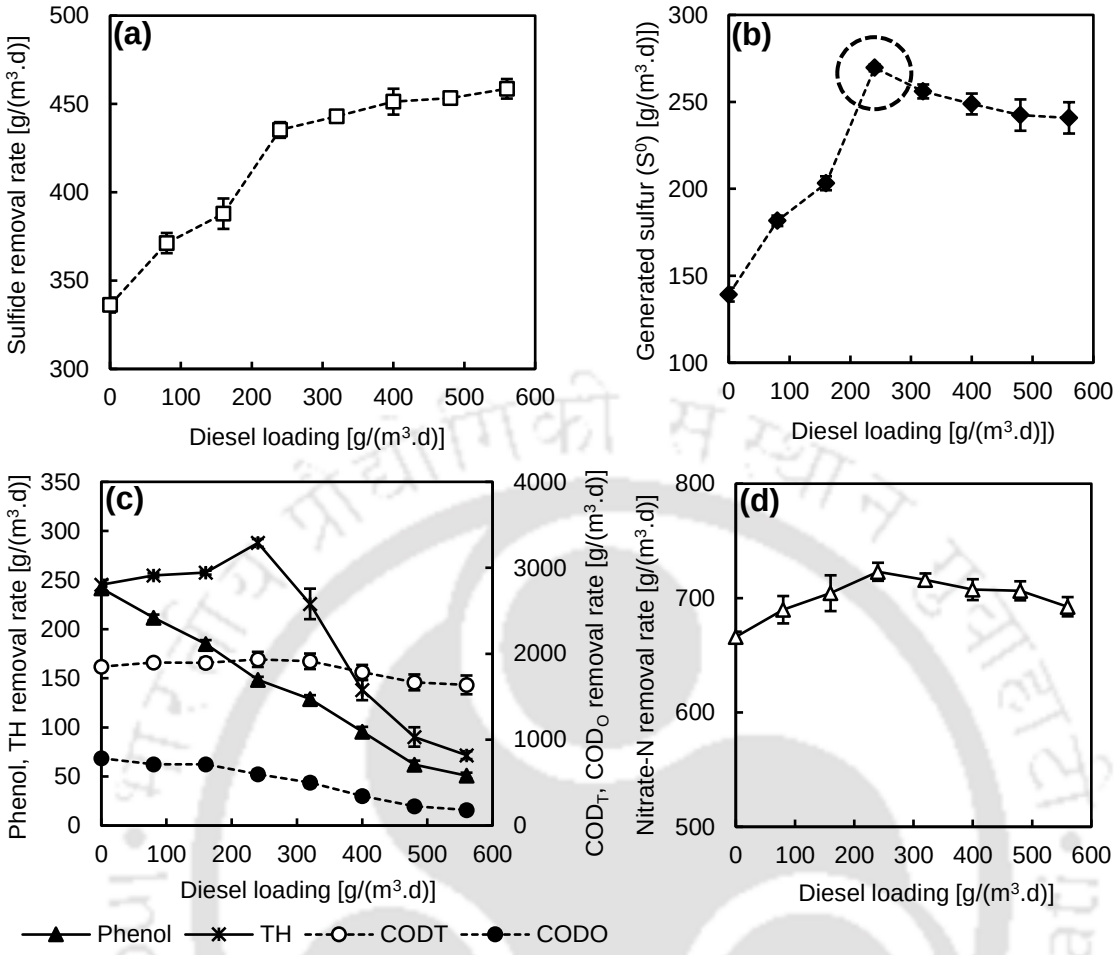

Fig. 2.8: Effect of diesel loading on (a) sulfide removal rate, (b) sulfur production, (c) removal rate of organics, (d) nitrate-N removal rate

Effluent phenol, COD_T, COD_O and TH increased with increase in diesel (Table 2.5) and decrease in removal efficiency (phenol: 40% to 8%, TH: 43% to 6%, COD_T: 46% to 36%, COD_O: 41% to 8%) and removal rate (Fig. 2.8c) occurred. Degradation rate of TH and COD_T initially increased up to influent diesel load of 240 g/(m^3.d) and decreased at higher diesel load (Fig. 2.8c). Moussavi et al. (2016) treated kerosene in anoxic medium at initial load of 2200 g/(m^3.d) and obtained 79% removal efficiency at pH of 7.5. Petroleum hydrocarbon with higher density (diesel density: 0.810 g/mL, kerosene density: 0.732 g/mL) was treated in the presence of phenol, S^{2-} and NH_4^+-N at high alkaline pH (9.5 ± 0.1) in the present study. Phenol and COD_O degradation rate decreased with increase in diesel load (Fig. 2.8c). Decrease in the bacterial growth with increase in diesel during simultaneous removals of phenol and diesel has been reported (Ahmed et al., 2018). CODo removal rate was lower at maximum diesel load [560 ± 4 g/(m^3.d)] compared to the maximum phenol load [971 ± 4 g/(m^3.d)]. Hence, diesel had more profound effect on the COD_O removal compared to phenol.

Effluent NO_3^--N decreased initially up to 240 g/(m^3.d) of diesel load, then increased (Table 2.5). Removal efficiency (88%) and removal rate (Fig. 2.8d) were maximum at diesel load of 240 g/(m^3.d). Simultaneous removals of S^{2-} and TH at low diesel load led to increase in NO_3^--N consumption. Similarly, effluent NO_2^--N started to increase beyond diesel load of 240 g/(m^3.d) (Table 2.5).

Inhibition on TH removal beyond diesel loading of 240 g/(m^3.d), led to more available NO_3^--N for oxidation of S^{2-} and reaction shifted to the formation of more SO_4^{2-} and $S_2O_3^{2-}$. Therefore, generation of S^0 decreased beyond diesel loading of 240 g/(m^3.d). Also, at higher diesel loadings [> 240 g/(m^3.d)], increase in NO_2^--N was observed due to lower oxidation of hydrocarbons as electron donor. Diesel had more detrimental effect on NO_3^--N removal rate compared to phenol at similar loads.

2.4.4 Effect of initial ammonia-N (NH_4^+-N) feed

NH_4^+-N was varied from 0 to 450 ± 4 mg/L in R1 to R8. Influent S^{2-} (750 ± 7 mg/L), phenol (750 ± 5 mg/L), COD_T (5250 ± 22 mg O_2/L), COD_O (2650 ± 17 mg O_2/L) and NO_3^--N (1000 ± 10 mg/L) were kept constant (Table 2.6). Infeed diesel was kept at 300 mg/L as maximum S^0 generation occurred at that concentration (section 2.4.3). Reactor pH (9.5 ± 0.1) and salinity (4.27 ± 0.04 g/L) were constant and slight increase in conductivity (5.51 ± 0.02 - 5.87 ± 0.03 mS/cm) and TDS (4.50 ± 0.02 - 5.00 ± 0.03 g/L) was observed. The whole study was conducted for 70 days (day 361 to 430).

Removal of S^{2-} remained constant (72%) up to NH_4^+-N load of 284 ± 9 g/(m^3.d) (354 ± 9 mg/L) and decreased to 68% at maximum load [406 ± 4 mg/(L.d)] (Table 2.6). Similarly degradation rate of S^{2-} decreased beyond NH_4^+-N loading of 284 ± 9 g/(m^3.d) (Fig. 2.9a). It was reported that degradation of S^{2-} and benzene were not affected by lower loads of NH_4^+-N [21-44 g/(m^3.d)] in fluidized bed reactor and biofilter (Chong-woo et al., 2003). In the present study, degradation of S^{2-} was not hampered up to a significantly higher load. Production of S^0 from the oxidation of S^{2-} decreased at higher NH_4^+-N loadings [> 284 ± 7 g/(m^3.d)] (Fig. 2.9b). Generation of $S_2O_3^{2-}$ was below 10 mg/L and unaffected by NH_4^+-N. Conversion of S^{2-} to SO_4^{2-} was constant up to NH_4^+-N loading of 284 ± 7 g/(m^3.d) and increased beyond that (Table 2.6).

Organics removal remained unaffected up to influent NH_4^+-N load of 284 ± 9 g/(m^3.d). With further increase in NH_4^+-N load, effluent organics increased (Table 2.6) and there was decrease in the removal efficiencies (Phenol: 25% to 16%, TH: 27% to 17%, COD_T: 46% to 39% and COD_O: 26% to 16%) and removal rates (Fig. 2.9c).

Table 2.6: Effluent concentrations of the pollutants at feed ammonia-N (NH_4^+-N) variation

NH_4^+-N variation feed: NH_4^+-N: 0 - 456 ± 4 mg/L, Phenol: 750 ± 5, Sulfide: 750 ± 7 mg/L, Diesel: 300 mg/L, NO_3^--N: 1000 ± 10 mg/L, SO_4^{2-}: 44 ± 3 mg/L, pH: 9.5 ± 0.1														
Reactor	NH_4^+-N (mg/L)			COD_T (mg O_2/L)	COD_O (mg O_2/L)	Phenol (mg/L)	TH (mg/L)	S^{2-} (mg/L)	SO_4^{2-} (mg/L)	$S_2O_3^{2-}$ (mg/L)	S^0 (mg/L)	NO_3^--N (mg/L)	NO_2^--N (mg/L)	pH
	Inf	Eff	Free ammonia	Inf	Eff	Eff	Eff	Eff	Eff	Eff	Eff	Eff	Eff	Eff
R1	Absent	-	-	5243 ± 11	2653 ± 10	569 ± 8	731 ± 7	213 ± 6	711 ± 9	3 ± 1	318 ± 2	124 ± 6	115 ± 4	8.9 ± 0.1
R2	55 ± 2	68 ± 3	27 ± 2	5250 ± 18	2657 ± 14	570 ± 9	731 ± 9	214 ± 3	706 ± 8	6 ± 1	318 ± 3	126 ± 7	115 ± 2	9.0 ± 0.1
R3	106 ± 4	114 ± 6	46 ± 2	5244 ± 22	2658 ± 11	570 ± 6	731 ± 7	218 ± 7	705 ± 6	6 ± 1	312 ± 2	124 ± 5	116 ± 2	9.0 ± 0.1
R4	202 ± 5	224 ± 8	103 ± 3	5232 ± 11	2656 ± 18	565 ± 8	729 ± 6	210 ± 2	705 ± 9	7 ± 1	316 ± 2	123 ± 6	117 ± 4	9.1 ± 0.1
R5	304 ± 8	299 ± 6	105 ± 1	5227 ± 18	2656 ± 11	570 ± 6	740 ± 7	209 ± 4	704 ± 4	8 ± 2	316 ± 3	123 ± 3	117 ± 2	8.9 ± 0.1
R6	354 ± 9	349 ± 7	141 ± 4	5238 ± 10	2653 ± 17	568 ± 4	746 ± 8	211 ± 6	705 ± 9	5 ± 1	320 ± 3	122 ± 4	118 ± 3	9.0 ± 0.1
R7	404 ± 3	400 ± 6	161 ± 2	5234 ± 19	2651 ± 19	607 ± 7	801 ± 9	223 ± 2	665 ± 5	9 ± 2	304 ± 2	133 ± 2	118 ± 4	9.0 ± 0.1
R8	456 ± 4	452 ± 2	182 ± 3	5225 ± 10	2653 ± 11	634 ± 3	840 ± 8	242 ± 4	652 ± 2	7 ± 1	293 ± 2	140 ± 2	122 ± 2	9.0 ± 0.1

Inf: Influent, Eff: Effluent
TH: Total hydrocarbon
COD_T: Total COD
COD_O: Organic COD

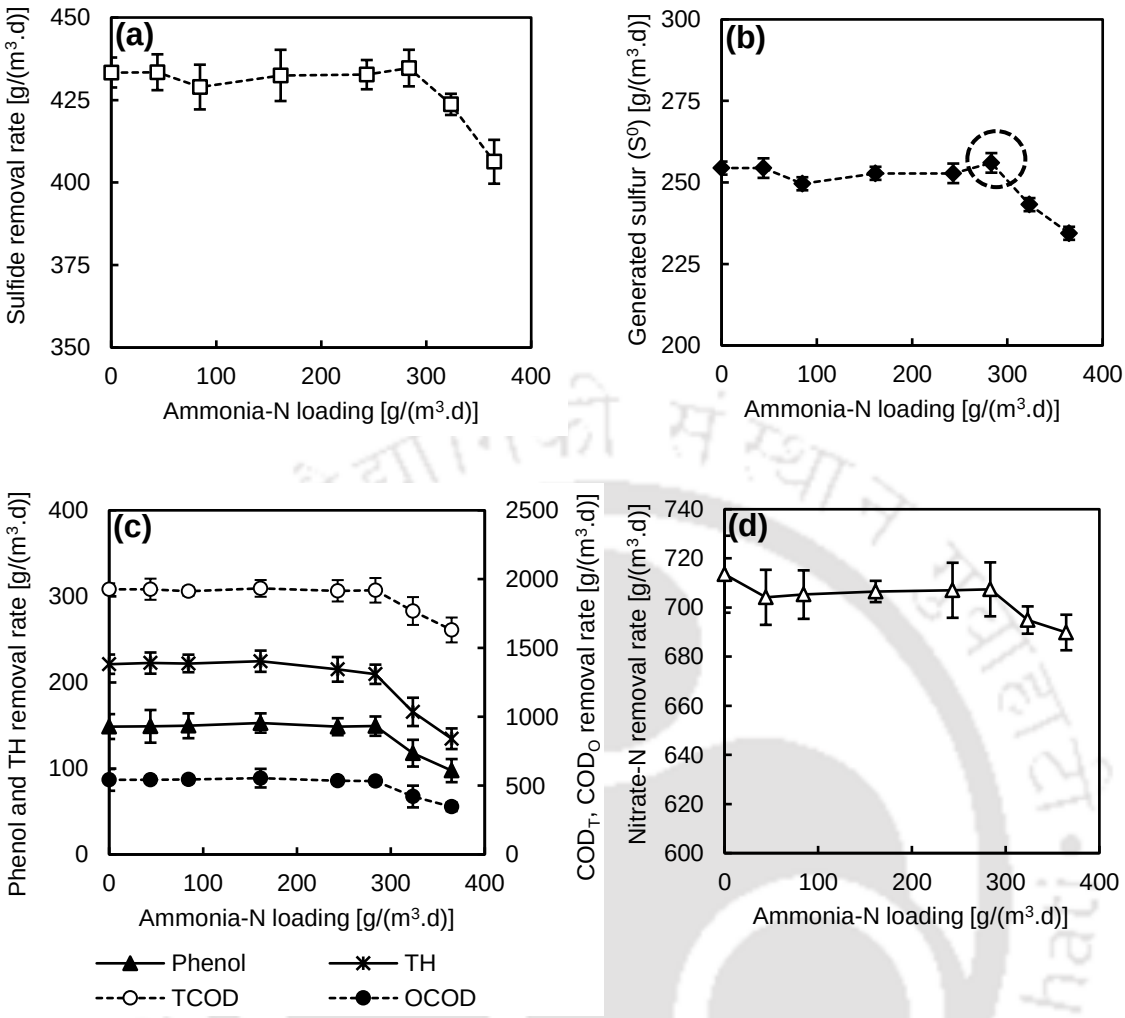

Fig. 2.9: Effect of ammonia-N loading on (a) sulfide removal rate, (b) sulfur production, (c) removal rate of organics, (d) nitrate-N removal rate

Reactors were operated at high alkaline pH and free ammonia (summarized in Table 2.6) was calculated as per Eq. 2.13 (Vadivelu et al., 2007). There was increase in free ammonia with increase in NH_4^+-N load.

$$\text{Free ammonia} = \frac{[NH_4^+ - N] \times 10^{pH}}{\exp\left[\frac{6334}{273+t}\right] + 10^{pH}} \quad \ldots (2.13)$$

Abd-El-Haleem et al. (2003) observed no effect on phenol degradation [load: 100 g/(m^3.d)] up to NH_4^+-N load of 5.2 g/(m^3.d) in anoxic condition and degradation reduced to more than 90% at NH_4^+-N load of 51.2 g/(m^3.d). In the present study, anoxic biomass tolerated much higher influent NH_4^+-N load and performance decreased at higher load due to the existence of excessive free NH_3 (> 150 mg/L) at high alkaline pH (pH > 9.5) which is in corroboration with

the literature (Muller et al., 2006; Liu and Tay, 2001). Increase in effluent NO_3^--N was observed (Table 2.6) beyond NH_4^+-N loading of 284 ± 9 g/(m^3.d) and removal efficiency (88% to 86%) and removal rate decreased (Fig. 2.9d) due to decrease in the oxidation of electron donors. Formation of NO_2^--N marginally increased (Table 2.6). Degradation of both organics and S^{2-} were hampered at higher NH_4^+-N. Conversion of S^{2-} to SO_4^{2-} decreased at higher NH_4^+-N load, suggesting inhibition to both heterotrophs and autotrophs in the presence of higher free ammonia at high alkaline pH.

2.4.5 Effect of initial nitrate-N (NO_3^--N) feed

NO_3^--N was varied from 0 to 2009 ± 9 mg/L in R1 to R8. Influent phenol (750 ± 5 mg/L), S^{2-} (750 ± 7 mg/L), TH (1000 ± 10 mg/L), COD_T (5250 ± 22 mg O_2/L) and COD_O (2650 ± 16 mg O_2/L) were constant. Influent NH_4^+-N was kept constant at 350 mg/L, as maximum S^0 generated at that concentration (section 2.4.4). Influent pH (9.5 ± 0.1) and salinity (4.28 ± 0.03 g/L) were constant and increase in conductivity (5.40 ± 0.02 - 5.99 ± 0.04 mS/cm) and TDS (3.99 ± 0.02 - 5.46 ± 0.04 g/L) was observed. The study was done for 70 days (day 431-500).

Effluent S^{2-} decreased with increase in NO_3^--N (Table 2.7) and increase in removal efficiency (7% to 75%) and removal rate were observed (Fig. 2.10a). Mass of generated S^0 was maximum when NO_3^--N loading was 811 ± 6 g/(m^3.d) (1014 ± 8 mg/L) and decreased with further increase in NO_3^--N (Fig. 2.10b). With increase in NO_3^--N, conversion of removed S^{2-} to $S_2O_3^{2-}$ and SO_4^{2-} increased (Table 2.7), as availability of more electron donor led to complete oxidation of intermediate S^0 to SO_4^{2-}.

With increase in the feed NO_3^--N, effluent phenol, TH, COD_T and COD_O decreased (Table 2.7) and there was increase in removal efficiency (phenol: 11% to 46%, TH: 6% to 50%, COD_T: 8% to 57%, COD_O: 9% to 47%) and removal rates (Fig. 2.10c). Sahariah and Chakraborty (2012) observed increase in the removals of phenol, thiocyanate (SCN-) and COD with increase in the feed NO_3^--N in anoxic fed batch reactors due to more availability of the electron acceptor. Increase in the removals of phenols and cresols was observed in a UASB reactor with increase in NO_3^--N (Ramakrishnan and Gupta, 2008).

Complete utilization of NO_3^--N occurred up to influent loading of 404 ± 4 g/(m^3.d) and effluent NO_3^--N increased beyond that load (Table 2.7). Formation of NO_2^--N started at influent NO_3^--N load of 603 ± 4 g/(m^3.d) and increased with increase in NO_3^--N load, suggesting incomplete utilization of NO_3^--N at higher loadings. NO_3^--N removal rate increased with increase in NO_3^--N loading (Fig. 2.10d), suggesting higher consumption at higher loading.

Table 2.7: Effluent concentrations of the pollutants at feed nitrate-N (NO_3^--N) variation

NO_3^--N variation feed: NO_3^--N: 0 - 2009 ± 9 mg/L, phenol: 750 ± 5, S^{2-}: 750 ± 7 mg/L, Diesel: 300 mg/L, NH_4^+-N: 350 ± 5 mg/L, SO_4^{2-}: 44 ± 3 mg/L, pH: 9.5 ± 0.1													
Reactor	NO_3^--N (mg/L)		NO_2^--N (mg/L)	COD_T (mg O_2/L)	COD_O (mg O_2/L)	Phenol (mg/L)	TH (mg/L)	S^{2-} (mg/L)	SO_4^{2-} (mg/L)	$S_2O_3^{2-}$ (mg/L)	S^0 (mg/L)	NH_4^+-N (mg/L)	pH
	Inf	Eff	Inf	Eff	Eff	Eff	Eff	Eff	Eff	Eff	Eff	Eff	Eff
R1	Absent	ND	ND	4813 ± 16	2413 ± 17	675 ± 4	950 ± 8	700 ± 9	59 ± 2	ND	47 ± 2	308 ± 3	9.3 ± 0.1
R2	254 ± 6	1 ± 1	1 ± 1	3844 ± 19	2238 ± 19	630 ± 8	870 ± 9	468 ± 5	142 ± 3	ND	247 ± 3	339 ± 7	9.2 ± 0.1
R3	505 ± 7	4 ± 1	5 ± 1	3235 ± 26	2176 ± 11	619 ± 9	828 ± 6	307 ± 7	576 ± 4	ND	268 ± 2	334 ± 2	9.1 ± 0.1
R4	754 ± 5	99 ± 2	17 ± 3	3075 ± 22	2098 ± 18	603 ± 4	779 ± 7	273 ± 8	651 ± 6	3 ± 1	277 ± 3	340 ± 2	8.9 ± 0.1
R5	1014 ± 8	131 ± 4	119 ± 8	2928 ± 27	1982 ± 16	574 ± 2	723 ± 9	237 ± 8	722 ± 4	8 ± 1	288 ± 4	333 ± 2	8.9 ± 0.1
R6	1259 ± 6	237 ± 2	123 ± 5	2654 ± 22	1792 ± 24	521 ± 8	651 ± 7	209 ± 7	889 ±11	28 ± 1	252 ± 3	332 ± 6	8.8 ± 0.1
R7	1509 ± 7	417 ± 6	155 ± 2	2468 ± 10	1624 ± 12	474 ± 5	583 ± 5	192 ± 5	987 ± 12	39 ± 2	227 ± 4	337 ± 7	8.8 ± 0.1
R8	2009 ± 9	704 ± 3	160 ± 4	2232 ± 18	1406 ± 21	412 ± 4	502 ± 6	184 ± 4	1155 ± 21	44 ± 2	179 ± 6	334 ± 2	8.7 ± 0.1

Inf: Influent, Eff: Effluent
ND: Not detectable
TH: Total hydrocarbon
COD_T: Total COD
COD_O: Organic COD

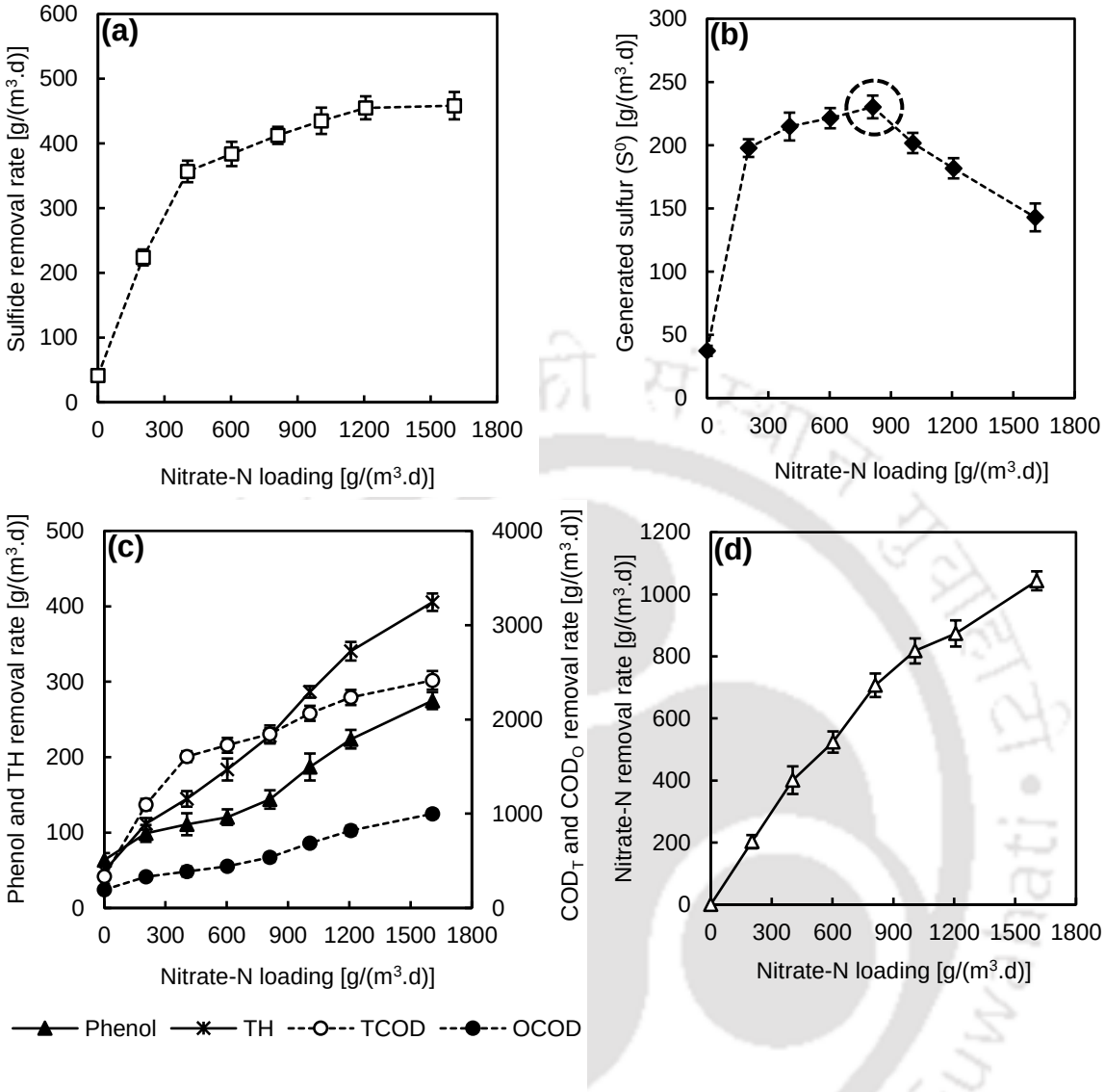

Fig. 2.10: Effect of nitrate-N loading on (a) sulfide removal rate, (b) sulfur production, (c) removal rate of organics, (d) nitrate-N removal rate

Mirbagheri et al. (2014) treated oil wastewater in an RBC with varied NO_3^--N [225-360 g/(m^3.d)] and obtained complete degradation of NO_3^--N at 8h HRT. However, accumulation of NO_2^--N started at influent NO_3^--N loading of 315 g/(m^3.d) in that study, which was lower as compared to the present study.

NO_3^--N was readily available for the degradation of both organics and S^{2-} at high loadings and continuous increase in the degradation rate was observed unlike the observations made during phenol and diesel variation studies. Hence, degradation of both organics and S^{2-} were independent of each other at high influent NO_3^--N load and availability of more NO_3^--N shifted the oxidation of S^{2-} towards SO_4^{2-}. Increase in SO_4^{2-} with increase in NO_3^--N was observed

(Table 2.7). $S_2O_3^{2-}$ increased beyond influent NO_3^--N loading of 811 ± 6 g/(m^3.d). Therefore, S^0 generation was maximum when NO_3^--N loading was 811 ± 6 g/(m^3.d) (feed NO_3^--N 1014 mg/L) and decreased with increase in influent NO_3^--N (Table 2.7). Increase in the molar ratio of NO_3^--N: S^{2-} supports complete conversion of S^{2-} to SO_4^{2-} (An et al., 2010). Jing et al. (2008) observed maximum conversion of S^{2-} to S^0 at N/S molar ratio of 0.4 in the absence of any organics and NH_4^+-N, which was equal to the stoichiometric value. Bayrakdar et al. (2015) used the similar N/S molar ratio of 0.4 during desulfurization through autotrophic denitrification in upflow fixed bed reactor by using NO_3^--N as electron acceptor in the absence of organics. However, N/S molar ratio of 3.04 provided maximum precipitation of S^0 due to utilization of NO_3^--N for the degradation of two organic co-substrates (phenol and diesel) during the present analysis. Same ratio was obtained during S^{2-} variation study for maximum S^0 generation. COD_O to NO_3^--N ratio was varied from 0.7 to 8.8 and maximum S^0 generation was observed at COD_O : NO_3^--N ratio of 1.95.

2.5 SUMMARY OF THE STUDY

Maximum conversion of sulfide as sulfur (S^0) occurred at the following influent pollutants concentrations: sulfide 750 mg/L, phenol 750 mg/L, diesel 300 mg/L, ammonia-N 350 mg/L and nitrate-N 1000 mg/L. Removal of organics was inhibited beyond phenol and diesel concentrations of 750 mg/L and 300 mg/L, respectively, at constant sulfide, ammonia-N and nitrate-N. Removals of organics and sulfide were hampered at higher ammonia-N (> 350 mg/L). Both organics and sulfide removal increased with increase in nitrate-N due to more availability of the electron donor. Maximum conversion of sulfide to sulfur (S^0) occurred at nitrate-N to sulfide molar ratio of 3.04 due to the competition posed by phenol and diesel (organics), which was higher than the stoichiometric value. Increase in nitrate-N to sulfide ratio beyond 3.04 (nitrate-N > 1000 mg/L) enhanced the oxidation of sulfide beyond S^0 to sulfate due to more available nitrate-N.

References

Abd-El-Haleem, D., Beshay, U., Abdelhamid, A. O., Moawad, H., Zaki, S. 2003. Effect of mixed nitrogen sources on biodegradation of phenol by immobilized Acinetobacter sp. strain W-17. African Journal of Chemistry 1(2): 67-70.

Ahmed, F., Fakhruddin, A. N. M., Kabir, M. M. 2018. Degradation of diesel and phenol using bacteria isolated from petroleum hydrocarbon contaminated soil. Bangladesh Journal of Scientific and Industrial Research 53(1): 53-62.

Alcantara, S., Velasco., A., Munoz, A., Cid, J., Revah, S., Razo-Flores, E. 2004. Hydrogen sulfide oxidation by a microbial consortium in a recirculation reactor system: sulfur formation under oxygen limitation and removal of phenols. Environmental Science and Technology 38: 918-923.

An, S., Tang, K., Nemat, M. 2010. Simultaneous bio desulphurization and denitrification using an oil reservoir microbial culture: Effects of sulphide loading rate and sulphide to nitrate loading ratio. Water Research 44(5): 1531-1541.

APHA, AWWA, WPCF, Standard Methods for the Examination of Water and Wastewater, 21st ed., American Public Health Association, Washington DC, 2005.

Bayrakdar, A., Tilahun, E., Baris, C. 2015. Biogas desulfurization using autotrophic denitrification process. Applied Microbiology and Biotechnology 100(2): 939-948.

Buisman, C., Post, R., Ijspeert, P., Geraats, G., Lettinga, G. 1989. Biotechnological process for sulphide removal with sulfur reclamation. Acta Biotechnologica 9: 255-267.

Can-Dogan, E., Turker, M., Dagasan, L., Arslan, A. 2010. Sulfide removal from industrial wastewaters by lithotrophic denitrification using nitrate as an electron acceptor. Water Science and Technology 62 (10): 2286-2293.

Cardoso, R. B., Sierra-Alvarez, R., Rowlette, P., Flores, E. R., Go´mez, J., Field, J. A. 2006. Sulfide oxidation under chemolithoautotrophic denitrifying conditions. Biotechnology and Bioengineering 95(6): 1148-1157.

Cardoso, R. B., Texier, A. C., Solis, A. A., Gomez, J., Flores, E. R. 2009. Phenol and sulfide oxidation in a denitrifying biofilm reactor and its microbial community analysis. Process Biochemistry 44: 23-28.

Chakraborty, S., Veeramani, H. 2006. Effect of HRT and recycle ratio on removal of cyanide, phenol, thiocyanate and ammonia in anaerobic-anoxic-aerobic continuous system. Process Biochemistry 41: 96-105.

Chavan, A., Mukherji, S. 2008. Treatment of hydrocarbon-rich wastewater using oil degrading bacteria and phototrophic microorganisms in rotating biological contactor: effect of N:P ratio. Journal of Hazardous Materials 154(1-3): 63-72.

Chong-woo, K., Park, J. S., Cho, S. ., Oh, K. J., Kim, Y. S., Kim, D. 2003. Removal of hydrogen sulfide, ammonia, and benzene by fluidized bed reactor and biofilter. Journal of Microbiology and Biotechnology 13(2): 301-304.

Diya'uddeen, B. H., Daud, W. M. A. W., Aziz, A. R. A. 2011. Treatment technologies for petroleum refinery effluents: a review. Process Safety and Environmental Protection 89 (2): 95-105.

Eiroa, M., Vilar, A., Amor, L., Kennes, C., Veiga, M. C. 2005. Biodegradation and effect of formaldehyde and phenol on the denitrification process. Water Research 39: 449-455.

Escalante, E. R., Texier, A., Lopez, F., Go´mez, J., Cervantes, F. J. 2008. Inhibition of sulfide on the simultaneous removal of nitrate and p-cresol by a denitrifying sludge. Journal of Chemical Technology and Biotechnology 83: 372-377.

Ghorbanian, M., Moussavi, G., Farzadkia, M. 2014. Investigating the performance of an up-flow anoxic fixed-bed bioreactor and a sequencing anoxic batch reactor for the biodegradation of hydrocarbons in petroleum-contaminated saline water. International Biodeterioration and Biodegradation 90: 106-114.

Ghaima, K. K., Rahal, B. S., Mohamed, M. M. 2017. Biodegradation of phenol by Pseudomonas aeruginosa isolated from soil contaminated with diesel fuel. Bioscience Research 14(4): 713-720.

Graaff, M. D., Bijmans, M. F. M., Abbas, B., Euverink, G. W., Muyzer, G., Janssen, A. J. H. 2011. Biological treatment of refinery spent caustics under halo-alkaline conditions. Bioresource Technology 102: 7257-7264.

Hariz, I. B., Halleb, A., Adhoum, N., Monser, L. 2013. Treatment of petroleum refinery sulfidic spent caustic wastes by electrocoagulation. Separation Purification Technology 107: 150-157.

Janssen, A. J. H., Lettinga, G., de Keizer, A. 1999. Removal of hydrogen sulphide from wastewater and waste gases by biological conversion to elemental sulphur. Colloidal and interfacial aspects of biologically produced sulphur particles. Colloids and Surfaces A: Physicochemical and Engineering Aspects 151(1-2): 389-397.

Jing, C., Ping, Z., Mahmood, Q. 2008. Effect of sulfide to nitrate ratios on the simultaneous anaerobic sulfide and nitrate removal. Bioresource Technology 99(13): 5520-5527.

Kleinjan, W. E., de Keizer, A., Janssen, A. J. H. 2005a. Equilibrium of the reaction between dissolved sodium sulfide and biologically produced sulfur. Colloids and Surfaces A: Physicochemical and Engineering Aspects 43(3-4): 228-237.

Liu, Y., Tay, J. H. 2001. Factors affecting nitrite buildup in nitrifying biofilm reactor. Journal of Environmental Science and Health 36: 1027-1040.

Liu, C., Han, K., Lee, D., Wang, Q. 2016a. Simultaneous biological removal of phenol, sulfide and nitrate using expanded granular sludge bed reactor. Applied Microbiology and Biotechnology 100: 4211-4217.

Lora, P. O., Flores, E. R. 2004. Anaerobic biodegradation of phenol in sulfide-rich media. Journal of Chemical Technology and Biotechnology 79: 554-561.

Mahmood, Q., Zheng, P., Hayat, Y., Islam, E., Wu, D., Ren-Cun, J. 2008. Effect of pH on anoxic sulfide oxidizing reactor performance. Bioresource Technology 99: 3291-3296.

Margesin, R., Schinner, F. 2001. Biodegradation and bioremediation of hydrocarbons in extreme environments. Applied microbiology and biotechnology 56: 650-663.

Mirbagheri, S. A., Ahmadi, S., Biglari-joo, N. 2014. Denitrification of nitrate-contaminated groundwater in an anoxic rotating biological contactor: a case study. Desalination and Water Treatment 57(10): 4694-4700.

Moraes, B. S., Orru, J. G. T., Foresti, E. 2013. Nitrogen and sulfide removal from effluent of UASAB reactor in a sequencing fed-batch biofilm reactor under intermittent aeration. Journal of Biotechnology 164 (3): 378-385.

Moussavi, G., Shekhoohiyan, S., Naddafi, K. 2016. Anoxic biodegradation of petroleum hydrocarbons in saline media using denitrifer biogranules. Ecotoxicology and Environment Safety 129: 51-56.

Müller, T., Walter, B., Wirtz, A., Burkovski, A. 2006. Ammonium toxicity in bacteria. Current Microbiology 52: 400-406.

Park, J., Byun, I., Park, S., Lee, J., Park, S., Park, T., Lee, T. 2009. Use of spent sulfidic caustic for autotrophic denitrification in the biological nitrogen removal processes: Lab-scale and pilot-scale experiments. Journal of Industrial Engineering and Chemistry 15: 316-322.

Ramakrishnan, A., Gupta, S.K. 2008. Effect of COD/NO_3^--N ratio on the performance of a hybrid UASB reactor treating phenolic wastewater. Desalination 232: 123-138.

Sahariah, B. P., Chakraborty, S. 2011. Kinetic analysis of phenol, thiocyanate and ammonia-nitrogen removals in an anaerobic-anoxic-aerobic moving bed bioreactor system. Journal of Hazardous Materials 190: 260-267.

Sahariah, B. P., Chakraborty, S. 2012. Effect of feed concentration and hydraulic retention time on removal of phenol, thiocyanate, and nitrate-nitrogen in anoxic fed batch moving bed reactor. Toxicological and Environmental Chemistry 94(9): 1629-1645.

Sharma, N. K., Philip, L. 2014. Effect of cyanide on phenolics and aromatic hydrocarbons biodegradation under anaerobic and anoxic conditions. Chemical Engineering Journal 256: 255-267.

Thomas, S., Sarfaraz, S., Mishra, L. C., Iyengar, L. 2002. Degradation of phenol and phenolic compounds by defined denitrifying bacterial culture. World journal of microbiology and biotechnology 18: 57-63.

Vadivelu, V. M., Keller, J., Yuan, Z. 2007. Effect of free ammonia on the respiration and growth processes of an enriched nitrobacter culture. Water Research 41: 826-834.

Xu, J., Fan, Y., Li, Z. 2016. Effect of pH on elemental sulfur conversion and microbial communities by autotrophic simultaneous desulfurization and denitrification. Environmental Technology 37(23): 3014-3023.

3

CHAPTER

EFFECT OF AGITATION SPEED AND HYDRAULIC RETENTION TIME ON THE PERFORMANCE OF ANOXIC-AEROBIC SEQUENTIAL MOVING BED REACTORS

CHAPTER 3

EFFECT OF AGITATION SPEED AND HYDRAULIC RETENTION TIME ON THE PERFORMANCE OF ANOXIC-AEROBIC SEQUENTIAL MOVING BED REACTORS

3.1 INTRODUCTION

Sulfide in refinery wastewater is volatile in nature and may escape to atmosphere during aerobic treatment prior to biodegradation. Sulfide present in refinery wastewater inhibits methanogenic activity in anaerobic reactor (Lens et al., 1998). Anoxic treatment of refinery wastewater could be a better alternative than aerobic and anaerobic ones, to overcome toxicity on anaerobic biomass and to prevent volatilization of sulfide.

Several researchers have reported successful biodegradation of sulfide in anoxic condition with end product as sulfate/elemental sulfur either in the absence of organic (Jing et al., 2010) or in the presence of acetate and methanol, which are absent in petroleum refinery wastewater (An et al., 2010). In refinery effluent, diesel is many times associated with emulsifier at high pH (> 9.0), which makes biodegradation further difficult (Zolfaghari et al., 2016). Moussavi et al. (2016) reported successful degradation of crude diesel in anoxic granular reactor without sulfide and emulsifier at pH 7.5. Liu et al. (2016) reported anoxic degradation of phenol, sulfide in expanded granular sludge bed reactor without hydrocarbon in feed at pH 7.5. Literature report on biodegradation of high sulfide containing alkaline wastewater (pH > 9.0) in the presence of phenol and other hydrocarbons is scanty.

For the treatment of wastewater having sulfide, phenol, diesel and ammonia, sequential anoxic-aerobic reactors may be highly suitable, where volatile sulfide can be oxidized using nitrate as electron acceptor in the anoxic reactor along with partial removal of phenol and diesel. Ammonia and residual organic removal may be achieved in aerobic reactor.

In the present work, treatment of synthetic petroleum refinery wastewater containing emulsified diesel, phenol and sulfide was attempted in an anoxic vertical disc reactor (A1) and the effluent from the disc reactor was treated in aerobic moving bed reactor (A2). In sulfur rich wastewater, sulfide conversion to elemental sulfur and recovery of elemental sulfur are highly

desirable options. A conical hopper bottom was provided for better separation of elemental sulfur from the system by centrifugal action of the moving discs in reactor A1. The objective of the present study was simultaneous biodegradation of sulfide, phenol, emulsified diesel and ammonia containing synthetic petroleum refinery wastewater in anoxic-aerobic sequential reactors and sulfur recovery from sulfide. Mixing speed and hydraulic retention time (HRT) of anoxic disc reactor and HRT of aerobic reactor were considered as variable parameters.

3.2 MATERIALS AND METHODS

3.2.1 Chemicals and Reagents

Chemicals and reagents used in this study were of AR grade and purchased from either Merck, India or CDH, India as mentioned in section 2.2.1. Nonylphenol monoethoxylate (9M) used as surfactant was purchased from Sigma-Aldrich and a stock solution of 0.9M was prepared using mili-Q water. Feed to the reactors was prepared with tap water (pH 8.0 ± 0.2) and all the stock solutions were prepared by milli-Q water (pH 7.0 ± 0.1).

3.2.2 Experimental setup and reactor operation

A1 was fabricated out of a Perspex tube. A schematic diagram of the reactor assembly is given in Fig. 3.1 and dimensions are summarized in Appendix F. Photograph of the reactor system is given in Fig. 3.2. The reactor was of 70 cm height and 15 cm diameter with working volume of 10L. The bottom of the reactor was made of a tapered shaped structure for an effective collection of solids. The disc bed consisted of 41 circular discs (10 cm diameter and 1 cm height of each disc) made out of polyurethane foam. A stainless steel shaft (0.9 cm diameter) was passed through the middle of the discs. Disc holders were provided at the top and bottom of the axial shaft to prevent the discs from getting out of the axial shaft. The shaft with holders and PUF discs were passed through an airtight bearing and attached to a mechanical stirrer (Model: REMI 126D) which provided clockwise rotational motion to the disc bed. Airtight bearing provided the smooth revolution of the bed. Temperature (27 ± 3 ºC) of the reactor was controlled by a hot air blower. A gas collection port was provided at the top of the reactor and gas was collected by water displacement method.

A2 was made using Perspex tube (height 33 cm and diameter 15 cm) of 5L working volume. Sponge cubes (1550 numbers, 60 g, each cube of size 1 cm × 1 cm × 1 cm, density 0.039 g/cm^3, porosity 0.81, specific surface area 600 m^2/m^3) were added in this reactor to support the biomass. Bottom of A2 was made tapered for effective collection of sludge. Airflow

was provided at 2 L/min by a small aquarium pump, purchased from a local aquarium shop, which provided movement to the cubes. Airflow was controlled by a rotameter (CWG, India).

Feeding to both the reactors was done by a peristaltic pump (Miclins PP 20x, 100 mL/min) in up flow mode from the bottom port of the reactors. Effluent was released from the same port. Sampling ports were provided at pre-determined heights in both of the reactors. Reactors were operated in sequential batch mode and operational conditions are summarized in Table 3.1. HRT (d), loading rate [g/(m^3.d)], removal (%) and removal rate [g/(m^3.d)] were calculated by equations (2.1), (2.2), (2.3) and (2.4) respectively as mentioned in Chapter 2.

Table 3.1: Operational conditions of anoxic and aerobic reactors during agitation speed and hydraulic retention time (HRT) variation

Reactor	Day	Variable parameter	Speed (rpm)	HRT (day)	Decant volume (L)	Decant time (min)	Fill time (min)	Reaction time (min)	Cycle time (h)
Anoxic reactor (A1)	106 - 210	Speed	0	1.25	8	30	80	1330	24
			20						
			40						
			60						
			80						
			100						
			120						
	211 - 330	HRT	20	1.25	8	30	80	1330	
				1.5	6.67	25	67	1348	
				2	5	20	50	1370	
				2.5	4	15	40	1385	
Aerobic reactor (A2)	331 - 410	HRT	Airflow rate 2L/min	0.21	4	15	40	185	4
				0.31				305	6
				0.42				425	8
				0.63				665	12
				0.83				905	16

3.2.3 Seed sludge

For A1, inoculum was collected from the anaerobic storage tank of Indian Oil Corporation Limited (IOCL), Noonmati, Assam, India. The collected sludge had total solids of 7.52 ± 0.21 g/L and volatile solids of 5.02 ± 0.24 g/L. Six liter sludge was used in A1. For A2, inoculum was collected from the activated sludge tank of Indian Oil Corporation Limited (IOCL), Noonmati, Assam, India. The collected sludge had total and volatile solids of 9.04 ± 0.23 g/L and 8.54 ± 0.23 g/L, respectively. Three liters of sludge was used in A2. After sludge was introduced, remaining volume was made up with tap water. Seed sludge properties are mentioned in Appendix G.

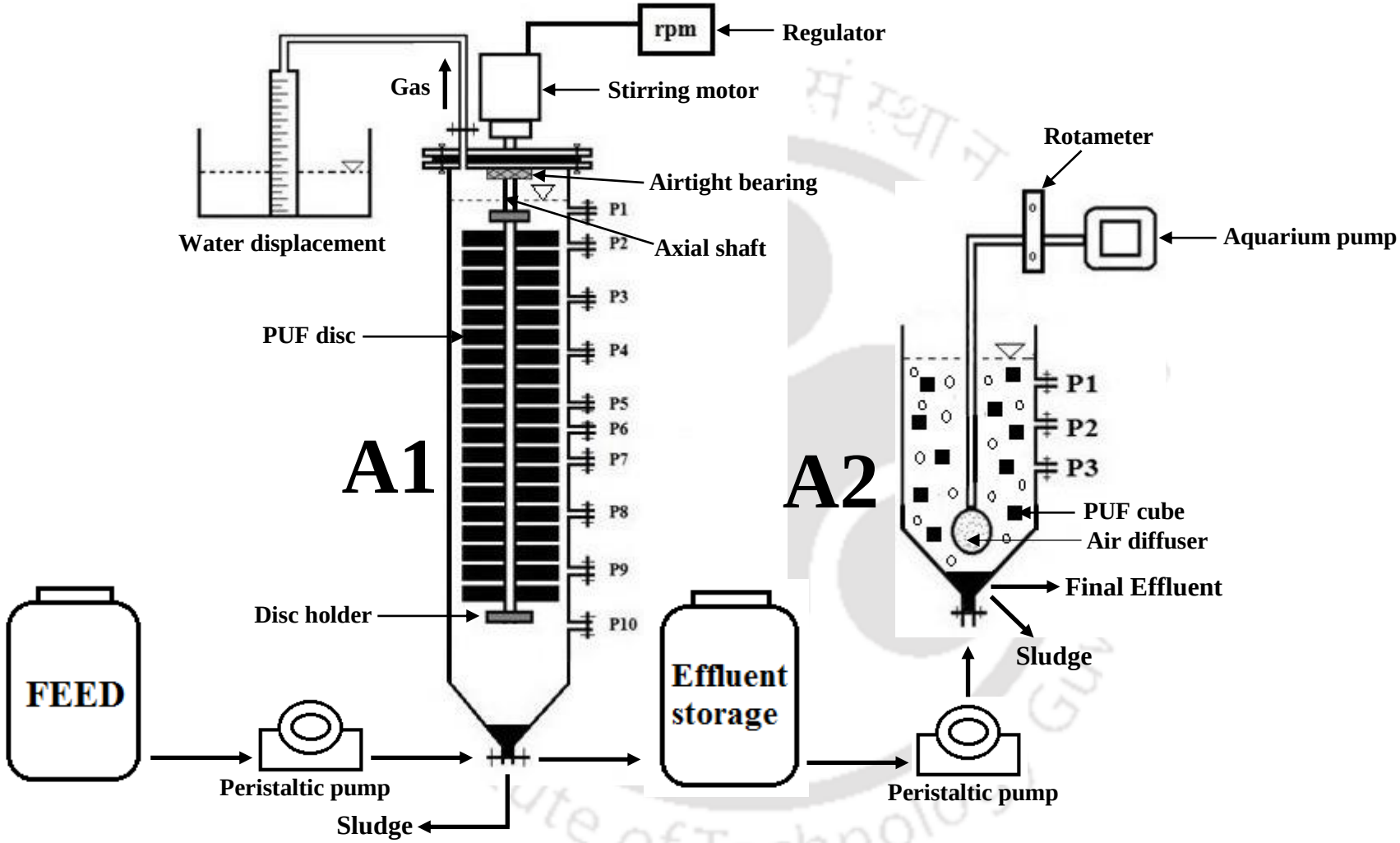

Fig. 3.1: Schematic diagram of anoxic (A1) - aerobic (A2) sequential moving bed system during combined treatment

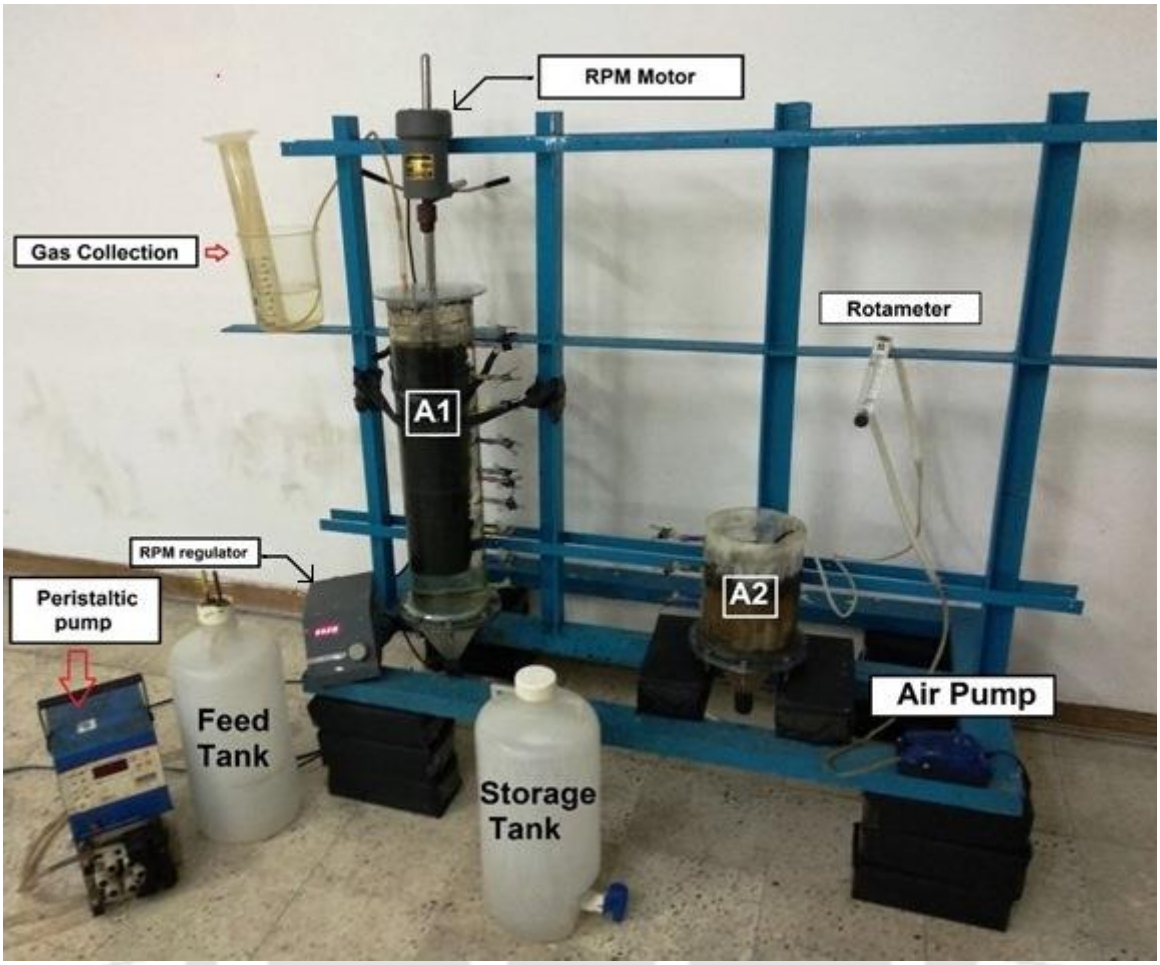

Fig. 3.2: Photographic image of the anoxic (A1)-aerobic (A2) reactor setup

3.2.4 Emulsification of diesel

Emulsifier required to keep diesel distributed inside the reactor was determined by adding different concentrations of surfactant (1.0, 0.5, 0.2 and 0.1 mM) to 300 mg/L of diesel and mixed thoroughly. The solution was kept in A1 without disc and biomass for 72h. Samples were collected from the bottom most port and COD was measured instantly and after 72h. At emulsifier concentration ≥ 0.2 mM, COD was similar for the samples collected instantly and after 72h (Fig. 3.3a). Diesel lost its mixed regime at surfactant < 0.2 mM and accumulated on the water surface. Therefore, 0.2 mM concentration was chosen for the emulsification of diesel.

3.2.5 Optimization of airflow rate in aerobic reactor (A2)

Emulsifiers/surfactants have a tendency to vaporize by foaming at high air flowrate. Air flowrate was optimized by supplying air at different flow rates (1, 2, 3, 4, 5 L/min) through a rotameter (CWG, India) to a solution of emulsified diesel for 24h kept in A2 (without biomass).

Loss of surfactant was minimum (5%) at flowrates of 1 and 2 L/min and loss was more beyond 2L/min (Fig. 3.3b). Hence, 2 L/min was chosen as the optimum airflow rate and this flowrate was observed to be sufficient to keep the biomass-loaded PUF cubes move inside A2.

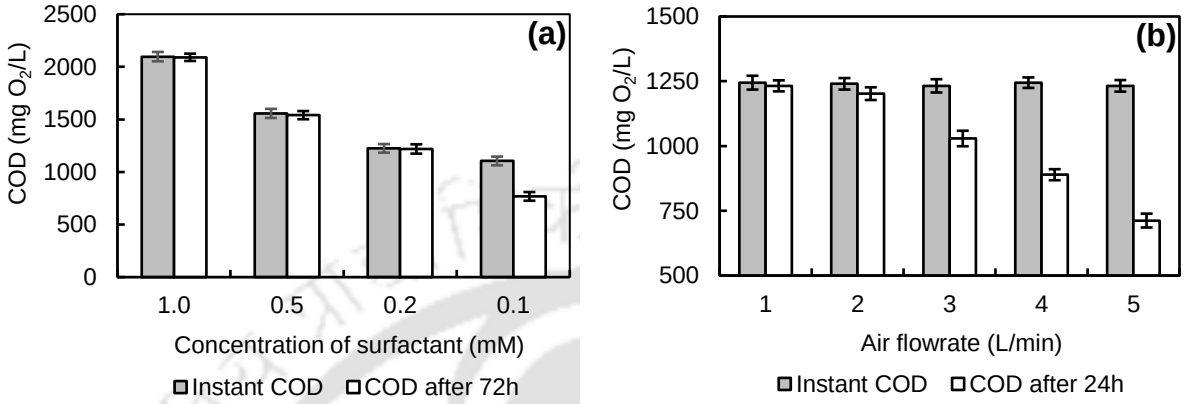

Fig. 3.3: (a) effect of surfactant concentration on COD, (b) effect of airflow rate on the COD of emulsified diesel (300 mg/L)

3.2.6 Synthetic feed

Feed concentrations were kept the same at which maximum S^0 generation was achieved (optimized in Chapter 2). Influent to A1 consisted of phenol (750 mg/L as C_6H_5OH), S^{2-} (750 mg/L as $Na_2S.xH_2O$), diesel (300 mg/L), NH_4^+-N (350 mg/L as NH_4Cl) and NO_3^--N (1000 mg/L as KNO_3). Diesel was emulsified by using a surfactant (nonylphenolmonoethoxylate) for its better distribution in the influent. To avoid abiotic loss, freshly prepared feed without emulsified diesel and S^{2-} was purged with N_2 gas and then emulsified diesel and S^{2-} were added just before the start of feeding operation. Feed was supplemented with phosphate buffer (1 mL/L), yeast extract (10 mg/L) and trace metals solution (1 mL/L) as mentioned in section 2.2.4 of Chapter 2. Feed pH was 9.5 ± 0.1 during the whole study due to the presence of Na_2S.

3.2.7 Acclimatization

Reactor A1 was fed with phenol, NH_4^+-N and NO_3^--N. Concentrations of pollutants were increased gradually and at each concentration, the reactor was operated for 5 days. Phenol concentration was increased from 5 to 10, 20, 50, 75 and 100 mg/L in 26 days and then it was increased by 50 mg/L after each 5 days up to 750 mg/L. NH_4^+-N concentration was increased from 10–20–30 mg/L up to 15th day and then increased by 25 mg/L after each 5 days. Initially 100 mg/L of NO_3^--N was added and after 5 days, its concentration was increased by 100 mg/L in each feed. Sulfide (10 mg/L) was added in A1 on 46th day and was increased to 20, 50 and

100 mg/L after each 5 days. Then increment was 100 mg/L up to 750 mg/L. Emulsified diesel of 10 mg/L was introduced in A1 on 71st day and increment was 50 mg/L after each 5 days.

Acclimatization of the aerobic reactor A2 was initialized with phenol (50 mg/L), emulsified diesel (15 mg/L), NH_4^+- N (50 mg/L) and $S_2O_3^{2-}$ (10 mg/L) on day 1. Increments were as follows: phenol 50 mg/L, NH_4^+-N 50 mg/L, emulsified diesel 100 mg/L and $S_2O_3^{2-}$ 10 mg/L. After each increment, A2 was operated for 5 days. Total acclimatization period was 105 days for A1 and 50 days for A2. Image of virgin PUF disc (Fig. 3.4a), biomass loaded PUF disc from A1 (Fig. 3.4b), virgin PUF cube (Fig. 3.4c) and biomass loaded PUF cube from A2 (Fig. 3.4d) are illustrated below.

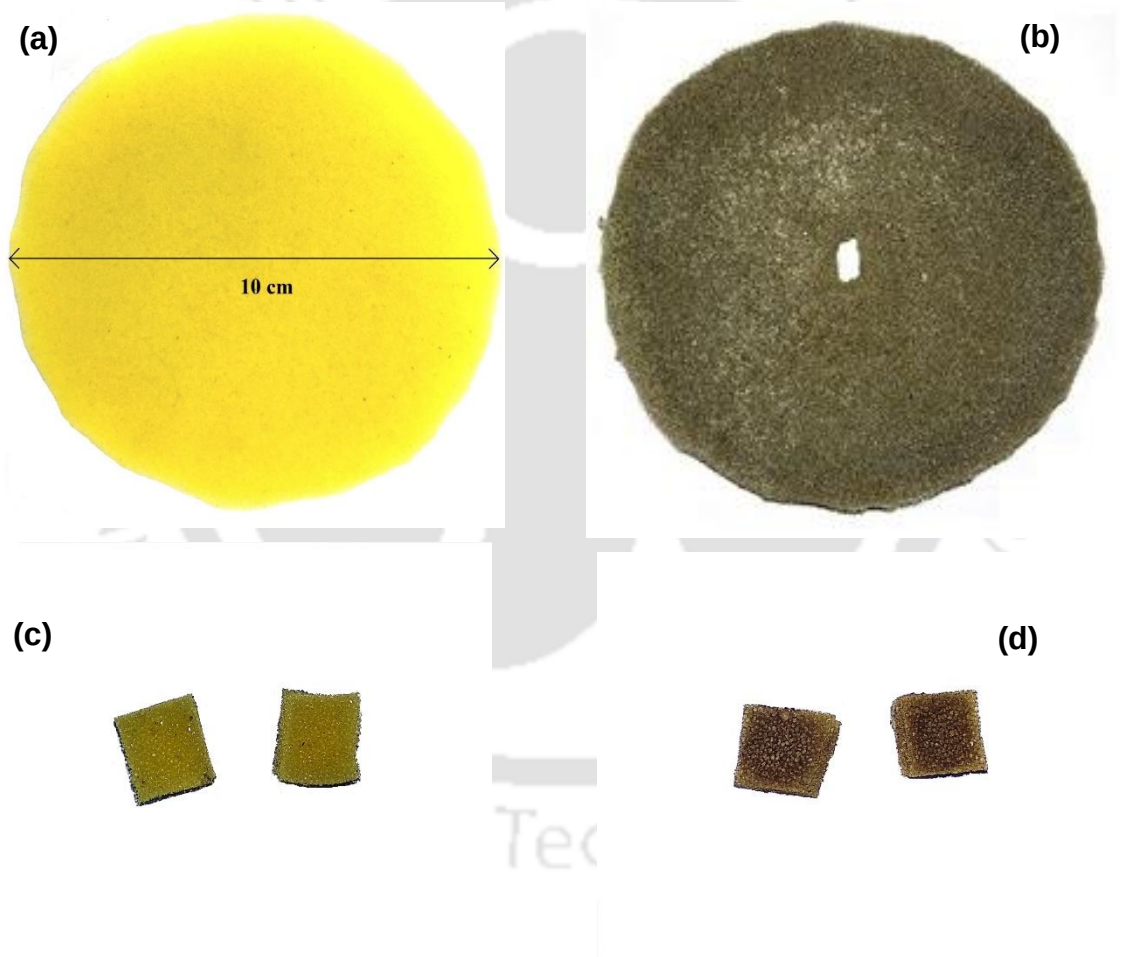

Fig. 3.4: (a) virgin PUF disc, (b) PUF disc loaded with biomass, (c) virgin PUF cube, (d) PUF cube loaded with biomass

3.2.8 Analytical procedure

Analysis of phenol, S^{2-}, SO_4^{2-}, $S_2O_3^{2-}$, emulsified diesel as total hydrocarbon, NO_3^--N, NO_2^--N, COD in the samples were done as per section 2.2.6 in Chapter 2.

3.3 RESULTS AND DISCUSSIONS

3.3.1 Performance of anoxic disc-bed reactor (A1)

3.3.1.1 Effect of mixing speed on pollutant degradation

Anoxic disc reactor (A1) was initially operated without agitation (105 - 120th day) and then rotational speed was increased from 20 to 120 rpm stepwise. Effluent concentrations of phenol (Fig. 3.5a), COD_O (Fig. 3.5b), TH (Fig. 3.5c) and NO_3^--N (Fig. 3.5d) at varying mixing speed are shown in Fig. 3.5. When there was no mixing, 18% COD_O and 17% TH removals were observed along with 60% denitrification (ΣNO_3^--N + NO_2^--N). When mixing speed was increased to 20 rpm, a steep decrease in effluent concentration was observed for all pollutants. With further increase in the mixing speed above 20 rpm, no significant change in effluent concentration was observed. NH_4^+-N of 350 ± 5 mg/L as influent was provided to the reactor and no removal was achieved throughout the study.

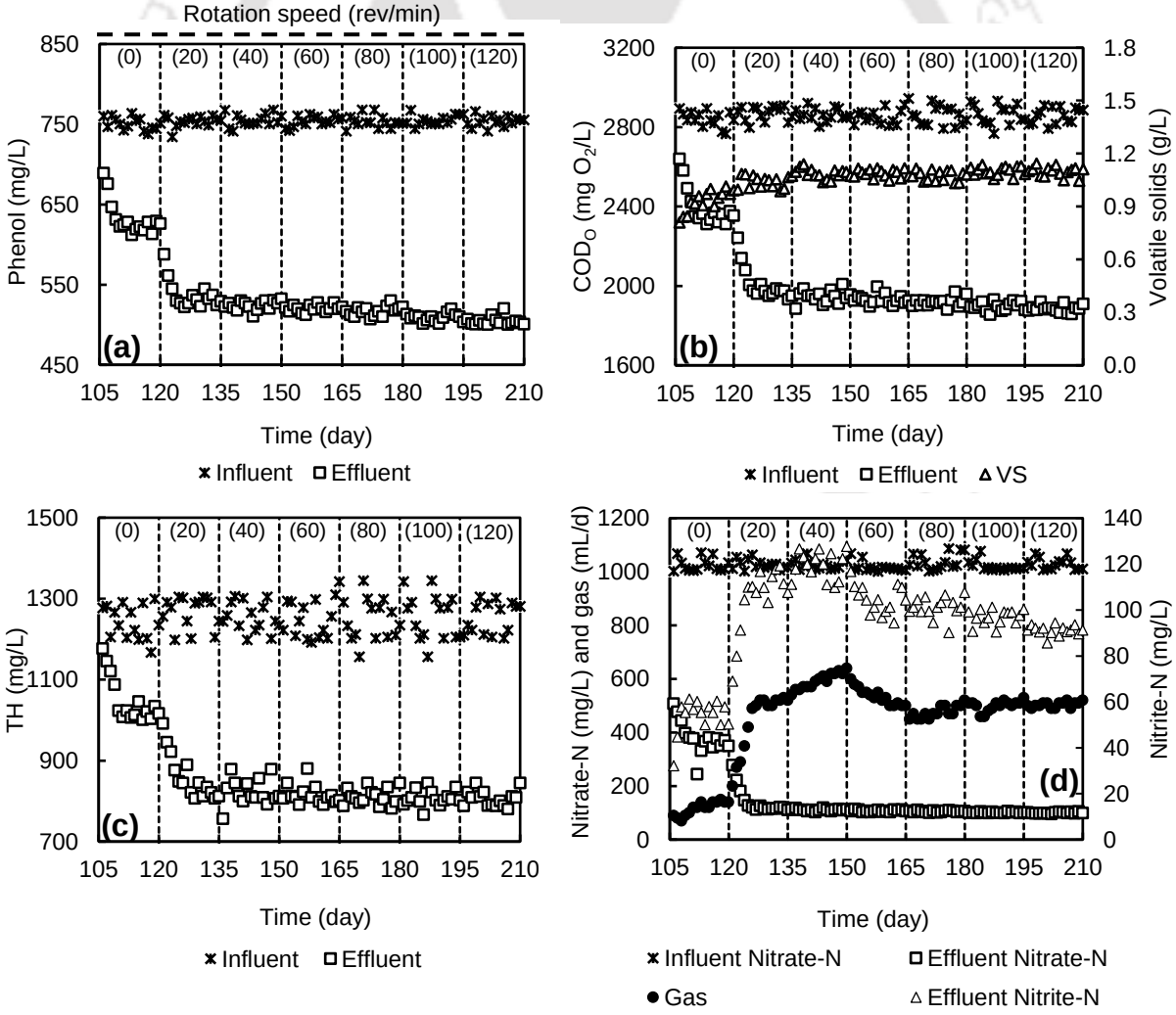

Fig. 3.5: Effect of agitation speed of anoxic reactor on the degradation of: (a) phenol, (b) COD_O, (c) TH, (d) nitrate-N and gas generation

Gas generation (mL/d) is shown in Fig. 3.5d. At no mixing condition, gas generation was less (average 134 ± 4 mL/d) and increased by threefold to 454 ± 6 mL/d at mixing speed of 20 rpm and increased further to 590 ± 11 mL/d at 40 rpm speed. In the mixing speed of 60–120 rpm, daily gas generation was almost constant at 530-590 mL/d. Initially, higher speed favored dispersion and release of gas bubbles from sludge and gas generation increased.

With an increase in mixing speed from 0 to 20 rpm, removal efficiency of A1 increased. Higher mixing speed was responsible for higher mass transfer of pollutants, resulting in more available substrate to microorganisms with higher degradation of all pollutants. Therefore, 20 rpm of rotational speed was adequate to transfer substrate to the biofilm. Lu et al. (1997) studied effect of rotational speed on performance of an anaerobic rotating biological contactor (RBC) and reported increase in COD removal efficiency (45% to 75%) with an increase in speed from 0 to 12 rpm and efficiency decreased when speed was more than 12 rpm.

With an increase in rotational speed, effluent SO_4^{2-} increased by more than two-fold (445 ± 27 to 1035 ± 27 mg/L), though S^{2-} removal remained the same when rotational speed was 20 rpm and above (Fig. 3.6a). Small amount of $S_2O_3^{2-}$ was also generated in the reactor (4 -19 mg/L), and increased with mixing speed. Cardoso et al. (2009) also observed formation of $S_2O_3^{2-}$ from S^{2-} oxidation in oxygen limiting conditions. Generated SO_4^{2-} was 38-62% and $S_2O_3^{2-}$ was 0-2% of removed S^{2-} and increased with increase in the mixing speed. Formation of S^0 initially increased at 20 rpm and decreased at higher speeds (Fig. 3.6b) as more S^{2-} was converted to SO_4^{2-}. Hence, conversion of removed S^{2-} to S^0 decreased from 62% to 35%.

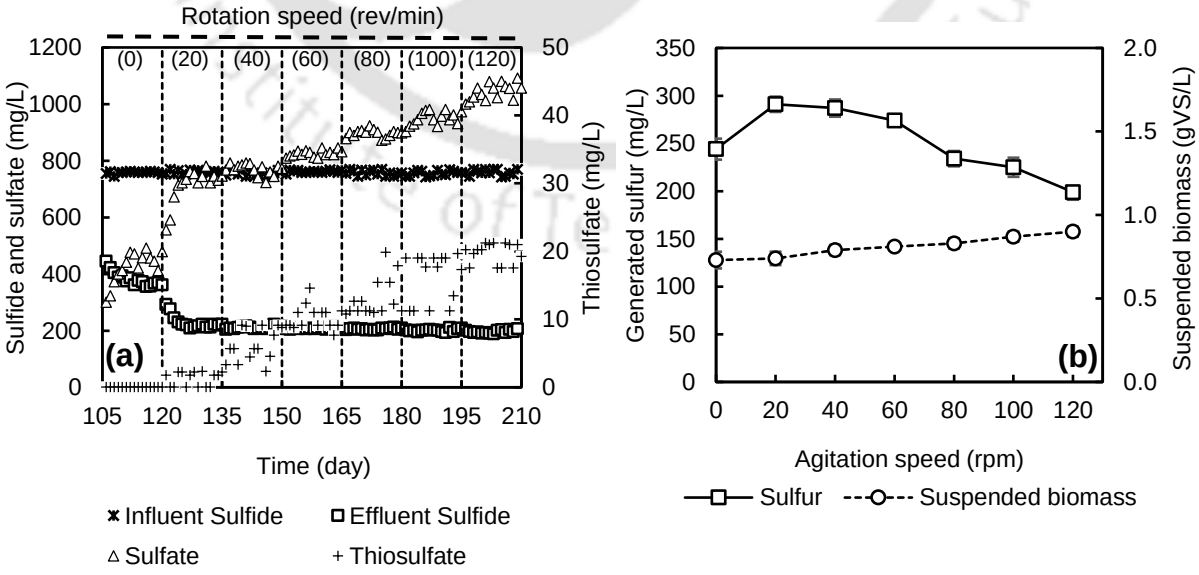

Fig. 3.6: Effect of agitation speed of anoxic reactor (a) on the degradation of sulfide, (b) generation of sulfur and suspended biomass

In the present study, when mixing was not done/mixing speed was very less, S^0 produced from S^{2-} settled as solid at the bottom of the reactor and unavailable for further oxidation to SO_4^{2-}, even though NO_3^--N was available; hence SO_4^{2-} formation in A1 increased with mixing speed. Removal of S^{2-}, denitrification and partial removals of phenol, TH and COD_O suggest that autotrophic and heterotrophic denitrification occurred simultaneously in A1.

Mass of suspended volatile solids (VS) collected from the bottom of the reactor is shown in Fig. 3.5b. With increase in mixing speed, mass of suspended VS increased. These VS consisted of sloughed biomass and elemental S^0, since both volatilized at 550 ºC. From VS values, calculated elemental S^0 values from the sulfur mass balance were subtracted and average biomass at varying mixing speed is shown in Fig. 3.6b. Suspended biomass concentration increased slightly from 0.72 ± 0.02 to 0.89 ± 0.04 g/L with an increase in mixing speed. Higher mixing speed resulted in higher shear force and more sloughing of biomass from disc surface, which is in agreement with Lu et al. (1997).

3.3.1.2 Effect of hydraulic retention time

Effect of hydraulic retention time (HRT) on the degradation of the pollutants in the disc reactor was studied for a period of 120 days (from day 161 to 281). HRT of the reactor was varied at four levels: 1.25, 1.5, 2 and 2.5 days. At each HRT, the reactor was operated for 30 days. There was transient phase for initial 10 - 15 days and then the reactor became stable. Influent pH was 9.5 ± 0.1 and insignificant change in pH was observed during the HRT study. HRT study was carried out using influent phenol 750 ± 5 mg/L, total hydrocarbons (TH) 1242 ± 16 mg/L; S^{2-} 750 ± 7 mg/L, COD_O 2850 ± 19 mg O_2/L and NO_3^--N of 1000 ± 10 mg/L.

Effluent phenol (Fig. 3.7a), TH (Fig. 3.7b), COD_O (Fig. 3.7c) and NO_3^--N (Fig. 3.7d) decreased with increase in HRT. Maximum removals of phenol, total hydrocarbon and COD of 52%, 60% and 61% were observed at 2.5d HRT at respective loadings of 302 ± 2, 507 ± 4 and 1107 ± 5 g/(m^3.d). Removal rate of total hydrocarbon was slightly higher than that of phenol, since total hydrocarbon was a combination of phenol and diesel along with hydrocarbons generated from diesel degradation. NO_3^--N was completely exhausted in A1 when HRT was 2.5d. 9-13% of feed NO_3^--N was converted to NO_2^--N as intermediate (Fig. 3.7d). Initially, with increase in disc reactor HRT up to 2d, effluent NO_2^--N concentration increased and beyond 2d, decreased. Hence, NO_2^--N reduction was kinetically slower than NO_3^--N reduction. Overall denitrification in A1 was 90% at loading of 400 ± 5 g/(m^3.d). Gas generation (Fig. 3.7d) also increased due to degradations of more COD and NO_3^--N.

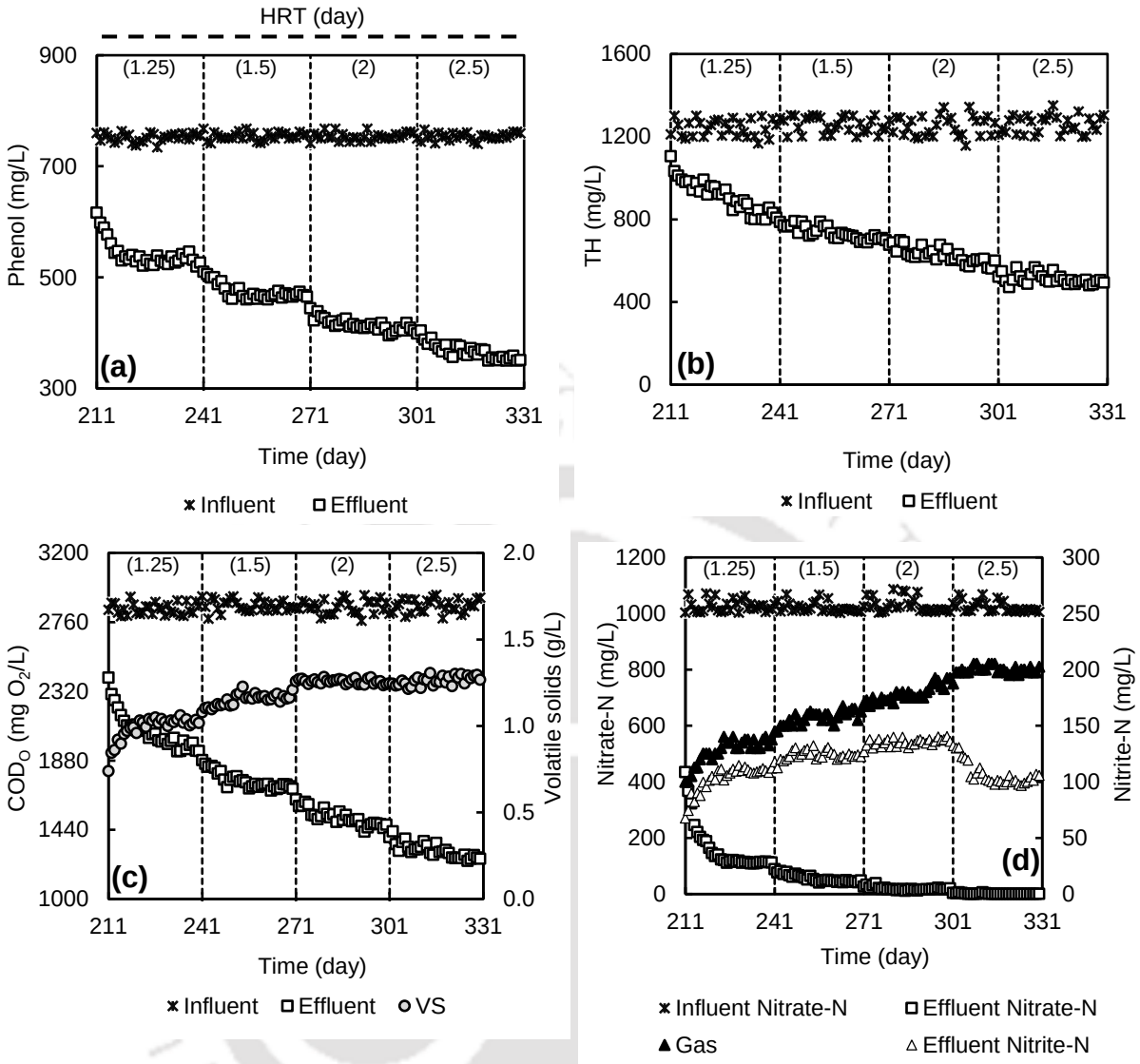

Fig. 3.7: Effect of HRT of anoxic reactor on the degradation of: (a) phenol, (b) TH, (c) COD, (d) nitrate-N and gas generation

At HRT of 2.5d, effluent S^{2-} was not detectable from influent loading of 300 ± 3 g/(m^3.d) (Fig. 3.8a). Conversion of removed S^{2-} to SO_4^{2-} was 45-56%, 1-3% of removed S^{2-} was in the form of $S_2O_3^{2-}$ and remaining 45-66% was S^0. In Fig. 3.8b, suspended biomass and S^0 at varying HRTs are shown. It can be seen that suspended biomass concentration increased from 0.75 ± 0.02 to 0.86 ± 0.03 g/L with an increase in HRT. The higher the HRT of the disc reactor, the lower was elemental S^0. This suggests that initially S^{2-} was oxidized using NO_3^- as electron acceptor to S^0 and then with an increase in HRT, this S^0 was further oxidized to SO_4^{2-}. The present observation is in good agreement with literature report (An et al., 2010) where short residence time favored formation of S^0 over SO_4^{2-} in the effluent. At A1 HRT of 2.5d, S^{2-} removal was complete with 40-45% recovery of S^{2-} in the form of S^0, but effluent had phenol

(410 ± 4 mg/L), TH (600 ± 9 mg/L), COD_O (1100 ± 11 mg/L) and NH_4^+-N of 350 ± 5 mg/L. With further increase of disc reactor HRT, effluent phenol, COD_O and TH decreased, but no removal of NH_4^+-N was achieved. The optimum HRT of the anoxic disc reactor was 2.5d with complete removal of volatile S^{2-}, and further treatment is suggested in a downstream aerobic reactor.

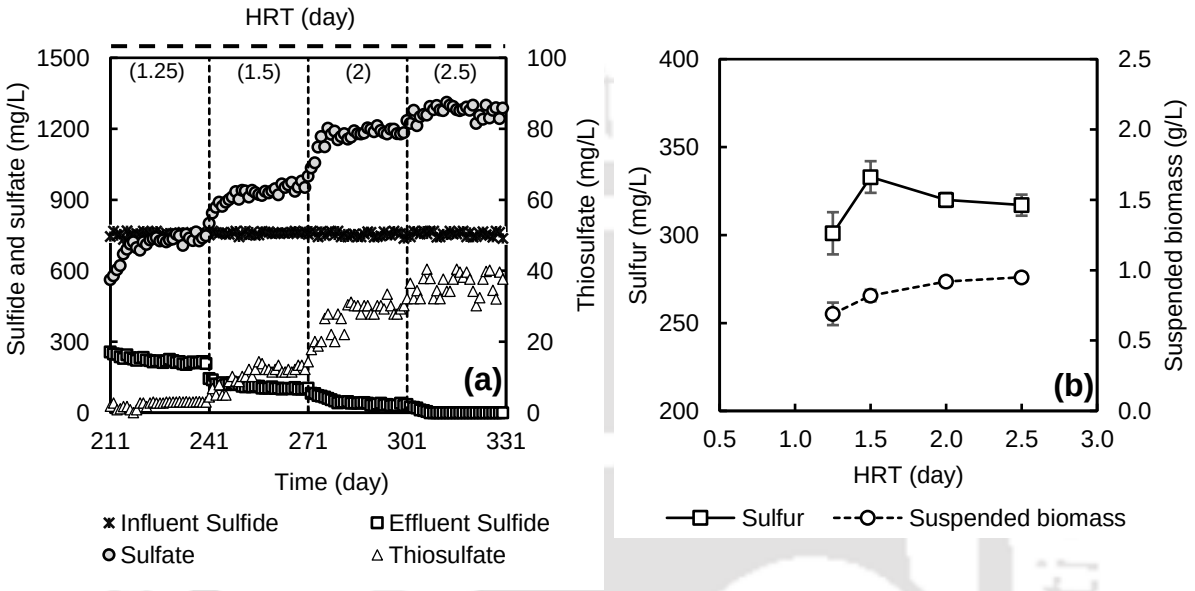

Fig. 3.8: Effect of HRT of anoxic reactor (a) on the degradation of sulfide, (b) generation of sulfur and suspended biomass

Cardoso et al. (2009) studied complete phenol and S^{2-} removals in an inverse fluidized bed reactor at phenol and S^{2-} loadings of 180 and 37 g/(m^3.d), respectively. An et al. (2010) reported simultaneous S^{2-} and NO_3^--N removals of 95% and 98%, respectively, at loadings of 1612 gS^{2-}/(m^3.d) and 1361 g NO_3^--N/(m^3.d) in the presence of acetate in a continuous stirred reactor. Ghorbanian et al. (2014) reported complete removal of hydrocarbons in an anoxic up flow fixed bed reactor at loading of 1450 g/(m^3.d), in absence of S^{2-} in feed. Moussavi et al. (2016) reported complete removal of hydrocarbon (added as kerosene) at influent loading of 2200 g/(m^3.d) without any S^{2-}. An anoxic expanded granular sludge bed reactor (Liu et al., 2016) was reported for complete S^{2-}, phenol removal and 92% NO_3^--N removal at loadings of 600 g S^{2-}/(m^3.d), 585 g phenol/(m^3.d) and 900 gNO_3^--N/(m^3.d), respectively, without any hydrocarbon feed and feed pH was adjusted to 7.5. Adjustment of feed to neutral level requires high quantity of acid/buffers for industrial wastewater having large volume. The present study was carried out at feed pH 9.5 ± 0.1, without pH adjustment.

Profile study of the reactors was done by drawing effluent samples from A1 from the ports provided at predetermined interval of heights during the HRT variation study. Ports were numbered as P1 to P10 from top to bottom (Fig. 3.1). Effluent concentrations with respect to port numbers at different HRTs are illustrated in Fig. 3.7. Effluent phenol (Fig. 3.9a), total hydrocarbon (Fig. 3.9b), S^{2-} (Fig. 3.9c) and NO_3^--N (Fig. 3.9d) remained unchanged with the height of the reactor. This suggests, there was complete mixed condition of the feed inside the reactor and microbial distribution with height of the biomass bed was uniform.

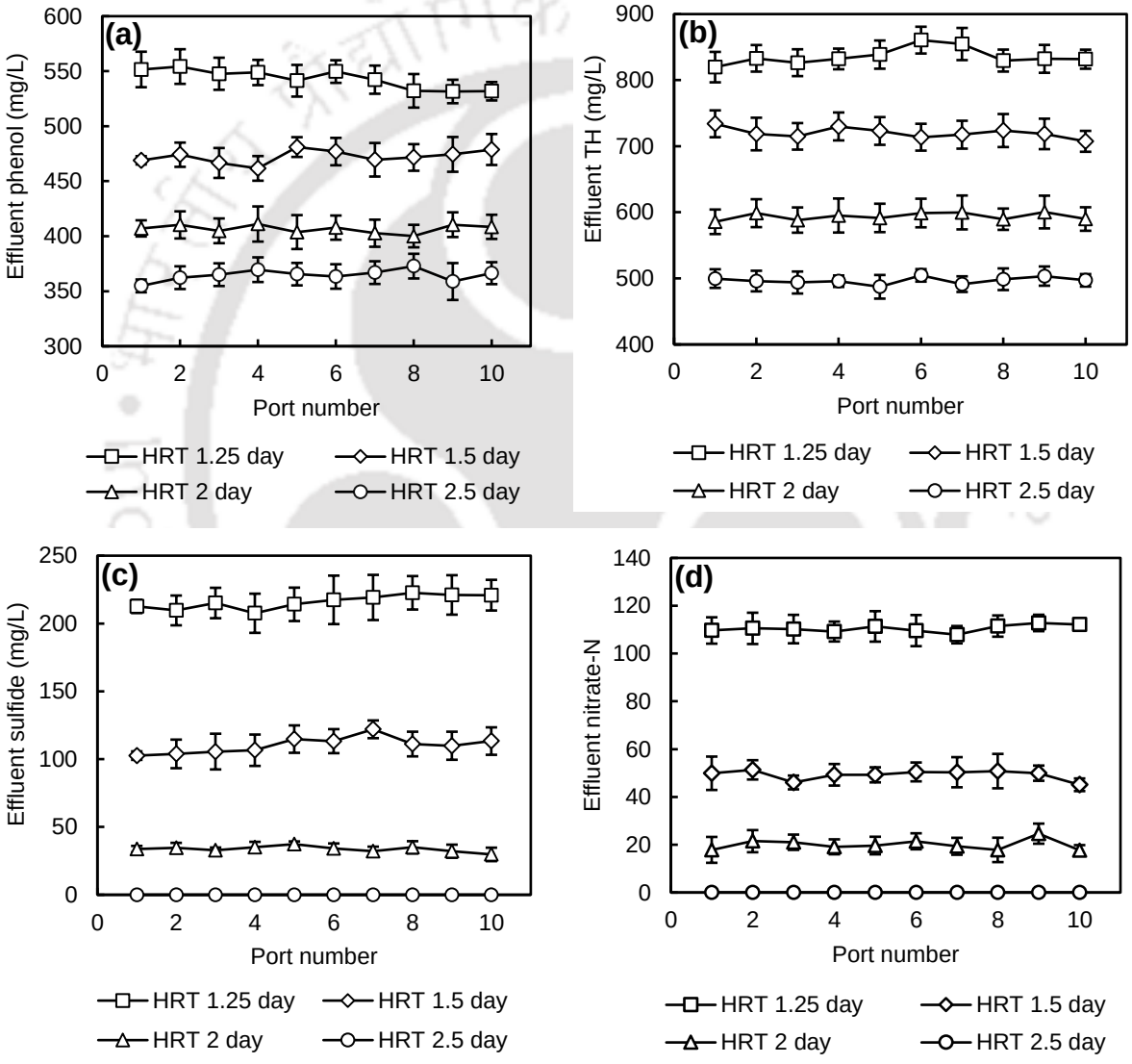

Fig. 3.9: Effluent concentrations of (a) phenol, (b) TH, (c) sulfide, (d) nitrate-N of anoxic reactor (A1) at different heights during profile sampling analysis

3.3.2 Performance of aerobic reactor A2 (Effect of hydraulic retention time)

Effect of hydraulic retention time for the removal of remaining pollutants from the effluent of the anoxic reactor was studied at five different levels: 5, 7.5, 10, 15 and 20h HRT and studied for 16 days at each HRT in A2. Simulated synthetic wastewater as per the effluent of the anoxic reactor at 2.5d HRT (phenol 450 ± 5 mg/L, TH 650 ± 7 mg/L, NH_4^+-N 350 ± 5 mg/L, COD_O 1650 ± 16 mg/L, $S_2O_3^{2-}$ 55 ± 3 mg/L, SO_4^{2-} 2500 ± 20 mg/L) was provided to the reactor during the study and steady state data was considered for further analysis.

Phenol (Fig. 3.10a), TH (Fig. 3.10b) and COD_O (Fig. 3.10c) removal in reactor A2 increased with increase in reactor HRT. Complete removals of phenol was achieved in 10h. Complete removal of TH was achieved at 15h HRT of A2 reactor. Effluent COD_O was below dischargeable limit when HRT of A2 was ≥ 15h. Complete removal of $S_2O_3^{2-}$ was achieved in A2 and effluent SO_4^{2-} concentration increased beyond 2500 mg/L. This could be due to further oxidation of $S_2O_3^{2-}$ in aerobic environment to SO_4^{2-} (Fig. 3.10d).

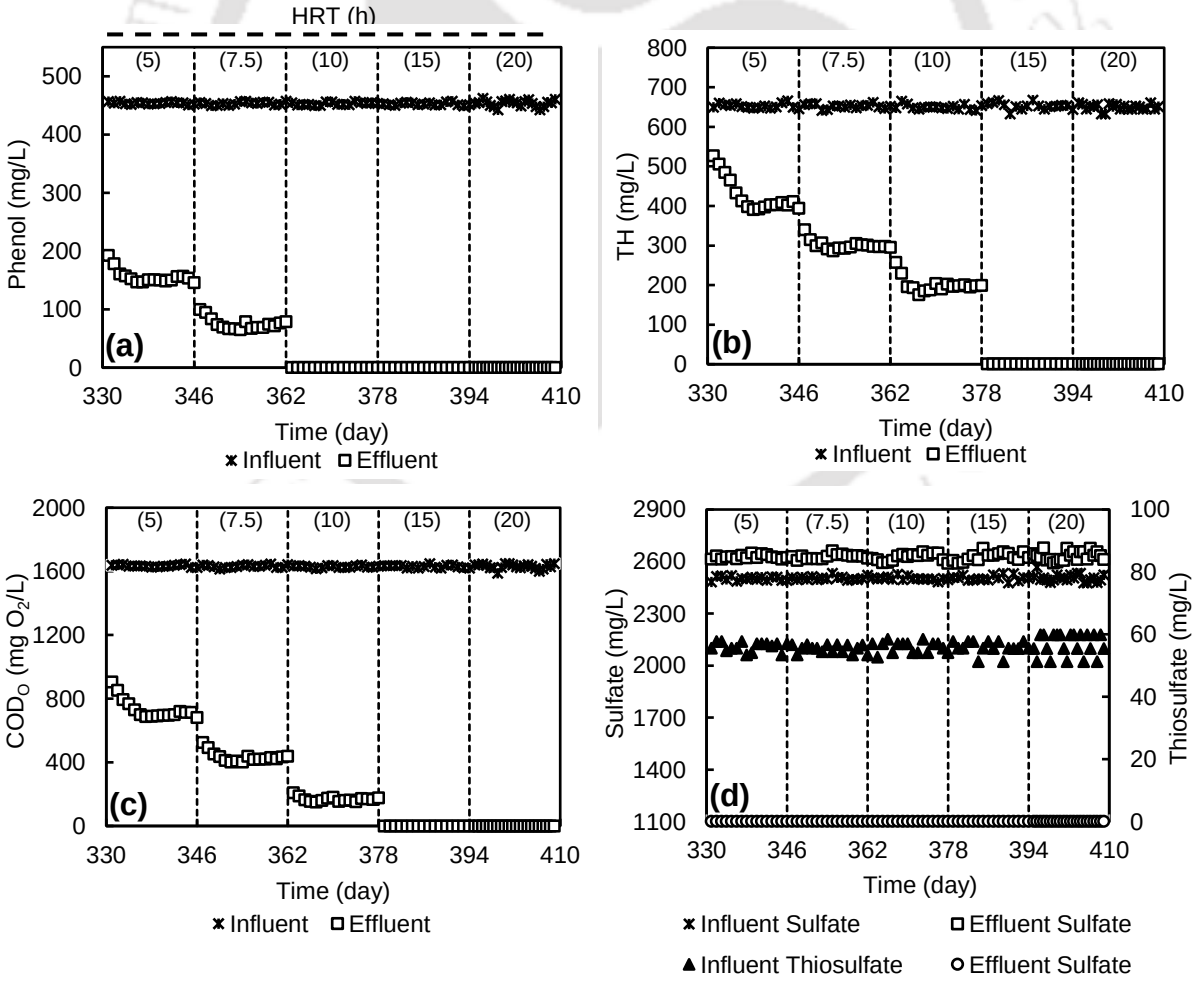

Fig. 3.10: Effect of HRT of aerobic reactor (A2) on the degradation of: (a) phenol, (b) TH, (c) COD_O, (d) thiosulfate

Degradation of NH_4^+-N required longer cycle time of 16h with corresponding HRT of 20h as compared to degradation of organics in A2 (Fig. 3.11a). This could be due to slow growing autotrophic bacteria, responsible for NH_4^+-N oxidation. Fig. 3.11b shows that effluent NO_2^--N increased up to reactor HRT of 8h and then decreased. Effluent NO_3^--N in A2 increased steadily from 43 ± 2 to 209 ± 3 mg/L with increase in HRT. NH_4^+-N oxidation to NO_3^- in aerobic environment occurs with NO_2^- as intermediate. With increase in HRT, NH_4^+-N oxidation increased and more NO_2^--N accumulated and at higher HRT, NO_2^--N further oxidized to NO_3^--N. A balance was made on amount of NH_4^+-N removed in A2 and amount of NH_4^+-N oxidized to NO_2^--N and NO_3^--N and unaccounted nitrogen fraction was 14-37%.

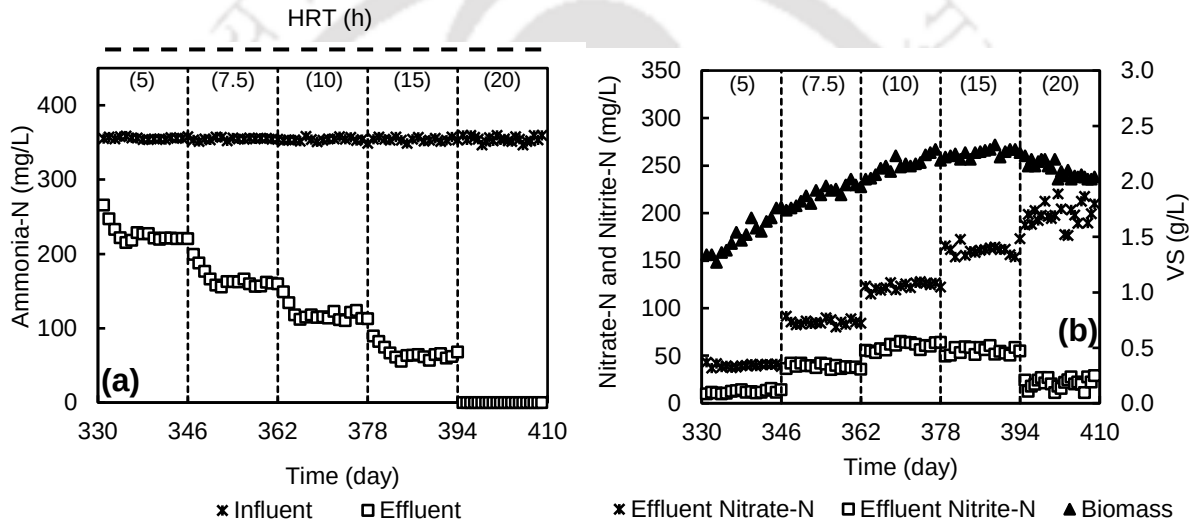

Fig. 3.11: Effect of HRT of aerobic reactor (A2) (a) on the degradation of and (b) generation of nitrate-N and nitrite-N from the oxidation of ammonia-N

3.3.3 Combined anoxic and aerobic reactor operation

Study on the variation in HRT revealed that complete degradation of volatile S^{2-} was achieved at 2.5d HRT in A1 and remaining pollutants were completely degraded at maximum of 20h HRT by A2 with total HRT of 80h.

A1 was operated at 48h cycle time (HRT 60h) in fed-batch mode. Released effluent (8L) from A1 had to be treated by A2 in 16h cycle time (HRT 20h) which was three times lesser compared to A1. Therefore, the volume of A2 was reduced three times to 3.33L (volume of A1 was 10L) and operated in 3 cycles at 16h cycle time (HRT 20h). The effluent of A1 was stored in a closed container and 2.67L was provided to A2 in each cycle. The study was done for 30

days and the influent and effluent concentrations from this study are summarized in Table 3.2. In reactor A1, at HRT of 60h, complete S^{2-} removal was achieved with NO_3^--N as electron acceptor with denitrification efficiency of 85%. COD reduction was only 53%.

In A2 reactor, phenol, TH and COD_O were oxidized. $S_2O_3^{2-}$ and NH_4^+-N were oxidized to SO_4^{2-} and NO_3^--N, respectively. A schematic diagram on removal of several pollutants in anoxic–aerobic sequential reactors is shown in Fig. 3.12. The final effluent had pH 8.5 ± 0.1, phenol, NH_4^+-N, TH, COD_O and SO_4^{2-} within dischargeable limit when total HRT of anoxic disc reactor and aerobic moving bed reactor was 80h as per CPCB, India (1986). Effluent NO_3^--N and NO_2^--N were on the higher side. However, these products are in reduced form and do not consume oxygen in case of discharge to surface water source.

Table 3.2: Effluents after treatment by anoxic-aerobic moving bed reactors

Parameters	Feed with emulsified diesel				
	Anoxic			Aerobic	
	Influent	Effluent#	Rem (%)	Effluent*	Overall rem (%)
Phenol	756 ± 4	321 ± 18	57	3 ± 1	99
TH	1228 ± 29	532 ± 27	56	5 ± 1	99
Sulfide	750 ± 7	2 ± 1	99	ND	100
COD_T	5413 ± 27	1420 ± 43	74	100 ± 5	98
COD_O	2842 ± 25	1215 ± 44	57	9 ± 2	99
Thiosulfate	-	26 ± 4	-	ND	100
Sulfate	40 ± 4	1164 ± 10	-	1201 ± 12	-
Sulfur	-	359 ± 9	-	-	-
Ammonia-N	350 ± 6	336 ± 5	4	5 ± 1	99
Nitrate-N	1032 ± 17	1 ± 1	99	192 ± 15	-
Nitrite-N	-	166 ± 5	-	114 ± 8	-
pH	9.5 ± 0.1	9.1 ± 0.1	-	8.5 ± 0.1	-
VS (g/L)	-	1.1 ± 0.1	-	2.3 ± 0.2	-
Gas (mL)	-	800 ± 23	-	-	-

ND: Not detectable
TH: Total hydrocarbon
COD_T: Total COD
COD_O: Organic COD
Rem: Removal
Units of all parameters except pH, gas and VS are in mg/L

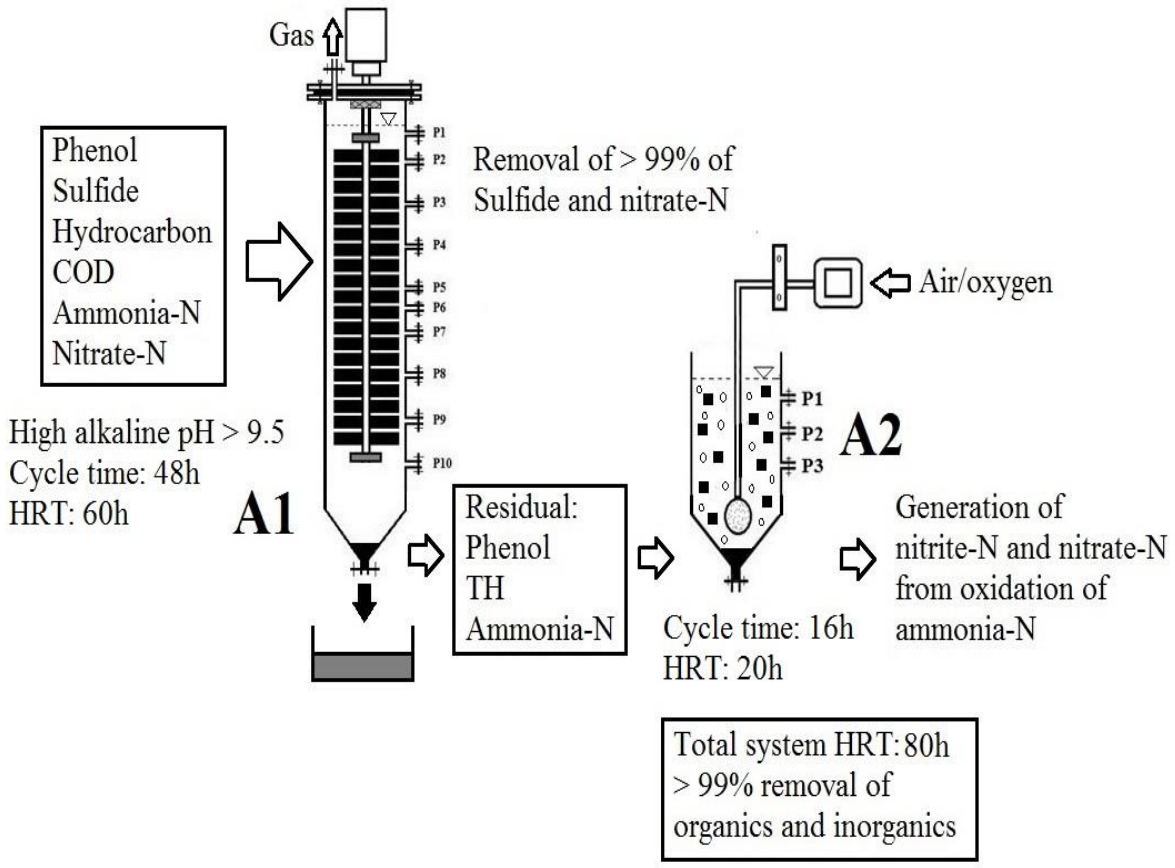

Fig. 3.12: Schematic diagram of treatment of synthetic petroleum refinery wastewater in anoxic-aerobic reactors

3.4 SUMMARY OF THE STUDY

The present study discussed anoxic and aerobic biodegradation of synthetic refinery wastewater having phenol, emulsified diesel, nitrate, ammonia and sulfide in anoxic vertical disc reactor (A1) and aerobic moving bed reactor (A2). Both reactors were operated in fed-batch mode. Mixing speed of 20 rpm was optimum and removal of pollutants remained constant beyond this speed in A1. The optimum HRT of A1 was observed as 2.5d, for complete removal of S^{2-} and maximum recovery of S^{2-} as S^0. Removals of organic compounds like phenol, COD and TH were partial (45% - 51%) and marginal for NH_4^+-N from influent of 756 ± 4, 1228 ± 29, 2842 ± 25 and 350 ± 5 mg/L, respectively, in A1 at HRT of 60h. Effluent of A1 was further treated in an aerobic moving bed reactor (A2) and the optimum HRT was observed as 20h. Total HRT of the combined anoxic-aerobic reactor was observed as 80h for complete removal of phenol, COD_O, total hydrocarbons, S^{2-} and NH_4^+-N.

References

An, S., Tang, K., Nemat, M. 2010. Simultaneous biodesulfurization and denitrification using diesel reservoir microbial culture: Effects of sulphide loading rate and sulphide to nitrate loading ratio. Water Research 44(5): 1531–1541.

Cardoso, R. B., Texier, A. C., Alvarez, R. S., Flores, E. R., Field, J. A., Gomez, J. 2009. Effect of initial sulfide concentration on sulfide and phenol oxidation under denitrifying conditions. Chemosphere 74: 200-205.

Central Pollution Control Board India 1986. The Environment (Protection) Rules. Schedule VI

Ghorbanian, M., Moussavi, G., Farzadkia, M. 2014. Investigating the performance of an up-flow anoxic fixed-bed bioreactor and a sequencing anoxic batch reactor for the biodegradation of hydrocarbons in petroleum-contaminated saline water. International Biodeterioration and Biodegradation 90: 106–114.

Jing, C. Ping, Z., Mahmood, Q. 2010. Influence of various electron acceptors on the anaerobic sulphide oxidation. Bioresource Technology 101: 2931–2937.

Lens, P. N. L., Visser, A., Janssen, A. J. H., Hulshoff Pol, L. W., Lettinga, G. 1998. Biotechnological treatment of sulfate-rich wastewaters. Critical Reviews in Environmental Science and Technology 28: 41-88.

Liu, C., Han, K., Lee, D., Wang, Q. 2016. Simultaneous biological removal of phenol, sulfide, and nitrate using expanded granular sludge bed reactor. Applied Microbiology and Biotechnology 100: 4211–4217.

Lu, C., Li, H., Lee, L.Y. 1997. Effects of disc rotational speed and submergence on the performance of an anaerobic rotating biological contactor. Environment International 23(2): 253-263.

Moussavi, G., Shekoohiyan, S., Naddafi, K. 2016. Anoxic biodegradation of petroleum hydrocarbons in saline media using denitrifier biogranules. Ecotoxicology and Environmental Safety 129: 51–56.

Zolfaghari, R., Fakhru'l-Razi, A., Abdullah, A. C., Elnashaie, S. S. E. H., Pendashteh, A. 2016. Demulsification techniques of water-in-oil and oil- in-water emulsions in petroleum industry. Separation and Purification Technology 170(1): 377–407.

4

CHAPTER

INFLUENCE OF DIFFERENT HYDROCARBONS ON THE PERFORMANCE OF ANOXIC-AEROBIC SEQUENTIAL MOVING BED REACTORS

CHAPTER 4

INFLUENCE OF DIFFERENT HYDROCARBONS ON THE PERFORMANCE OF ANOXIC-AEROBIC SEQUENTIAL MOVING BED REACTORS

4.1 INTRODUCTION

Refining and processing of crude petroleum oil invariably culminates into the generation of oily wastewater rich with complex hydrocarbons. Aqueous effluents (pH 8.0-10.0) from petroleum refineries encompass hydrocarbons diverse in density, structure (straight, branched, cyclic etc.), viscosity, volatility, carbon atoms (C_5-C_{44} per molecule) and volatile carcinogenic inorganics such as sulfides and ammonia (Diya'uddin et al., 2011; Sharghi et al. 2013; Razavi and Miri, 2015). Different sections of a refinery such as fractional distillation, cooling tower, hydrocrackers, coking, ballast water units release hydrocarbons with inconsistent concentration and physico-chemical properties (MoEF, 2010). For example, kerosene is volatile and of short chain length (C_{12}-C_{15} per molecule) (Wang et al., 2015; Khan et al., 2015) and heavy oil is non-volatile and is of longer chain length (C_{18}-C_{44} per molecule) (Zhrong et al., 2018). Some of the hydrocarbon may contain merceptans and organic sulfur compounds (MoEF, 2010).

Although biological assimilation of refinery wastewater is an attractive option (Gasim et al., 2012), presence of immiscible, recalcitrant and volatile compounds pose quite a challenge for their biodegradation (Sonwani et al., 2019). Simultaneous removals of different types of hydrocarbons like diesel, kerosene, heavy oil and crude oil having different physico-shemical properties can cause toxic effects on microorganisms (Heipieper et al., 2010). Wang et al. (2016) reported shift in performance of anaerobic reactor while treating heavy oil. Literature reports on biodegradation using different types of hydrocarbons are very scanty.

Agitation speed and hydraulic retention times were optimized in the previous chapter (Chapter 3). The aim of the present study was to analyze the effects of different types of hydrocarbons (kerosene, heavy oil and their mixtures with diesel) and crude oil on characteristics of biomass, microbial activity and performance of anoxic-aerobic sequential moving bed reactors while removing S^{2-}, hydrocarbons, NH_4^+-N and NO_3^--N.

4.2 MATERIALS AND METHODS

4.2.1 Chemicals and Reagents

Chemicals used were of AR grade and purchased from either Merck or CDH, India. Kerosene was purchased from the local market. Diesel was procured from an Indian Oil petrol station. Laal ghoda engine oil (Hindustan Petroleum) was purchased form a local shop and used as heavy oil. Crude oil was procured from Indian Oil Corporation Limited, Guwahati. Nonylphenolmonoethoxylate (9M) was purchased from Sigma-Aldrich. Feed was prepared with tap water (pH 8.0 ± 0.2) and stocks were prepared by milli-Q water (pH 7.0 ± 0.1).

4.2.2 Experimental set up and reactor operation

Anoxic (A1) - Aerobic (A2) reactors mentioned in Chapter 3 (section 3.2.2) were used during the present study at fixed HRT of 60h and 20h, respectively, with an overall 80h system HRT. Operational conditions of the reactors can be found in Table 4.1.

Table 4.1: Operational conditions of A1 and A2 during variation in hydrocarbons

Hydrocarbons	Days	Agitation		Reactor volume (L)		Decant volume (L)		Cycle time (h)		HRT (h)	
		A1	A2	A1	A2	A1	A2	A1	A2	A1	A2
K	442-483	20 rpm	Airflow 2L/min	10	3.33	8	2.67	48	16	60	20
HO	485-526										
K+HO	528-569										
K+HO+D	571-612										
Crude oil	614-652										

K: Kerosene, HO: Heavy oil, D: Diesel,
A1: Anoxic reactor, A2: Aerobic reactor

4.2.3 Feed characteristics

Feed was prepared by adding phenol (750 ± 5 mg/L as C_6H_5OH), NH_4^+-N (350 ± 4 mg/L as NH_4Cl) and NO_3^--N (1000 ± 10 mg/L as KNO_3) in tap water and purged with N_2 gas. Concentration of hydrocarbon was kept constant at 300 mg/L. In the feed solution, required hydrocarbons (300 mg/L) and S^{2-} (750 ± 4 mg/L as $Na_2S.xH_2O$) were added to avoid abiotic loss by purging. Then emulsifier (nonylphenolmonoethoxylate) of 0.2 mM was added in the feed. Synthetic feed also contained phosphate buffer (1 mL/L), yeast extract (10 mg/L) and trace metal solutions (1 mL/L) as nutrients as per section 2.2.4. Initial feed pH was 9.5 ± 0.1 during the study due to the presence of Na_2S. Images of hydrocarbons and their emulsified feed are illustrated in Fig. 4.1 and Table 4.2 shows the properties of the synthetic emulsified feed.

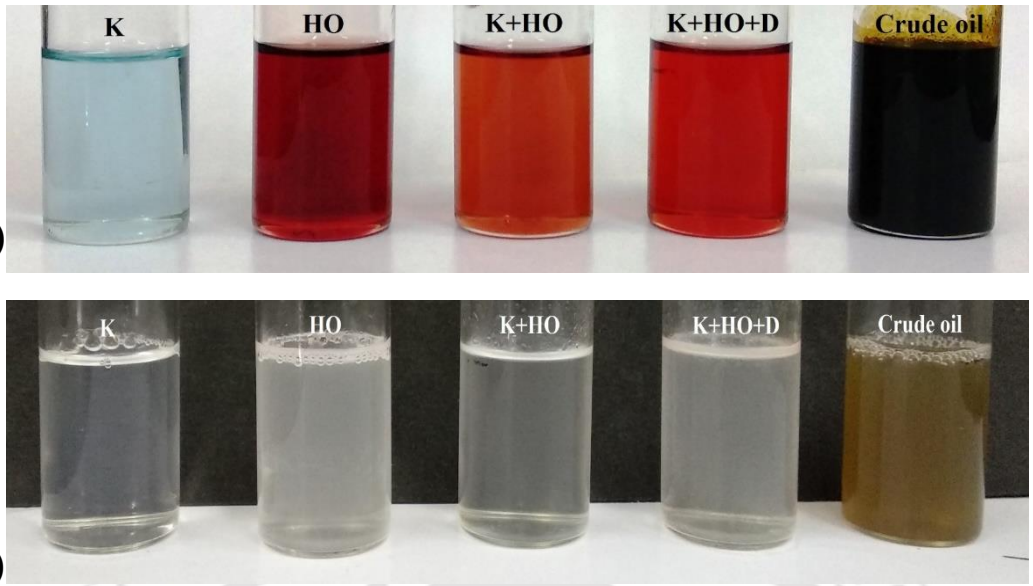

Fig. 4.1: Image of (a) raw hydrocarbons, (b) emulsified feed with hydrocarbons

Table 4.2: Properties of the hydrocarbons, surfactant and emulsified feed

Properties of the hydrocarbons and surfactant			
Hydrocarbons	Physical properties		
	Density (g/mL)	Dynamic Viscosity (Poise)	COD* (mg/L)
K	0.712 ± 0.029	0.048 ± 0.002	912 ± 12
HO	0.875 ± 0.017	0.097 ± 0.003	999 ± 10
K+HO	0.783 ± 0.049	0.064 ± 0.002	934 ± 17
K+HO+D	0.797 ± 0.029	0.076 ± 0.002	978 ± 22
Crude oil	1.024 ±0.049	0.182 ± 0.003	1012 ± 19

Properties of the emulsified feed					
Parameters	**K**	**HO**	**K+HO**	**K+HO+D**	**Crude oil**
Required volume (mL/10L feed)	4.21	3.43	K: 2.11 HO: 1.73	K: 1.40 HO : 1.14 D:1.23	3.25 mL crude oil
Turbidity (NTU)	28.22 ± 2.11	60.41 ± 3.23	39.12 ± 2.21	40.91 ± 1.21	96.81 ± 4.11
SS (mg/L)	6.22 ± 0.91	42.13 ± 1.92	18.12 ± 2.04	22.32 ± 1.01	79.34 ± 3.11
Conductivity (mS/cm)	5.33 ± 0.05	6.01 ± 0.04	5.77 ± 0.02	5.89 ± 0.05	7.79 ± 0.04
Salinity (g/L)	4.29 ± 0.03	4.35 ± 0.02	4.31 ± 0.02	4.33 ± 0.01	5.04 ± 0.11
TDS (g/L)	4.70 ± 0.01	4.82 ± 0.02	4.74 ± 0.02	4.76 ± 0.09	4.98 ± 0.08

Turbidity was measured at twice dilution

Surfactant of 0.22 mL was added for 10L feed, *COD was measured for 300 mg/L of hydrocarbon

K: Kerosene, HO: Heavy oil, D: Diesel,

SS: suspended solids, TDS: Total dissolved solids

4.2.4 Analytical procedure

Analysis of phenol, sulfide, sulfate, thiosulfate, diesel as total hydrocarbon, nitrate-N, nitrite-N, density and viscosity of hydrocarbons, TDS, salinity and conductivity were done as mentioned in section 2.2.6 of Chapter 2. Measurement of suspended solids of influent feed was done by filtration method as per APHA (2005). Initial weight of an oven-dried Whatman 41 filter paper were measured. Sample of 50 mL volume was filtered through the filter paper. Then the filter paper was dried in hot air oven (ICT, India) at 105º C for 24h. Final weight of the filter paper was measured after 24h and suspended solids were determined from the difference between the final and initial weight of the filter paper. Turbidity of the samples was determined by Nephelometric Turbidity meter (Systronics, India).

COD of the hydrocarbons was determined as mentioned in section 2.2.6 and results are illustrated in Appendix H. Increase in COD was observed with increase in digestion time and after 8h digestion, COD was constant. Hence, 8h digestion time was selected for the determination of COD.

Minimum concentration of the emulsifier needed to keep the hydrocarbons completely mixed in the reactor was determined as mentioned in section 3.2.4 of Chapter 3 and results are illustrated in Appendix I. Similar results were obtained as it was observed in case of diesel. Hence, 0.2 mM emulsifier concentration was chosen for the emulsification of hydrocarbons.

Air flowrate to A2 was optimized by supplying air at different flow rates as mentioned in section 3.2.5 of Chapter 3 for different emulsified hydrocarbons and similar results were observed (Appendix J). Hence, 2 L/min was supplied to A2.

4.2.5 Quantification of biomass

Three discs from top, middle and bottom were removed, their surfaces were washed with milli-Q water and n-Hexane to remove any hydrocarbons and analyzed for volatile solids (VS) by ignition method (APHA, 2005). VS due to only biomass was measured by subtracting the weight of virgin disc. Average VS was calculated and multiplied with the total number of discs to obtain the total attached biomass in A1. Six random cubes were collected from A2 and same procedure was repeated for the analysis of attached biomass in A2. To determine the total suspended solids, 50 mL sample was collected, centrifuged and supernatant was discarded to remove organics. Volume refilled to 50 mL with milli-Q water and VS was measured by ignition method (APHA, 2005). Suspended volatile solids as biomass were calculated by subtracting the generated S^0 values from total volatile suspended solids as per section 3.3.1.1.

4.2.6 Abiotic study

Abiotic removal (adsorption and volatilization) in A1 was done by collecting one disc from A1 as attached biomass and 250 mL effluent sample having suspended solids. Abiotic removal in A2 was determined by collecting 78 PUF cubes and 250 mL effluent liquor with proportion to A2. Both the attached and suspended biomass were autoclaved and further dried in a hot air oven at 105 ºC. The dried biomass of A1 was put in 500 mL wide mouth plastic bottles with 250 mL simulated feed and shaken at 20 rpm in a rotary shaker for 48h. The plastic bottles were capped and a port (0.5 cm ϕ) was provided at the top to release volatilization. Dried biomass of A2 was put in similar uncapped bottles with simulated feed at 2L/min aeration for 16h. Difference of influent and effluent concentrations was the abiotic removal (C_A, mg/L).

4.2.7 Determination of biomass activity

Biomass activity was measured as heterotrophic activity (HA) and chemolithotrophic activity (CA) by modified method suggested by Jawed and Tare (1999). HA was done with biomass collected from A1 and A2 separately, whereas CA was done with A1 biomass only. Biomass of 1g was used for each analysis in the same attached to suspended ratio available in the reactors. Nutrients were not used to prevent biomass growth.

HA of anoxic sludge was done in an aspirator bottle (1L) having opening for gas and sample collection (Fig. 4.2a). A magnetic stirrer was used for mixing and sample was collected from the bottom port with a syringe. Feed COD was maintained at 3000 mg O_2/L (using dextrose) and NO_3^--N of 1000 mg/L similar to feed of A1 reactor. HA analysis of the aerobic sludge was done in a beaker (1L) with aeration (2L/min) and feed COD was 2000 mg O_2/L using dextrose, same as COD_O of reactor A2 (Fig. 4.2b). Measurement of COD was done at predetermined time interval for 48h and 16h for A1 and A2 biomass respectively. CA was done in a similar way using A1 sludge having only S^{2-} (750 mg/L) and NO_3^-N (1000 mg/L). Activity was done for three cycles and data obtained in the third cycle was considered (Jawed and Tare, 1999). Graph was plotted with time in X-axis and cumulative COD removed (difference of initial COD and COD after particular interval of time) in Y-axis. Straight line passing through origin was plotted for the linear portion of the curve. Calculation of activity was done as follows,

$$\text{Activity } \left(\frac{\text{mg}}{\text{g VS.day}}\right) = \frac{\text{Slope of the linearized portion } \left(\frac{\text{mg}}{\text{L.h}}\right) \times 24 \left(\frac{\text{h}}{\text{day}}\right)}{\text{Total biomass } \left(\text{g.}\frac{\text{VS}}{\text{day}}\right)} \quad \ldots (4.1)$$

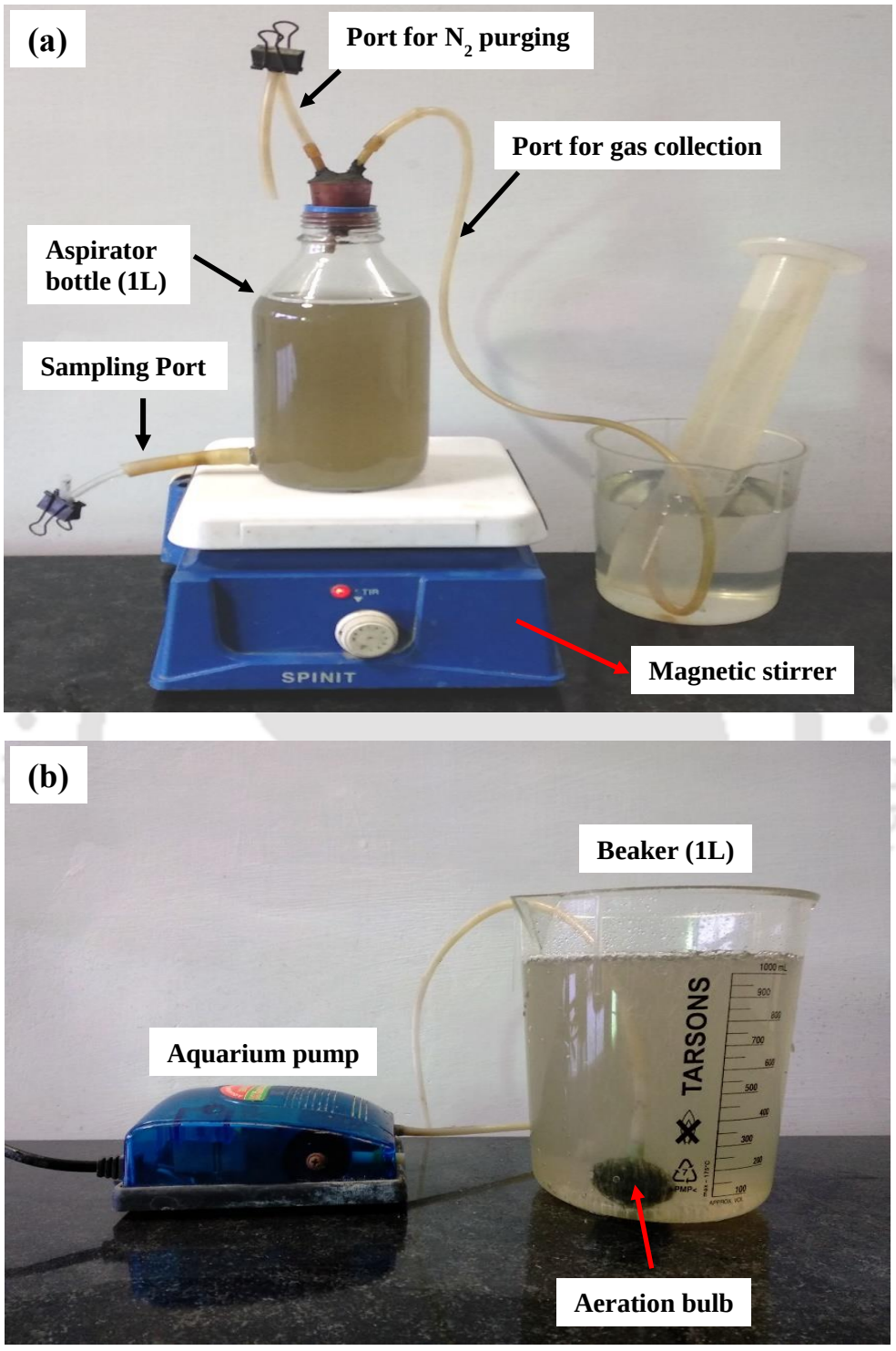

Fig. 4.2: Arrangement for biomass activity test of (a) anoxic biomass, (b) aerobic biomass

4.2.8 Analysis of gas samples

Gas samples were analyzed for nitrogen (N_2), methane (CH_4), carbon dioxide (CO_2) and hydrogen sulfide (H_2S). N_2, CH_4 and CO_2 were determined by a gas chromatograph (Dhruva, Gujrat, India) by thermal conductivity detector (TCD). Temperatures of the oven and detector were kept at 250 ºC and 80 ºC, respectively. Argon (99.99% pure) was used as carrier gas at 30 mL/min. Instrument was calibrated with a standard mixture of known N_2 (40%), CO_2 (15%) and CH_4 (10%) (Ultra Pure Gases, Baroda, India). One mL sample was injected through the septum installed at the injection port by using a graduated syringe. N_2 and CH_4 were analyzed using Molecular Sieve 5A column and CO_2 was measured using Porapak Q column as percentage present in the sample and converted to volume from the total generated gas of the reactors. Gas from anoxic reactor was passed through a solution of potassium hydroxide (1M KOH), which absorbed H_2S gas. This H_2S was determined in the form of molar S^{2-} by methylene blue method (APHA, 2005) and converted to volume as per ideal gas law PV = nRT. where, P = standard atmospheric pressure (1 bar), V = volume of the gas (m^3), n = number of moles of S^{2-} or H_2S, R = ideal gas constant (8.314 kg m^2 s^{-2} K^{-1} mol^{-1}), T = absolute temp. (K).

4.2.9 FTIR analysis of the samples

Samples were centrifuged at 8500 rpm for 10 minutes for the removal of sulfur and biomass and supernatant was examined for infrared spectrum using Fourier Transform Infra-red Spectroscopy (Model No: IRAffinity-1; M/s Shimadzu, Japan) by attenuated total reflection (ATR) technique. Sample volume of 50 µL was used for analysis in a wavelength range of 400-4000 cm^{-1} and at a scan rate of 40.

4.3 EFFECT OF HYDROCARBONS ON THE PERFORMANCE OF ANOXIC-AEROBIC SEQUENTIAL MOVING BED REACTORS

Treatment of synthetic refinery wastewater laden with commercial hydrocarbons and crude oil of different physicochemical properties was done in between day 442 to 652 in a study period of 210 days. Hydrocarbons were varied in the following order: K, HO, (K+HO), (K+HO+D) and crude oil. Influent phenol (750 ± 5 mg/L), S^{2-} (750 ± 4 mg/L), hydrocarbons (300 mg/L), NH_4^+-N (350 ± 4 mg/L), NO_3^--N (1000 ± 20 mg/L) and surfactant (0.2 mM) were kept constant during the study. Anoxic (A1) and aerobic (A2) reactors were operated at 48h cycle time (60h HRT) and 16h cycle time (20h HRT) respectively. Feed pH was constant at 9.5 ± 0.1 during the study due to the presence of S^{2-} as Na_2S.

4.3.1 Biomass concentration

Total and attached biomass in A1 were maximum in the presence of kerosene (K) having the lowest density and viscosity. Heavy oil (HO) and crude oil being denser and viscous, triggered sloughing of the anoxic biomass and marginal increase in the suspended biomass was discerned (Fig. 4.3a). Total and attached biomass in A1 were intermediate in the presence of either (K+HO) or (K+HO+D), as their density and viscosity were lower compared to HO and crude oil and higher than K. Solids retention time (SRT) was calculated as follows,

$$\text{SRT (d)} = \frac{\text{Total biomass (g)}}{\text{biomass wasted/day } (\frac{\text{g}}{\text{d}})} \quad \ldots (4.2)$$

SRT of A1 was lower in the presence of HO and crude oil (Fig. 4.3b). The concentrated raw feed was first received by A1. For successful degradation, substrate needs to be transported effectively through the support media (Sahariah et al., 2016). Increase in the viscosity hampered the relative flow of substrate into the porous discs leading to lesser growth of the attached biomass. Distribution of aerobic biomass was unaffected (Fig. 4.3c) and SRT of A2 did not change during the study (Fig. 4.3d), suggesting its steady performance. Since, A2 was downstream, it received less concentrated feed and exposed to lower toxicity.

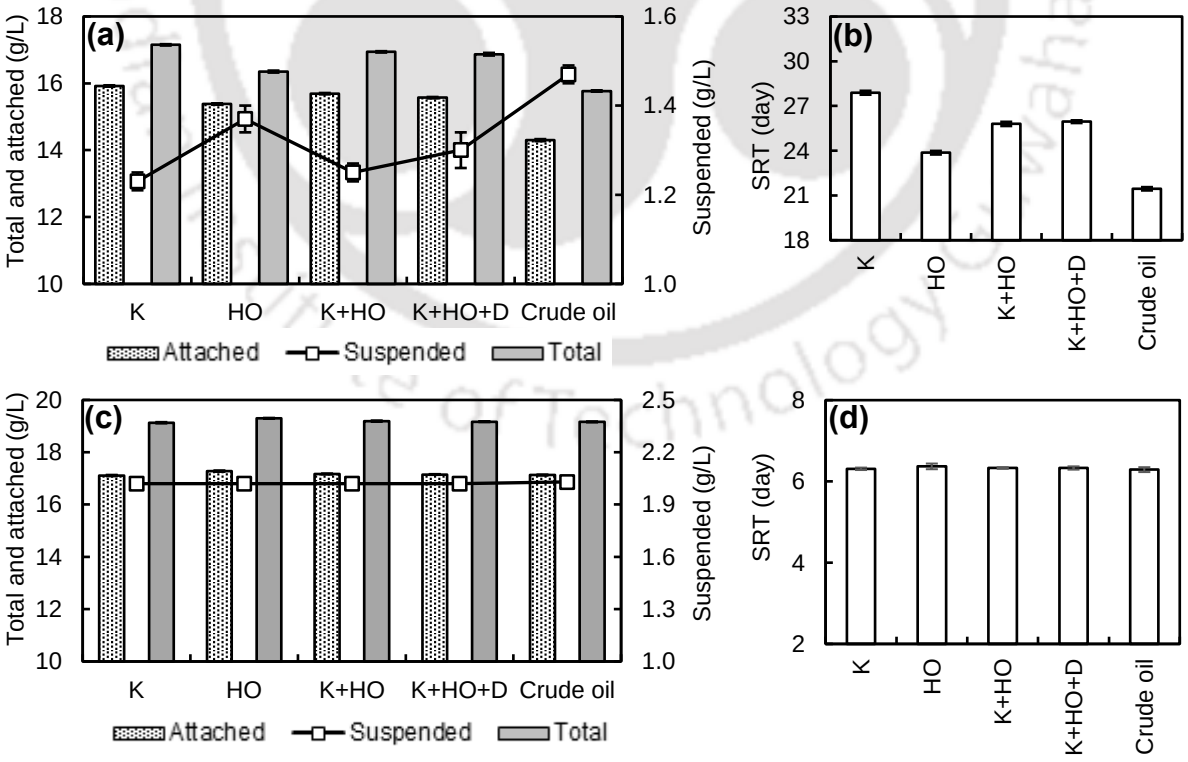

Fig. 4.3: (a) distribution of biomass in A1, (b) SRT of A1, (c) distribution of biomass in A2 , (d) SRT of A2

Immobilized biomass (total, attached and suspended) per gram of the biomass support material (PUF) with respect to different influent hydrocarbons are summarized in Table 4.3. Similar trend of biomass distribution was observed and attached biomass in A1 was least when crude oil was used as hydrocarbon. Sahariah and Chakraborty (2013) have reported total biomass per gram of biomass support (total 100g biomass support material) material as 1.1 to 1.2 during the treatment of phenol, thiocyanate and ammonia in anaerobic-anoxic-aerobic fed batch sequential moving bed reactors. Higher biomass concentration was observed in the present study shows better growth of biomass inside the support material while degrading phenol, hydrocarbons, S^{2-} and ammonia at high alkaline pH (9.53 ± 0.02). Total biomass to packing material (alginate beads of total 70g) ratio of 0.24 to 0.26 was reported by Banerjee and Ghoshal (2016) during the biodegradation of real petroleum refinery wastewater. This suggests PUF to be a better biomass support material compared to alginate beads.

Table 4.3: Immobilized biomass per gram of the biomass support material

Hydrocarbons	Biomass per gram of the support material (gVS/g of PUF)					
	Reactor A1			Reactor A2		
	Attached	Suspended	Total	Attached	Suspended	Total
K	1.33 ± 0.01	0.10 ± 0.01	1.43 ± 0.01	1.42 ± 0.01	0.17 ± 0.01	1.59 ± 0.01
HO	1.28 ± 0.01	0.11 ± 0.01	1.39 ± 0.01	1.44 ± 0.01	0.17 ± 0.01	1.61 ± 0.01
K+HO	1.31 ± 0.01	0.10 ± 0.01	1.41 ± 0.01	1.43 ± 0.01	0.17 ± 0.01	1.60 ± 0.01
K+HO+D	1.30 ± 0.01	0.11 ± 0.01	1.41 ± 0.01	1.43 ± 0.01	0.17 ± 0.01	1.60 ± 0.01
Crude oil	1.19 ± 0.01	0.12 ± 0.01	1.31 ± 0.01	1.43 ± 0.01	0.17 ± 0.01	1.60 ± 0.01

- A1: Anoxic moving bed reactor
- A2: Aerobic moving bed reactor
- K: Kerosene, HO: Heavy oil, D: Diesel
- VS: Volatile solids
- PUF: Poly Urethane Foam

4.3.2 Performance of the bioreactors

4.3.2.1 Abiotic removals of the pollutants

Abiotic removals of phenol and TH were 1-3% and 5-10%, respectively, through adsorption and volatilization (Appendix K) in anoxic-aerobic sequential reactors. S^{2-} removal was 4-5% in anoxic reactor due to its volatile nature and $S_2O_3^{2-}$ removal was 33-45% in aerobic reactor due to chemical oxidation. Abiotic removals of COD_T and COD_O were 6-9% and removals of NO_3^--N and NO_2^--N were less than 1% during the study.

4.3.2.2 Removal of organics

Initial rise in effluent phenol (Fig. 4.4a), TH (Fig. 4.4b), COD_T (Fig. 4.4c) and COD_O (Fig. 4.4d) was monitored with each change in the hydrocarbons in the effluent of A1 at 48h cycle time (60h HRT) (Fig. 4.4). Steady state was achieved within 10-12 days after any change in feed hydrocarbon. Steady state phenol removal was maximum with kerosene (K) and decreased in the order of K > (K+HO) > (K+HO+D) > HO > crude oil in A1. Residual phenol was completely removed in A2 at 16h cycle time (20h HRT) with a total system HRT of 80h regardless of the influent hydrocarbons. Total hydrocarbon (TH) removal was similar to phenol removal in sequential anoxic-aerobic reactors (Fig. 4.4b). Phenol and TH removal rates were 224 ± 2 and 377 ± 3 g/(m^3.d) by the anoxic-aerobic sequential reactors and were constant irrespective of the hydrocarbon type. Higher TH removal rate of 2340 g/(m^3.d) is reported by Ghorbanian et al. (2014) during the sole assimilation of petroleum hydrocarbons in up flow anoxic fixed bed reactor. In the final effluent from A2, phenol and TH were less than 5 mg/L, and COD_O and COD_T were within dischargeable limit (Table 4.3), suggesting more than 99% removals of TH, phenol and COD_O and 97% removal of COD_T. Abass et al. (2018) used anoxic-oxic membrane bioreactor system for the treatment of oil refinery wastewater (pH 7.1 ± 0.2) and reported COD (influent 7850 mg O_2/L) and oil (influent 260 mg/L) removals of 97% and 99%, respectively at a lesser total system HRT of 17.4h compared to the present study. However, membrane fouling was reported beyond oil concentration of 250 mg/L. Although, the present study required more HRT (80h) for the degradation of S^{2-} and NH_4^+-N including hydrocarbons (phenol and emulsified crude oil), the reactor system was stable at higher oil concentrations (300 mg/L, TH: 1250 ± 10 mg/L). In the same study by Abass et al. (2018), SRT of 35d was reported for both anoxic and aerobic reactors, which was higher compared to the present study.

Biomass activity cycles and specific removal rates of organics are illustrated in Fig. 4.5. Specific removal rate was calculated as follows,

$$\text{Specific removal rate } \left[\frac{\text{mg}}{\text{gVS.d}}\right] = \frac{C_i - C_f - C_A}{X.HRT} \quad \ldots (4.3)$$

where, C_A = abiotic removal (mg/L), C_i = influent to anoxic or aerobic reactor (mg/L), C_f = effluent from anoxic or aerobic reactor (mg/L), X = biomass concentration (g/L)

Specific removal rates of phenol and TH were lower in A1 and higher in A2 in the presence of HO and crude oil. With HO and crude oil in feed, efficiency of anoxic reactor

decreased and downstream reactor received higher organics (Fig. 4.6a). Similarly, specific removals of COD_T and COD_O were lower in the presence of HO and crude oil (Fig. 4.6b). TH utilization of 9310 mg/(gVS.d) at pH 7.2 (Talaiekhozani et al., 2015), 290 mg/(gVS.d) in UASB reactor (Moussavi and Ghorbanian, 2015), 2600 mg/(gVS.d) (Moussavi et al., 2016) in anoxic condition and COD utilization of 332-767 mg/(gVS.d) in activated sludge process (pH 7.1) has been reported (Ebrahimi et al., 2016). Much lower utilization in the present study was due to high alkaline pH and presence of phenol and S^{2-} as competing energy source available for mixed microbial consortia.

Biomass activity of a biological system indicates the maximum organic degradation capacity (McHugh et al., 2004; Hussain and Dubey, 2017). Biomass activity of anoxic biomass decreased and that of aerobic biomass increased when HO and crude oil were used (Fig. 4.6b). Aerobic biomass showed higher activity than anoxic biomass due to higher free energy change (Schink, 2006; Metcalf and Eddy, 2011). Specific COD_O removal rate of the reactors was higher whenever biomass activity was on the higher side. Hence, a direct correlation of biomass activity with organics degradation efficiency was confirmed and biomass activity can be used as a potential tool for the prediction of organic removal efficiency in bioreactors. Specific COD_O removal of both anoxic and aerobic reactors were quite less compared to their respective biomass activity (Fig. 4.6b). Low specific removal rates in the present study were due to much toxic pollutants, high alkaline pH and presence of high biomass in the reactors. Dextrose being relatively much benign was utilized more efficiently by both the anoxic and aerobic biomass.

FTIR spectra of the influent and effluent from A1 and A2 showed the common presence of alkyl halides (500-600 cm^{-1}), alkanes (700-850 cm^{-1}), distributed benzenes (850-950 cm^{-1}), carboxylic acids (1300-1350 cm^{-1} and 2600-2800 cm^{-1}), aliphatic (2900-3000 cm^{-1}) and aromatic (3000-3300 cm^{-1}) hydrocarbons in all types of feed (Revathy et al., 2015; Ramasamy et al., 2014; Miller et al., 1952; Sharma et al., 2014; Segneanu et al. 2012; Qasim et al. 2017) (Appendix L). Mercaptans (400-500 cm^{-1}) and organo-nitrogens (3400-3700 cm^{-1}) were detected in the feed containing HO and crude oil (Sharma et al., 2014). Significant reduction of the peaks in the effluent spectra of A1 was observed. Peaks for alkanes and other aromatics were significantly decreased. Esters (1700-1800 cm^{-1}) and carboxylic acids were detected as degradation products of alkanes (Sharma et al., 2014). Effluent of A2 contained only the extracellular polymeric substances (EPS) and no other corresponding peaks for organics were detected confirming the complete removal of the intermediate products generated in A1.

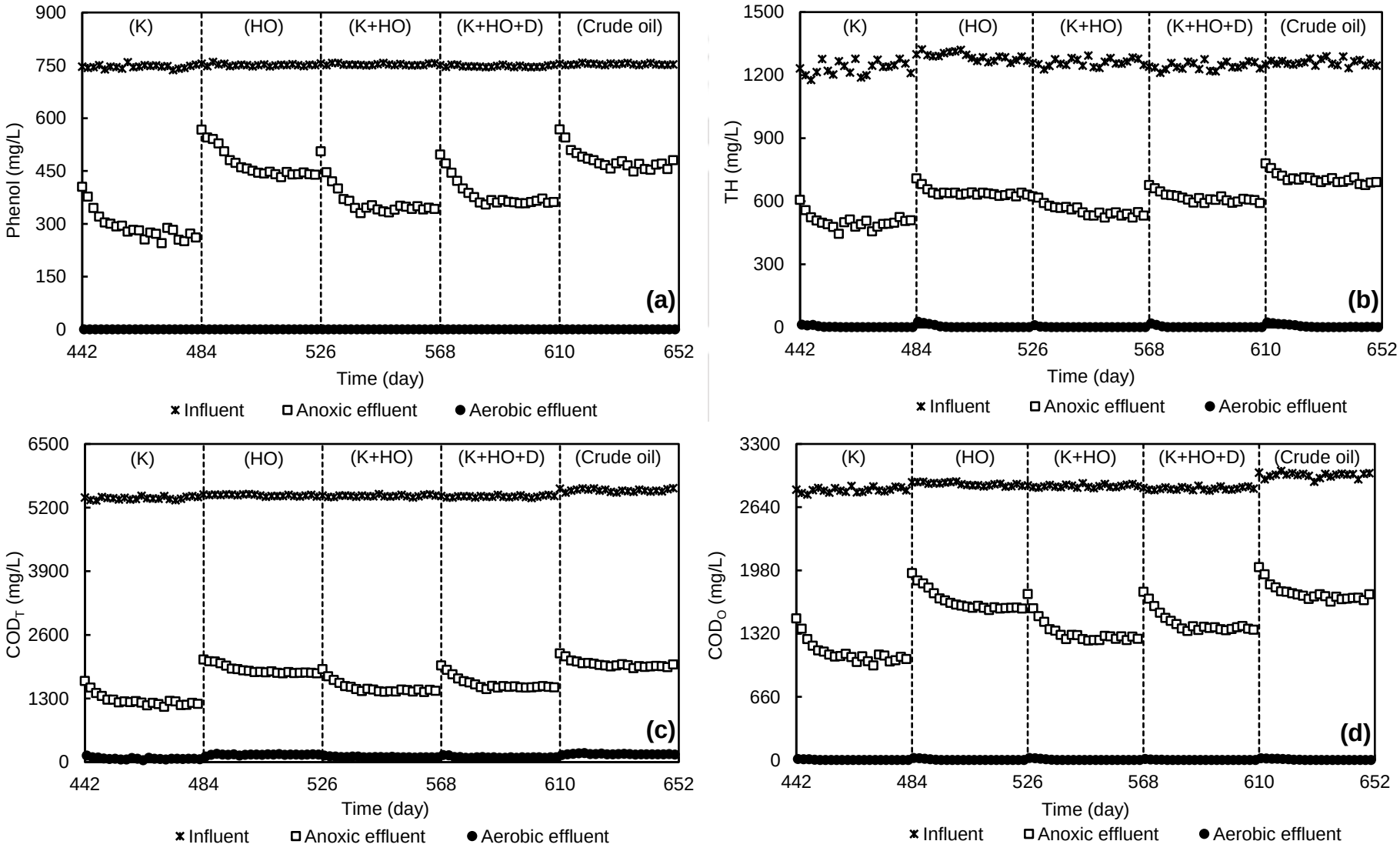

Fig. 4.4: Influent and effluent concentrations of (a) Phenol, (b) TH, (c) COD$_T$ and (d) COD$_O$ during varied hydrocarbons

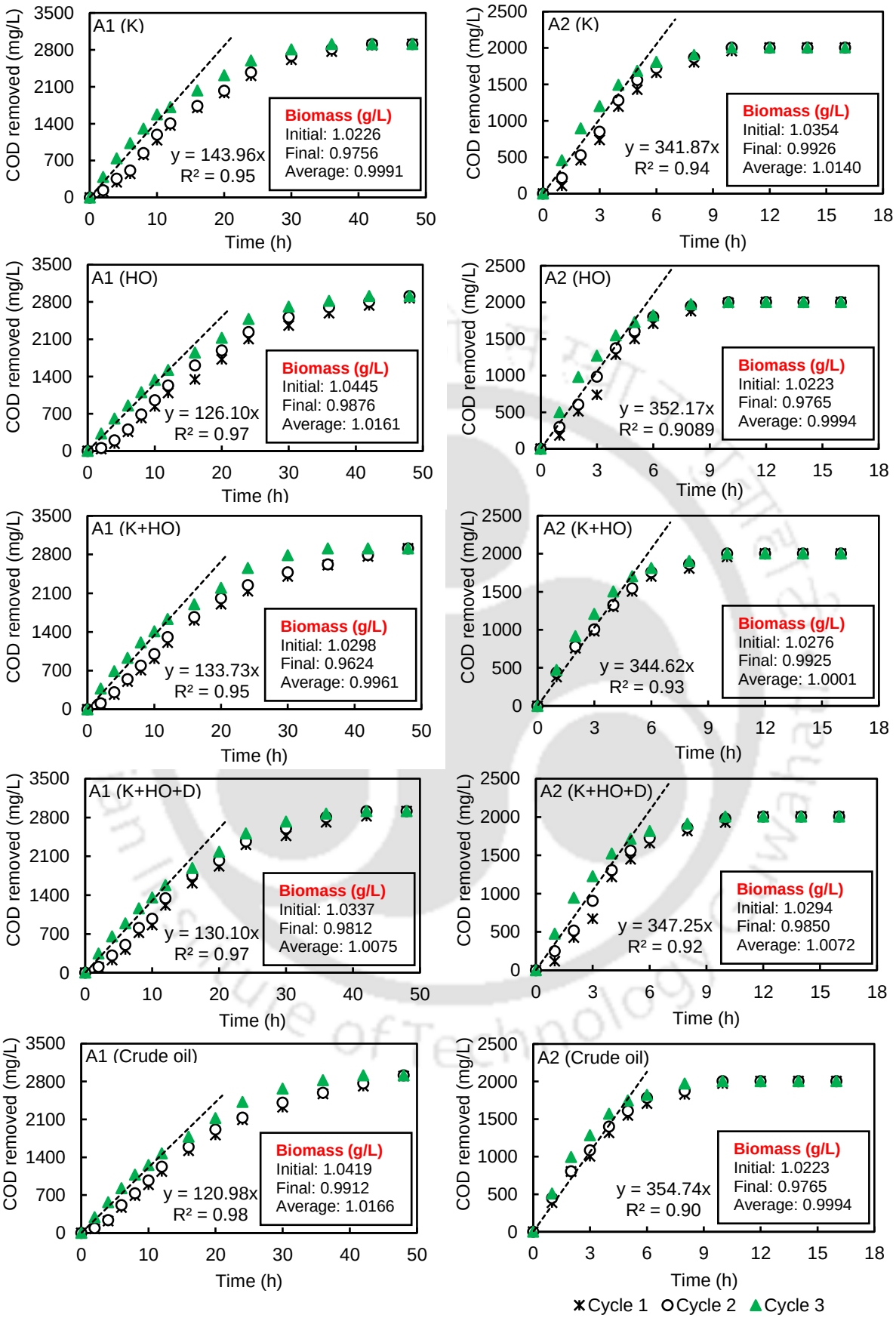

Fig. 4.5: Heterotrophic activity (HA) cycles of anoxic and aerobic biomass during variation in feed hydrocarbons properties

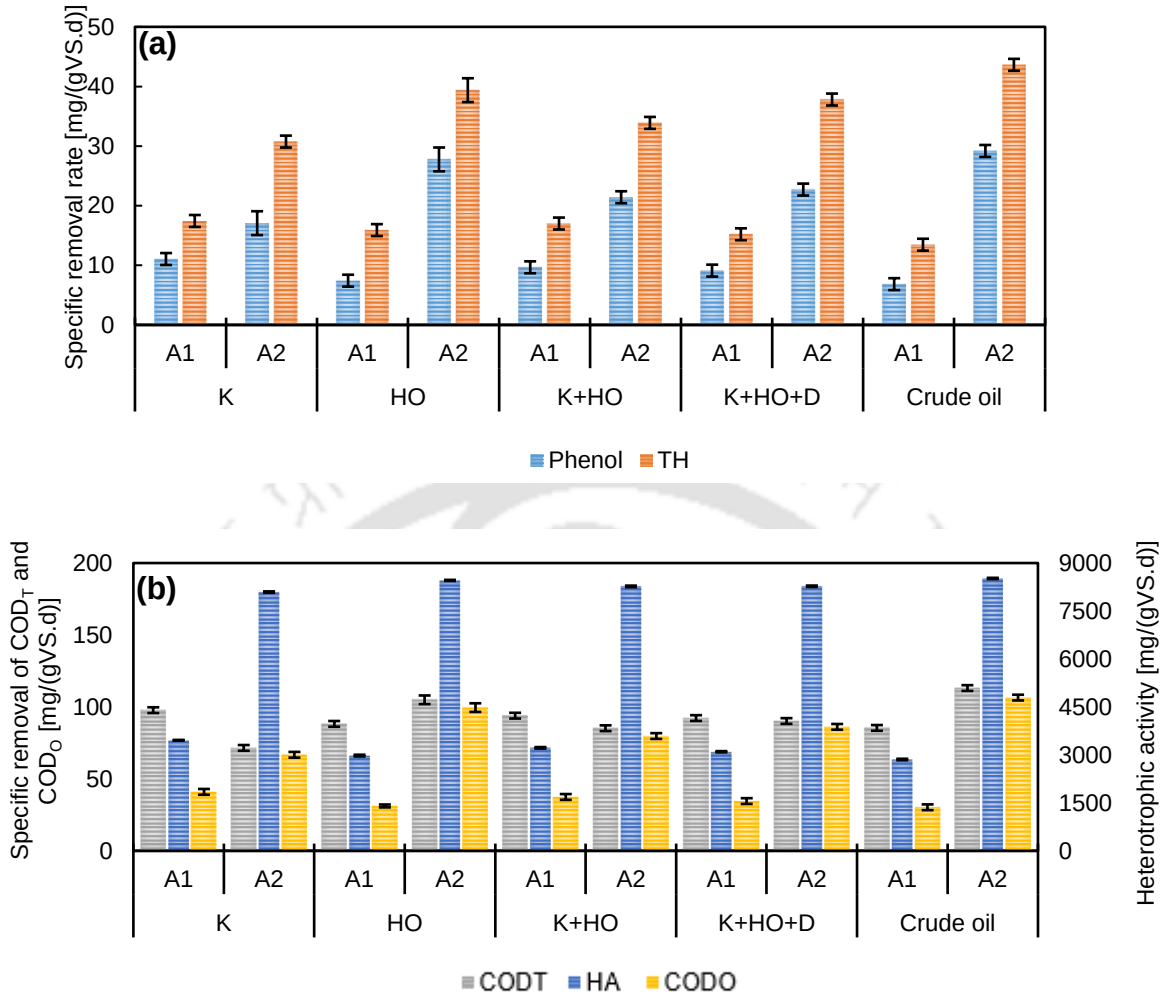

Fig. 4.6: (a) specific removal rate of phenol and TH, (b) specific removal rate of COD_T, COD_O and heterotrophic activity during hydrocarbon variation

4.3.2.3 Removal of sulfide

Effluent S^{2-} from A1 was quite low in all the cases (Fig. 4.7a) and specific removal of S^{2-} in A1 remained constant (Fig. 4.7b). Effect of hydrocarbons and decrease in SRT could not affect oxidation of S^{2-} in A1. S^{2-} oxidation in anoxic environment is a two-step process with formation of S^0 in the first step and further oxidation to SO_4^{2-} (An et al., 2010). Generation of SO_4^{2-} in A1 was maximum when kerosene was the sole hydrocarbon and minimum in the presence of crude oil (Fig. 4.7a). Inhibition on S^{2-} oxidation to SO_4^{2-} increased with increase in hydrocarbon viscosity and density. Degradation of S^{2-} was faster in A1 compared to phenol, as S^{2-} was completely oxidized at 60h HRT but residual phenol remained after anoxic treatment despite of the same initial concentration (Table 4.4).

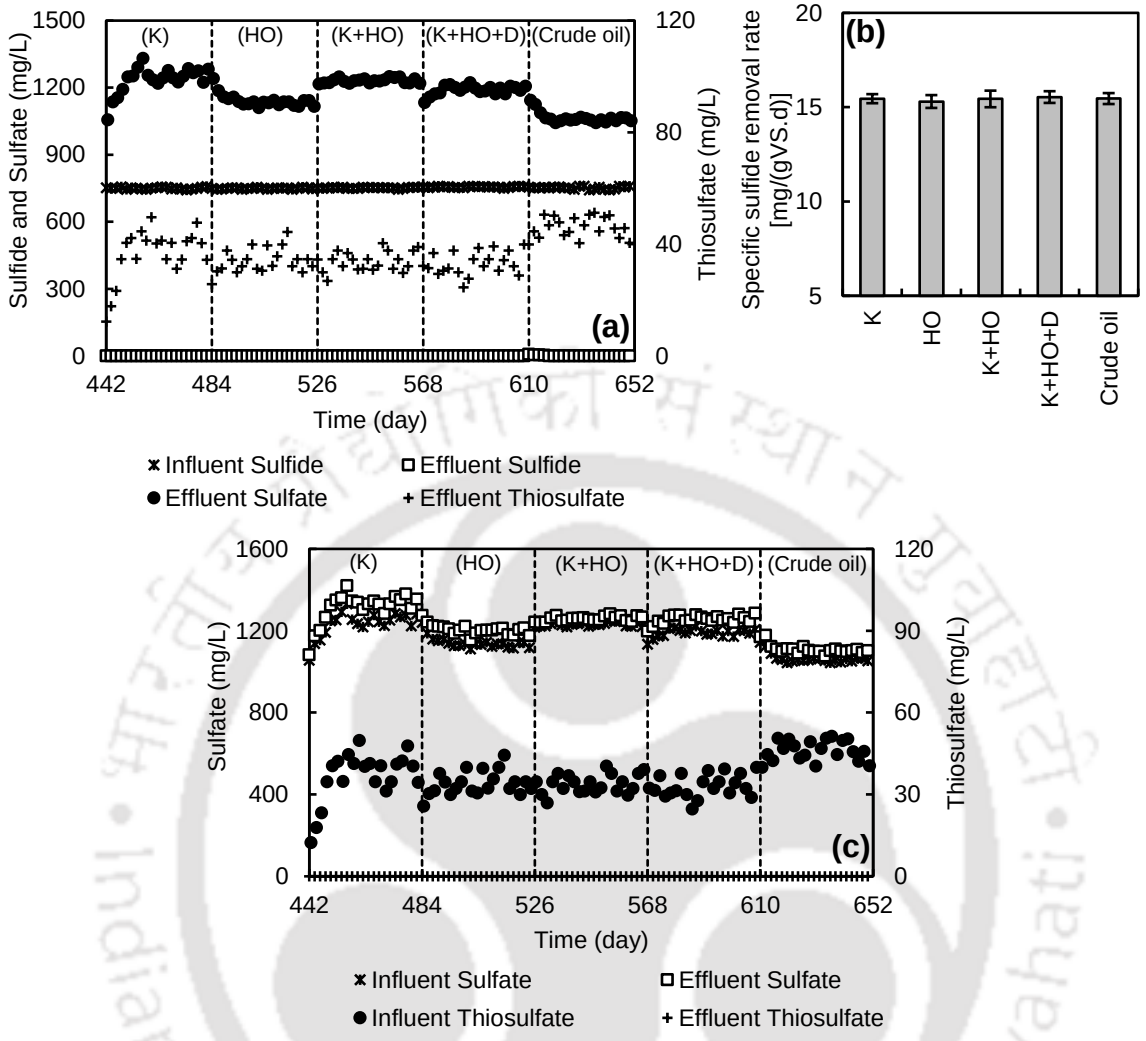

Fig. 4.7: (a) influent and effluent sulfide, sulfate and thiosulfate in A1, (b) specific sulfide removal rate in A1, (c) influent and effluent sulfate and thiosulfate in A2

$S_2O_3^{2-}$ generation was less than 5% of the removed S^{2-} in the presence of any of the hydrocarbon source and no significant change was observed (Fig. 4.7c). Rest of the removed S^{2-} was chiefly S^0 (320 ± 4 to 387 ± 7 mg/L) and precipitated metal-sulfide. Generated $S_2O_3^{2-}$ was oxidized in A2 (Fig. 4.7c) and effluent SO_4^{2-} increased (Table 4.4). Chemolithotrophic activity (CA) cycles and average CA are summarized in Fig. 4.8. CA of A1 biomass was much lower than the observed heterotrophic activity (HA). CA was higher in the presence of HO and crude oil compared to the other types of hydrocarbons. Hence, anoxic biomass was able to degrade S^{2-} with NO_3^--N as electron acceptor in the absence of organics. These results indicate that in reactor A1, both CA and HA existed. Heterotrophic degradation was severely affected in the presence of either HO or crude oil with increase in density and viscosity. S^{2-} was oxidized by autotrophic action in A1 reactor remained unaffected by change in hydrocarbon type.

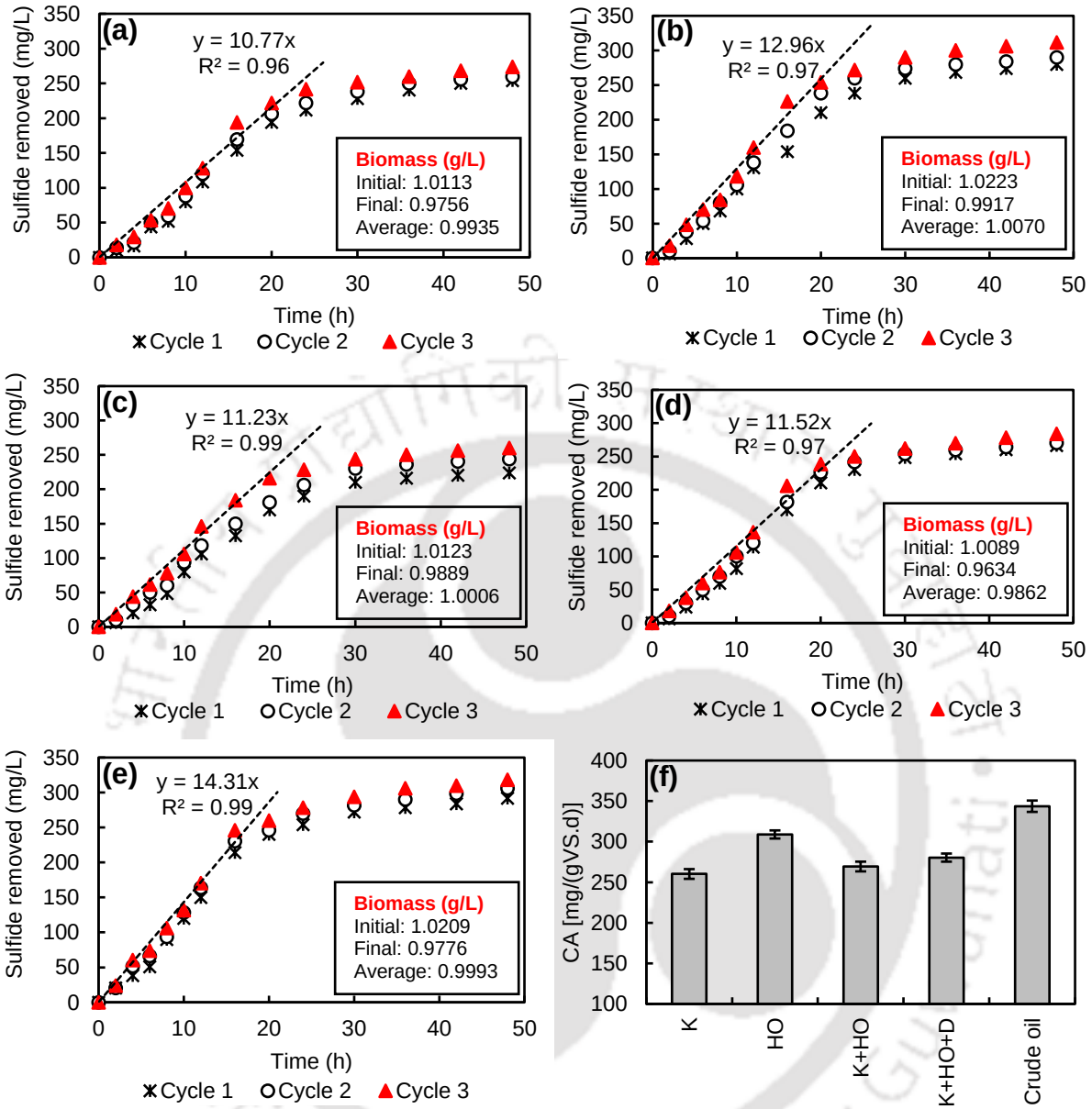

Fig. 4.8: Chemolithotrophic activity (CA) cycles of anoxic biomass in the presence of (a) K, (b) HO, (c) K+HO, (d) K+HO+D, (e) crude oil, (f) average CA

4.3.2.4 Removal of nitrogen

More than 99% of the electron acceptor (NO_3^--N) was utilized in A1 and type of hydrocarbon source had no effect on the reduction of NO_3^--N at 60h HRT (Fig. 4.9a). Accumulation of NO_2^--N was minimum in the presence of kerosene and increased (>2 times in the presence of either HO or crude oil) when hydrocarbon of higher density was supplied (Table 4.4). Denitrification (%) was calculated as follows,

$$\text{Denitrification } (\%) = \frac{[\text{Inf. } NO_3^-] - [\text{Eff.}NO_3^-] - [\text{Eff.}NO_2^-]}{[\text{Inf.}NO_3^-]} \times 100 \quad \ldots (4.4)$$

Less number of electrons were released due to decrease in the removals of organics in the presence of HO and crude oil leading to increase in the partial reduction of NO_3^--N to NO_2^--N. Hence, denitrification decreased from 91% to 80% in the presence of crude oil.

Maximum gas was produced in the presence of kerosene and decreased with increase in hydrocarbon density and viscosity (Table 4.4). Nitrogen (N_2) consisted of 97% of the generated gas when kerosene was used as hydrocarbon source, decreased in the presence of other hydrocarbons and remained within 90-94% of the total generated gas (Fig. 4.9b). Decrease in N_2 in the presence of either HO or crude oil confirms the decrease in denitrification. Carbon dioxide (CO_2) and (H_2S) were 1-2% of the total generated gas and CH_4 was never observed. Effect of hydrocarbons was never observed in the generation of either CO_2 or H_2S. Rest of the gaseous species was termed as unaccounted and could be the mixture of intermediate nitrogen species like N_2O, NO and NO_2 and volatile NH_3 at high alkaline pH. Removal of NH_4^+-N in A1 was paltry (4-6%) and completely oxidized in A2 (Fig. 4.10a). Effect of hydrocarbons could not affect NH_4^+-N. Specific removal rate of NH_4^+-N was quite high in A2 compared to A1, as more than 95% was oxidized in A2 (Fig. 4.10b). Oxidation of NH_4^+-N generated NO_3^--N in A2, which moderately decreased in the presence of residual HO and crude oil (Fig. 4.10c).

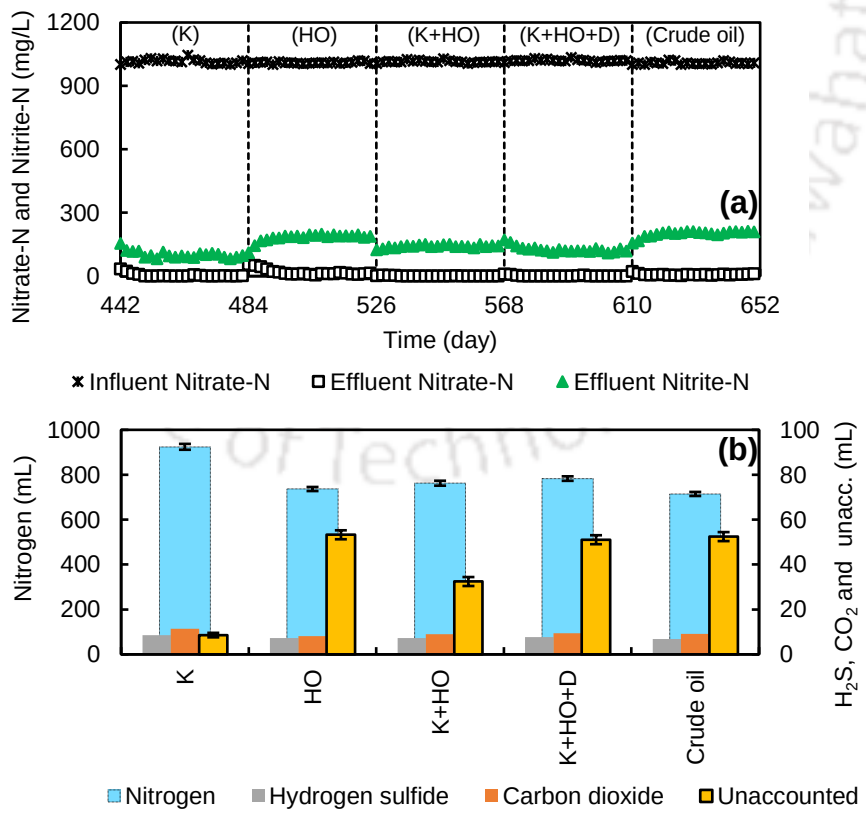

Fig. 4.9: (a) influent and effluent nitrate-N and nitrite-N in A1, (b) gas composition

Total nitrification rate in A2 was calculated based on the generation of NO_3^--N, consumption of NO_2^--N and reactor HRT. Nitrification rates were 182 ± 5, 146 ± 3 and 178 ± 2, 158 ± 3 and 117 ± 2 g/(m^3.d) in the presence of residual K, HO, (K+HO), (K+HO+D) and crude oil, respectively. Slow growth of nitrifying bacteria compared to heterotrophic bacteria (Rittman et al., 1999; Dolinsek et al., 2013) in A2 resulted in the decline in nitrifying rate when either HO or crude oil was used. This suggests that nitrifiers remained active even in the presence of more toxic colloidal matter but the rate slowed down. Effluent pH of aerobic reactor was 8.4-8.6 during the study. Free ammonia (FA) was calculated as per Eq. 2.13 in Chapter 2.

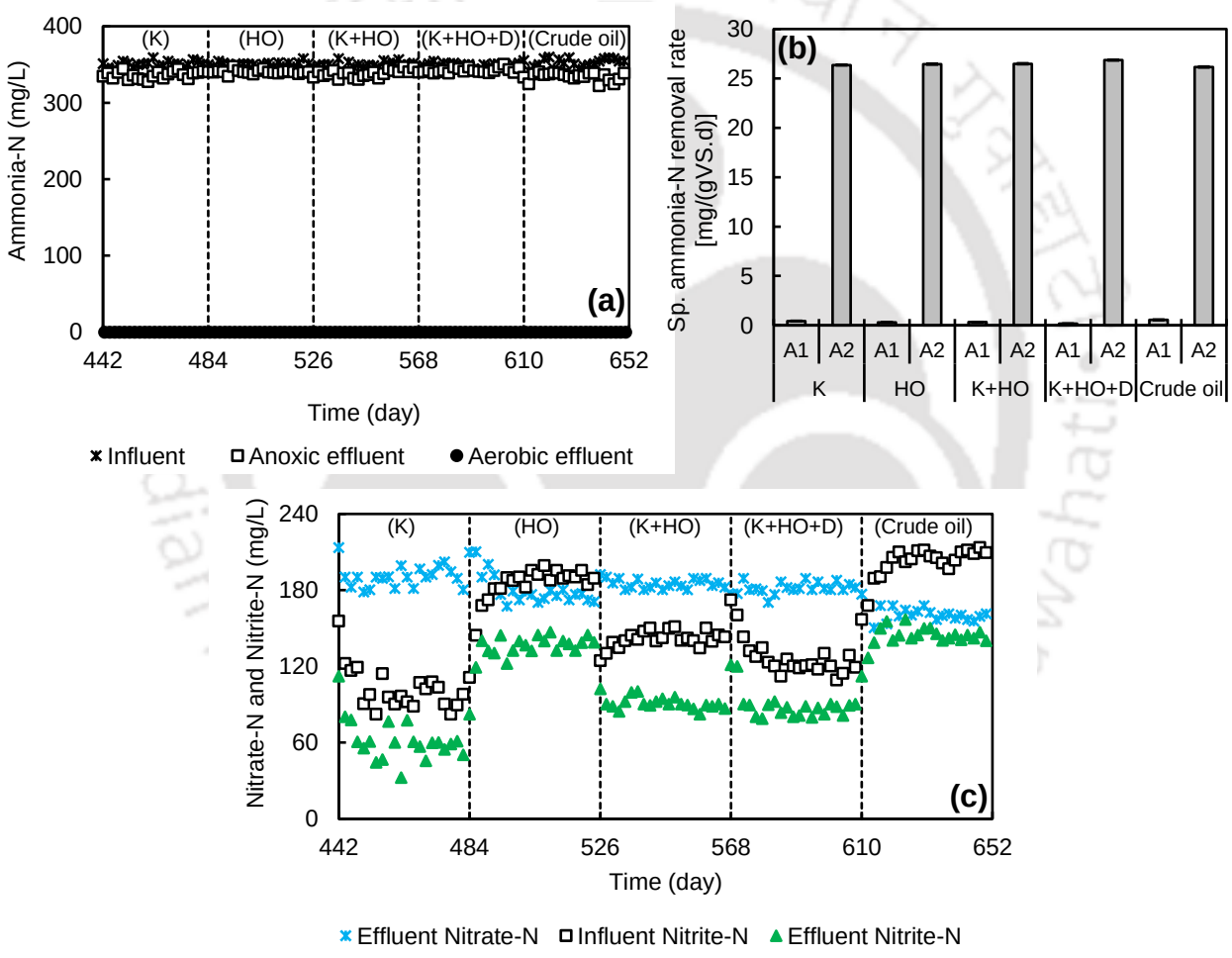

Fig. 4.10: (a) removal of ammonia-N in A1 and A2, (b) specific removal rate of ammonia-N, (c) influent and effluent nitrate-N and nitrate-N in A2

FA remained within 60-70 mg/L (Table 4.4). Higher FA (10-150 mg/L) causes inhibitory effect to the nitrite and NH_4^+-N oxidizing organisms (Liu and Tay, 2001). In the present study, all of the NH_4^+-N was degraded by aerobic reactor but NO_2^--N degradation remained incomplete.

4.3.3 Mechanism of pollutants removal in anoxic reactor (A1)

Mechanism of the pollutants degradation in anoxic condition is shown in Fig. 4.11. Soluble phenol, S^{2-} and NO_3^--N directly diffused into the bacterial cell wall but direct interaction of hydrocarbons with the microorganisms depended upon the structure of cell wall and hydrophobicity. Previous literature reported that long chain hydrocarbons are resistant to biodegradation due to hydrophobic nature (Delarco and De Francea, 2001). Hydrocarbons with lower molecular weight are more soluble in water (Vajrani and Upasani, 2017). Hydrocarbons reach the cell wall as sub microscopic droplets and penetrate through the grooves formed by the cell wall just before the interaction (Vajrani and Upasani, 2017). Diffusion of K was easier compared to HO and crude oil due to its smaller size and chain length (Delarco and De Francea, 2001). Fig. 4.1 shows almost aqueous solution after the emulsification of K. Emulsified HO and crude oil looked like white and brownish colloidal suspensions. Table 4.2 shows that with K as sole hydrocarbon source, turbidity and suspended solids in feed were minimum and higher when HO and crude oil was hydrocarbon source. It seems that when either HO or crude oil was added, a non-aqueous colloidal suspension was formed. On the other hand, inorganics like NO_3^-, S^{2-} and NH_4^+ were soluble in aqueous solution and directly penetrated through the cell wall. Removal of S^{2-} was unaffected by hydrocarbon type. NO_3^--N removal was unaffected, since it was the sole electron acceptor for oxidation of organics. Poorer diffusion of organics resulted in lower denitrification and higher NO_2^--N accumulation. NH_4^+-N removal was unaffected and no removal was achieved in the anoxic reactor.

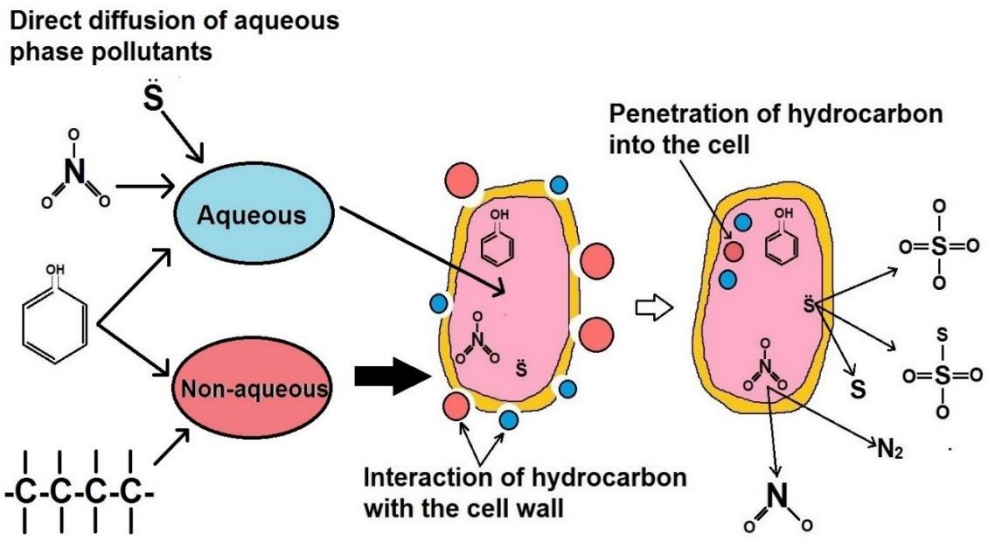

Fig. 4.11: Removal mechanism of pollutants in A1

Table 4.4: Effluent concentrations of pollutants during variation in hydrocarbon density and viscosity

Parameters	K			HO			K+HO			K+HO+D			Crude oil		
	Anoxic		Aerobic	Anoxic		Aerobic	Anoxic		Aerobic	Anoxic		Aerobic	Anoxic		Aerobic
	Influent	Effluent	Effluent	Influent	Effluent	Effluent	Influent	Effluent	Effluent	Influent	Effluent	Effluent	Influent	Effluent	Effluent
Phenol	746 ± 5	272 ± 16	3 ± 1	750 ± 2	447 ± 10	4 ± 1	751 ± 2	342 ±16	4 ± 1	747 ± 2	363 ± 6	4 ± 1	753 ± 2	466 ± 10	5 ± 1
TH	1238 ± 30	490 ± 21	5 ± 2	1244 ± 19	633 ± 6	5 ± 2	1262 ± 18	542 ±16	4 ±2	1245 ±18	604 ±10	4 ±2	1261 ± 17	697 ± 11	5 ± 2
Sulfide	750 ±5	2 ±1	-	749 ±13	2 ±1	-	752 ±3	2 ±1	-	756 ±3	3 ±1	-	751 ± 6	3 ± 1	-
COD_T	5395 ±28	1203 ±37	62 ±13	5446 ± 18	1839 ± 25	151 ±7	5441 ± 20	1462 ± 22	95 ±5	5428 ± 20	1536 ± 21	100 ± 5	5549 ±27	1967 ± 25	160 ± 5
COD_O	2802 ±23	1064 ±35	12 ± 3	2876 ±17	1601 ±26	14 ±2	2862 ± 15	1276 ±22	11 ±2	2835 ±15	1377 ±19	11 ±2	2971 ±27	1701 ± 25	16 ± 2
Thiosulfate	-	40 ±5	ND	-	46 ±4	ND	-	34 ±3	ND	-	33 ± 5	ND	-	46 ± 4	ND
Sulfate	38 ±5	1260 ± 31	1343 ± 33	35 ±4	1129 ±11	1196 ± 18	47 ±4	1232 ±10	1301 ± 12	40 ±4	1194 ±13	1261 ±14	44 ±3	1056 ± 7	1141 ± 11
Sulfur	-	320 ±4	-	-	365 ±6	-	-	333 ±7	-	-	352 ±4	-	-	387 ± 7	-
Ammonia-N	351 ±4	336 ±5	4 ±1	351 ±3	340 ±12	5 ±2	350 ±4	339 ±5	5 ±2	349 ±3	343 ±3	4 ±2	351 ±3	340 ± 2	5 ± 2
Nitrate-N	1017 ±11	1 ±1	191 ±7	1010 ±6	11 ±3	175 ±4	1016 ±5	1 ±1	182 ±13	1021 ±5	1 ±1	185 ±5	1010 ± 6	7 ± 2	160 ± 3
Nitrite-N	-	96 ±9	56 ±12	-	191 ±4	137 ±6	-	120 ±6	86 ±4	-	144 ±5	90 ±4	-	208 ± 8	145 ± 5
FA	-	-	60 ±2	-	-	71 ±2	-	-	71 ±2	-	-	86 ±3	-	-	70 ± 3
pH	9.5 ± 0.1	9.1 ±0.1	8.4 ± 0.1	9.5 ±0.1	9.0 ± 0.1	8.5 ± 0.1	9.5 ±0.1	9.1 ±0.1	8.5 ± 0.1	9.5 ±0.1	9.1 ± 0.1	8.6 ±0.1	9.5 ±0.1	9.0 ± 0.1	8.5 ± 0.1
Gas (mL)	-	953 ±27	-	-	-	805 ±13	-	-	851 ±24	-	-	811 ± 11	-	-	760 ± 20

K: kerosene, HO: Heavy oil, D: Diesel
TH: Total hydrocarbon, ND: not detected, FA: Free ammonia
COD_T: Total chemical oxygen demand
COD_O: Organic chemical oxygen demand
All units except gas and pH are in mg/L

4.4 SUMMARY OF THE STUDY

Anoxic-aerobic sequential reactor system was highly efficient to biodegrade petroleum refinery wastewater in the presence of different hydrocarbons like kerosene (K), heavy oil (HO), mixtures of kerosene and heavy oil (K+HO), mixture of kerosene, heavy oil and diesel (K+HO+D) and crude oil at total hydraulic retention time of 80h. Heavy oil and crude oil with higher density caused more biomass washout in the anoxic reactor, lowering solid retention time and poorer organic removal. Removal of organics in anoxic reactor decreased in the order of K > (K+HO) > (K+HO+D) > HO > crude oil. Complete degradation of the remaining organics occurred in the aerobic reactor irrelevant of the density and viscosity of the hydrocarbons. Activity of aerobic biomass was higher compared to anoxic biomass due to higher degradation of organics at lesser hydraulic retention time. A direct correlation was observed between biomass activity and organics removal performance of the reactors. Complete oxidation of sulfide was observed in anoxic reactor. Ammonia-N was completely oxidized in the aerobic reactor with final products as nitrate and nitrite in effluent.

References

Abass, O. K., Fang, F., Zhuo, M., Zhang, K. 2018. Integrated interrogation of causes of membrane fouling in a pilot scale anoxic-oxic membrane bioreactor treating oil refinery wastewater. Science of the Total Environment 642: 77-89.

An, S., Tang, K., Nemat, M. 2010. Simultaneous biodesulphurization and denitrification using diesel reservoir microbial culture: Effects of sulfide loading rate and sulfide to nitrate loading ratio. Water Research 44(5): 1531-1541.

APHA, AWWA, WPCF. Standard Methods for the Examination of Water and Wastewater. 21st ed., American Public Health Association, Washington DC, 2005.

Banerjee, A., Ghoshal, A. K. 2016. Biodegradation of real petroleum wastewater by immobilized hyper phenol-tolerant strains of Bacillus cereus in a fluidized bed bioreactor. 3 Biotech 6: article 137. DOI 10.1007/s13205-016-0447-1

Delarco, J. P., De Francea, F. P. 2001. Influence of oil contamination levels on hydrocarbon biodegradation in sandy sediment. Environmental Pollution 110: 515-519.

Diya'uddin, B. H., Daud, W. M. A. W., Aziz, A. R. A. 2011. Treatment technologies for petroleum refinery effluents: a review. Process Safety and Environmental Protection 89(2): 95-105.

Dolinsek, J., Lagkouvardos, I., Wanek, W., Wagner, M., Holger, Daims. 2013. Interactions of nitrifying bacteria and heterotrophs: Identification of a Micavibrio-Like putative predator of nitrospira. Applied and Environmental Microbiology 79(6): 2027-2037.

Ebrahimi, M., Kazemi, H., Mirbagheri, S. A., Rockaway, T. D. 2016. An optimized biological approach for treatment of petroleum refinery wastewater. Journal of Environmental Chemical Engineering 4: 3401-3408.

Gasim, H. A., Kutty, S. R. M., Isa, M. P. M. 2012. Treatment of petroleum refinery wastewater by using UASB reactors. International Journal of Chemical and Biological Engineering 6: 174-177.

Ghorbanian, M., Moussavi, G., Farzadkia, M. 2014. Investigating the performance of an up-flow anoxic fixed-bed bioreactor and a sequencing anoxic batch reactor for the biodegradation of hydrocarbons in petroleum-contaminated saline water. International Biodeterioration and Biodegradation 90: 106-114.

Heipieper, H. J., Martinez, P. M. 2010. Toxicity of hydrocarbons to microorganisms, In: Timmis K.N. (eds) Handbook of Hydrocarbon and Lipid Microbiology. Springer, Berlin, Heidelberg.

Hussain, A., Dubey, S. K. 2017. Specific methanogenic activity test for anaerobic degradation of influents. Applied Water Science 7: 535-542.

Jawed, M., Tare, V. 1999. Microbial composition assessment of anaerobic biomass through methanogenic activity tests. Water SA 25: 346-350.

Khan, S. R., Nirmal, J. I. K., Kumar, R. N., Patel, J. G. 2015. Biodegradation of kerosene: Study of growth optimization and metabolic fate of *P. janthenellum* SDX7. Brazilian Journal of Microbiology 46(2): 397-406.

Liu, Y., Tay, J. H. 2001. Factors affecting nitrite buildup in nitrifying biofilm reactor. Journal of Environmental Science and Health 36: 1027-1040.

McHugh, S., Carton, M., Collins, G., O'Flaherty, V. 2004. Reactor performance and microbial community dynamics during anaerobic biological treatment of wastewaters at 16-37 ºC. FEMS Microbiology and Ecology 48: 369-378.

Metcalf and Eddy. 2011. Wastewater Engineering, Treatment and reuse, Seventh Edition. Tata McGraw-Hill Edition.

Miller, F. A., Wilkins, C. H. 1952. Infrared spectra and characteristic frequencies of inorganic ions. Analytical Chemistry 24(8): 1253-1294.

Moussavi, G., Ghorbanian, M. 2015. The biodegradation of petroleum hydrocarbons in an upflow sludge blanket/fixed film hybrid bioreactor under nitrate-reducing conditions: Performance evaluation and microbial identification. Chemical Engineering Journal 280: 121-131.

Moussavi, G., Shekoohiyan, S., Naddafi, K. 2016. Anoxic biodegradation of petroleum hydrocarbons in saline media using denitrifier biogranules. Ecotoxicology and Environment Safety 129: 51-56.

Qasim, M., Ansari, T. M., Hussain, M. 2017. Combustion, performance, and emission evaluation of a diesel engine with biodiesel like fuel blends derived from a mixture of Pakistani waste canola and waste transformer oils. Energies 10: Article 1023.

Ramasamy, S., Mathiyalagan, M., Chandran, P. 2014. Characterization and optimization of EPS-producing and diesel oil-degrading Orchobacterium anthropic MP3 isolated from refinery wastewater. Petroleum Science 11: 439-445.

Razavi, S. M. R., Miri, T. 2015. A real petroleum refinery wastewater treatment using hollow fiber membrane bioreactor (HF-MBR). Journal of Water Process Engineering 8: 136-141.

Revathy, T., Jayasri, M. A., Suthindharan, K. 2015. Biodegradation of PAHs by Burkholderia sp. VITRSB1 isolated from marine sediments. Hindawi Publishing Corporation Scientifica 2015: 1-9.

Rittman, B., Laspidou, C. S., Flax, J., Stahl, D. A., Urbain, V., Harduin, H., Van Der Waarde, J. J., Geurkink, B., Henssen, M. J. C., Brouwer, H., Klapwijk, A., Wetterauw, A. 1999. Molecular and modeling analysis of the structure and function of nitrifying activated sludge. Water Science and Technology 39: 51-59.

Sahariah, B. P., Chakraborty, S. (2013) Performance of anaerobic-anoxic-aerobic batch fed moving-bed reactor at varying phenol feed concentrations and hydraulic retention time. Clean Technology and Environmental Policy 15: 225-233.

Sahariah, B. P., Kumar, J. A., Chakraborty, S. 2016. Treatment of coke oven wastewater in an anaerobic-anoxic-aerobic moving bed bioreactor system. Desalination and Water Treatment 57(31): 14396-14402.

Schink, B. 2006. Microbially driven redox reactions in anoxic environments: pathways, energetics, and biochemical consequences. Engineering Life Science 6(3): 228-233.

Segneanu, A. E., Gozescu, I., Dabici, A., Sfirloaga, P., Szabadai, Z. 2012. Organic compounds FT-IR spectroscopy. Macro to Nano Spectroscopy, ISBN: 978-953-51-0664-7: InTech.

Sharghi, E. A., Bonakdarpour, B., Roustazade, P., Amoozegar, M. A., Rabbani, A. R. 2016. The biological treatment of high salinity synthetic oil field produced water in a submerged membrane bioreactor using a halophilic bacteria consortium. Journal of Chemical Technology and Biotechnology 88: 2016-2026.

Sharma, A., Kumar, P., Rehman, M. B. 2014. Biodegradation of diesel hydrocarbon in soil by bioaugmentation of Pseudomonas aeruginosa: A laboratory scale study. International Journal of Environmental Bioremediation and Biodegradation 2(4): 202-212.

Sonwani, R. K., Swain, G., Giri, B. S., Singh, R. S., Rai, B. N. 2019. A novel comparative study of modified carriers in moving bed biofilm reactor for the treatment of wastewater: Process optimization and kinetic study. Bioresource Technology 281: 335-342.

Talaiekhozani, A., Jafarzadeh, N., Fulazzaky, M. A., Talaie, M. R., Beheshti, M. 2015. Kinetics of substrate utilization and bacterial growth of crude oil degraded by Pseudomonas aeruginosa. Journal of Environmental Science and Engineering 13(64): 1-8.

Technical EIA guidance manual for petroleum refining industry. The ministry of Environment and Forests, Government of India, 2010.

Vajrani, S. J., Upasani, V. N. 2017. A new look on factors affecting microbial degradation of petroleum hydrocarbon pollutants. International Biodeterioration and Biodegradation 120: 71-83.

Wang, Y., Wang, Q., Li, M., Wang, Y., He, W., Yan, G., Guo, S. 2016. An alternative anaerobic treatment process for treatment of heavy oil refinery wastewater containing polar organics. Biochemical Engineering Journal 105: 44-51.

Wang, Y. T., Xu, J., Liu, X. F., Chen, M. H., Wang, S. T. 2015. Study of determination of oil mixture components based on Quasi-Monte Carlo Method. Guang Pu Xue Yu Guang Pu Fen Xi 35(5), 1312-1315.

Zhrong, L., Longfei, C., Mohammed, S. A. 2018. Comprehensive chemical characterization of lubricating oils used in modern vehicular engines utilizing GC × GC-TOFMS. Fuel 220: 792-799.

5

CHAPTER

IDENTIFICATION OF DOMINANT SPECIES AND BIOREMEDIATION OF AUTOMOBILE SERVICE STATION WASTEWATER

CHAPTER 5

IDENTIFICATION OF DOMINANT SPECIES AND BIOREMEDIATION OF AUTOMOBILE SERVICE STATION WASTEWATER

5.1 INTRODUCTION

Pollutants degradation by both heterotrophic and chemolithotrophic action was confirmed by activity analysis from Chapter 4. Microbial communities like *Bacillus sp.* (Mousssavi and Ghorbanian, 2015) and *Pseudomonas sp.* (Sharma et al., 2014) in anoxic condition and *Bacillus sp.* (Chhetri et al., 2016), *Proteobacteria*, *Actinobacteria* (Brzeszcz and Kaszycki, 2018) in aerobic conditions are capable of degrading petroleum pollutants. However, the reported literature works never used collective mixture of organics (phenol, hydrocarbons) and inorganics (S^{2-}, NH_4^+-N, NO_3^--N) as feed. Degradation of the mentioned pollutants was successfully achieved in anoxic-aerobic sequential reactors and identification of microbial species can give information about the diversity of microbial presence.

Maintenance of the vehicles in service stations includes cleansing and washing by pressurized wax-mediated water and detergents rich in phosphates, ammonia-N and nitrate-N (Asha et al., 2016). Incomplete combustion products of motor oil, hydrocarbons and organometallics are the staple constituents that impart COD to the released wastewater from automobile service stations (Boonchan et al., 2000). Concentrations of hydrocarbons (80-700 mg/L) and COD (100-1000 mg/L) of such wastewaters can vary depending upon the type and number of vehicular services (Ganiyu et al., 2018; Boularte et al., 2016). Presence of phenol (Zaneti et al., 2011) and nitrogen compounds (NO_3^--N, NO_2^--N) (Boularte et al. 2016) in the automobile service station wastewater are reported. Single vehicular wash generates 150-600 L of wastewater (Lau et al., 2013) and directly discharged to the municipal sewage drains by most of the service stations (Sires et al., 2012). This leads to hazardous effects on the environment, heavy load on sewage systems and metallic deposits in sewer networks (Paxeus et al., 1996). Developed countries have incorporated legislations on the freshwater usage, on-site treatment and reuse of the treated wastewater in service stations (Ganiyu et al., 2018).

Biological systems are cost friendly and do not require any external chemical addition as all the nutrients for the microorganisms are already present in the wastewater. In addition, effluent pH (6.2 - 8.8) of such wastewater varies from moderate acidic to alkaline range (Boularte et al., 2016), which makes it a suitable candidate for bio-treatment. Few studies for the treatment of vehicle wash wastewater by activated sludge process (ASPs) (Asha et al., 2016; Mazumder et al., 2011) and membrane bioreactors (Boularte et al., 2016) have been reported. However, abiotic loss of emulsified oils in ASPs cannot be avoided. Hence, treatment of such wastewater in a closed anaerobic/anoxic system is a viable option and reported literature works are available (Sharma and Philip, 2014; Moussavi and Ghorbanian, 2015; Ramos et al., 2016). However, ammonia-N oxidation is difficult in anoxic condition and downstream aerobic treatment becomes necessary for its oxidation.

Anoxic and aerobic reactors operated in series are advantageous as they eliminate volatilization of emulsified oil in anoxic systems, provide nitrification of ammonia-N in aerobic systems and encourage the reuse of the treated water (Nasirpour et al., 2015). However, performance evaluation of anoxic-aerobic sequential systems for the treatment of automobile service station wastewater is not reported yet. Analysis of dominant microbial species and sludge characteristics of the bioreactors in terms of metals content during the degradation of automobile service station wastewater is also missing from the literature reports.

In the present study, attempt was made to identify the dominant microbial species in both anoxic and aerobic reactors. In addition, characterization and treatment of real automobile service station wastewater was done in anoxic-aerobic sequential system to achieve effective reuse quality. Furthermore, metals content in the reactor-generated sludge was measured for potential land disposal.

5.2 MATEIALS AND METHODS

5.2.1 Chemicals and Reagents

Chemicals and reagents used in the present study were of AR grade and same as described in section 2.2.1 of Chapter 2. All the stock solutions and reagents were prepared by milli-Q water (pH 7.0 ± 0.1). Nutrient agar and nutrient broth were purchased from SRL, India. Gram staining kit was purchased from HIMedia. The gram staining kit contained solubilized crystalline blue dye, decolorizing reagent (95% ethyl alchohol), iodine solution and solubilized safranin dye. Glass microscopic slides were purchased from India Gold, India.

5.2.2 Isolation of dominant microorganisms

To find out the viable microorganisms responsible for the degradation of the pollutants in both anoxic and aerobic reactors, biomass was isolated by nutrient agar media by pour plate method. Biomass samples were collected in the same ratio available in the reactors and diluted 10^8 times by serial dilution with sterilized milli-Q water. Diluted sample (1 mL) was taken and grown in nutrient agar media by pour plate method (APHA, 2005). After incubation for 24h at 30 °C, individual colonies were picked and streaked for further isolation in nutrient agar media.

5.2.3 Gram staining test

To perform the gram-staining test, a microscopic slide was taken and a circle was marked in the middle by a pencil. A drop of sterilized water was put on it and spread by a sterilized inoculating loop. A small fraction of the bacterial colony was picked up and spread over the water to form smear by a sterilized inoculating loop. The smear was allowed to dry and heat fixed by passing the bottom of the smear containing area over the flame of a spirit lamp three times. The heat fixed smear was gently flooded with crystal violet and let stand for one minute. The slide was tilted slightly and gently washed with sterilized water using a wash bottle. The smear was decolorized using decolorizing agent (95% ethyl alcohol or acetone). The slide was tilted slightly, alcohol was applied drop by drop for 5 to 10 seconds, and care was taken not to over decolorize and was immediately rinsed with sterilized water. Safranin was gently flooded to counter strain and let stand for 1 minute. Then it was washed with sterilized water, allowed to dry and viewed under microscope. If the cells appear blue color, then they are termed as gram-positive bacteria and if they appear red, then they were termed gram-negative bacteria.

5.2.4 Growth of pure culture and pollutant removal characteristics

Single isolated colony was picked and grown in nutrient broth (100 mL) for 24h at 30 ºC and cells were harvested by centrifugation at 8500 rpm. Cells harvested were added to 100 mL sterilized milli-Q water so that the optical density at 600 nm was within 1.0 - 1.2 (Padhi and Gokhale, 2016). Cells isolated from A1 were subjected to degrade simulated pollutants in a 250 mL plastic conical flask with 100 mL working volume. Conical flasks loaded with feed and biomass were kept in anoxic condition on a shaking incubator (150 rpm) at 30 ºC and concentrations were measured after 48h. Biomass isolated from A2 was subjected to degrade pollutants as per the effluent of A1 in glass beakers (250 mL) with 100 mL working volume at an aeration rate of 2L/min and concentrations were measured after 16h.

5.2.5 Identification of the isolated microbial species

Isolated microbial colonies were grown on plastic petri plates (Tarsons) in nutrient agar media. Samples were packed in polystyrene packs with arranged ice packing to keep the temperature regulated and to arrest the microbial growth. Microorganisms isolated from anoxic biomass were sent to Xceleris, India and microorganisms isolated from aerobic biomass were sent to Pathcarelabs, India for identification. The procedure followed for the identification of microorganisms by Xceleris, India and Pathcarelabs, India are summarized below.

5.2.5.1 Anoxic microorganisms

DNA of the cultures were isolated and quality was evaluated on 0.8% agarose gel. A single band of high molecular weight DNA was observed. Isolated DNA was amplified with 16S rRNA specific primer (8F and 1492R) using Vertii 99 well thermal cycler (Model No. 9902). A single discrete PCR amplicon of 1500 bp was observed. The PCR amplicon was enzymatically purified and further subjected to Sanger Sequencing. Bi-directional DNA sequencing reaction of PCR was carried out with 704F and 907R primers using BDT v3.1 Cycle sequencing kit on ABI 3730 × 1 Genetic Analyzer. Consensus sequence of 1374 bp 16S rDNA was generated from forward and reverse sequence data using aligner software. The *16SrDNA* sequence was used to carry out BLAST alignment search tool of NCBI GenBank database. Based on minimum identity score, first fifteen sequences were selected and aligned using multiple alignment software program ClustalW. Distance matrix was generated using RDP database and the phylogenetic tree was constructed using MEGA5.

5.2.5.2 Aerobic microorganisms

The colonies were sub-cultured and DNA was isolated from the cultures. The DNA was subjected to quality check and quantification. The 16S amplicon was generated using primers 8F and 1492R. The amplicons were subjected to quality check and quantification. The amplicon was sequenced by capillary electrophoresis using the Sanger Big Dye Termination Chemisrty (BDT v3.1 Cycle Sequencing Kit) generating the forward and reverse sequences on ABI 3500 genetic Analyzer. The data was curated, if necessary. A consensus sequence of the 16S region was generated from forward and reverse sequence data using aligner software. The 16S rDNA gene sequence was BLASTed against the nr-database of NCBI Genbank database. The first ten sequences were selected based on maximum identity score. These sequences were aligned using Clustal W (multiple alignment software program). The analysis for number of

base substitutions per site from between sequences were conducted using the Maximum-Composite Likelihood Model (Tamura et al., 2004). The analysis involved 11 nucleotide sequqnces. All positions containing gaps and missing data were eliminated. There were a total of 1391 positions in the final dataset. Evolutionary analysis were conducted in MEGA7 (Kumar et al., 2016). The evolutionary history was inferred by using the Maximum Likelihood method based on the Tamura-Nei model (Tamura and Nei, 1993). The analysis involved 11 nucleotide sequences. All positions containing gaps and missing data were eliminated. There were a total of 1391 positions in the final data set. Evolutionary analyses were conducted in MEGA7 (Kumar et al., 2018).

5.2.6 Reactor operation for real wastewater treatment

Anoxic (A1) - Aerobic (A2) reactors mentioned in section 3.2.2 were used for the present study. Treatment of automobile service station wastewater was performed at total cycle time of 24h (18h for A1 and 6h for A2) and HRT of 30h (22.5h for A1 and 7.5h for A2) for 10 days. Operational conditions of the reactors during the study can be found in Table 5.1.

Table 5.1: Operating conditions of A1 and A2 during the treatment of real automobile service station wastewater

Source	Days	Agitation		Cycle time (h)		HRT (h)	
		A1	A2	A1	A2	A1	A2
Automobile service station wastewater	658-667	20 rpm	Airflow 2L/min	18	6	22.5	7.5

A1: Anoxic reactor, A2: Aerobic reactor

5.2.7 Wastewater collection from service station and characteristics

Wastewater was collected in a plastic bottle with screw cap (Tarsons, 10L) from a combined effluent discharge point of a motor garage and vehicle-washing unit situated near Jayguru chowk of Assam, India. Physico-chemical properties and metallic constituents were analyzed and averages are summarized in Table 5.2. Wastewater was supplemented with phosphate buffer (pH 6.8, 1 mL/L), yeast extract (10 mg/L) and trace metals solution (1 mL/L) as mentioned in section 2.2.4.

Table 5.2: Properties of wastewater from automobile service station

Pollutant	Concentration
Petroleum properties (mg/L)	
Phenol	37 ± 3
Total hydrocarbon	475 ± 11
COD	506 ± 12
Nitrate-N	135 ± 6
Ammonia-N	170 ± 7
Phosphate	20 ± 2
Metallic properties (mg/L)	
Na^{+}	20.13 ± 3.21
K^{+}	37.44 ± 6.13
Ca^{2+}	21.87 ± 6.33
Cr^{3+}	0.14 ± 0.02
Fe^{2+}	0.45 ± 0.02
Mg^{2+}	1.09 ± 0.07
Cu^{2+}	0.67 ± 0.04
Zn^{2+}	0.85 ± 0.06
Co^{2+}	1.99 ± 0.04
Ni^{2+}	0.44 ± 0.02
Mn^{2+}	1.22 ± 0.01
As^{3+}	0.04 ± 0.01
Pb^{2+}	1.02 ± 0.02
Cd^{2+}	0.22 ± 0.01
Physical properties	
Total solids (g/L)	5.11 ± 0.12
pH	7.88 ± 0.04
Conductivity (mS/cm)	44.13 ± 0.12
Salinity (g/L)	1.23 ± 0.11
Total dissolved solids (g/L)	4.13 ± 0.14
Turbidity (NTU)	67.5 ± 1.8

5.2.8 Analytical procedure

5.2.8.1 Analysis of pollutants

Analysis of phenol, S^{2-}, SO_4^{2-}, $S_2O_3^{2-}$, TH, NO_3^{-}-N, NO_2^{-}-N, PO_4^{3-}-P and COD was done as mentioned in section 2.2.6 of Chapter 2. Measurements of suspended solids, turbidity (section 4.2.4), quantification of biomass (section 4.2.5), analysis of gas (section 4.2.8) and FTIR study (section 4.2.9) were done as mentioned in Chapter 4.

5.2.8.2 Analysis of sludge generated from reactors

Metal concentrations in sludge from A1 and A2 were determined by acid digestion method as per Method 3050B of USEPA (1996) (Gueven and Akinci, 2011). Dried sludge samples of 1g was heated for 2h at 95 ºC with 10 mL of 50% HNO_3 in a 250 mL glass conical flask and allowed to cool. The samples were refluxed repeatedly with 65% HNO_3 until the disappearance of brown fumes and evaporated in a hot plate until the volume reduced to 5 mL. After cooling, 10 mL of 30% H_2O_2 was added slowly. The mixture was refluxed with 10 mL 37% HCl at 95 ºC for 15 minutes, filtered through membrane filter paper and diluted to 100 mL before being analyzed. Analysis of metals was done by atomic absorption spectroscopy (AAS, Varian). Sodium (Na^+), potassium (K^+) and calcium (Ca^{2+}) were measured by flame photometer (Systronics, India). Chloride (Cl^-) was measured by argentometric method (APHA, 2005).

5.3 MICROBIAL SPECIES AND PURE CULTURE ANALYSIS

5.3.1 Anoxic biomass

Isolation of the anoxic culture revealed presence of two distinct cultures of orange and white color. Appearance, morphology and microscopic images of both cultures are illustrated in Fig. 5.1. Both cultures were gram negative and rod shaped. Colony formation of both the cultures were circular, raised elevated and entire in margin. Both colonies were subjected to the degradation of individual pollutants separately. Concentrations of phenol and S^{2-} were varied from 0 to 1200 ± 10 mg/L and that of diesel oil was varied from 0 to 700 mg/L (TH 700 ± 12 to 1400 ± 14 mg/L) at constant infeed NO_3^--N of 1000 ± 20 mg/L.

Anoxic orange culture degraded all the pollutants (phenol, S^{2-}, TH and NO_3^--N). Removal of S^{2-} by orange culture decreased from 57% to 12% with increase in S^{2-}. Similarly, degradation of phenol, TH and NO_3^--N also decreased with increase in S^{2-} (Fig. 5.2a). Degradation of phenol (56% to 7%) and TH (41% to 8%) decreased with increase in phenol. However, degradation of S^{2-} and NO_3^--N increased (Fig. 5.2b). Increase in influent TH led to decrease in the removals of phenol and TH. However, removal of S^{2-} and NO_3^--N increased as it happened when influent phenol was varied (Fig. 5.2c). Orange culture was further analyzed for the anoxic degradation of different concentrations of S^{2-} (0-1200 ± 10 mg/L) with and without the presence of organics at constant NO_3^--N (1000 ± 20 mg/L). S^{2-} removal was negligible (2-4%) in the absence of organics (Fig. 5.2d) and significant increase in S^{2-} removal was observed both in the presence of phenol (750 ± 5 mg/L) (Fig. 5.2e) and diesel (TH 350 ± 12 mg/L) (Fig. 5.2f). Hence, the orange culture could not utilize S^{2-} as sole source of energy.

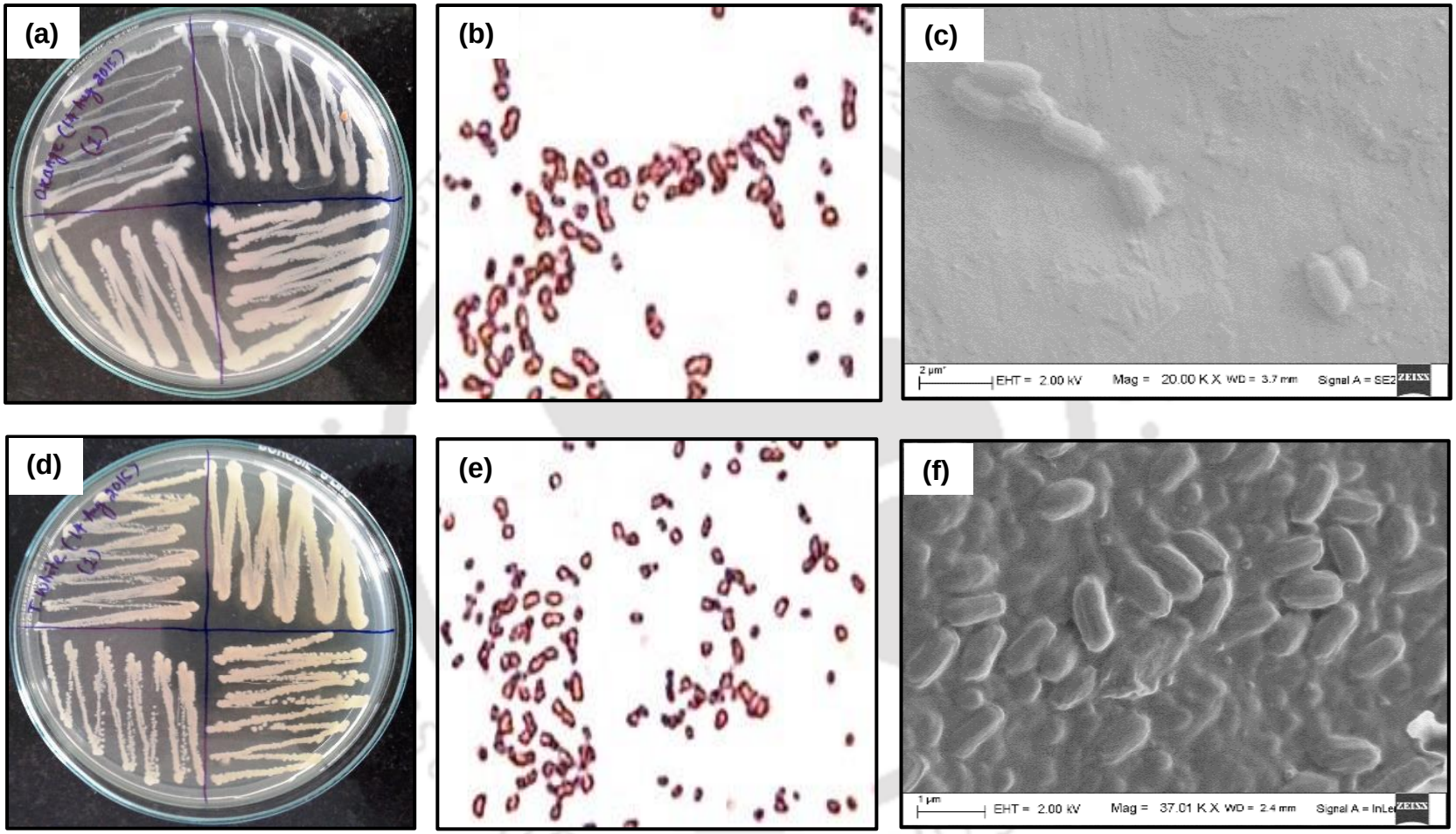

Fig. 5.1: (a) Streaked culture, (b) gram staining results and (c) FESEM image of anoxic orange culture; (d) Streaked culture, (e) gram staining test and (f) FESEM image of anoxic white culture

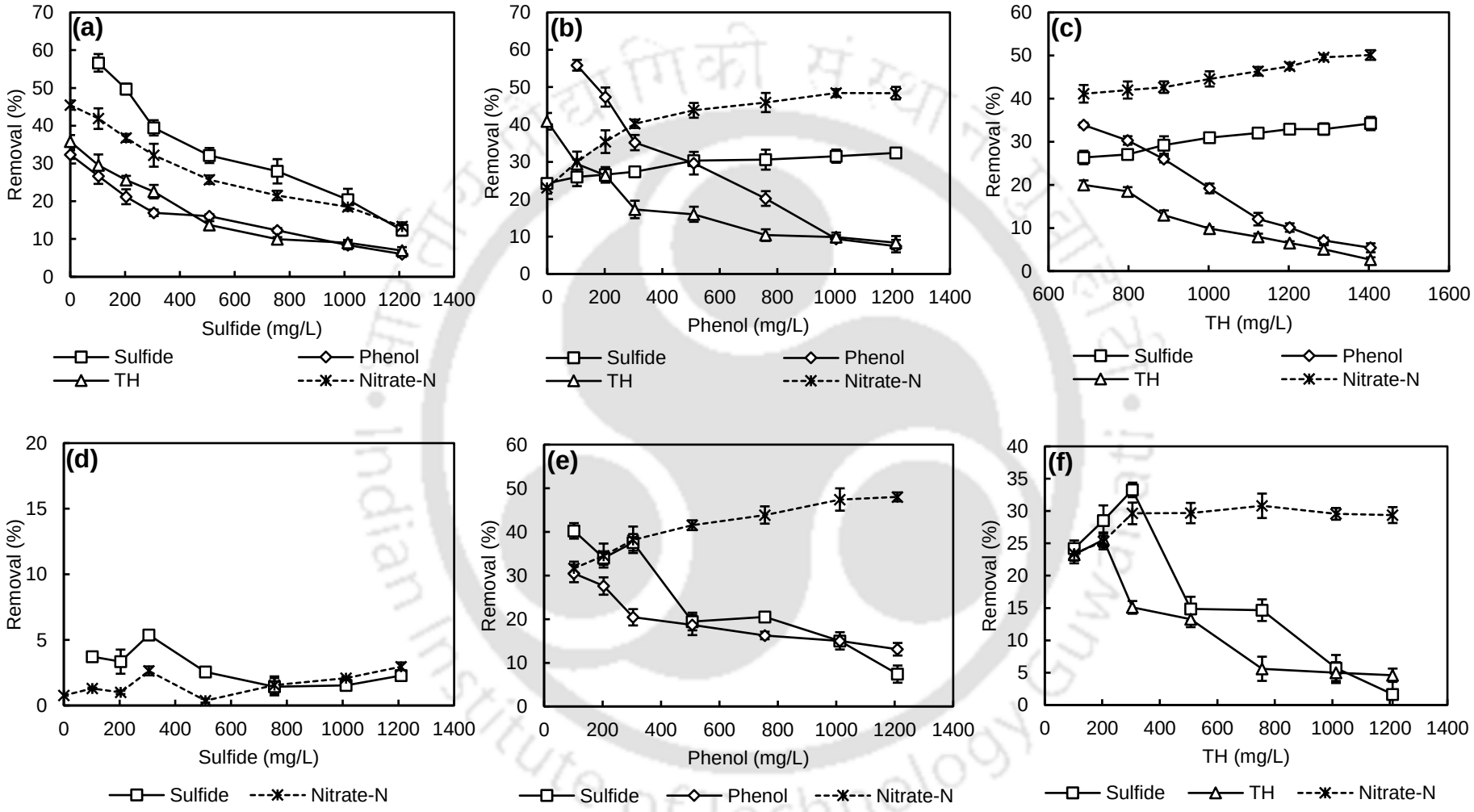

Fig. 5.2: Removals of individual pollutants by anoxic orange culture at (a) sulfide variation, (b) phenol variation, (c) TH variation; Removal of sulfide (d) without organics, (e) in the presence of phenol, (f) in the presence of diesel

Anoxic white culture also degraded all the pollutants but to a lesser extent compared to the orange culture (Fig. 5.3). S^{2-} removal decreased from 35% to 6% with increase in S^{2-} concentration (Fig. 5.3a). Similarly, removal of phenol, TH and NO_3^--N also decreased with increase in the S^{2-} feed. Phenol removal decreased from 41% to 6% with increase in phenol along with decrease in the TH removal from 28% to 4% (Fig. 5.3b). However, removal of both S^{2-} and NO_3^--N was observed similar to the orange culture. Similar trend was observed when TH was increased (Fig. 5.3c) White culture when subjected to the degradation of S^{2-} without any carbon source, showed promising results and survived in the absence of any carbon source (Fig. 5.3d). Therefore, white culture in the reactor showed chemolithotrophic characteristics. Hence, white culture was responsible for the chemolithotrophic activity (CA) of the anoxic biomass mentioned in Chapter 4.

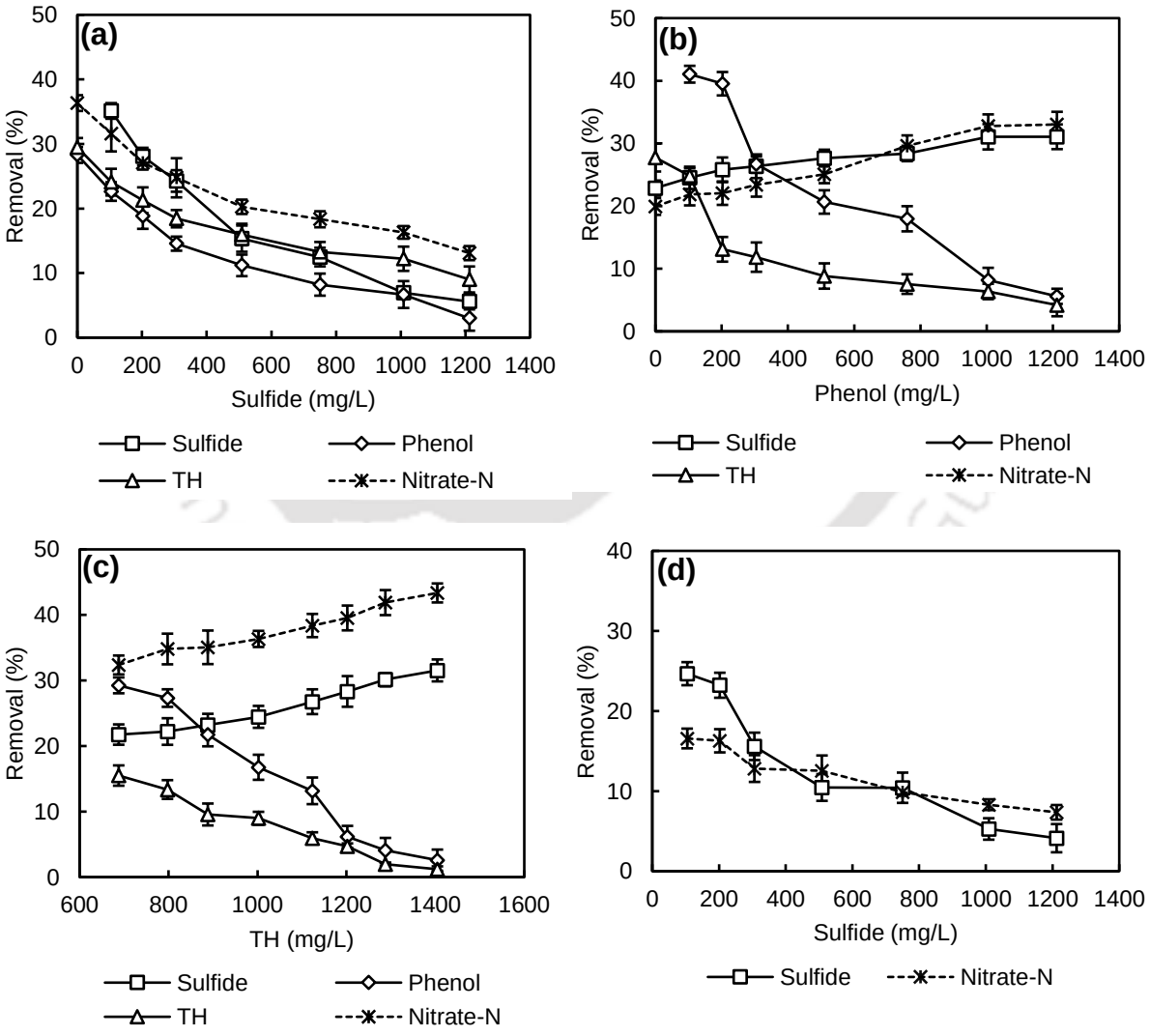

Fig. 5.3: Removals of individual pollutants by anoxic white culture at (a) S^{2-} variation, (b) phenol variation , (c) TH variation, and (d) removal of S^{2-} without organics

Identification of both cultures was done as mentioned in section 5.2.5 and cells in the orange colony showed 99% similarity with the strain *Pseudomonas aeruginosa* **KT894767.1**. Therefore, it was identified as a new strain and named as *Pseudomonas aeruginosa* **SKM2013** with Genbank accession number of **KY238114**. However, cells in the white colony matched 97% with the strain *Pseudomonas aeruginosa* **KLU02**. Therefore, it was identified as a new strain and named as *Pseudomonas aeruginosa* **SC2013** with Genbank accession number of **KY421078**. However, *Pseudomonas aeruginosa* falls into the category of is facultative gram-negative microbial identity. It is known to grow both in aerobic and anaerobic conditions and can degrade nitrate when suitable environment is provided (Davies et al., 1989). Degradation of phenolics and hydrocarbon compounds by *Pseudomonas aeruginosa* has been reported (Romero et al., 1998) but no literature was obtained for the degradation of S^{2-}. Phylogenetic trees of range and white cultures are illustrated in Fig. 5.4a and 5.4b, respectively.

5.3.2 Aerobic biomass

Isolation of the aerobic culture revealed the presence of four distinct cultures of red, yellow, white and grey color. Appearance, morphology and microscopic images of the red and yellow cultures are illustrated in Fig. 5.5 and those of aerobic white and grey cultures are shown in Fig. 5.6. Red culture was gram positive and rod shaped. Whereas, aerobic yellow culture was gram negative and round shaped. White and grey cultures were gram negative and rod shaped. All the colonies were subjected to the degradation of individual pollutants separately as received by A2 during the whole work. Concentrations of NH_4^+-N (0-350 ± 7 mg/L), phenol (0-450 ± 5 mg/L), crude oil as TH (450 ± 7 – 650 ± 8 mg/L) and NO_2^--N (0-150 ± 5 mg/L) were varied and $S_2O_3^{2-}$was kept constant (50 ± 4 mg/L) during the pure culture degradation analysis. Once a pollutant was varied, concentration of others were kept constant.

Red culture was able to degrade all the pollutants (NH_4^+-N, phenol, TH, NO_2^--N and $S_2O_3^{2-}$). Removal of NH_4^+-N decreased and those of phenol and NO_2^--N increased with increase in NH_4^+-N concentration (Fig. 5.7a). Removal of TH (initial 650 ± 8 mg/L) was asymptotic and remained within 28-32%. Increase in phenol supported the oxidation of both NH_4^+-N (Initial 350 ± 5 mg/L) and NO_2^--N (initial 150 ± 5 mg/L) by the red culture, but decrease in the removal (%) of phenol and TH was observed due to increase in their initial concentrations (Fig. 5.7b). Increase in TH had similar effect on the oxidation of NH_4^+-N (initial 350 ± 5 mg/L), NO_2^--N (initial 150 ± 5 mg/L), phenol (initial 450 ± 5 mg/L) and TH as happened during the

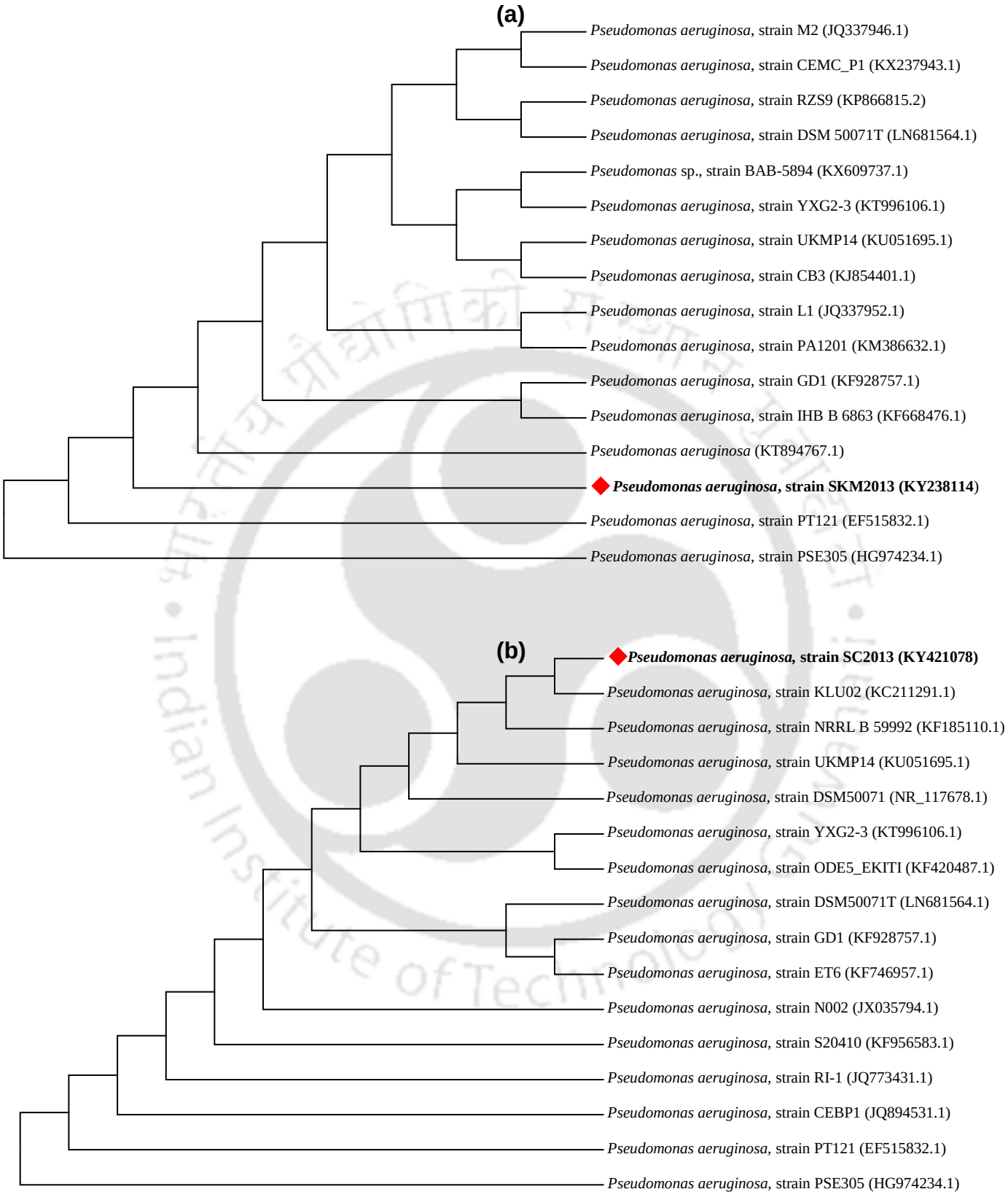

Fig. 5.4: Phylogenetic tree of (a) anoxic orange culture and (b) anoxic white culture

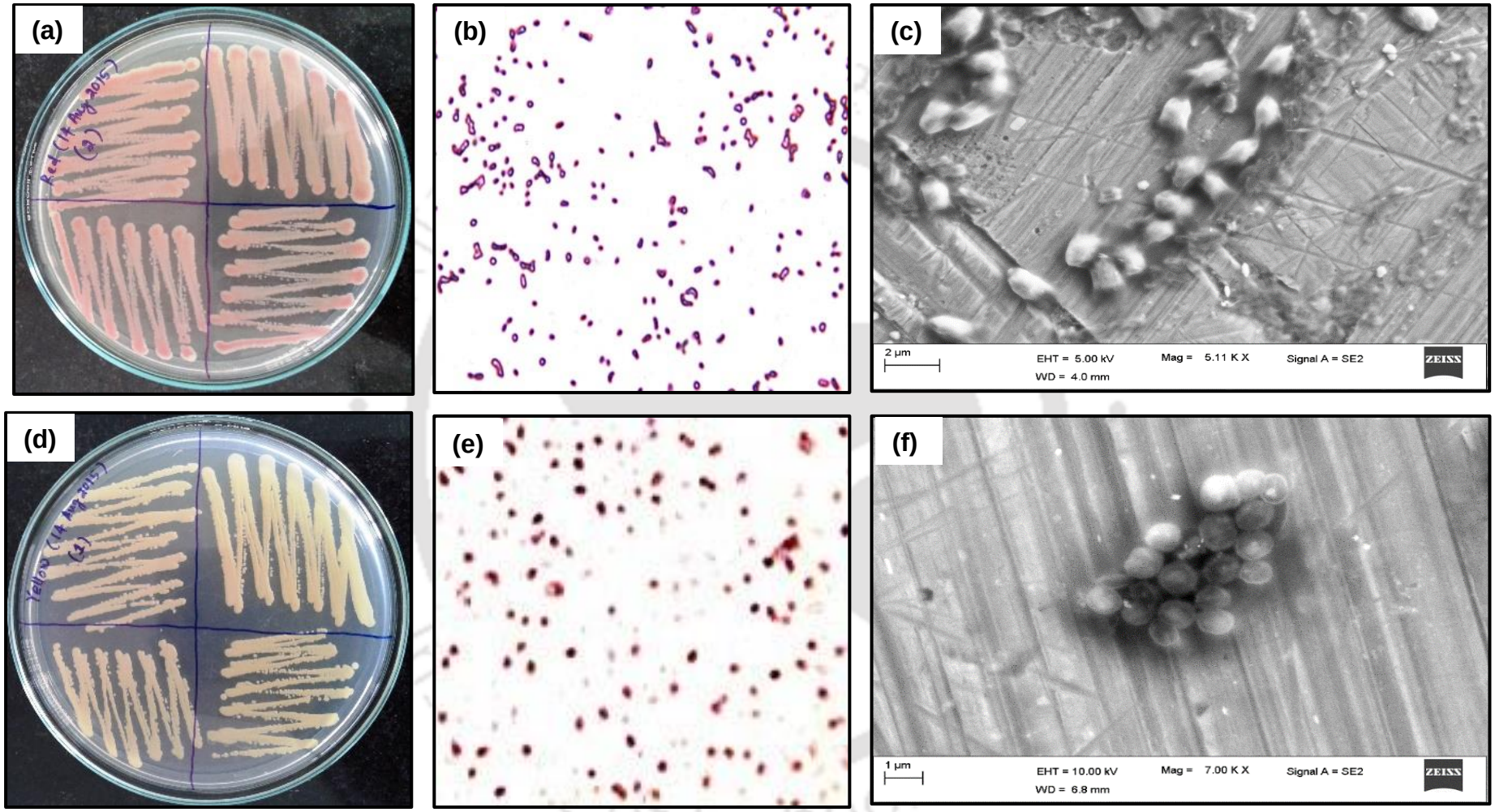

Fig. 5.5: (a) Streaked culture, (b) gram staining test and (c) FESEM image of aerobic red culture; (d) Streaked culture, (e) gram staining test and (f) FESEM image of aerobic yellow culture

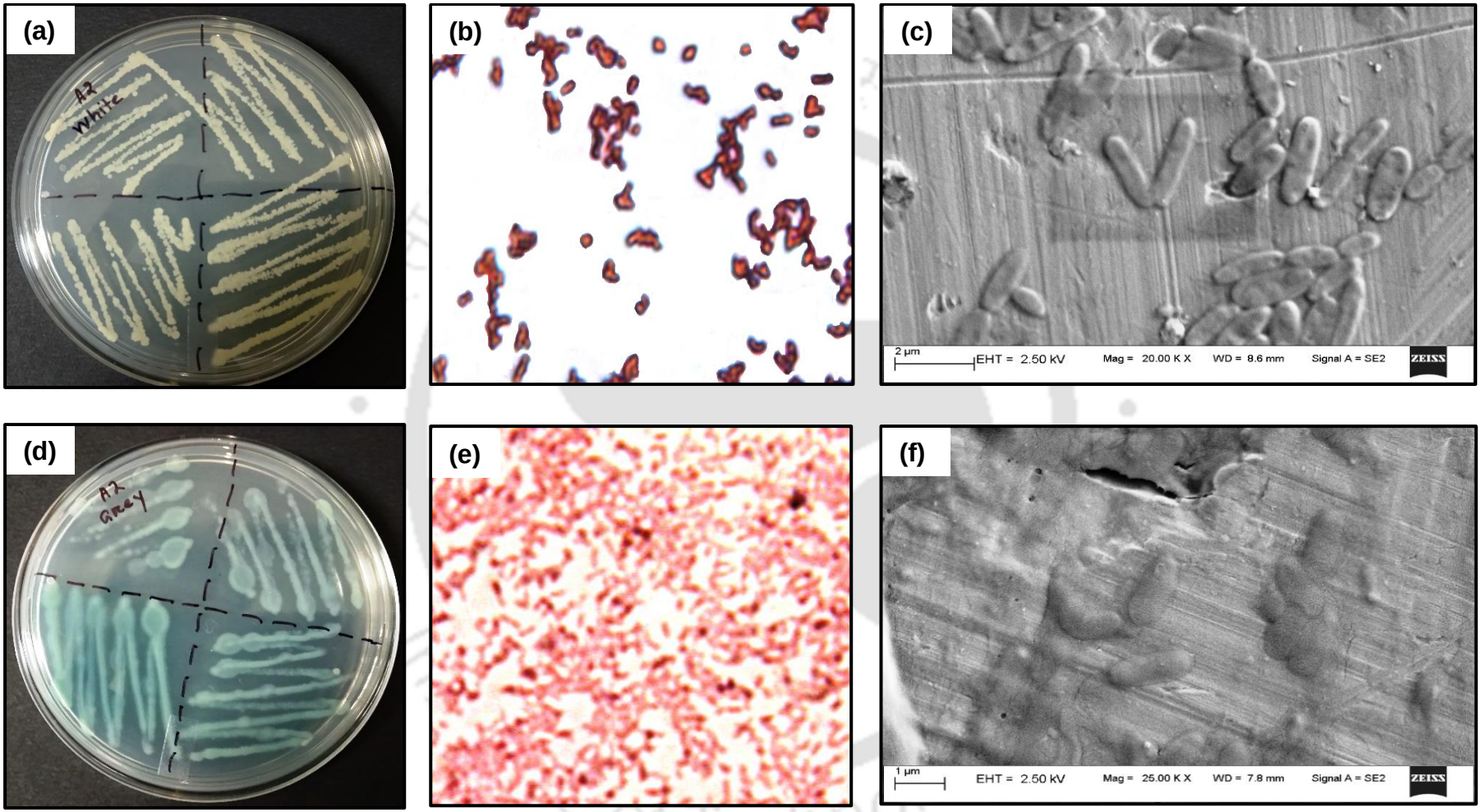

Fig. 5.6: (a) Streaked culture, (b) gram staining test and (c) FESEM image of aerobic white culture; (d) Streaked culture, (e) gram staining test and (f) FESEM image of aerobic grey culture

influent phenol variation (Fig. 5.7c), suggesting increase in nitrogen removal by red culture with increase in organic feed. Increase in the influent NO_2^--N did not have any effect on the removal of NH_4^+-N (initial 350 ± 5 mg/L) which remained within 33-35%. Decrease in the removal (%) of NO_2^--N was observed due to increase in its concentration and increase in the removals of phenol (initial 450 ± 5 mg/L) and TH (initial 650 ± 8 mg/L) was observed due to more availability of the electron acceptor (Fig. 5.7d).

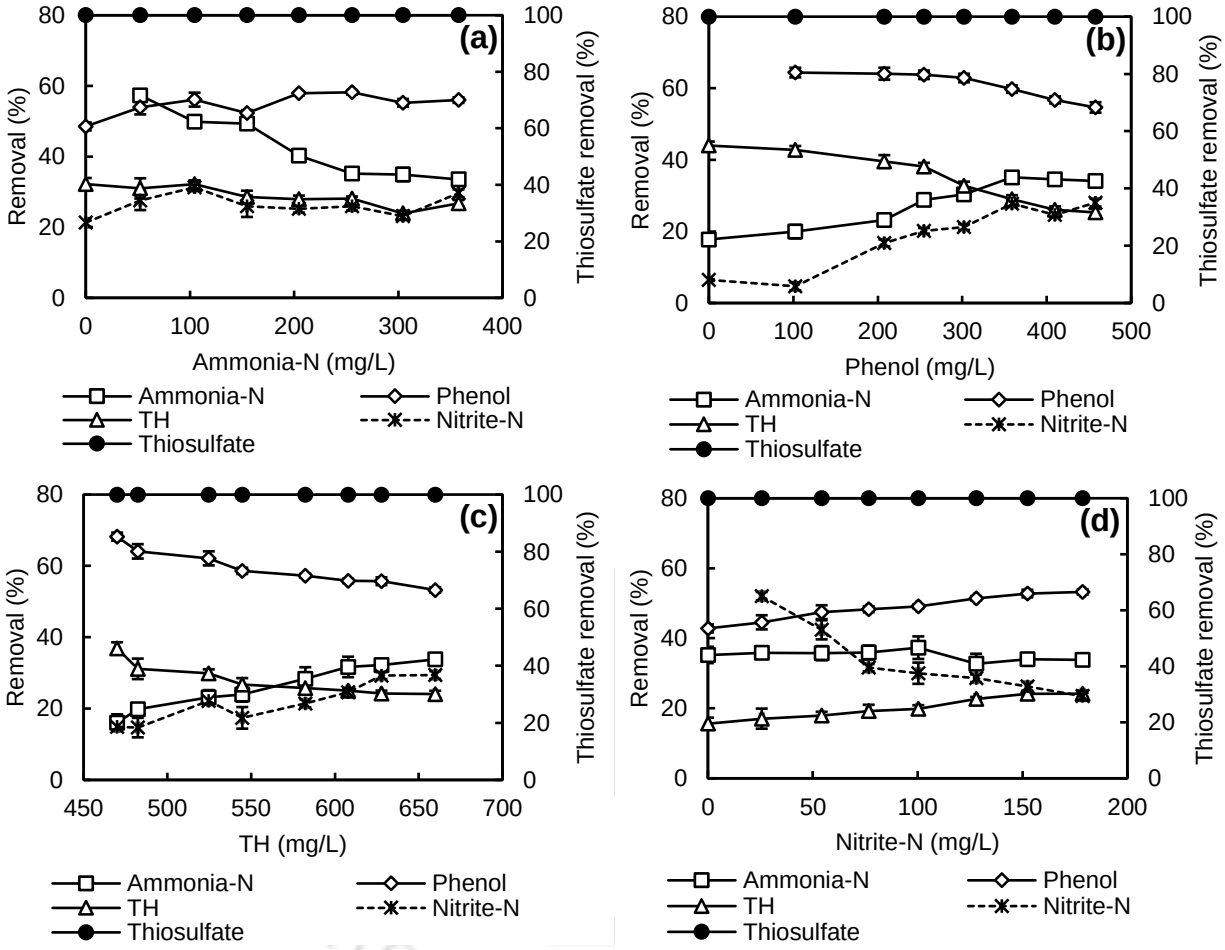

Fig. 5.7: Removals of individual pollutants by aerobic red culture at (a) NH_4^+-N variation, (b) phenol variation , (c) TH variation, (d) NO_2^--N variation

Yellow culture was also able to degrade all the pollutants but was less efficient compared to the red culture. Removals of phenol (initial 350 ± 5 mg/L) and TH (initial 650 ± 8 mg/L) were supported by increase in NH_4^+-N (Fig. 5.8a). Removal of NO_2^--N (initial 150 ± 5 mg/L) was asymptotic and remained within 20-30% and decrease in the removal (%) of NH_4^+-N was observed due to its initial influent concentration. Increase in phenol led to increase in the removals of NH_4^+-N (initial 350 ± 5 mg/L) and NO_2^--N (initial 150 ± 5 mg/L) and decrease in

the removals of phenol and TH (Fig. 5.8b). Similar removal pattern was shown by the yellow culture when concentration of TH was varied (Fig. 5.8c). Hence, yellow culture showed better nitrogen removal in the presence of organics as it happened for red culture. Removals of NH_4^+-N (initial 350 ± 5 mg/L) and NO_2^--N were asymptotic and remained within 14-18% and 10-20%, respectively, with increase in influent NO_2^--N (Fig. 5.8d). However, removals of phenol (initial 450 ± 5 mg/L) and TH (initial 650 ± 8 mg/L) increased due to the presence of more electron acceptor. Although yellow culture was also able to degrade all the pollutants, removal (%) of all the pollutants were comparatively low as observed in case of red culture.

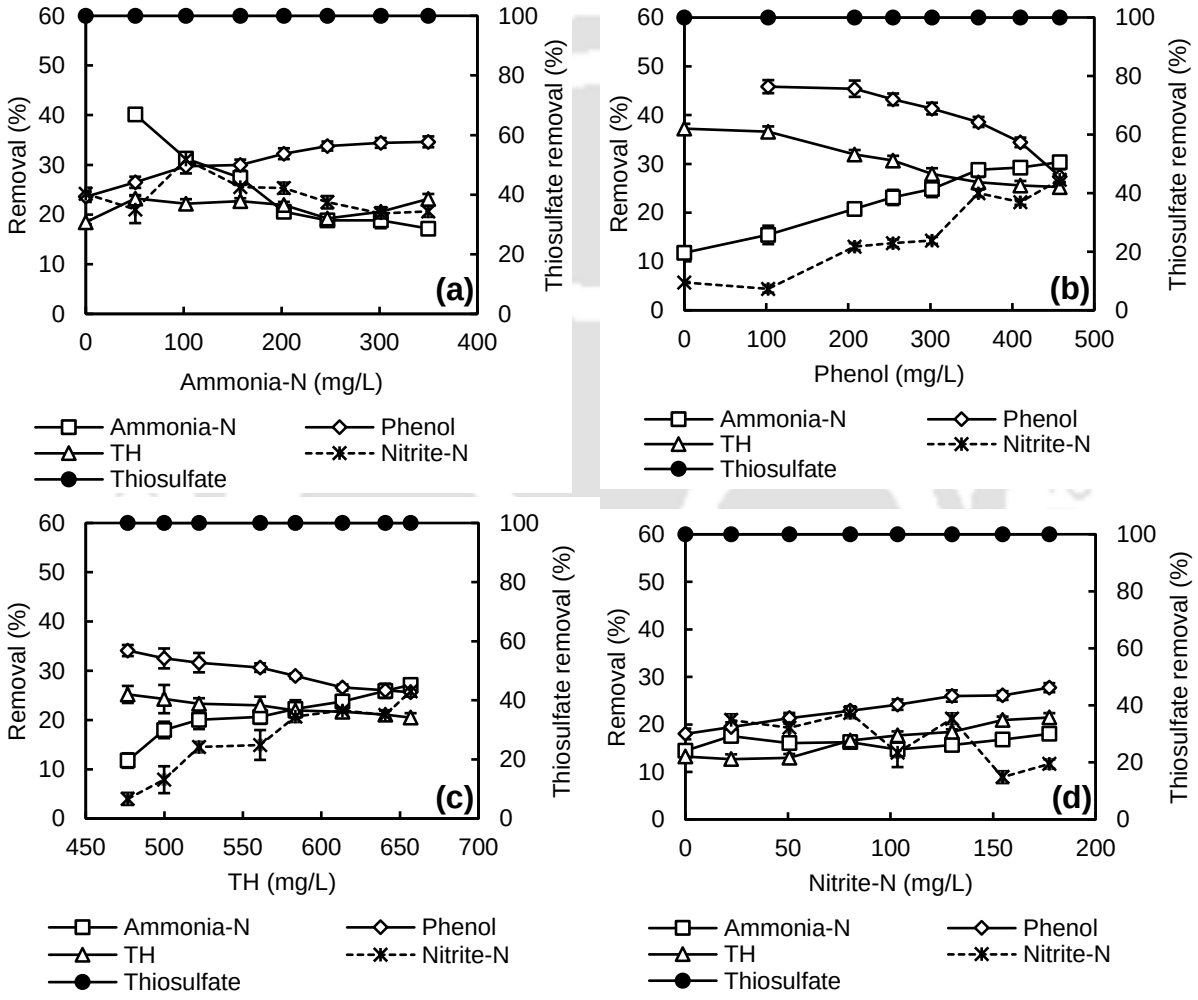

Fig. 5.8: Removals of individual pollutants by aerobic yellow culture at (a) NH_4^+-N variation, (b) Phenol variation, (c) TH variation and (d) NO_2^--N variation

Pollutants removal by the grey culture is shown in Fig. 5.9. NH_4^+-N removal (%) was quite low, but phenol and TH removals were similar to the red culture. Increase in the removals of phenol (initial 450 ± 5 mg/L), TH (initial 650 ± 8 mg/L) and NO_2^--N (initial 150 ± 5 mg/L)

occurred with increase in NH_4^+-N (Fig. 5.9a). Increase in phenol had no effect on the removal of NH_4^+-N (initial 350 ± 5 mg/L) which remained within 13-15% and increase in the removal of NO_2^--N (initial 150 ± 5 mg/L) was observed (Fig. 5.9b). However, there was decrease in the removals of phenol and TH due to increase in phenol. Increase in TH had no effect on the removal (%) of NH_4^+-N (initial 350 ± 5 mg/L) and slight increase in the removal of NO_2^--N (150 ± 5 mg/L) was observed (Fig. 5.9c). Similar removal pattern was observed for phenol and TH during the variation of TH, as observed during the variation of phenol. Increase in the removal (%) of phenol (initial 450 ± 5 mg/L) and TH (initial 650 ± 8 mg/L) was observed with increase in NO_2^--N due to more availability of the electron acceptor (Fig. 5.9d) and NH_4^+-N (initial 350 ± 5 mg/L) removal was unaffected. Removal of NH_4^+-N by grey culture was quite low compared to red and yellow culture.

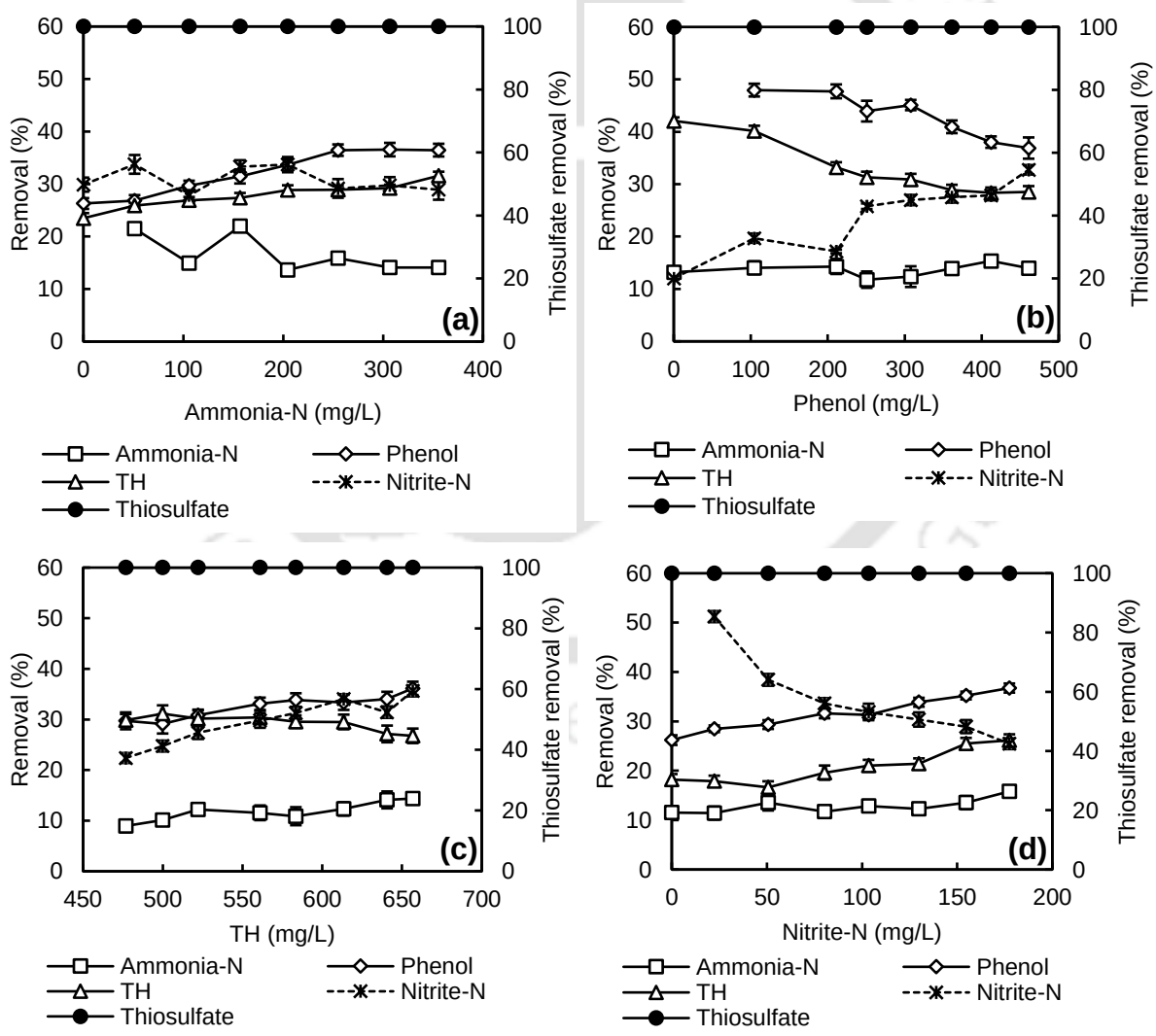

Fig. 5.9: Removals of individual pollutants by aerobic grey culture at (a) NH_4^+-N variation, (b) Phenol variation, (c) TH variation and (d) NO_2^--N variation

Aerobic white culture was not able to degrade NH_4^+-N in any circumstances and removal was always less than 4%. Slight increase in the removals of phenol (initial 450 ± 5 mg/L) and TH (initial 650 ± 8 mg/L) was observed with increase in NH_4^+-N (Fig. 5.10a). There was no change in the removal of NO_2^--N. Removals of phenol and TH marginally decreased with increase in phenol. Removal of NH_4^+-N (initial 350 ± 5 mg/L) was negligible and no altercation in the degradation of NO_2^--N (initial 150 ± 5 mg/L) was observed and removal always remained close to 40% (Fig. 5.10b). Similar observation was made when TH was varied in the presence of aerobic white culture (Fig. 5.10c). Increase in NO_2^--N led to slight increase in the removals of both phenol (initial 450 ± 5 mg/L) and TH (initial 650 ± 8 mg/L) and NH_4^+-N removal remained below 4%. NO_2^--N removal decreased, but remained more than 35% at maximum initial concentration of 175 ± 8 mg/L (Fig. 5.10d).

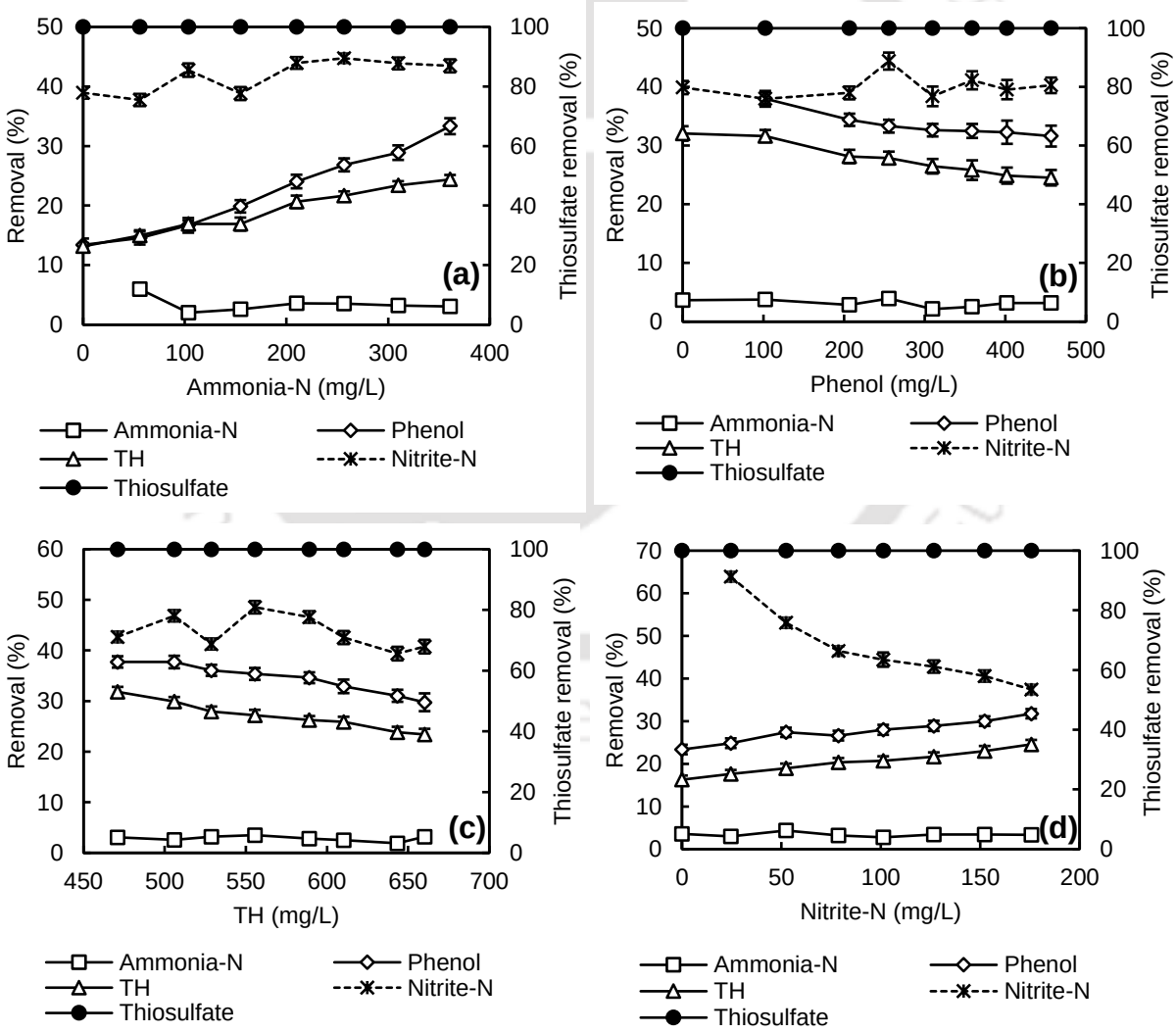

Fig. 5.10: Removals of individual pollutants by aerobic white culture at (a) NH_4^+-N variation, (b) Phenol variation, (c) TH variation and (d) NO_2^--N variation

Identification of the cultures were done as described in section 5.2.5.2. Based on the nucleotide homology and phylogenetic analysis, red culture had 100% homology with *Lysinibacillus sp.* strain **H200-510** with GenBank accession number **MG754438.1**, yellow culture had 100% homology with *Stenotrophomonas sp.* strain **LW-34** with GenBank accession number **KR258782.1**, grey culture had 100% homology with *Pseudomonas aeruginosa* strain **ISB4** with GenBank Accession number **KJ507205.1** and aerobic white culture had 100% homology with *Pseudomonas aeruginosa* strain **LZS8436** with GenBank accession number **MF143547.1**. Phylogenetic trees of red and yellow cultures are shown in Fig. 5.11 and those of grey and aerobic white cultures are shown in Fig. 5.12.

Lysinibacillus sp. can utilize various forms of organic carbons for their survival. Utilization of methanol and pyruvate by as carbon source by this species in aerobic condition has been already reported (Mishra et. al., 2015). In the same study, the authors have reported the utilization of both NH_4^+-N and NO_2^--N by *Lysinibacillus sp.* for the first time in aerobic condition. Similar properties were furnished by *Lysinibacillus sp.* strain **H200-150** in the present study. Lin et al. (2010) also have reported heterotrophic NH_4^+-N oxidation in synthetic feed by *Bacillus sp.* in aerobic condition. *Stenotrophomonas* is gram-negative and some species have been reported to utilize NO_2^--N (Hauben et al., 1999). NH_4^+-N oxidation by *Stenotrophomonas sp.* has been reported by Wu et al. (2011). In the present study, the identified culture *Stenotrophomonas sp.* strain **LW-34** was able to oxidize both NH_4^+-N and NO_2^--N in the presence of hydrocarbons.

Pseudomonas aeruginosa is a facultative gram-negative microorganism reported to degrade petroleum products in aerobic (Nawaz et al., 1991; Hamzah et al., 2013) and anoxic conditions (Davies et al., 1989; Romero et al., 1998). Literature reports are also available on the degradation of NH_4^+-N and organo-nitrogen compounds (Wu et al., 2011) by *Pseudomonas aeruginosa* in aerobic condition. In the present study, different strains of *Pseudomonas aeruginosa* were isolated from both anoxic and aerobic reactors, which confirmed their wide range of survival and well supported by literature. However, *Pseudomonas aeruginosa* strain **SKM2013** with GenBank accession number **KY238114** showed chemolithotrophic nature which is reported for the first time. An initial concentration of 50 ± 4 mg/L of $S_2O_3^{2-}$ was also supplied to the aerobic biomass and 100% removal was observed in all the cases. Such exhibit was possibly due to its self-oxidation to SO_4^{2-}.

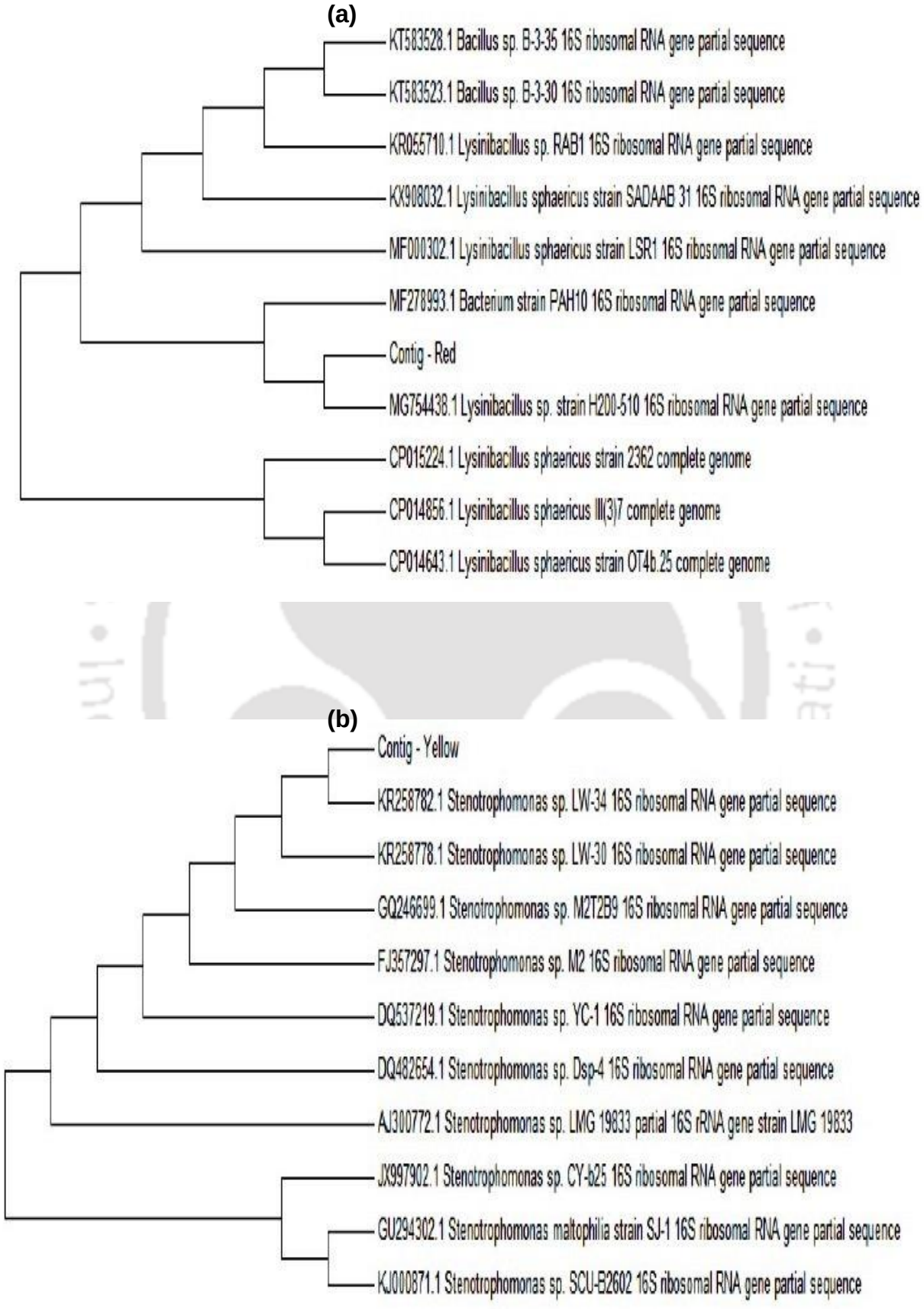

Fig. 5.11: Phylogenetic tree of (a) aerobic red culture and (b) aerobic yellow culture

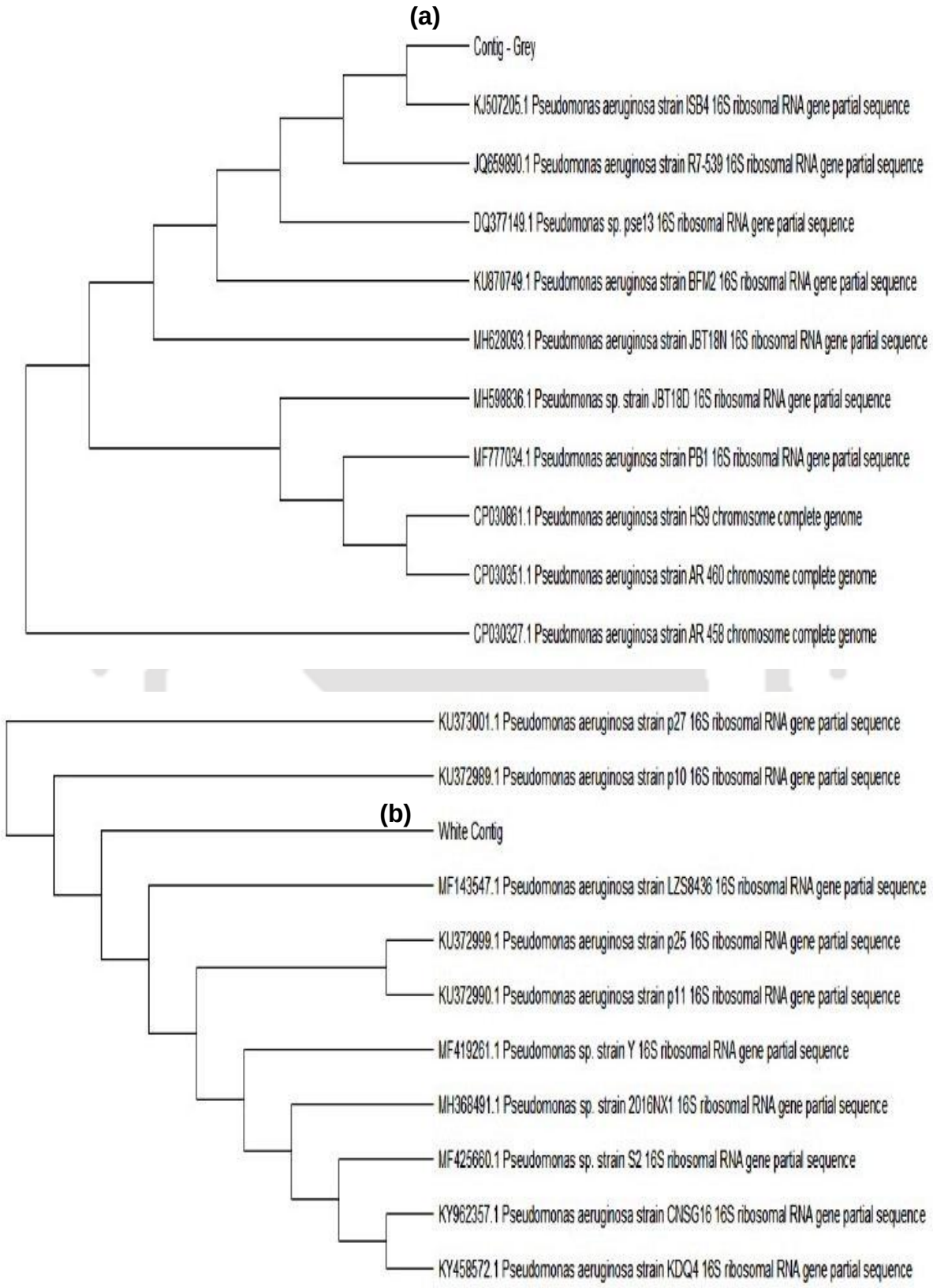

Fig. 5.12: Phylogenetic tree of (a) aerobic grey culture and (b) aerobic white culture

5.4 REAL WASTEWATER TREATMENT BY ANOXIC-AEROBIC REACTORS

Kinetics study was done in both anoxic and aerobic reactors to determine the cycle time requirement for the complete removals of all the compounds (Fig. 5.13). Complete degradation of phenol and NO_3^--N were achieved at 6h and 14h, respectively. Degradation of TH took a longer duration and was completely removed by A1 in 16-18h (Fig. 5.13a). Formation of NO_2^--N increased up to 8h and then completely removed at 18h (Fig. 5.13a). NH_4^+-N degradation in A1 was negligible (< 5%) within 18h time. Remaining NH_4^+-N from A1 was degraded in A2 and complete degradation occurred in 6h (Fig. 5.13b). Hence, cycle times of A1 and A2 were chosen as 18h (HRT 22.5h) and 6h (HRT 7.5h), respectively, with a total HRT of 30h.

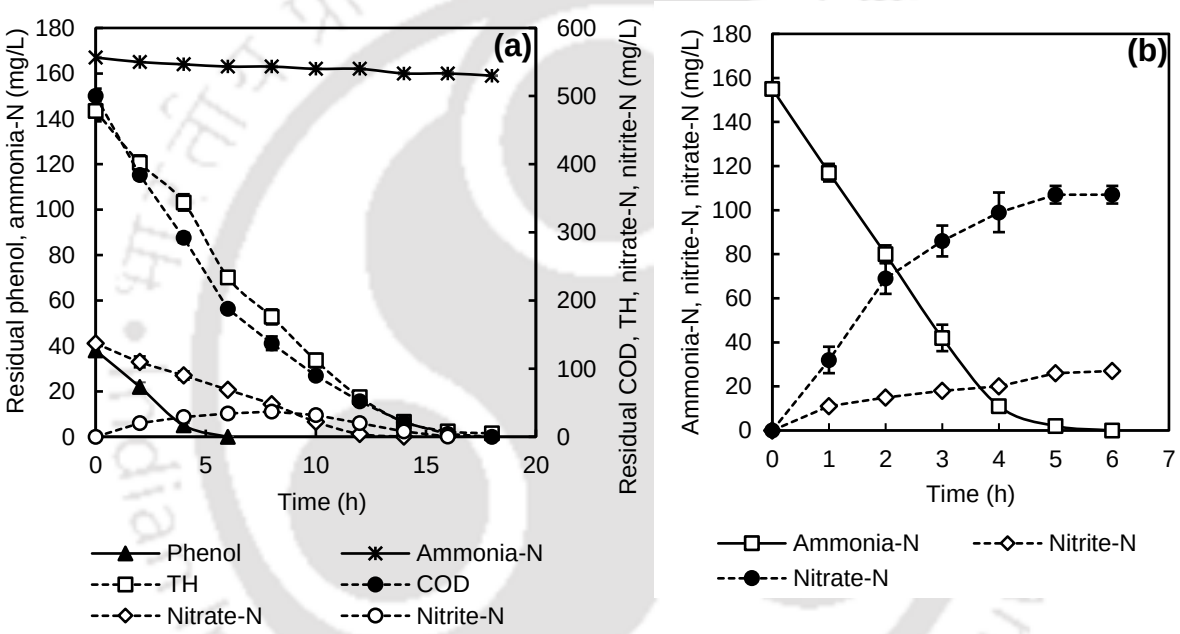

Fig. 5.13: Removal kinetics of pollutants in (a) A1 and (b) A2 during the treatment of automobile service station wastewater

Day wise performance of A1 and A2 for the removal of pollutants is illustrated in Fig. 5.14 and average concentrations are summarized in Table 5.3. Complete removals of phenol (Fig. 5.14a) and TH (Fig. 5.14b) were achieved in A1 at 22.5h HRT. Effluent COD was always below discharge limit after the treatment from A1 and further decreased in the effluent of A2. FTIR analysis of the influent revealed the presence of merceptans, aromatics, esters, alkynes, carboxylic acids and oximes as organics (Revathy et al., 2015; Segneanu et al., 2012; Ramasamy et al., 2014) along with NO_3^--N and PO_4^{3-} (Miller and Wilkins, 1952). Complete removals of all the organics were confirmed and there were no intermediate organics as no distinguishable peak for hydrocarbons were observed and only peaks observed were for the

OH bending of water molecule (Sharma et al., 2014) and extracellular polymeric substances (EPS) (Ramasamy et al., 2014) (Fig. 5.15). Removal rates of phenol, TH and COD were 30 ± 2 g/(m^3.d), 378 ± 6 g/(m^3.d) and 381 ± 9 g/(m^3.d), respectively, during the study. Yang et al. (2015) treated actual petroleum wastewater by anoxic-aerobic process and obtained maximum COD degradation rate of 501 ± 9 g/(m^3.d) at 20h HRT accounted to 79% removal of the influent COD and was higher than the present findings. Ghorbanian et al. (2014) reported higher total hydrocarbon removal rate of 2340 g/(m^3.d) in an upflow anoxic fixed bed reactor at HRT of 1d. Tong et al. (2013) operated conventional activated sludge process coupled with an immobilized biological filter to achieve 179 g/(m^3.d) of total hydrocarbon removal, which was lesser compared to the present study.

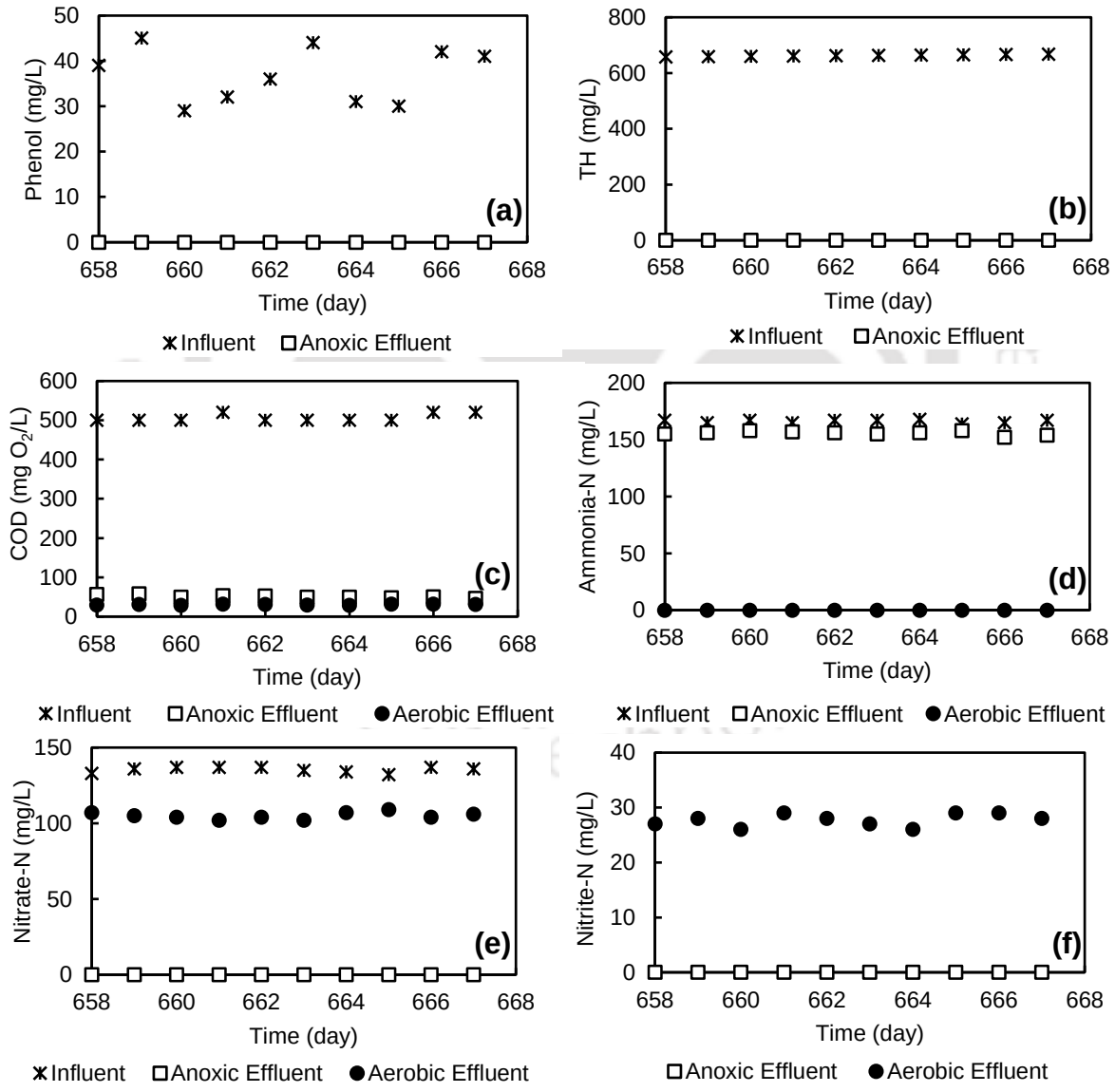

Fig. 5.14: Influent and effluent (a) phenol, (b) TH, (c) COD, (d) ammonia-N, (e) nitrate-N and (f) nitrite-N in A1-A2 reactors

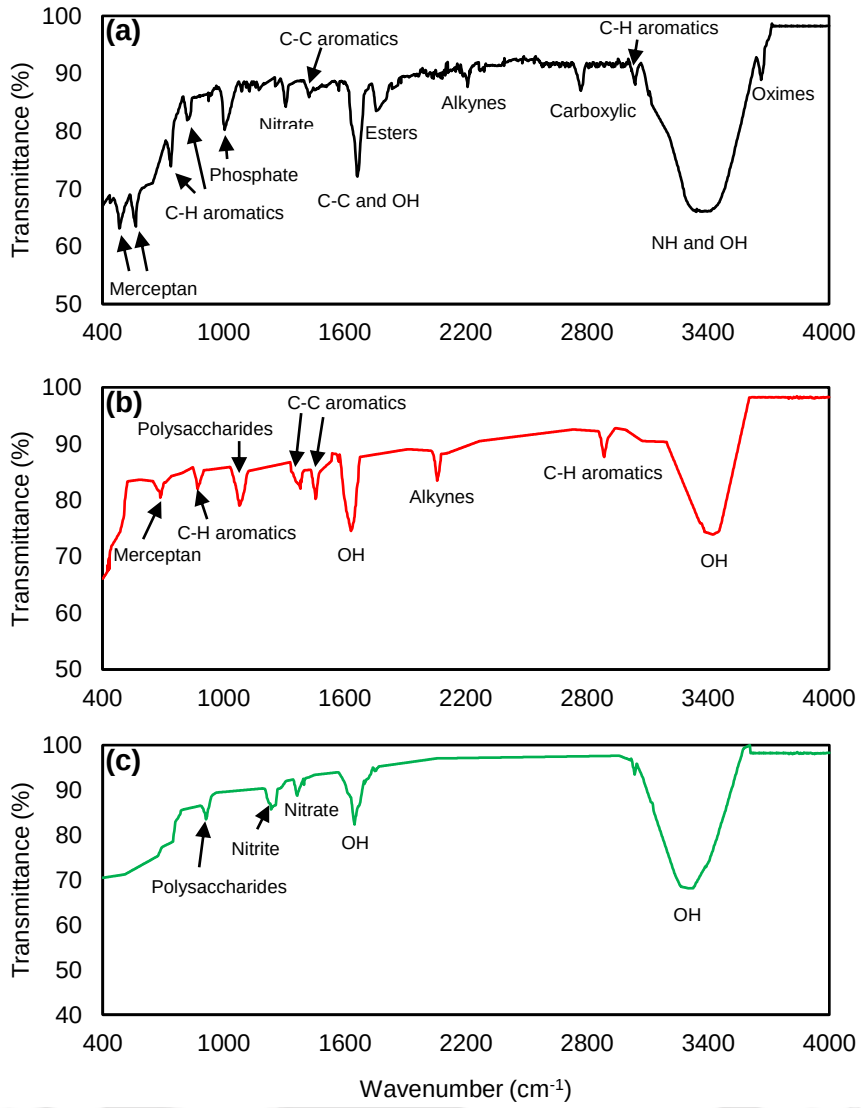

Fig. 5.15: FTIR spectra of the (a) influent, (b) anoxic effluent and (c) aerobic effluent

NO_3^--N was completely reduced in A1 and NO_2^--N as intermediate was never observed. Disappearance of NO_3^- peak in the effluent of A1 confirmed such exhibit (Fig. 5.15). Denitrification rate of 143 ± 1 g/(m^3.d) was observed for A1. Mirbagheri et al. (2014) observed higher denitrification rate [300 g/(m^3.d)] in anoxic reactor in the presence of acetate as carbon source. However, Sahariah and Chakraborty (2013) reported denitrification rate of 160 g/(m^3.d) with phenol as carbon source in an anoxic moving bed reactor.

Removal of NH_4^+-N was negligible in A1 and completely removed in A2 with generation of NO_3^--N and NO_2^--N (Table 5.3). Overall, 67% of the influent NH_4^+-N in A2 was oxidized to NO_3^--N and 18% was oxidized to NO_2^--N with a nitrification rate of 426 ± 2 g/(m^3.d). Remaining 15% of NH_4^+-N was probably converted to biomass in A2. Corresponding total

nitrogen removal was 44% by the A1-A2 sequential reactors. Vazquez et al. (2006) reported maximum nitrification rate of 180 g/(m^3.d) in aerobic suspended growth reactor at influent NH_4^+-N of 1095 mg/L in presence of phenol. Sahariah et al. (2016) reported nitrification rate of 192 g/(m^3.d) in an aerobic moving bed reactor from influent NH_4^+-N of 405 mg/L with 710 mg/L of phenol. Nitrification rate of 500 g/(m^3.d) was reported by Rostron et al. (2001) without any COD loading and observed reduction in nitrification due to the growth of heterotrophic bacteria when glucose was supplied to the feed, which was similar to the present findings.

Table 5.3: Effluent concentrations during the treatment of real automobile service station wastewater

Parameters	Anoxic reactor (A1)		Aerobic reactor (A2)
	Influent	Effluent	Effluent
Phenol (mg/L)	37 ± 6	0.04 ± 0.01	0.02 ± 0.01
Total hydrocarbon (mg/L)	475 ± 11	5 ± 1	3 ± 1
COD (mg/L)	506 ± 12	55 ± 3	30 ± 2
Ammonia-N (mg/L)	170 ± 7	156 ± 2	0.2 ± 0.1
Nitrate-N (mg/L)	135 ± 2	0.4 ± 0.1	105 ± 2
Nitrite-N (mg/L)	-	0.3 ± 0.1	28 ± 2
Total-N (mg/L)	302 ± 2	156 ± 2	133 ± 2
Dissolved oxygen (DO) (mg/L)	0.9 ± 0.1	0.2 ± 0.1	6.4 ± 0.2
pH	7.81 ± 0.02	7.95 ± 0.02	7.45 ± 0.21
Gas (mL)	145 ± 9		-
Total biomass (g/L)	15.24 ± 0.02		17.99 ± 0.03
Attached biomass (g/L)	14.72 ± 0.02		17.10 ± 0.02
Suspended biomass (g/L)	0.52 ± 0.01		0.89 ± 0.02
Total suspended solids (g/L)	0.79 ± 0.03		1.11 ± 0.01
SRT (day)	21.98 ± 0.11		5.05 ± 0.06

COD: Chemical oxygen demand,

SRT: Solids retention time

Effluent pH of A1 slightly increased possibly due to alkalinity generated by anoxic process and decreased after aerobic treatment. An image of influent and effluent of A1 and A2 is illustrated in Fig. 5.16. Gas generated from A1 was composed of 90% of N_2 and 7% of CO_2 from the anoxic degradation. CH_4 was never observed in the samples and rest (3%) was unaccounted.

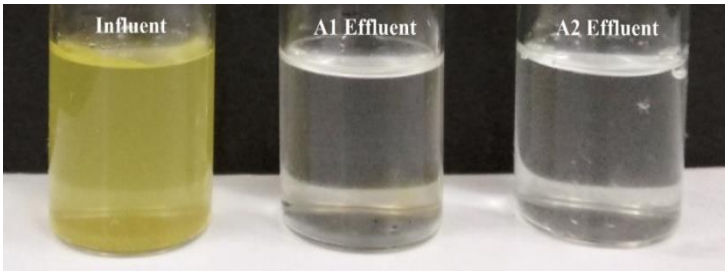

Fig. 5.16: Image of influent and effluent from A1 and A2

Both attached and suspended biomass were higher in A2 and total biomass in A2 was 18% more compared to A1 (Table 5.3). Cycle time of A2 was three times less compared to A1. Hence, effluent was withdrawn from A2 more frequently. At steady state, suspended biomass in A2 was more. Therefore, there was more loss of biomass as A2 was operated at 6h cycle time compared to 18h cycle time of A1. Consequently, anoxic biomass spent more time inside the reactor compared to the aerobic biomass and SRT of A1 (21.98 day) was almost four times higher compared to A2 (5.10 day), even if A2 had higher total biomass. Wastewater used as influent had both metallic and ionic properties (Table 5.2). Hence, presence of possible ions and heavy metals was examined in the sludge generated by both A1 and A2 and shown in Table 5.4. Metals content in A1 sludge was more compared to A2. Because, concentrated raw feed was first received by A1 and partially treated effluent was received by A2. Most of the metals were precipitated in A1, resulted in their comparative higher concentrations. Concentrations of Fe^{2+}, Zn^{2+} and Pb^{2+} were higher compared to other metal equivalents (Table 5.4).

Final effluent from the A1-A2 sequential system had dischargeable COD and was devoid of phenol, hydrocarbons, NH_4^+-N and metallic sludge (Table 5.3). Effluent from A2 contained generated NO_3^--N and NO_2^--N from the oxidation of NH_4^+-N. Hence, the treated water can be proposed to be reused for vehicle washing purposes. This may eliminate discharge of the vehicle wash wastewater in the public sewer system and reduce the load on municipal sewage treatment plants. Physico-chemical methods are reported to have generated reusable water from the treatment of vehicle wash wastewater (Ganiyu et al., 2018; Boularte et al., 2016). In the present study, anoxic-aerobic sequential biological system was able to produce reusable quality of water from the treatment of vehicle wash wastewater. Heavy metal contents in the reactor-generated sludge were within permissible limits and could be applicable to agricultural lands as per guidelines (USEPA, 1994) (Table 5.4).

Table 5.4: Metals content in reactor-generated sludge and permissible limits (mg/kg of dry weight)

Reactor	Na^{+}	K^{+}	Ca^{2+}	Cr^{3+}	Fe^{2+}	Mg^{2+}	Cu^{2+}	Zn^{2+}	Co^{2+}	Ni^{2+}	Mn^{2+}	As^{3+}	Pb^{2+}	Cd^{2+}
Anoxic (A1)	40 ± 3	68 ± 3	35 ± 2	9 ± 1	51 ± 5	29 ± 1	31 ± 3	26 ± 2	17 ± 2	20 ± 3	19 ± 1	4 ± 1	19 ± 1	11 ± 1
Aerobic (A2)	45 ± 5	72 ± 4	23 ± 3	7 ± 1	28 ± 4	10 ± 2	23 ± 3	17 ± 3	8 ± 1	9 ± 1	11 ± 1	1 ± 1	11 ± 2	7 ± 1
Permissible limits	-	-	-	1200*	-	-	1500*	2800*	-	420*	-	41*	300*	39*

* USEPA, 1994

5.5 PURE CULTURE ANALYSIS FOR SIMULATED AUTOMOBILE SERVICE STATION WASTEWATER

In a separate experiment, each of the isolated colonies (both anoxic and aerobic) were subjected to degradation of pollutants found in automobile service station wastewater with simulated synthetic pollutants. Isolated anoxic cultures were exposed to feed containing phenol (55 ± 2 mg/L), crude oil (TH: 480 ± 5 mg/L), NH_4^+-N (170 ± 5 mg/L) and NO_3^--N (135 ± 5 mg/L) and effluent concentrations were measured after 18h. Aerobic cultures were exposed to feed containing only NH_4^+-N (160 ± 5 mg/L) without organics and effluent concentration was measured after 6h. Both the isolated anoxic cultures were able to degrade phenol and TH and utilize NO_3^--N as electron acceptor (Fig. 5.17a). Orange culture (*Pseudomonas aeruginosa* strain **SKM2013**) showed higher potential for organics degradation compared to the anoxic-white culture (*Pseudomonas aeruginosa* strain **SC2013**). Neither of the cultures showed promise for NH_4^+-N removal.

Out of the four isolated aerobic cultures, red (*Lysinibacillus sp*. strain **H200-510**), yellow (Stenotrophomonas *sp.* strain **LW-34**) and grey (*Pseudomonas aeruginosa* strain **ISB4**) cultures showed potential NH_4^+-N removal without organics. Removal of NH_4^+-N by aerobic-white culture (*Pseudomonas aeruginosa* strain **LW-34**) was quite low in the absence of organics (Fig. 5.17b). Previously it was observed that aerobic white culture did not remove NH_4^+-N in the presence of organics. In the present study, different strains of *Pseudomonas aeruginosa* were isolated from both anoxic and aerobic reactors, which confirmed their wide range of survival.

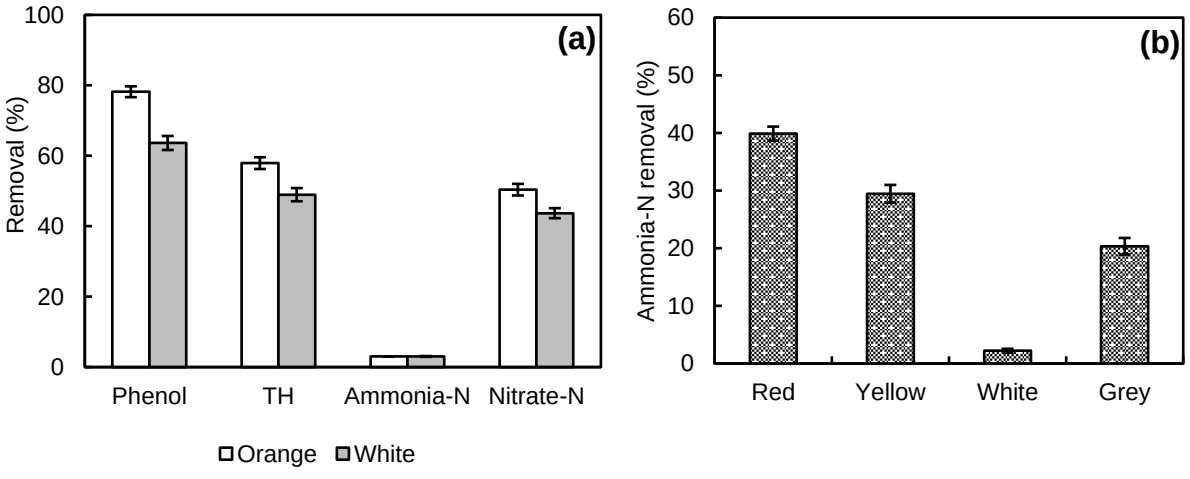

Fig. 5.17: (a) Removals of organics and nitrate-N by anoxic culture, (b) removal of ammonia-N by aerobic culture

5.6 SUMMARY OF THE STUDY

Identification of microbial species revealed the presence of *Pseudomonas aeruginosa* strain **SKM2013** and *Pseudomonas aeruginosa* strain **SC2013** in anoxic culture. Both were found to degrade organics and sulfide. In addition, *Pseudomonas aeruginosa* strain **SC2013** was able to utilize sulfide in the absence of organics in anoxic condition and showed chemolithotrophic characteristics. Identification of aerobic culture revealed the presence of *Lysinibacillus sp.* strain **H200-510**, *Stenotrophomonas sp.* strain **LZS8436**, *Pseudomonas aeruginosa* strain **ISB4** and *Pseudomonas aeruginosa* strain **LZS8436**. The first three mentioned cultures were able to oxidize ammonia-N in aerobic condition. Complete removals of phenol, hydrocarbon, nitrate-N and ammonia-N in real automobile service station wastewater were achieved by anoxic-aerobic sequential bioreactors at 30h HRT. Anoxic reactor carried out degradation of organics and nitrate-N and residual ammonia-N was oxidized to nitrite-N and nitrate-N in aerobic reactor. Potential reuse of the treated water and land application of the generated sludge were proposed.

References

APHA, AWWA, WPCF. Standard Methods for the Examination of Water and Wastewater. 21st ed., American Public Health Association, Washington DC.

Asha, M. N., Chandan, K. S., Harish, H. P., NikhileshwarReddy, S., Sharath, K. S., Mini Liza, G. 2016. Recycling of wastewater collected from automobile service station. Procedia Environmental Sciences 35: 289-297.

Boonchan, S., Britz, M. L., Stanley, G. A. 2000. Degradation and mineralization of high-molecular-weight polycyclic aromatic hydrocarbons by defined fungal-bacterial cocultures. Applied Environmental Microbiology 66(3): 1007-1019.

Boularte, I. A. R., Andersen, M., Parmanik, B. K., Chang, C. Y., Bagshaw, S., Farago, Jegatheesan, V., Shu, L. 2016. Reuse of car wash wastewater by chemical coagulation and membrane bioreactor treatment process, International Biodeterioration and Biodegradation 113: 44-48.

Brzeszcz, J., Kaszycki, P. 2018. Aerobic bacteria degrading both n-alkanes and aromatic hydrocarbons: an undervalued strategy for metabolic diversity and flexibility. Biodegradation 29: 359-407.

Chhetri, B., Mukherjee, A., Langpoklakpam, J. S., Chattopadhyay, D., Singh, A. K. 2016. Kinetics of nutrient enhanced crude oil degradation by Pseudomonas Aeruginosa AKS1 and Bacillus sp. AKS2 isolated from Guwahati refinery, India. Environmental Pollution 216: 548-558.

Davies, K. J. P., Lloyd, D., Boddy, L. 1998. The effect of oxygen on the denitrification in *Paracoccusdenitrificans* and *Pseudomonas aeruginosa*. Microbiology 135: 2445-2451.

Ganiyu, S. O., dos Santos, E. V., E. de Araujo Costa, E. C. T., Martinez-Huitle, C. A. 2018. Electrochemical advanced oxidation processes (EAOPs) as alternative treatment techniques for carwash wastewater reclamation. Chemosphere 211: 998-1006.

Ghorbanian, M., Moussavi, G., Farzadkia, M. 2014. Investigating the performance of an up-flow anoxic fixed-bed bioreactor and a sequencing anoxic batch reactor for the biodegradation of hydrocarbons in petroleum-contaminated saline water. International Biodeterioration and Biodegradation 90: 106-114.

Gueven, D. E., Akinci, G. 2011. Comparison of acid digestion techniques to determine heavy metals in sediment and soil samples. Gazi University Journal of Science 24(1): 29-34.

Hamzah, A., Phan, C. W., Abu Bakar, N. F., Wong, K. K. 2013. Biodegradation of crude oil by constructed bacterial consortia and the constituent single bacteria isolated from Malaysia. Bioremediation Journal 17(1): 1-10.

Hauben, R., Woods, S., Ferguson, J., Benjamin, M. 1999. Genomic diversity of the genus *Stenotrophomonas*. International Journal of Systematic Bacteriology 49: 1749-1760.

Kumar, S., Stretcher, G., Li, M., Knyaz, C., Tamura, K. 2018. MEGA X: Molecular Evolutionary Genetics Analysis across computing platforms. Molecular Biology and Evolution 35: 1547-1549.

Kumar, S., Stretcher, G., Tamura, K. 2016. MEGA 7: Molecular Evolutionary Genetics Analysis version 7.0 for bigger dtatsets. Molecular Biology and Evolution 33: 1870-1874.

Lau, W. J., Ismail, A. F., Firdaus, S. 2013. Car wash industry in Malaysia: treatment of car wash effluent using ultrafiltration and nanofiltration membranes. Separation and Purification Technology 104: 26-31.

Lin, Y., Kong, H., Wu, D., Li, C., Wang, R., Tanaka, S. 2010. Physiological and molecular biological characteristics of heterotrophic ammonia oxidation by Bacillus sp. LY. World Journal of Microbiology and Biotechnology 26: 1605-1612.

Mazumder, D., Mukherjee, S. 2011. Treatment of automobile service station wastewater by coagulation and activated sludge process, Int. J. Env. Sci. Develop. 2(1) (2011), 64-69.

Miller, F. A., Wilkins, C. H. 1952. Infrared spectra and characteristic frequencies of inorganic ions. Analytical Chemistry 24(8): 1253-1294.

Mirbagheri, S. A., Ahmadi, S., Biglari-joo, N. 2014. Denitrification of nitrate-contaminated groundwater in an anoxic rotating biological contactor: a case study. Desalination and. Water Treatment 57(10): 4694-4700.

Mishra, S. S., Markande, A. R., Keluskar, R. P., Karunasagar, I., Nayak, B. B. 2015. Simultaneous nitrification and denitrification by novel heterotrophs in remediation of fish processing effluent. Journal of Basic Microbiology 55: 772-779.

Moussavi, G., Ghorbanian, M. 2015. The biodegradation of petroleum hydrocarbons in an upflow sludge-blanket/fixed-film hybrid bioreactor under nitrate-reducing conditions: Performance evaluation and microbial identification. Chemical Engineering Journal 280: 121-131.

Nasirpour, N., Mousavi, S. M., Shojaosadati, S. A. 2015. Biodegradation potential of hydrocarbons in petroleum refinery effluents using a continuous anaerobic-aerobic hybrid system. Korean Journal of Chemical Engineering 32(5): 874-881.

Nawaz, M. S., Davis, J. W., Wolfram, J. H., Chapatwala, K. D. 1991. Degradation of organic cyanides by *Pseudomonas aeruginosa*. Applied Biochemistry and Biotechnology 28: 865-875.

Padhi, S. K., Gokhale, S. 2016. Benzene control from waste gas streams with a sponge-medium based rotating biological contactor. International Biodeterioration and Biodegradation 109: 96-103.

Paxeus, N. 1996. Organic pollutants in the effluents of large wastewater treatment plants in Sweden. Water Research 30(5): 1115-1122.

Ramasamy, S., Mathiyalagan, P., Chandran, P. 2014. Characterization and optimization of EPS-producing and diesel oil-degrading Orchobacterium anthropic MP3 isolated from refinery wastewater. Petroleum Science 11: 439-445.

Ramos, C., Suarez-Ojeda, M. E., Carrera, J. 2016. Denitrification in anoxic granular reactor using phenol as sole organics carbon source. Chemical Engineering Journal 288: 289-297.

Revathy, T., Jayasri, M. A., Suthindharan, K. 2015. Biodegradation of PAHs by *Burkholderia* sp. VITRSB1 isolated from marine sediments, Hindawi Publications Co. Science. DOI: http://dx.doi.org/10.1155/2015/867586

Romero, M. C., Cazau, M. C., Giorgieri, S., Arambarri, A. M. 1998. Phenanthrene degradation by microorganisms isolated from a contaminated stream. Environmental Pollution 101: 355-359.

Rostron, W. M., Stuckey, D. C., Young, A. A. 2001. Nitrification of high strength ammonia wastewaters: comparative study of immobilisation media. Water Research 35(5): 1169-1178.

Sahariah, B. P., Chakraborty, S. 2013. Performance of anaerobic-anoxic-aerobic batch fed moving-bed reactor at varying phenol feed concentrations and hydraulic retention time. Clean Technology and Environment Policy 15: 225-233.

Sahariah, B. P., Kumar, J. A., Chakraborty, S. 2016. Treatment of coke oven wastewater in an anaerobic-anoxic-aerobic moving bed bioreactor system. Desalination and Water Treatment 57(31): 14396-14402.

Segneanu, A. E., Gozescu, I., Dabici, A., Sfirloaga, P., Szabadai, Z. 2012. Organic compounds FT-IR spectroscopy. Macro to Nano Spectroscopy, ISBN: 978-953-51-0664-7, InTech.

Sharma, A., Kumar, P., Rehman, M. B. 2014. Biodegradation of diesel hydrocarbon in soil by bioaugmentation of Pseudomonas aeruginosa: A laboratory scale study. International Journal of Environmental Bioremediation and Biodegradation 2(4): 202-212.

Sharma, N. K., Philip, L. 2014. Effect of cyanide on phenolics and aromatic hydrocarbons biodegradation under anaerobic and anoxic conditions. Chemical Engineering Journal 256: 255-267.

Sires, I., Brillas, E. 2012. Remediation of water pollution caused by pharmaceutical residues based on electrochemical separation and degradation technologies: a review. Environment International 40: 212-229.

Tamura, K., Nei, M. 1993. Estimation of the number of neucleotide substitutions in the control region of mitochondrial DNA in humans and chimpanzees. Molecular Biology and Evolution 10: 512-526.

Tamura, K., Nei, M., Kumar, S. 2004. Prospects for inferring very large phylogenies by using the neighbor-joining method. Proceedings of the National Academy of Sciences (USA) 101: 11030-11035.

Tong, K., Zhang, Y., Liu, G., Ye, Z., Chu, P. K. 2013. Treatment of heavy oil wastewater by a conventional activated sludge process coupled with immobilized biological filter. International Biodeterioration and Biodegradation 85: 65-71.

United States Environment and Protection Agency, 1996. Method 3050B Acid digestion of sediments, sludges and soils. Revision 2, Washington, USA 3-5.

United States Environment and Protection Agency, Land application of sewage sludge 1994. EPA/831-B-93-002B.

Vazquez, I., Rodriguez, J., Maranon, E., Castrillon, L., Fernandez, Y. 2006. Study of the aerobic biodegradation of coke wastewater in a two and three-step activated sludge process. Journal of Hazardous Materials B137: 1681-1688.

Wu, L. C., Kuo, C. L., Chung, Y. C. 2011. Removal of high concentrations of NH(3) by a combined photoreactor and biotrickling filter system. Journal of Environmental Science and Health Part A 46(14): 1675-1682.

Zaneti, R., Etchepare, R., Rubio, J. 2011. Car wash wastewater reclamation. Full-scale application and upcoming features. Resources, Conservation and Recycling 55: 953-959.

6

CHAPTER

EFFECTS OF SALINITY AND SHOCK LOAD DURING THE TREATMENT OF PETROLEUM REFINERY WASTEWATER BY ANOXIC-AEROBIC SEQUENTIAL REACTORS

CHAPTER 6

EFFECTS OF SALINITY AND SHOCK LOAD DURING THE TREATMENT OF PETROELUM REFINERY WASTEWATER BY ANOXIC-AEROBIC SEQUENTIAL REACTORS

6.1 INTRODUCTION

A mixed brine of high salinity and chemicals is formed during the crude oil extraction process due to leaching of various salts from aquifer to extracted oil (Diya'Uddin et al., 2011). Sometimes saline water or seawater is used to maintain oil reservoir pressure in the aquifer zone, subsequently generating wastewater with high organics and total dissolved solids (TDS) (Mahmoud et al., 2017). Surfactants and polymers are also used for the better recovery of oil from reservoirs (Son et al., 2014). Hence, processed water generated from petroleum refineries becomes a chemical soup characterized by high conductivity, salinity and TDS, in which the salt concentration can range from a few to 300 g/L (Sharghi et al., 2013). Excess of salt is harmful for the growth of microbial biomass (Alipour et al., 2017). Still Biodegradation being a cheap option for the treatment of industrial wastewater have been applied for the assimilation of pollutants in saline refinery wastewater by aerobic (Ahmadi et al., 2017; Veenagayathri and Vasudevan, 2017; Jamal and Pugazhendi, 2018) and anaerobic (Dincer and Kargi, 1999; Shuler and Kargi, 2002; Ghorbanian et al., 2014) processes to meet discharge standards. All the mentioned literature works have operated single reactor systems with moderate influent salinity and pollutants concentrations. Simultaneous degradation of petroleum hydrocarbons and inorganics at varied concentrations of salt is yet to be studied.

Production rates vary within industries and wastewater with intermittent concentration of pollutants is generated. Sudden change in load to a bio-treatment system can occur during industrial operations due to accidental spills, introduction of new operations, manufacturing of new products and increase in material demand. Microbes inside bioreactors can face huge altercations when exposed to abrupt change in the pollutants loads and efficiency of the system can decrease. Hence, stability of the treatment systems to the instantaneous change in pollutants/shock loads needs to be tested in lab scale prior to their practical application.

In the present study, effect of feed salt (NaCl) concentration on the performance of anoxic-aerobic sequential moving bed reactors was investigated. Then effect of sudden increase of crude oil on the stability of the anoxic-aerobic sequential reactor system was also studied.

6.2 MATERIALS AND METHODS

6.2.1 Chemicals and Reagents

Chemicals and reagents described in Chapter 4 were used during the present study. Crude oil was used as hydrocarbon and NaCl was purchased from Merck, India. Feed prepared by tap water (pH 8.0 ± 0.2) and stock solutions were prepared by milli-Q water (pH 7.0 ± 0.1).

6.2.2 Reactor operation at different NaCl dose

Anoxic (A1) - Aerobic (A2) reactors mentioned in section 3.2.2 were used during the present study at fixed cycle times 48h (HRT 60h) and 16h (HRT 20h), respectively, with an overall 80h system HRT. Operational conditions of the reactors can be found in Table 6.1.

Table 6.1: Operational conditions of A1 and A2 during variation in NaCl concentration

NaCl (g/L)	Days	Agitation		Reactor volume (L)		Decant volume (L)		Cycle time (h)		HRT (h)	
		A1	A2	A1	A2	A1	A2	A1	A2	A1	A2
0	670-708	20 rpm	Airflow 2L/min	10	3.33	8	2.67	48	16	60	20
10	711-749										
20	752-790										
25	793-831										
30	834-872										
35	875-913										
40	916-954										
45	957-995										
Rec.	998-1036										

A1: Anoxic reactor, A2: Aerobic reactor

6.2.3 Feed characteristics

Treatment of synthetic refinery wastewater with varied salinity levels was done in between day 670 to 1036 for a study period of 366 days. Influent phenol (750 ± 5 mg/L), S^{2-} (750 ± 7 mg/L), crude oil (300 mg/L), TH (1250 ± 14 mg/L), NH_4^+-N (350 ± 5 mg/L), NO_3^--N (1000 ± 10 mg/L) and surfactant (0.2 mM) were kept constant. Increase in feed conductivity, salinity and TDS was observed with increase in NaCl. NaCl was varied at eight levels: 0, 10, 20, 25, 30, 35, 40 and 45 g/L. NaCl was reduced to 0 g/L during the recovery study. Saline

properties of the feed are summarized in Table 6.2. N_2 purging was done before the addition of S^{2-} and emulsified crude oil to avoid abiotic loss. Compositions of the trace metal solutions, yeast extract and phosphate buffer were same as mentioned in section 2.2.4 previously.

Table 6.2: Properties of the feed at NaCl variation

NaCl (g/L)	Turbidity (NTU)	Conductivity (mS/cm)	Salinity (g/L)	Total dissolved solids (g/L)	Total suspended solids (g/L)
0	96.21 ± 4.19	7.79 ± 0.04	5.04 ± 0.11	4.98 ± 0.08	76.55 ± 2.07
10		21.60 ± 0.11	16.53 ± 0.09	14.30 ± 0.24	
20		44.40 ± 0.14	34.02 ± 0.18	29.20 ± 0.32	
25		56.05 ± 0.19	43.35 ± 0.21	38.35 ± 0.17	
30		63.35 ± 0.17	47.15 ± 0.39	41.70 ± 0.37	
35		76.80 ± 0.24	58.50 ± 0.44	51.20 ± 0.42	
40		87.90 ± 0.18	67.80 ± 0.37	58.70 ± 0.32	
45		98.90 ± 0.32	76.10 ± 0.38	65.70 ± 0.28	
Recovery		7.82 ± 0.04	5.02 ± 0.11	4.99 ± 0.08	

Turbidity was measured at twice dilution

Recovery study was done at 0 g/L of NaCl

6.2.4 Analytical procedure

Analysis of phenol, S^{2-}, SO_4^{2-}, $S_2O_3^{2-}$, total hydrocarbon, NO_3^--N, NO_2^--N, NH_4^+-N, salinity, conductivity, TDS, turbidity, gaseous samples and COD was done as mentioned in Chapter 2. Measurements of suspended solids (section 4.2.4), quantification of biomass (section 4.2.5) and biomass activity (section 4.2.7) were done as mentioned Chapter 4. Pure culture analysis was done as per section 5.2.4 in Chapter 5.

6.3 EFFECT OF VARIED SALINITY ON ANOXIC-AEROBIC REACTORS

6.3.1 Biomass concentration

Attached biomass was maximum in A1 in the absence of NaCl (Fig. 6.1a). Decrease in attached biomass and increase in suspended biomass were observed with increase in NaCl dose, suggesting sloughing of the anoxic biomass at high salinity. Presence of salts and increase in the ionic strength of water inhibited the catabolic and anabolic activity of the microbial community (Rath et al., 2016) and mineralization of feed source was hampered. This led to

endogenous respiration as well as rupture of cell biomass and resulted into sloughing. SRT of A1 decreased due to more sloughing from discs and washing out of biomass with increase in salinity (Fig. 6.1b). Anoxic biomass received the initial toxic load with high salinity and pollutants concentrations and aerobic biomass received comparatively lesser concentrations. Hence, NaCl had more profound effect on the anoxic biomass as change in the distribution of aerobic biomass was only observed beyond NaCl concentration of 30 g/L (Fig. 6.1c). Whereas, anoxic biomass got effected at three times lesser dose of NaCl. There was a decrease of 8% in the total anoxic biomass and 2% in the total aerobic biomass with increase in NaCl from 0 g/L to 45 g/L. SRT of A2 was not affected up to 30g/L of NaCl and decreased with further increase in NaCl (Fig. 6.1d). Total biomass of both A1 and A2 increased when NaCl was reduced to 0 g/L during recovery. Distribution of attached and suspended biomass in the total biomass of both A1 and A2 was observed to be similar as it was before the introduction of NaCl. This suggests full recovery of the reactor biomass after the withdrawal of NaCl load.

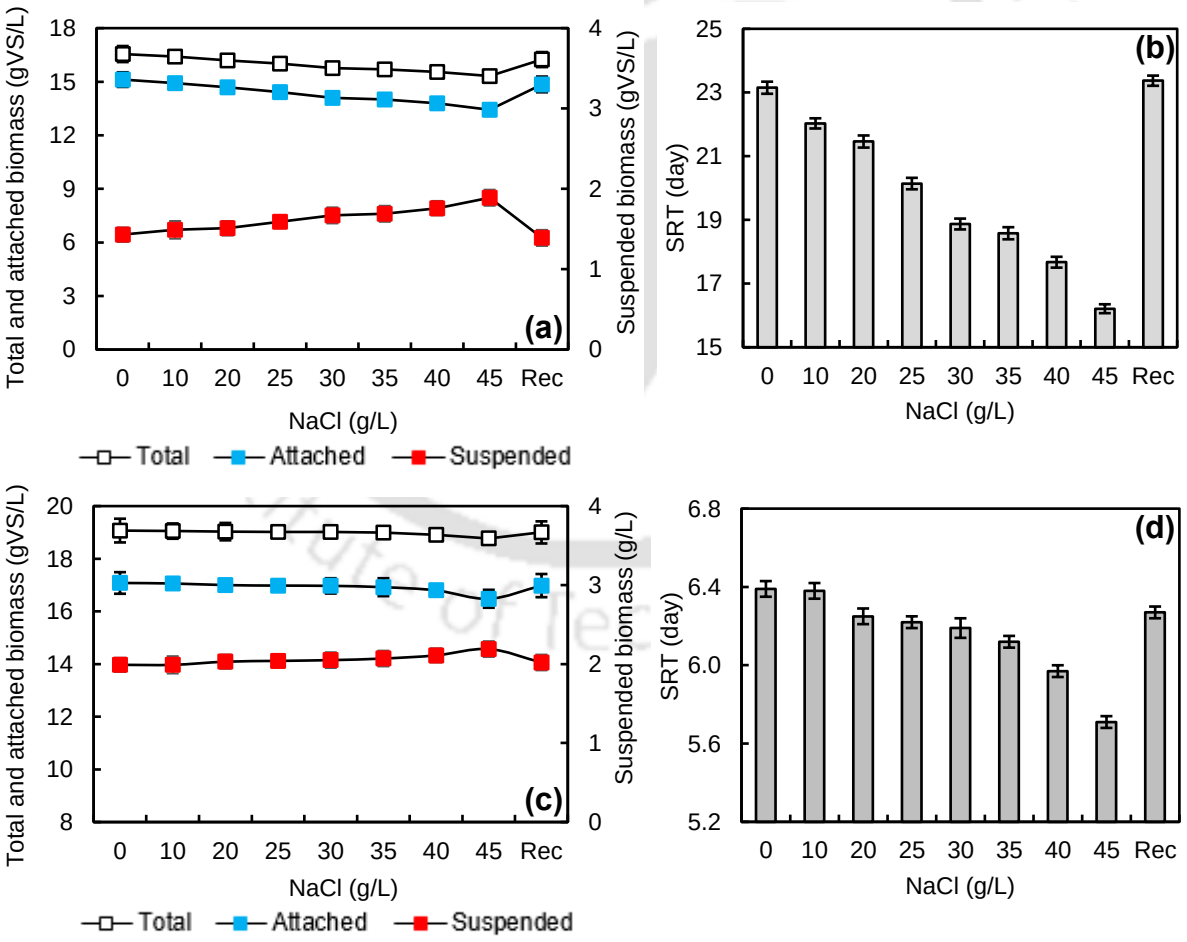

Fig. 6.1: (a) biomass distribution in A1, (b) SRT of A1, (c) biomass distribution in A2, (d) SRT of A2 during NaCl variation

6.3.2 Removal of organics

Effluent phenol (Fig. 6.2a), TH (Fig. 6.2b), COD_T (6.2c) and COD_O (Fig. 6.2d) from A1 increased with increase in NaCl with corresponding decrease in removal efficiencies from 38% to 14% (phenol), 45% to 23% (TH), 64% to 49% (COD_T) and 41% to 18% (COD_O) at 60h HRT. Decrease in SRT had negative effect on the efficiency of A1. Palanisamy et al. (2014) reported decrease in the removals of hydrocarbons beyond 10 g/L of NaCl and Alipour et al. (2017) observed decrease in COD removal at NaCl dose of 8 g/L in anoxic condition. Similarly, decrease in COD removal in A1 started with the introduction of 10 g/L of NaCl in the present study. However, Jafari et al. (2015) reported negative effect of NaCl up to 20 g/L during removal of catechol by denitrification. In the present study, inhibition on organics degradation occurred at lower NaCl dose due to the presence of much toxic compounds and high alkaline pH. Effluent of A1 was treated in A2 and effect of influent NaCl on A2 was never observed up to 30 g/L as complete removals of phenol (Fig. 6.2a), TH (Fig. 6.2b) and COD_O (Fig. 6.2d) was observed at 20h HRT with a total HRT of 80h. Beyond NaCl dose of 30 g/L, performance of A2 started to decline and overall efficiency of the A1-A2 system decreased. Aerobic degradation of poly aromatic hydrocarbons (influent TH: 1419 mg/L) was hampered beyond NaCl dose of 40 g/L as reported by Jamal and Pugazhendi (2018). In the present study, 30 g/L of NaCl caused problems for the aerobic biomass possibly due to the presence of hydrocarbons with higher density and viscosity and high pH. Increase in the final effluent of COD_T from the A1-A2 system was observed with increase in NaCl (Fig. 6.2c), as presence of more than 2 g/L of Cl^- could cause interference in the COD determination (APHA, 2005) and overall COD removal decreased. Efficiency of both A1 and A2 for the removal of organics increased during the recovery phase (NaCl 0g/L) and complete recovery of the reactors was achieved.

Heterotrophic activity (HA) was analyzed for both anoxic and aerobic biomass at every phase of NaCl dose variation and activity cycles are illustrated in Fig. 6.3a and Fig. 6.3b. HA of anoxic biomass was maximum in the absence of NaCl and decreased with increase in NaCl (Fig. 6.4a). HA of aerobic biomass was stable up to 30 g/L NaCl and decreased at higher concentrations (Fig. 6.4b). Decrease in activity of both anoxic and aerobic biomass was reflected in the reactor efficiency, as both SRT and organics removal decreased at higher influent NaCl concentrations. Hence, HA of the reactor biomass had direct correlation with the organics degradation efficiency. HA of both anoxic and aerobic biomass increased during the recovery period and were similar as they were before the introduction of NaCl.

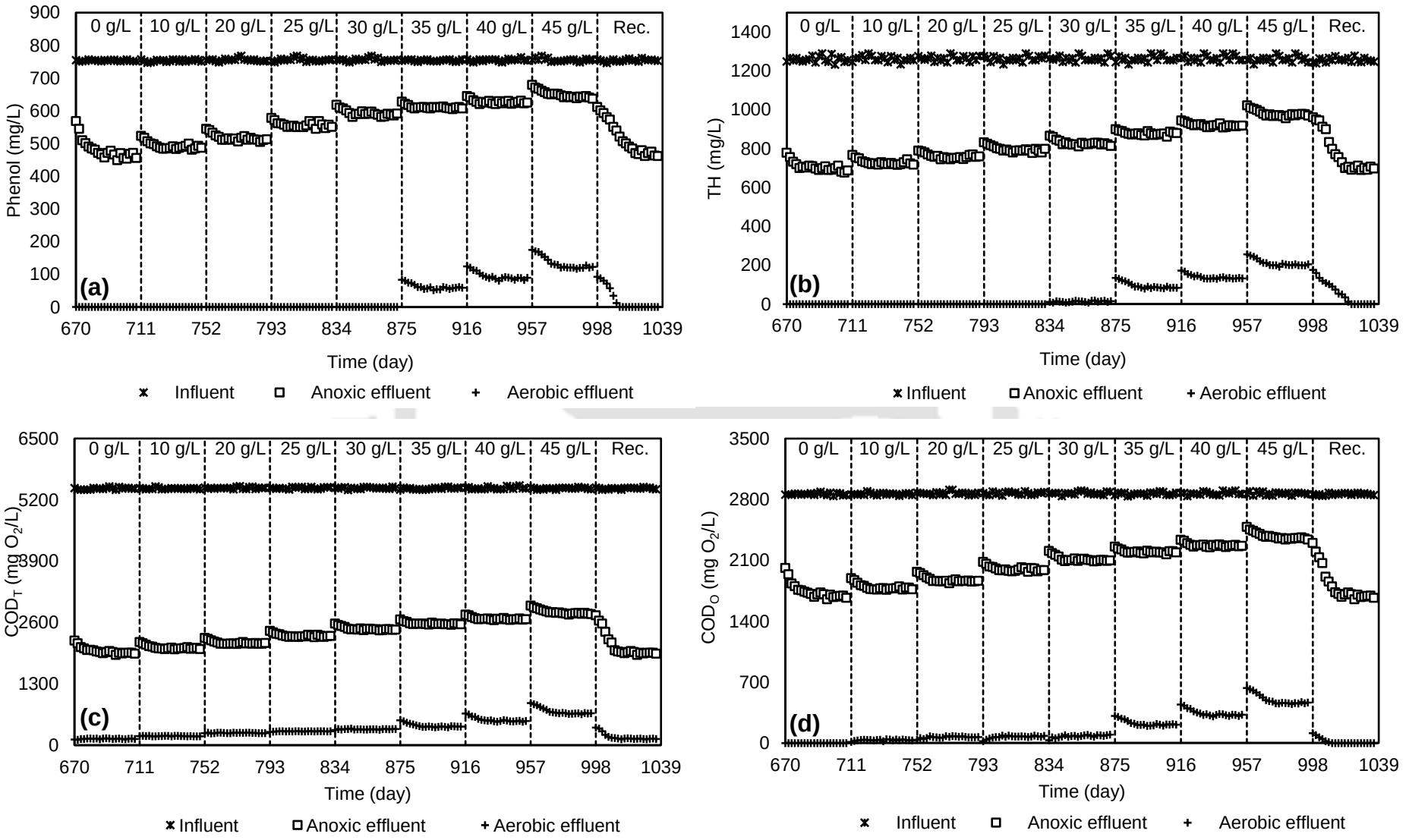

Fig. 6.2: Influent and effluent concentrations of (a) Phenol, (b) TH, (c) COD_T and (d) COD_O during NaCl variation

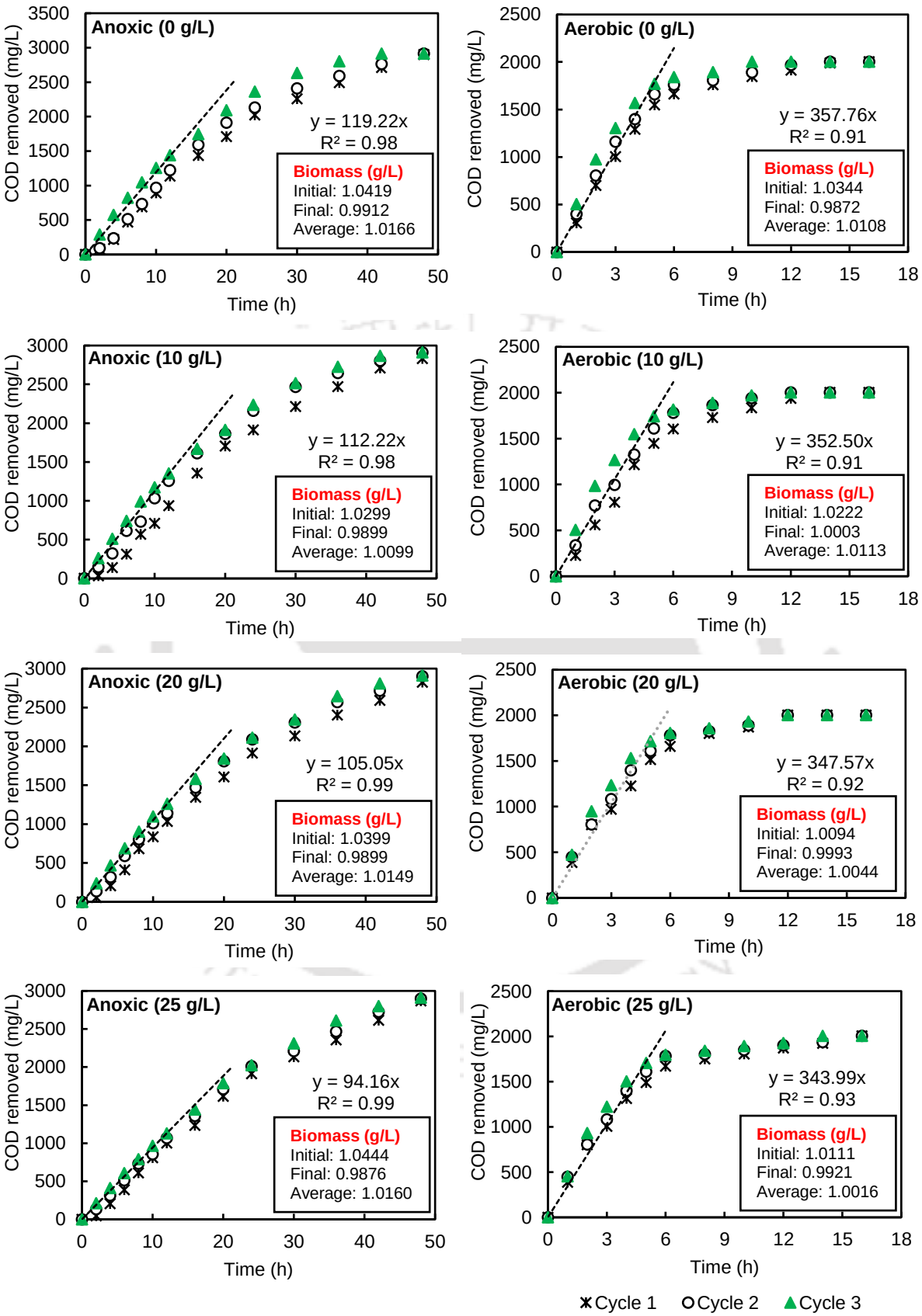

Fig. 6.3a: Heterotrophic activity cycles of anoxic and aerobic biomass at varied NaCl concentration (0, 10, 20, 25 g/L)

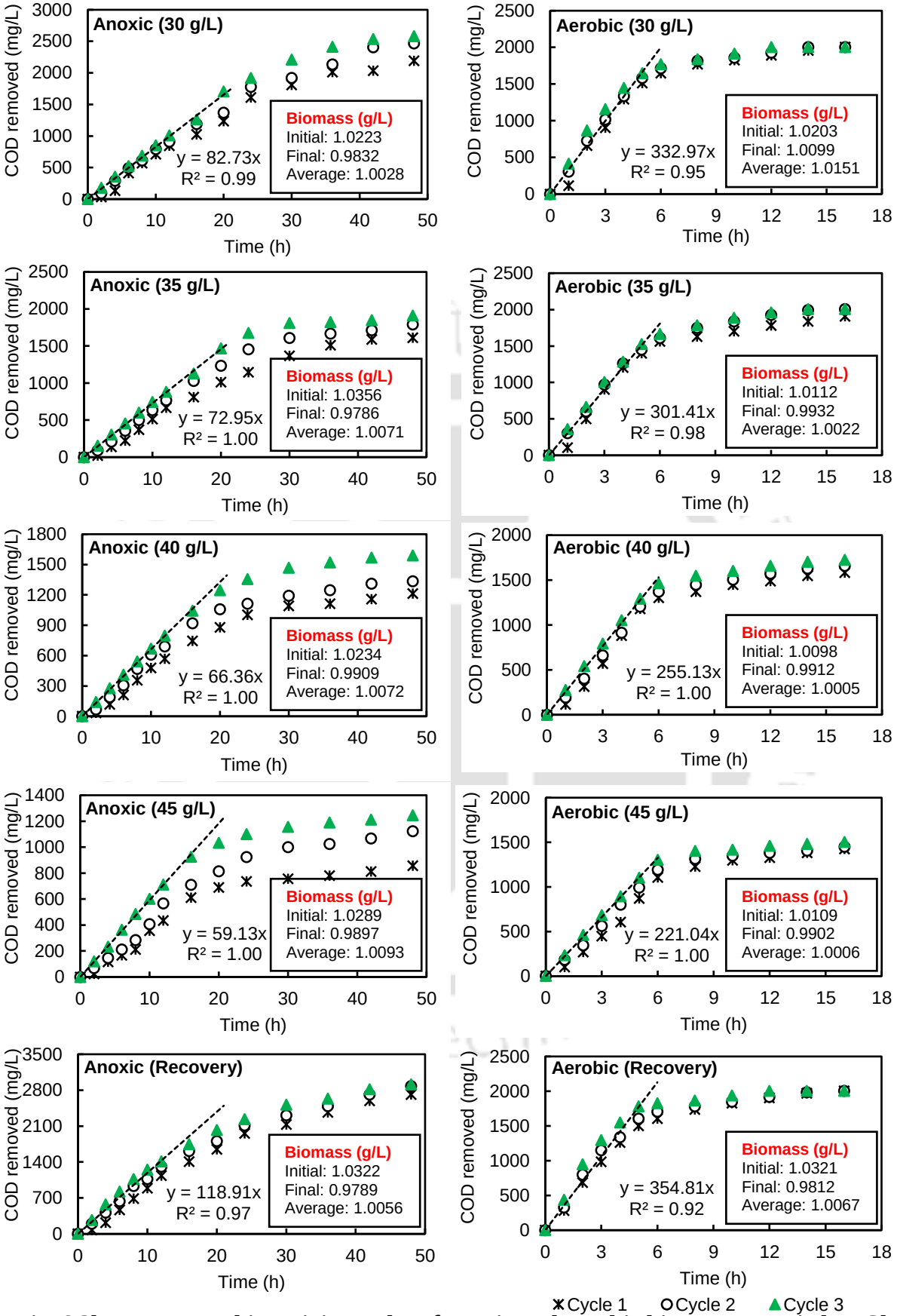

Fig. 6.3b: Heterotrophic activity cycles of anoxic and aerobic biomass at varied NaCl concentration (30, 35, 40, 45 g/L and recovery)

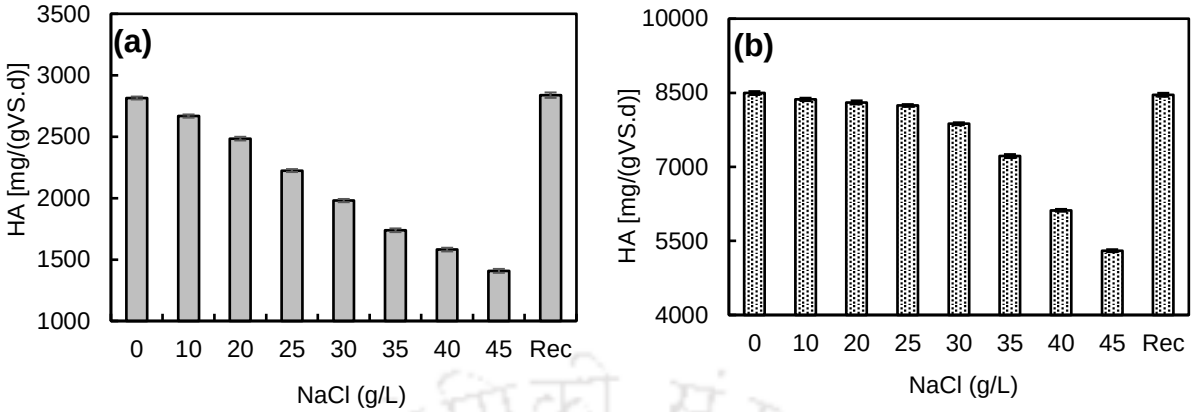

Fig. 6.4: Heterotrophic activity of (a) anoxic and (b) aerobic biomass at NaCl variation

6.3.3 Removal of sulfide

Influent and effluent concentrations of S^{2-}, $S_2O_3^{2-}$ and SO_4^{2-} are illustrated in Fig. 6.5 and average concentrations are summarized in Table 6.3a and 6.3b. Effect of NaCl dose and decrease in A1 reactor SRT did not affect removal of S^{2-} and complete removal of S^{2-} occurred in A1 at 60h HRT (Fig. 6.5a). Effluent SO_4^{2-} decreased, whereas, $S_2O_3^{2-}$ increased with increase in salinity levels in A1 (Fig. 6.5a). S^{2-} to SO_4^{2-} conversion hampered with increase in NaCl concentration and 38% of the removed S^{2-} was converted to SO_4^{2-} at 45 g/L of NaCl dose. Partial degradation of S^{2-} was supported by the increase in salinity as $S_2O_3^{2-}$ conversion increased from 3% to 8% of the removed S^{2-} with increase in NaCl dose of 0 g/L to 45 g/L (Fig. 6.5b). Remaining of the removed S^{2-} could attribute to the production of bio-sulfur (S^0) and the conversion was minimum in the absence of NaCl and increased with increase in NaCl concentration. Liu et al. (2016) observed decrease in SO_4^{2-} and increase in S^0 during oxidation of S^{2-} (influent 200 mg/L) in the presence of acetate in anoxic conditions with increase in NaCl (0-70 g/L). At 35 g/L of NaCl with 95% S^{2-} removal efficiency, 55% of the feed S^{2-} was converted to S^0 (Liu et al., 2016). However, in the present study with feed S^{2-} of 750 mg/L, 99% S^{2-} removal was achieved with 52% converted to S^0. Both the results supported that higher salinity favored incomplete oxidation of S^{2-} to S^0. Residual $S_2O_3^{2-}$ was oxidized to SO_4^{2-} in A2 and effect of NaCl was not observed (Fig. 6.5c)

Chemolithotrophic activity (CA) cycles are summarized in Fig. 6.6. CA was maximum in the absence of NaCl and decreased with increase in NaCl (Fig. 6.7). Decrease in CA was the potential reason for the decrease in the complete oxidation of S^{2-} to SO_4^{2-} and increase in the intermediate S^0 and $S_2O_3^{2-}$. When NaCl dose was reduced to 0 g/L in the recovery phase, CA of anoxic biomass increased and recovered to its original state (Fig. 6.7).

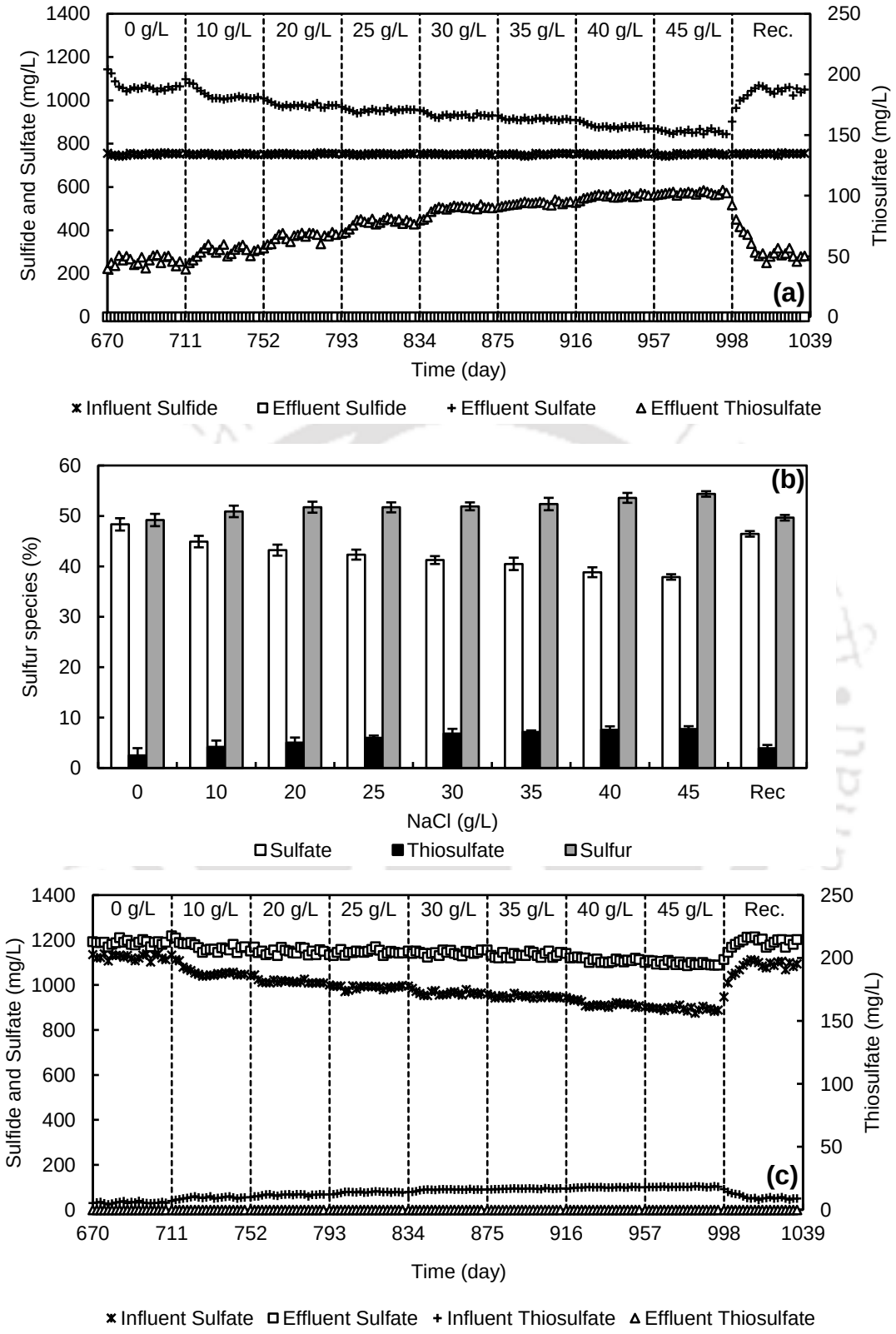

Fig. 6.5: (a) Influent and effluent S^{2-}, $S_2O_3^{2-}$ and SO_4^{2-} in A1, (b) Distribution of sulfur species, (c) Influent and effluent $S_2O_3^{2-}$ and SO_4^{2-} in A2

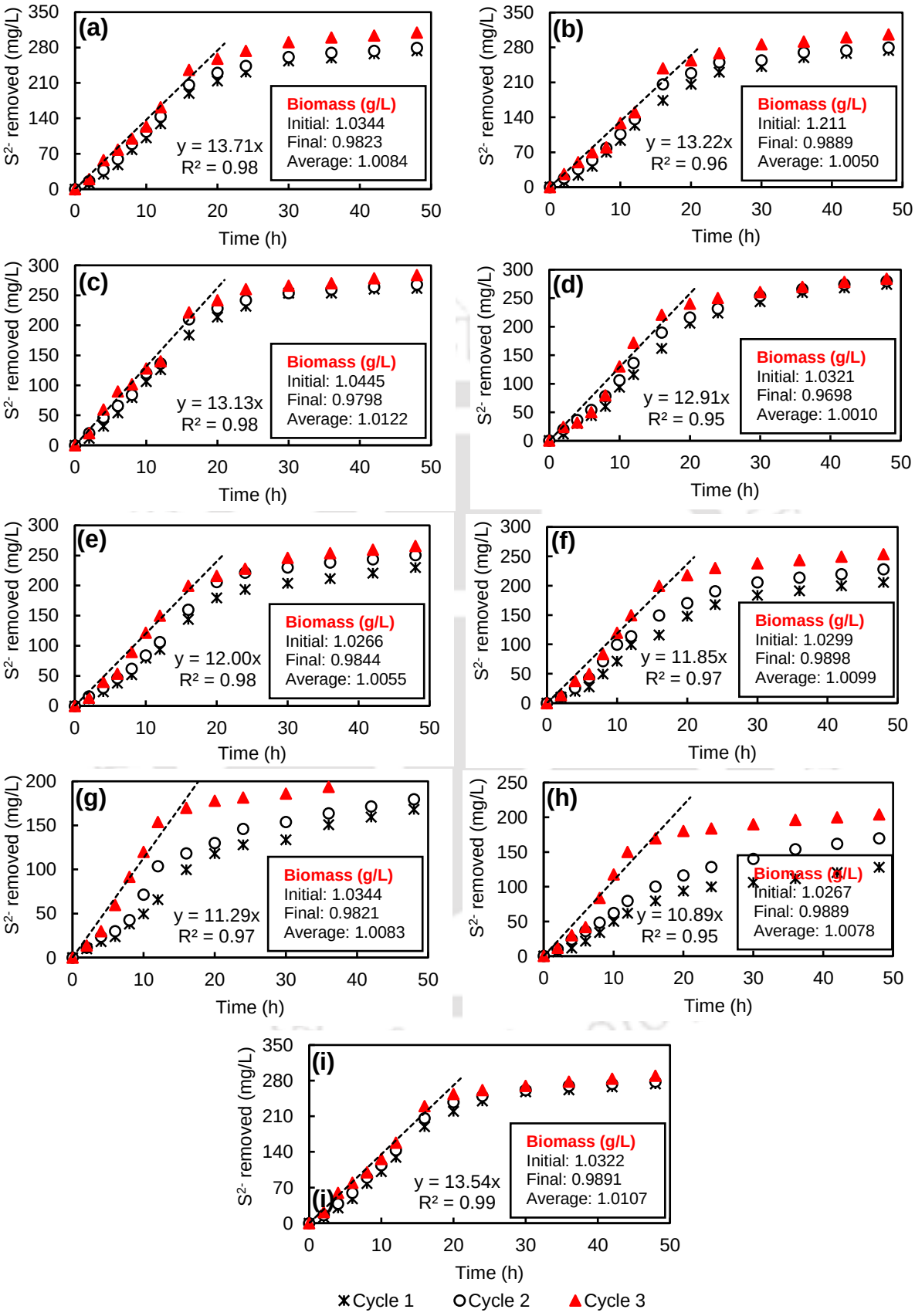

Fig. 6.6: Chemolithotrophic activity cycles of A1 biomass at varied NaCl of (a) 0 g/L, (b) 10 g/L, (c) 20 g/L, (d) 25 g/L, (e) 30 g/L, (f) 35 g/L, (g) 40 g/L, (h) 45 g/L and (i) recovery

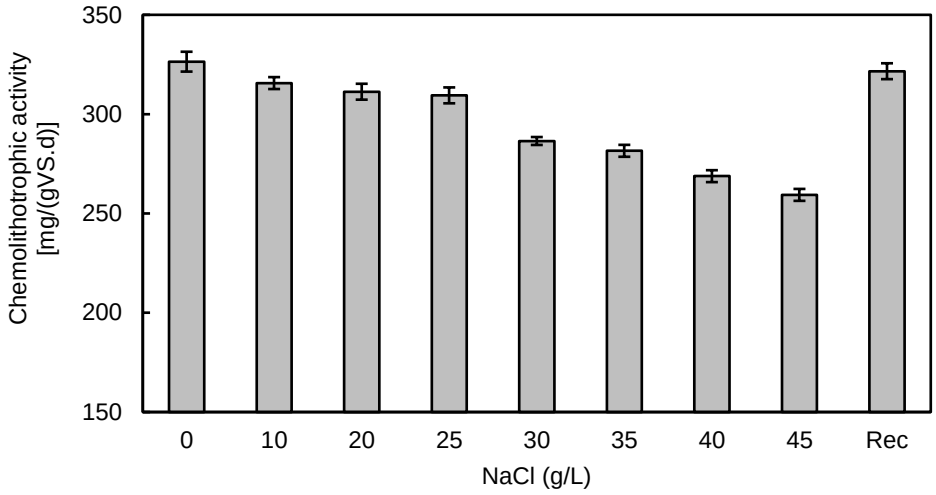

Fig. 6.7: Average chemolithotrophic activity of anoxic biomass at NaCl variation

6.3.4 Removal of nitrogen

Complete removal of NO_3^--N occurred in the absence of NaCl (Fig. 6.8a). Decrease in the removals of phenol and TH led to lower utilization of the electron acceptor. Reduction of NO_3^--N hampered and partial degradation was enhanced as NO_2^--N accumulation increased more than 1.5 times with increase in NaCl from 0 to 45 g/L in A1 (Table 6.3a and 6.3b). Diversity of microbial community decreased in the presence of salinity and nitrite reductase gene got affected at high salt concentration (Yoshie et al., 2004). Deng et al. (2017) have reported decrease in denitrifying community with increase in salinity during degradation of aromatic hydrocarbon. In the present study also, there was accumulation of NO_2^--N in A1 with increase in NaCl and denitrification efficiency decreased from 81% to 55% with increase in NaCl from 0 to 45 g/L. Ebrahimi et al. (2015) reported decrease in NO_3^--N removal (initial 113 mg/L) at 35 ºC with increase in NaCl from 20 to 60 g/L with acetate as carbon source. Anoxic biomass in the present study was exposed to more pernicious organic and inorganic pollutants along with high influent NO_3^--N (1000 ± 10 mg/L) and still showed more than 90% removal up to 35 g/L of NaCl.

Generated gas volume released by A1 is summarized in Table 6.3a and 6.3b and constituent analysis is shown in Fig. 6.8b. Gas production was maximum in the absence of NaCl and decreased with increase in NaCl. Volumes of CO_2 and H_2S were constant throughout and were not affected by the increase in salinity. CH_4 was never observed in any of the samples. Decrease in the reduction of NO_3^--N to N_2 was observed with increase in NaCl as fraction of N_2 decreased from 92% to 80% of the total gas generated.

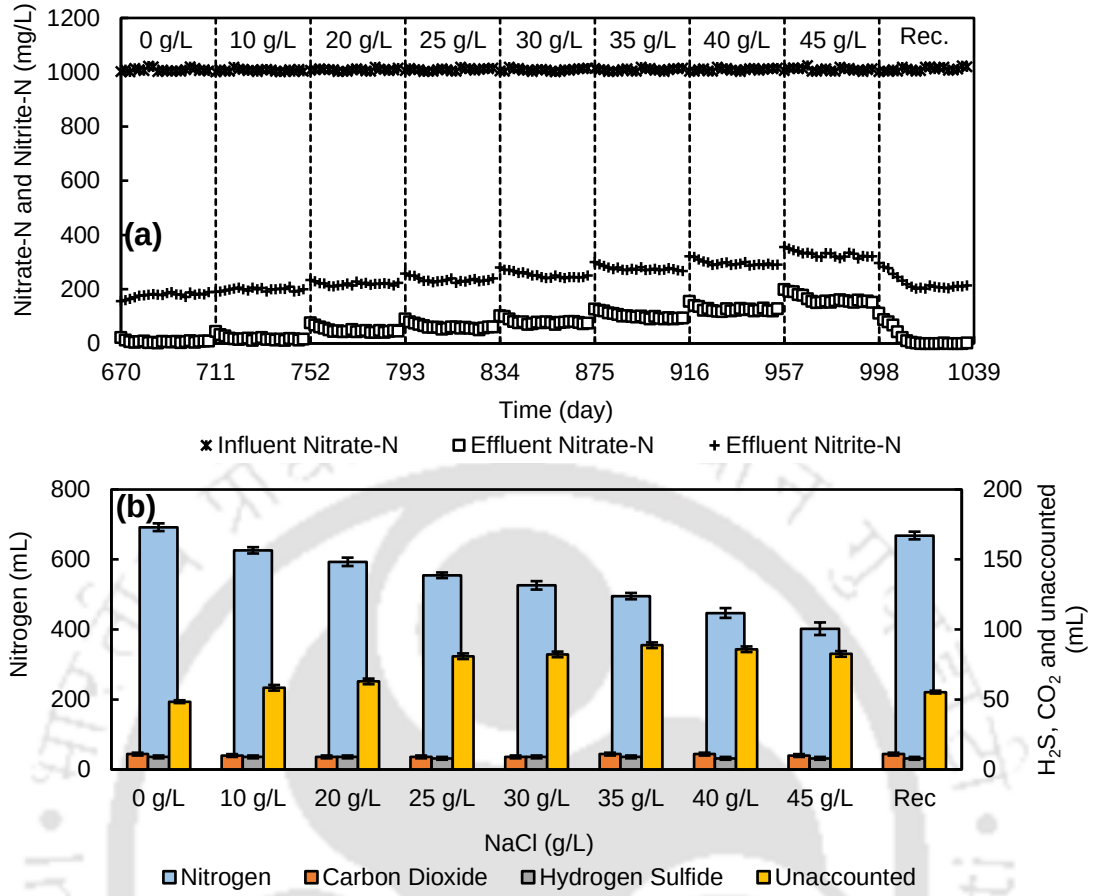

Fig. 6.8: (a) influent and effluent NO_3^--N and NO_2^--N in A1, (b) Gaseous species in A1 at NaCl variation

NH_4^+-N removal in A1 was quite low (3-5%) irrespective of the NaCl dose (Fig. 6.9a). Complete oxidation of NH_4^+-N was achieved up to NaCl dose of 30 g/L in A2 and higher NaCl (35 to 45 g/L) resulted in decrease in NH_4^+-N removal efficiency from 99% to 86% (Fig. 6.9a). Claros et al. (2016) reported decrease in activity of ammonia oxidizing bacteria with increase in salinity. Influent NO_3^--N and NO_2^--N to A2 increased with increase in NaCl as denitrification decreased in A1. NO_3^--N and NO_2^--N were formed from the oxidation of NH_4^+-N (Fig. 6.9b). Effluent NO_3^--N increased and NO_2^--N decreased in A2 (Table 6.3a and 6.3b) suggesting nitrification of the influent NH_4^+-N and NO_2^--N. Nitrification rate of NH_4^+-N in A2 was calculated as follows,

$$[(NO_3^- - N)_{eff} - (NO_3^- - N)_{inf}] - [(NO_2^- - N)_{inf} - (NO_2^- - N)_{eff}]/HRT \quad \ldots (6.1)$$

where,

$(NO_3^-N)_{eff}$: effluent nitrate (mg/L), $(NO_3^-N)_{inf}$: influent nitrate (mg/L), $(NO_2^-N)_{inf}$: influent nitrite-N, $(NO_2^-N)_{eff}$: effluent nitrite-N

Maximum nitrification rate of 138 ± 7 g/(m^3.d) was observed in the absence of NaCl and decreased with increase in salt concentration. Nitrification rates of 132 ± 5, 122 ± 4, 121 ± 3, 114 ± 2, 109 ± 2, 104 ± 4, 94 ± 3 g/(m^3.d) were observed at NaCl dose of 10, 20, 25, 30, 35, 40 and 45 g/L, respectively, suggesting nitrification was inhibited by salinity. Decrease in nitrification beyond 40 g/L of NaCl dose was reported by Cui et al. (2016) at influent NH_4^+-N of 60 mg/L. Nitrifying action of the microorganisms was hampered at smaller NaCl dose (30 g/L) due to higher NH_4^+-N concentration and presence of toxic hydrocarbons. Similarly, Cortes-Lorenzo et al. (2015) also obtained decrease in nitrification at NaCl ≥ 24 g/L. Complete NH_4^+-N oxidation was achieved after the removal of NaCl dose and improvement in the nitrification rate [136 ± 5 g/(m^3.d)] was observed, suggesting recovery of A2 after the removal of inhibiting salinity (NaCl) in the present study.

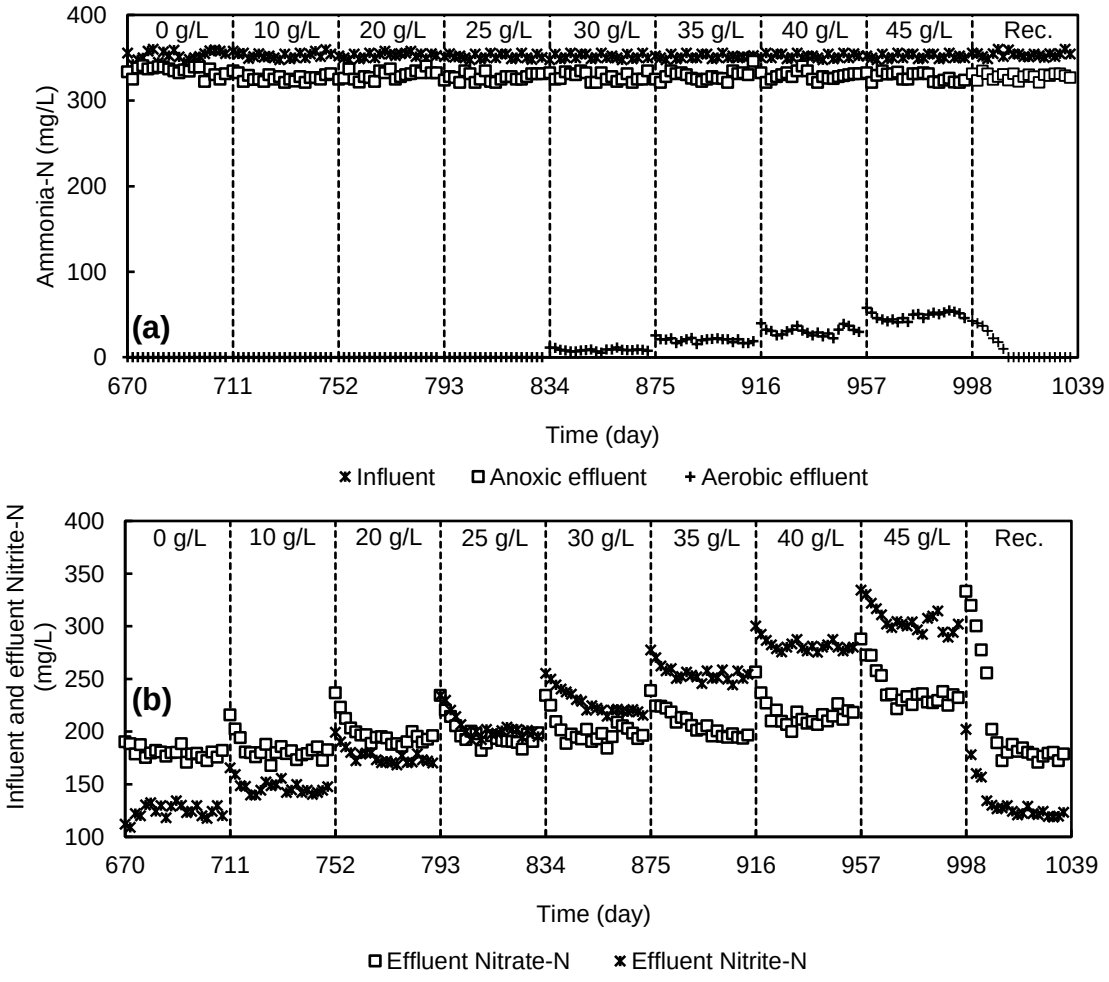

Fig. 6.9: (a) Influent and effluent NH_4^+-N in A1 and A2, (d) Effluent NO_3^--N and NO_2^--N from A2 during NaCl variation

Table 6.3 (a): Average influent and effluent of pollutants during NaCl variation (0, 10, 20, 25 and 30 g/L)

Parameters	0 g/L			10 g/L			20 g/L			25 g/L			30 g/L		
	Anoxic		Aerobic	Anoxic		Aerobic	Anoxic		Aerobic	Anoxic		Aerobic	Anoxic		Aerobic
	Influent	Effluent	Effluent	Influent	Effluent	Effluent	Influent	Effluent	Effluent	Influent	Effluent	Effluent	Influent	Effluent	Effluent
Phenol	753 ± 2	465 ± 10	4 ± 1	754 ± 3	488 ± 5	5 ± 1	756 ± 5	512 ± 5	4 ± 1	756 ± 5	554 ± 7	6 ± 1	757 ± 5	589 ± 5	4 ± 1
TH	1262 ± 17	697 ± 11	7 ± 2	1263 ± 15	724 ± 7	8 ± 2	1263 ± 14	755 ± 8	7 ± 2	1262 ± 14	790 ± 7	8 ± 2	1264 ± 15	825 ± 6	13 ± 4
Sulfide	754 ± 3	2 ± 1	-	752 ± 3	3 ± 1	-	753 ± 3	2 ± 1	-	752 ± 3	4 ± 1	-	752 ± 3	3 ± 1	-
COD	5449 ± 18	1965 ± 24	138 ± 6	5446 ± 17	2054 ± 12	195 ± 6	5455 ± 21	2157 ± 10	262 ± 4	5452 ± 20	2311 ± 17	295 ± 5	5455 ± 16	2455 ± 12	339 ± 7
Thiosulfate	-	47 ± 3	ND	-	55 ± 3	ND	-	67 ± 3	ND	-	79 ± 2	ND	-	91 ± 1	ND
Sulfate	34 ± 3	1125 ± 12	1189 ± 10	40 ± 2	1048 ± 5	1161 ± 12	42 ± 4	1014 ± 6	1150 ± 12	47 ± 3	991 ± 5	1148 ± 9	40 ± 2	965 ± 7	1143 ± 8
Sulfur	-	371 ± 5	-	-	382 ± 4	-	-	389 ± 5	-	-	389 ± 3	-	-	390 ± 3	-
Ammonia-N	353 ± 5	334 ± 5	4 ± 1	353 ± 4	325 ± 3	6 ± 1	354 ± 3	331 ± 5	4 ± 1	352 ± 3	327 ± 4	5 ± 1	352 ± 3	327 ± 5	8 ± 1
Nitrate-N	1010 ± 7	6 ± 2	179 ± 4	1007 ± 4	16 ± 3	180 ± 5	1009 ± 5	45 ± 3	193 ± 4	1011 ± 5	58 ± 3	192 ± 5	1009 ± 4	76 ± 4	197 ± 6
Nitrite-N	-	182 ± 5	125 ± 5	-	200 ± 3	146 ± 5	-	220 ± 4	173 ± 4	-	232 ± 5	199 ± 5	-	247 ± 3	221 ± 4
pH	9.5 ± 0.1	9.1 ± 0.1	8.5 ± 0.1	9.5 ± 0.1	9.1 ± 0.1	8.5 ± 0.1	9.5 ± 0.1	9.1 ± 0.1	8.5 ± 0.1	9.5 ± 0.1	9.19 ± 0.1	8.5 ± 0.1	9.5 ± 0.1	9.1 ± 0.1	8.5 ± 0.1
Gas (mL)	-	761 ± 21	-	-	-	704 ± 17	-	-	674 ± 5	-	-	653 ± 8	-	-	626 ± 7

TH: Total hydrocarbon
COD: chemical oxygen demand
ND: Not detected
All units except pH and gas are in mg/L

Table 6.3 (b): Average influent and effluent of pollutants during NaCl variation (35, 40, 45 g/L and recovery)

Parameters	35 g/L			40 g/L			45 g/L			Recovery		
	Anoxic		Aerobic	Anoxic		Aerobic	Anoxic		Aerobic	Anoxic		Aerobic
	Influent	Effluent	Effluent	Influent	Effluent	Effluent	Influent	Effluent	Effluent	Influent	Effluent	Effluent
Phenol	753 ± 3	609 ± 2	58 ± 3	755 ± 4	625 ± 4	88 ± 4	754 ± 4	645 ± 5	125 ± 7	755 ± 3	491 ± 9	5 ± 2
TH	1265 ± 14	876 ± 8	87 ± 5	1268 ± 16	918 ± 6	134 ± 4	1265 ± 15	972 ± 6	202 ± 5	1260 ± 11	728 ± 5	29 ± 7
Sulfide	751 ± 5	4 ± 2	-	752 ± 4	6 ± 1	-	753 ± 4	7 ± 2	-	754 ± 3	6 ± 2	-
COD	5443 ± 20	2573 ± 11	396 ± 11	5455 ± 29	2673 ± 12	518 ± 12	5450 ± 15	2802 ± 16	686 ± 23	5450 ± 15	1982 ± 61	142 ±9
Thiosulfate	-	94 ± 1	ND	-	100 ± 4	ND	-	102 ± 6	ND	-	52 ± 4	ND
Sulfate	38 ± 5	949 ± 6	1135 ± 10	41 ± 4	911 ± 6	1108 ± 7	44 ± 2	894 ± 10	1094 ± 7	40 ± 4	1094 ± 13	1195 ± 15
Sulfur	-	393 ± 3	-	-	403 ± 3	-	-	409 ± 4	-	-	374 ± 6	-
Ammonia-N	352 ± 3	328 ± 4	20 ± 2	351 ± 3	329 ± 5	31 ± 5	352 ± 3	327 ± 5	49 ± 4	354 ± 3	328 ± 3	5 ± 1
Nitrate-N	1010 ± 5	96 ± 4	201 ± 7	1011 ± 4	124 ± 4	213 ± 7	1009 ± 5	155 ± 3	231 ± 5	1014 ± 6	3 ± 1	180 ± 5
Nitrite-N	-	273 ± 4	253 ± 4	-	293 ± 4	281 ± 4	-	324 ± 7	301 ± 8	-	183 ± 5	124 ± 4
pH	9.5 ± 0.1	9.1 ± 0.1	8.5 ± 0.1	9.5 ± 0.1	9.1 ± 0.1	8.5 ± 0.1	9.5 ± 0.1	9.1 ± 0.1	8.5 ± 0.1	9.5 ± 0.1	9.1 ± 0.1	8.5 ± 0.1
Gas (mL)	-	604 ± 15	-	-	-	552 ± 19	-	-	503 ± 13	-	-	743 ± 15

TH: Total hydrocarbon
COD: chemical oxygen demand
ND: Not detected
All units except pH and gas are in mg/L

6.3.5 Effect of NaCl on the isolated microbial species

Effect of NaCl dose on the performance was analyzed for the pure cultures isolated from both anoxic and aerobic biomass with the simulated feed as supplied to the reactors A1 and A2 as mentioned in section 5.2.3. High NaCl had detrimental effect on *Pseudomonas aeruginosa* **SKM2013** (Fig. 6.10a) and effect on *Pseudomonas aeruginosa* **SC2013** (Fig. 6.10b) was marginal. Negative effect of increased salinity on denitrification efficiency of *Pseudomonas aeruginosa* is previously being reported (Yoshie et al., 2004). Out of the four dominant aerobic cultures, *Lysinibacillus sp.* **H200-150** could effectively resist the effect of NaCl up to 30 g/L and slight decrease in the removals of organics and NH_4^+-N were observed (Fig. 6.10c). Performance of *Stenotrophomonas sp.* **LW-34** was drastically hampered beyond 30 g/L of NaCl (Fig. 6.10d). In case of *Pseudomonas aeruginosa* **ISB4** (Fig. 6.10e) and *Pseudomonas aeruginosa* **LZS8436** (Fig. 6.10f), removals decreased continuously with increase in NaCl.

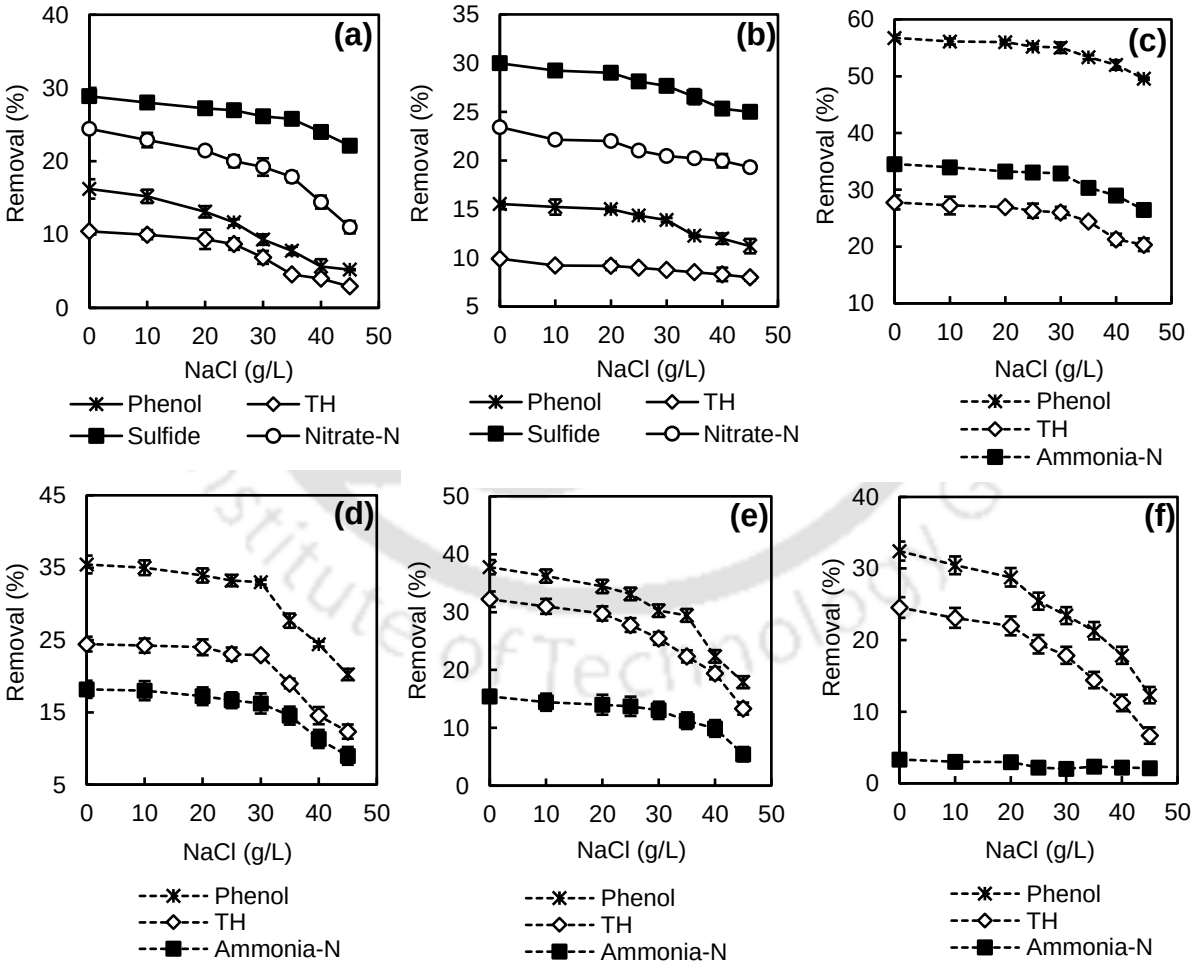

Fig. 6.10: Effect of NaCl on the performance of (a) *Pseudomonas aeruginosa* SKM2013, (b) *Pseudomonas aeruginosa* SC2013, (c) *Lysinibacillus* sp. H200-510, (d) *Stenotrophomonas* sp. LW-34, (e) *Pseudomonas aeruginosa* ISB4, (f) *Pseudomonas aeruginosa* LZS8436

6.4 EFFECT OF CRUDE OIL SHOCK LOADING

6.4.1 Feed and reactor operation

Effect of shock loading on the performance of A1 and A2 was examined by supplying sudden elevated loads of crude oil to the A1-A2 system. Concentrations of phenol (750 ± 5 mg/L), S^{2-} (750 ± 7 mg/L), NH_4^+-N (350 ± 5 mg/L) and NO_3^--N (1000 ± 10 mg/L) and HRT of the system (A1: 60h, A2: 20h, total: 80h) were kept constant. Shock load study was done at two different crude oil loadings named as shock 1 and shock 2 with each shock load being applied for thee cycles each. In shock 1, concentration of crude oil was increased twice (600 mg/L) and in shock 2, concentration was increased thrice (900 mg/L) compared to the original feed (300 mg/L). Operational conditions of the reactors during the study is summarized in Table 6.4. Emulsifier requirement test revealed a little higher concentration (0.3 mM) of surfactant was required to keep the oil distributed in the system and 8h of digestion time was sufficient for the determination of COD (Appendix M). After each shock load, recovery of the reactors was studied. During the recovery period, concentrations of crude oil (300 mg/L) and surfactant (0.2 mM) were brought back to the original as they were prior to shock feed.

Table 6.4: Operational conditions of A1 and A2 during crude oil shock load

Shock	Days	Crude oil (mg/L)	Surfactant (mM)	Agitation		Cycle time (h)		HRT (h)	
				A1	A2	A1	A2	A1	A2
Shock 1	1049-1053	600	0.3	20 rpm	Airflow 2L/min	48	16	60	20
Recovery after shock 1	1055-1085	300	0.2						
Shock 2	1087-1091	900	0.3						
Recovery after shock 2	1093-1143	300	0.2						

A1: Anoxic disc-bed reactor, A2: Aerobic moving bed reactor

6.4.2 Performance of the reactors

6.4.2.1 Removal of organics

Influent TH increased by 32% with the application of shock 1 resulting into rise in effluent TH (1.8 times), phenol (1.3 times), COD_T (2.0 times) and COD_O (2.1 times) from A1 (Fig. 6.11). Organics removal decreased (phenol: 43% to 21%, TH: 50% to 20%, COD_T: 65% to 44% and COD_O: 50% to 24%) with sudden increase in TH during shock 1 at 60h HRT. Aerobic reactor was marginally affected by shock 1 and overall organics removal efficiency slightly

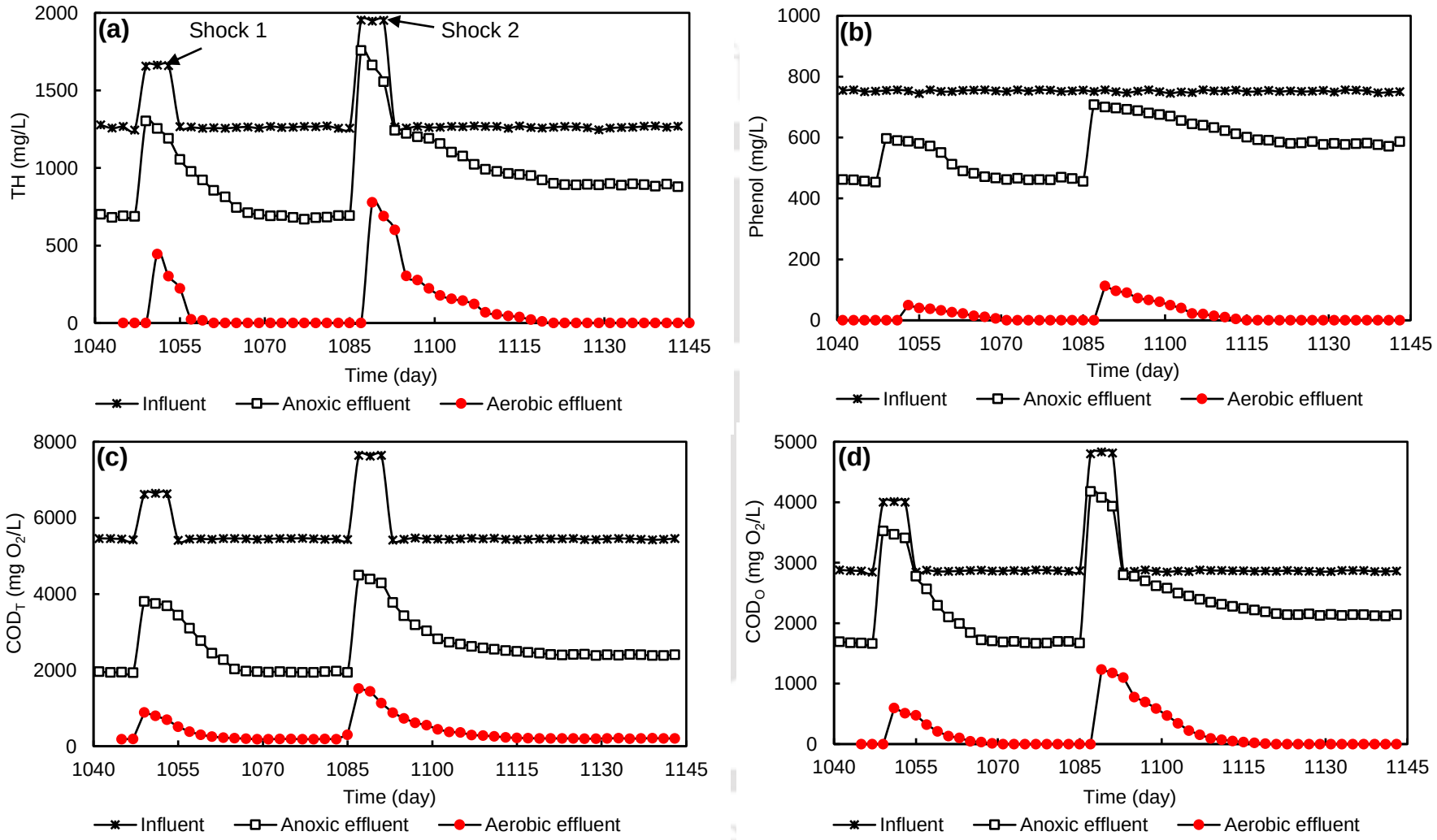

Fig. 6.11: Influent and effluent of (a) TH, (b) Phenol, (c) COD_T and (d) COD_O of A1 and A2 during shock load and recovery

decreased (phenol: 99% to 96%, TH: 99% to 94%, COD_T: 97% to 94% and COD_O: 99% to 94%) at total HRT of 80h. Decrease in the removal efficiency of anaerobic contact reactor (Senturk et al., 2014) and activated sludge reactor (Narayan et al., 2010) with application of organic shock loading have been reported. Both A1 and A2 recovered within 4 cycles after the resumption of the normal feed condition after shock 1. Removals of phenol, TH, COD_T and COD_O were 42%, 48%, 64% and 49%, respectively, in A1 and more than 99% removal of phenol, TH and COD_O was achieved after treatment from A2 during recovery and was comparable to the efficiency achieved prior to the application of shock 1.

Influent TH increased by 56% with the application of shock 2 and there was sudden rise in the effluent TH (3.5 times), phenol (2.7 times), COD_T (2.3 times) and COD_O (2.5 times) from A1 (Fig. 6.11). Removals of organics (phenol: 43% to 21%, TH: 50% to 20%, COD_T: 65% to 44% and COD_O: 50% to 24%) in A1 were severely hampered after shock 2. A2 also suffered from shock 2 and overall organics removal efficiencies during shock 2 (phenol: 99% to 96%, TH: 100% to 94%, COD_T: 99% to 94% and COD_O: 100% to 94%) were lesser compared to shock 1. Organics removal efficiency (phenol: 22% to 44%, TH, COD_T and COD_O) of A1 marginally increased during recovery after shock 2. However, full recovery to its original state did not happen even after 15 cycles of resumption of normal feed and A1 achieved a new effluent trend. Recovery of A2 was achieved within 8 cycles after shock 2 and more than 99% removal of phenol, TH and COD_O was achieved.

6.4.2.2 Removal of sulfide

Influent and effluent S^{2-} in A1 during shock load application are summarized in Fig. 6.12a and average concentrations are summarized in Table 6.5. S^{2-} removal was unaffected in A1 by the application of either of the shock loads. However, effluent SO_4^{2-} decreased and $S_2O_3^{2-}$ increased with the application of shock loads. Hence, conversion of S^{2-} to SO_4^{2-} was hampered, partial degradation of S^{2-} to $S_2O_3^{2-}$ was supported and effect of shock 2 was more profound compared to shock 1. Conversion of S^{2-} to SO_4^{2-} increased and $S_2O_3^{2-}$ decreased to their original state after the withdrawal of each shock loads. This suggests, S^{2-} degradation recovered completely in A1 even after shock 2 at high alkaline pH (> 9.5), unlike the organics degradation performance. Effluent released from A1 was passed to A2 where $S_2O_3^{2-}$ was oxidized Fig. 6.12b). Complete oxidation of $S_2O_3^{2-}$ was achieved during either shock 1 or shock 2 and increase in the effluent SO_4^{2-} from A2 during shock 1 and shock 2 confirmed the complete oxidation of $S_2O_3^{2-}$ even in shock loading condition.

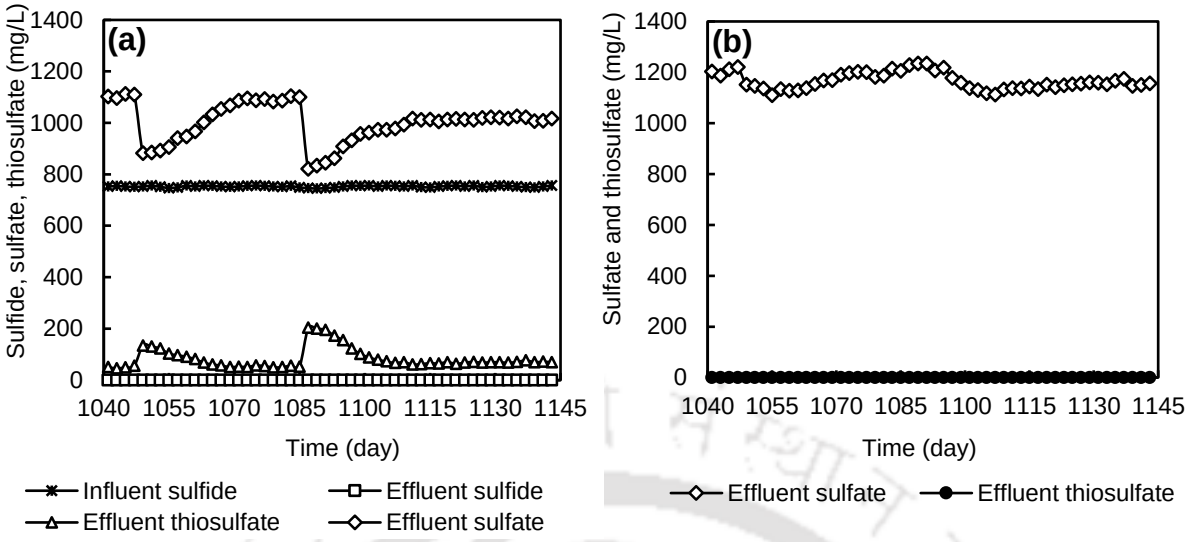

Fig. 6.12: (a) Influent and effluent sulfide, thiosulfate and sulfate in A1, (b) Influent and effluent thiosulfate and sulfate in A2 during shock application and recovery

6.4.2.3 Removal of nitrogen

Effluent NO_3^--N increased 44% and 56% with the application of shock 1 and shock 2, respectively, due to decrease in removal of the organics. Removal of NO_3^--N in A1 was less in case of shock 2 compared to shock 1. Effluent NO_3^--N decreased during the recovery period after each shock load as organics degradation as well as conversion of S^{2-} to SO_4^{2-} increased. Effluent NO_3^--N was negligible after recovery from shock 1. However, decrease in the efficiency of A1 for the removal of organics after shock 2 led to an upward shift in the effluent NO_3^--N after recovery from shock 2 (Fig. 6.13a). Denitrification decreased to 77% after shock 1 and recovered to 89% within 4 cycles of operation. Further decline in denitrification to 67% occurred during shock 2 and recovered to 80% due to reduction in the removal of NO_3^--N.

Effluent NH_4^+-N in A2 increased with the application of both shock 1 and shock 2 (Fig. 6.13b). Effect of shock 2 was more detrimental and removal efficiency decreased to 80%, which was 89% in the presence of shock 1. Removal increased to 99% during recovery after shock 1 and shock 2. There was increase in effluent NO_2^--N in A2 during the shock loads, suggesting oxidation of NH_4^+-N was mostly limited to NO_2^--N (Fig. 6.13c). Generation of NO_3^--N increased and effluent NO_2^--N decreased during recovery, suggesting complete oxidation of NH_4^+-N enhanced after the withdrawal of the shock load. Total nitrification rates from the oxidation of NH_4^+-N were 97 ± 3 g/(m^3.d) and 86 ± 2 g/(m^3.d) during shock 1 and shock 2, respectively, and increased to 106 ± 4 g/(m^3.d) during recovery period after each shock load.

.

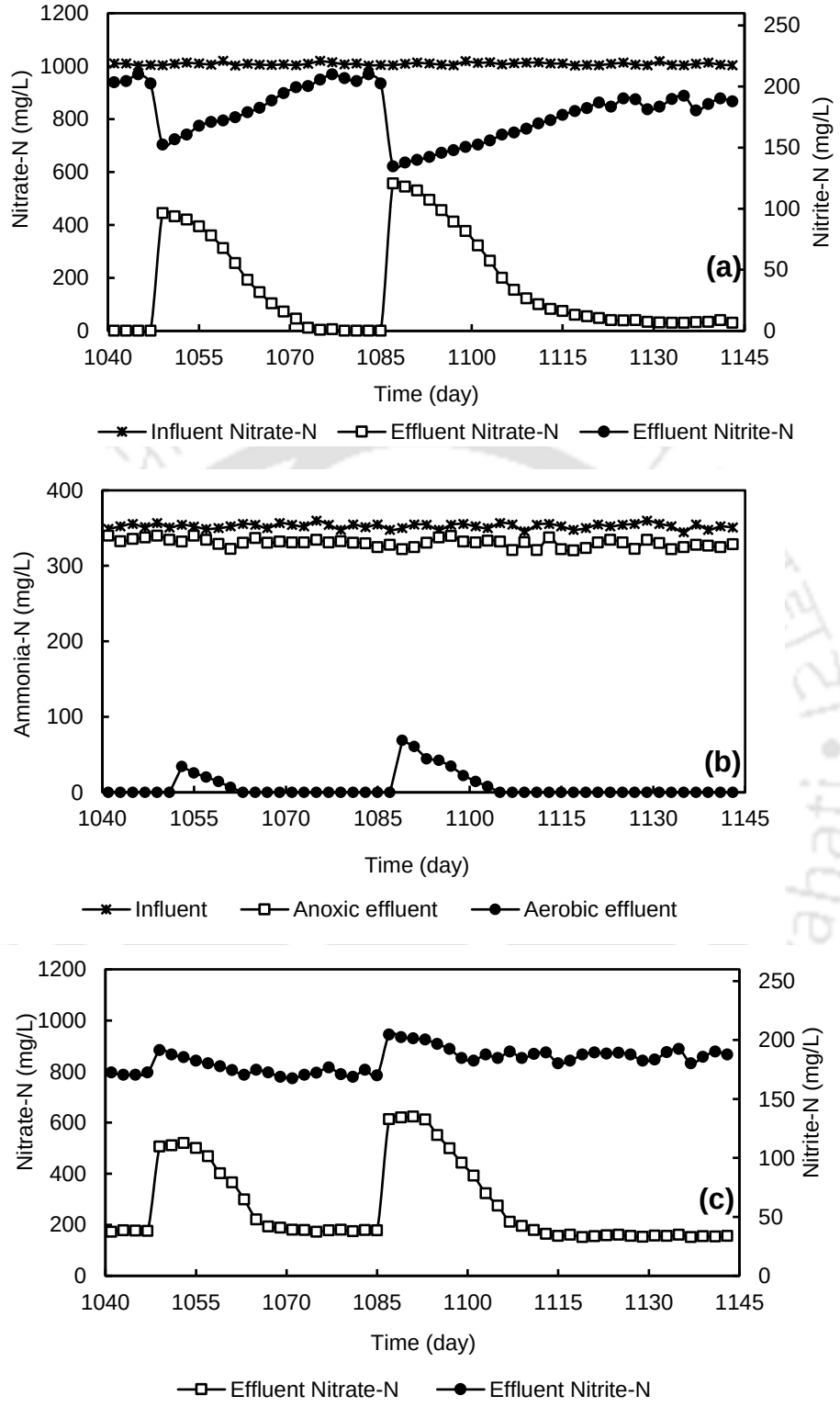

Fig. 6.13: (a) influent and effluent nitrate-N and nitrite-N in A1, (b) influent and effluent ammonia-N in A2, (c) effluent nitrate-N and nitrite-N in A2 during shock load and recovery

Table 6.5: Average influent and effluent concentrations of pollutants in A1 and A2 during shock application and recovery

Parameters	Shock 1			Recovery after shock 1			Shock 2			Recovery after shock 2		
	Anoxic		Aerobic	Anoxic		Aerobic	Anoxic		Aerobic	Anoxic		Aerobic
	Influent	Effluent	Effluent	Influent	Effluent	Effluent	Influent	Effluent	Effluent	Influent	Effluent	Effluent
Phenol	754 ± 3	583 ± 9	37 ± 6	751 ± 4	462 ± 8	4 ± 1	756 ± 5	701 ± 9	107 ± 6	753 ± 7	572 ± 8	5 ± 1
TH	1660 ± 22	1271 ± 19	220 ± 11	1266 ± 11	680 ± 9	6 ± 2	1945 ± 26	1660 ± 21	597 ± 11	1266 ± 8	890 ± 9	6 ± 2
Sulfide	753 ± 4	2 ± 1	-	755 ± 8	2 ± 1	-	756 ± 7	2 ± 1	-	752 ± 6	2 ± 1	-
COD_T	6630 ± 31	3686 ± 24	798 ± 17	5457 ± 21	1951 ± 14	199 ± 9	7622 ± 34	4399 ± 21	1443 ± 15	5466 ± 13	2400 ± 14	211 ± 7
COD_O	4011 ± 28	3407 ± 29	513 ± 11	2868 ± 11	1691 ± 22	16 ± 3	4836 ± 19	3956 ± 19	1170 ± 19	2866 ± 21	2130 ± 18	16 ± 3
Thiosulfate	-	135 ± 7	ND	-	55 ± 6	ND	-	200 ± 9	ND	-	71 ± 6	ND
Sulfate	44 ± 3	889 ± 23	1030 ± 39	41 ± 3	1092 ± 19	1178 ± 21	41 ± 2	834 ± 12	1002 ± 14	40 ± 4	1013 ± 14	1122 ± 23
Sulfur	-	398 ± 10	-	-	370 ± 9	-	-	365 ± 9	-	-	380 ± 11	-
Ammonia-N	355 ± 2	332 ± 4	22 ± 2	352 ± 4	327 ± 7	5 ± 1	353 ± 6	331 ± 4	42 ± 5	351 ± 4	331 ± 2	5 ± 1
Nitrate-N	1012 ± 10	419 ± 9	507 ± 11	1007 ± 6	6 ± 3	179 ± 7	1016 ± 5	539 ± 11	601 ± 18	1001 ± 5	41 ± 3	154 ± 5
Nitrite-N	-	153 ± 6	187 ± 8	-	201 ± 4	159 ± 8	-	135 ± 8	204 ± 11	-	184 ± 9	180 ± 7
pH	9.5 ± 0.1	9.1 ± 0.1	8.5 ± 0.1	9.5 ± 0.1	9.1 ± 0.1	8.5 ± 0.1	9.5 ± 0.1	9.1 ± 0.1	8.5 ± 0.1	9.5 ± 0.1	9.1 ± 0.1	8.5 ± 0.1
Gas (mL)	-	544 ± 11	-	-	-	767 ± 14	-	-	499 ± 10	-	-	723 ± 17

ND: Not detected

TH: Total hydrocarbon

All units except pH and gas are in mg/L

6.5 SUMMARY OF THE STUDY

Removal efficiency of organics, nitrate-N and heterotrophic activity of anoxic biomass deteriorated with increase in salinity. Sulfide removal remained unaffected. However, increase in NaCl caused decrease in sulfide to sulfate conversion along with chemolithotrophic activity of anoxic biomass. Aerobic biomass was more tolerant to high salinity and removals of both organics and ammonia-N started to decrease at NaCl > 30 g/L. High salinity caused toxic effect on the anoxic biomass and triggered sloughing, resulting in lower SRT of A1. Sloughing of the aerobic biomass was only observed beyond 30 g/L of NaCl. Complete recovery of biomass distribution, activity and performance of both anoxic and aerobic reactors was achieved after the withdrawal of NaCl. *Pseudomonas aeruginosa* **SC2013** and *Lysinibacillus sp.* **H200-150** could tolerate high salinity in anoxic and aerobic biomass, respectively. Effect of crude oil shock loading was readily observed for the removal of organics in both the reactors. Sulfide removal was not affected with shock load. However, conversion of sulfide to sulfate reduced with shock loading. Nitrate-N removal in anoxic reactor and ammonia-N removal in aerobic reactor were hampered with sudden increase in crude oil concentration. Complete recovery of the anoxic-aerobic system was achieved after the withdrawal of the shock loads.

References

Ahmadi, M., Jaafarzadeh, N., Rahmat, Z. G., Babaei, A. K., Alavi, N., Baboli, Z., Niri, M. V. 2017. Kinetic studies on the removal of phenol by MBBR from saline wastewater. Journal of Environmental Health Science and Engineering 15(22): 1-7.

Alipour, V., Moein, F., Rezaei, L. 2017. Determining the salt tolerance threshold for biological treatment of salty wastewater. Health Scope 6(1): 1-5.

APHA, AWWA, WPCF. 2005. Standard Methods for the Examination of Water and Wastewater. 21st ed., American Public Health Association, Washington DC.

Claros, J., Jimenez, E., Borras, L., Aguado, D., Seco, A., Ferrer, J., Serralta, J. 2010. Short-term effect of ammonia concentration and salinity on activity of ammonia oxidising bacteria. Water Science and Technology 61(12): 3008-3016.

Cortes-Lorenzo, C., Rodriguez-Diaz, M., Sipkema, D., Juarez-Jimenez, B., Rodelas, B., Smidt, H., Gonzalez-Lopez, J. 2015. Effect of salinity on nitrification efficiency and structure of ammonia-oxidizing bacterial communities in a submerged fixed bed reactor. Chemical Engineering Journal 266: 233-240.

Cui, Y. W., Zhang, H. Y., Ding, J. R., Peng, Y. Z. 2016. The effects of salinity on nitrification using halophilic nitrifiers in a sequencing batch reactor treating hypersaline wastewater. Scientific reports 6: 1-11.

Deng, Y. L., Ruan, Y. J., Zhu, S. M., Guo, X. S., Han, Z. Y., Ye, Z. Y., Liu, G., Shi, M. M. 2017. The impact of DO and salinity on microbial community in poly (butylene succinate) denitrification reactors for recirculating aquaculture system wastewater treatment. AMB Express 7(113): 1-11.

Dincer, A. R., Kargi, F. 1999 Salt inhibition of nitrification and denitrification in saline wastewater. Environmental Technology 20(11): 1147-1153.

Diya'uddin, B. H., Daud, W. M. A. W., Aziz, A. R. A. 2011. Treatment technologies for petroleum refinery effluents: a review. Process Safety and Environmental Protection 89(2): 95-105.

Ebrahimi, S., Nguyen, T.H., Roberts, D.J. 2015. Effect of temperature & salt concentration on salt tolerant nitrate-perchlorate reducing bacteria: Nitrate degradation kinetics. Water research 83: 345-353.

Ghorbanian, M., Moussavi, G., Farzadkia, M. 2014. Investigating the performance of an up-flow anoxic fixed-bed bioreactor and a sequencing anoxic batch reactor for the biodegradation of hydrocarbons in petroleum-contaminated saline water. International Biodeterioration and Biodegradation 90: 106-114.

Jafari, S. J., Moussavi, G., Yaghmaeian, K. 2015. High-rate biological denitrification in the cyclic rotating-bed biological reactor: Effect of COD/NO3-, nitrate concentration and salinity and the phylogenetic analysis of denitrifiers. Bioresource Technology 197: 482-488.

Jamal, M. T., Pugazhendi, A. 2018. Degradation of petroleum hydrocarbons and treatment of refinery wastewater under saline condition by a halophilic bacterial consortium enriched from marine environment (Red Sea), Jeddah, Saudi Arabia. 3 Biotech 8(276): 1-10.

Liu, C., Zhao, D., Ma, W., Guo, Y., Wang, A., Wang, Q., Lee, D.J. 2016. Denitrifying sulfide removal process on high-salinity wasetwaters in the presence of Halomonas sp. Applied Microbiology and Biotechnology 100: 1421-1426.

Mahmoud, M., Elkatatny, S., Abdelgawad, K. Z. 2017. Using high- and low-salinity seawater injection to maintain the oil reservoir pressure without damage. Journal of Petroleum Exploration and Production Technology 7(2): 589-596.

Narayan, S., Bhargava, R., Kumar, P. 2010. Effect of organic shock loads on a two-stage activated sludge-biofilm reactor. Bioresource Technology 101(9): 3060-3066.

Palanisamy, N., Ramya, J., Kumar, S., Vasanthi, N. S., Chandran, P., Khan, S. 2014. Diesel biodegradation capabilities of indigenous bacterial species isolated from diesel contaminated soil. Journal of Environmental Health Science and Engineering 12(1): 142-149.

Rath, K. M., Maheswari, A., Bengtson, P., Rousk, J. 2016 Comparative toxicities of salts on microbial processes in soil. Applied and Environmental Microbiology 82: 2012-2020.

Senturk, E., Ince, M., Engin, G. O. 2014. The effect of shock loading on the performance of a thermophilic anaerobic contact reactor at constant organic loading rate. Journal of Environmental Health Science and Engineering 12(1): 1-6.

Sharghi, E. A., Bonakdarpour, B., Roustazade, P., Amoozegar, M. A., Rabbani, A. 2013. The biological treatment of high salinity synthetic oil field produced water in a submerged membrane bioreactor using a halophilic bacteria consortium. Journal of Chemical Technology and Biotechnology 88: 2016-2026.

Shuler, M. L., Kargi, F. 2002. Bioprocess Engineering Basic concepts. 2nd edn., Prentice Hall India, New Delhi. pp. 67-73.

Son, H., Kim, H., Lee, G., Kim, J., Sung, W. 2014. Enhanced oil recovery using nanoparticle-stabilized oil/water emulsions. Korean Journal of Chemical Engineering 31(2): 338-342.

Veenagayathri, K., Vasudevan, N. 2017. Treatment of saline pharmaceutical wastewater by a moderately halophilic bacterial consortium. JSM Environmental Science & Ecology 5(1): 1-9.

Yoshie, S., Noda, N., Tsuneda, S., Hirata, A., Inamori, Y. 2004 Salinity decreases nitrite reductase gene diversity in denitrifying bacteria of wastewater treatment systems. Applied and Environmental Microbiology 70(5): 3152-3157.

7

CHAPTER

CONCLUSIONS AND FUTURE SCOPE

CHAPTER 7

CONCLUSIONS AND FUTURE SCOPE

Major findings of the research work carried out are summarized in this chapter. Research aim of the study was the treatment of synthetic petroleum refinery effluent containing phenol, hydrocarbons, sulfide, ammonia-N and nitrate-N and recovery of elemental sulfur. Concentration of pollutants were varied to maximize the generation of sulfur in anoxic fed-batch reactors. Anoxic-aerobic sequential moving bed system was operated with the pollutants concentrations previously optimized from the fed-batch study. Studied variable parameters were rotational speed, hydraulic retention time, types of hydrocarbons, feed salinity and hydrocarbon shock loads. Major conclusions obtained from the study are enlisted below:

1. Maximum removal of sulfide as sulfur (S^0) occurred at the following influent pollutants concentrations: sulfide 750 ± 7 mg/L, phenol 750 ± 5 mg/L, diesel 300 mg/L (TH: 1000 ± 9 mg/L), ammonia-N 350 ± 5 mg/L and nitrate-N 1000 ± 10 mg/L in anoxic fed-batch reactors at 1.25d HRT. Maximum S^0 was obtained at influent NO_3^--N: S^{2-} molar ratio of 3.04. Yellow solid precipitation was observed in the reactors and confirmed as sulfur (S^0) from elemental analysis.

2. Optimum agitation speed in anoxic disc bed reactor was 20 rpm and higher speed had no beneficial effect on the removals of pollutants. Sulfide (influent 750 ± 7 mg/L) and nitrate-N (Influent 1000 ± 10 mg/L) were removed (> 99 %) at 2.5d HRT in anoxic reactor along with partial removals of organics and marginal removal of ammonia-N. Aerobic moving bed reactor was fed with the effluent of anoxic reactor and more than 99% removals of ammonia-N and residual organics were achieved at 20h HRT. Phenol, total hydrocarbon (diesel) and ammonia-N were below 5 mg/L, sulfide was undetected and COD was below dischargeable limit in the final effluent of anoxic-aerobic sequential moving bed system at a total HRT of 80h (anoxic 60h + aerobic 20h).

3. Anoxic-aerobic sequential reactors were operated at 80h HRT (anoxic 60h + aerobic 20h) with five different types of hydrocarbons: kerosene (K), heavy oil (HO), kerosene with heavy oil (K+HO), kerosene with heavy oil and diesel (K+HO+D) and crude oil. Density

and viscosity of the hydrocarbons increased in the order of K < K+HO < K+HO+D < HO < crude oil. Removals of organics deteriorated in anoxic reactor in the presence of hydrocarbons with higher density and viscosity. However, removals of sulfide and nitrate-N in anoxic reactor remained unaffected. Attached biomass decreased and suspended biomass increased with increase in hydrocarbon density and viscosity and decrease in SRT of anoxic reactor occurred due to higher sloughing in anoxic reactor. Decrease in heterotrophic activity and increase in chemolithotrophic activity of anoxic biomass were observed with increase in hydrocarbon density and viscosity.

4. Effect of diverse hydrocarbons was not observed in aerobic reactor and complete removals of residual hydrocarbons and ammonia-N were achieved at overall HRT of 80h. Biomass distribution and SRT of aerobic reactor remained unaffected by the change in hydrocarbon properties. Heterotrophic activity of aerobic biomass was higher when hydrocarbons with higher density and viscosity were used in the feed due to more availability of carbon source. Removal rates of phenol, S^{2-}, TH, COD_T and NH_4^+-N were 227 ± 2, 378 ± 3, 1585 ± 30 and 105 ± 3 g/(m^3.d), respectively, by the anoxic-aerobic sequential system and were never hampered by the change in hydrocarbon properties.

5. Isolation of anoxic biomass revealed the dominance of two cultures; orange and white and were identified as *Pseudomonas aeruginosa* **SKM2013** and *Pseudomonas aeruginosa* **SC2013**. Both cultures degraded phenol, sulfide, hydrocarbons and nitrate-N, and could not degrade ammonia-N. *Pseudomonas aeruginosa* **SC2013** degraded sulfide in the absence of organics in denitrifying condition and showed chemolithotrophic characteristics. Isolation of aerobic biomass showed four cultures; red, yellow, white and grey and were identified as *Lysinibacillus sp.* **H200-150**, *Stenotrophomonas sp.* **LW-34**, *Pseudomonas aeruginosa* **LZS8436** and *Pseudomonas aeruginosa* **ISB4**. *Lysinibacillus sp.* **H200-150**, *Stenotrophomonas sp.* **LW-34** and *Pseudomonas aeruginosa* could degrade both organics and ammonia-N. *Pseudomonas aeruginosa* **LZS8436** could degrade organics using nitrite-N as electron acceptor but could not oxidize ammonia-N.

6. Real automobile service station wastewater was contaminated with phenol (37 ± 6 mg/L), hydrocarbons (475 ± 11 mg/L), NO_3^--N (135 ± 2 mg/L) and NH_4^+-N (170 ± 7 mg/L). During the treatment of real wastewater, organics, NO_3^--N and NO_2^--N were removed

(>99%) in anoxic reactor at 22.5h HRT and residual NH_4^+-N was removed in aerobic reactor at 7.5h HRT with an overall HRT of 30h.

7. Degradation of organics and nitrate-N deteriorated with increase in NaCl dose (0 to 45 g/L) in anoxic reactor. Sulfide removal remained intact, but complete conversion of S^{2-} to SO_4^{2-} was hampered. Higher salinity led to sloughing and decrease in SRT of anoxic reactor. Both heterotrophic activity and chemolithotrophic activity decreased with increase in NaCl. Residual organics and ammonia-N were completely removed in aerobic reactor up to NaCl dose of 30 g/L. Nitrification of ammonia-N was hampered with increase in salinity. Heterotrophic activity of aerobic biomass decreased at NaCl beyond 30 g/L. The anoxic-aerobic moving bed system recovered to its original state after the withdrawal of NaCl.

8. Heterotrophic activity of both anoxic and aerobic biomass were higher whenever degradation of organics were higher. Similarly, chemolithotrophic activity of anoxic biomass was higher when sulfide oxidation and conversion of sulfide to sulfate were higher. Direct correlation of biomass activity with the COD removal was observed. Hence, biomass activity test can be used as an indirect tool to predict bioreactor performance.

9. Crude oil shock load was applied to the anoxic-aerobic system at two phases by increasing its concentration twice (600 mg/L) and thrice (900 mg/L), respectively. Degradation of organics in both anoxic and aerobic reactors, nitrate-N in anoxic reactor and ammonia-N in aerobic reactor were hampered with the application of shock load. Performance of the anoxic-aerobic sequential system recovered after the withdrawal of shock load. However, there was permanent upward shift in the effluent of anoxic reactor after the second shock.

Future scope of the study:

The following future studies can be carried out based on the findings of the present study:

- Treatment of petroleum refinery wastewater containing benzene, toluene, ethylbenzene and xylene (BTEX), organo-sulfur and organo-nitrogen compounds.
- Bioremediation of real spent caustic wastewater to improve the versatility of the anoxic-aerobic sequential moving bed system.
- Bio-augmentation and culturing of annamox microbial species for the simultaneous removals of NH_4^+-N and NO_2^--N.
- Shock load application of other pollutants (sulfide, phenol, ammonia).

LIST OF PUBLICATIONS

International journal publications:

Mallick, S. K., Chakraborty, S. 2017. Treatment of synthetic refinery wastewater in anoxic-aerobic sequential moving bed reactors and sulphur recovery. Journal of Environmental Science and Health, Part A 52(13): 1257-1268.

Mallick, S. K., Chakraborty, S. 2017. Effect of nitrate-N on the degradation of petroleum refinery wastewater in anoxic moving bed reactors. CSVTU International Journal of Biotechnology, Bioinformatics and Biomedical 2(3): 33-38.

Mallick, S. K., Chakraborty, S. 2019. Bioremediation of wastewater from automobile service station in anoxic-aerobic sequential reactors and microbial analysis. Chemical Engineering Journal 361: 982-989.

Mallick, S. K., Chakraborty, S. 2019. Bioremediation of hydrocarbon containing wastewater in anoxic-aerobic sequential reactors. Environmental Technology (Accepted).

Mallick, S. K., Chakraborty, S. 2019. Varied infeed inorganics and organics for the assimilation of aqueous petrochemical products in anoxic fed-batch reactors: Maximizing precipitation of S^0. Separation and Purification Technology 219: 268-280.

Book Chapter:

Mallick, S. K., Chakraborty, S. 2018. Treatment of synthetic petroleum refinery wastewater in anoxic reactors at varied feed phenol. Water Quality Management, Water Science and Technology Library 79. Publisher: Springer Nature Singapore Pte Ltd.

Manuscripts under preparation:

Mallick, S. K., Chakraborty, S. Treatment of petroleum refinery wastewater loaded with crude oil in anoxic-aerobic sequential reactors and biomass activity. (Submitted)

Mallick, S. K., Chakraborty, S. Salinity footprint on the performance of anoxic-aerobic sequential reactors for the assimilation of petroleum refinery wastewater: Effect on dominant species. (Submitted)

Mallick, S. K., Chakraborty, S. Effect of crude oil shock load on the performance of anoxic-aerobic sequential reactors. (Submitted)

International conferences:

Mallick, S. K., Chakraborty, S. 2015. Treatment of petroleum refinery wastewater in anoxic fed batch moving bed reactor. National Conference on "**Challenges in Environmental Research (NCOCER)**", Indian Institute of Technology Guwahati, Assam India, **4-6 June 2015**.

Mallick, S. K., Chakraborty, S. 2015. Treatment of Synthetic Oil Refinery Wastewater in Anoxic Reactors at Varied Feed Sulfide Concentration. International Conference on "**New Horizons in Biotechnology (NHBT)**", Trivandrum, Kerala, India, **22-25 November 2015**.

Mallick, S. K., Chakraborty, S. 2016. Treatment of synthetic petroleum refinery wastewater in anoxic reactors at varied feed phenol. International Conference on "**Water, Environment, Energy and Society (ICWEES)**", AISECT University, Bhopal, India, **15-18 March 2016**.

Mallick, S. K., Chakraborty, S. 2016. Abiotic loss of volatile compounds in petroleum refinery wastewater by aeration. International Conference on "Waste Management", **Recycle 2016**, **1-2 April 2016**, IIT Guwahati.

Mallick, S. K., Chakraborty, S. 2016. Involvement of individual biomass during the anoxic degradation of pollutants in simulated petroleum refinery wastewater at varied feed phenol concentration. International conference on contaminated site remediation and international workshops "**Clean Up India 2016**", **13-16 December 2016**, Tamilnadu National Agricultural University, Coimbatore, India. (**Best Oral Presentation Award**).

Mallick, S. K., Chakraborty, S. 2018. Performance critique of anoxic-aerobic reactors during the assimilation of refinery wastewater: Importance of biomass activity and bio-solids retention time. International Conference on "**Bioprocess for Sustainable Environment and Energy (ICBSEE)**", National Institute of Technology Rourkela, India, 6-7 December 2018. (**Best Poster Award**).

APPENDIX

Appendix A: Characteristics of the tap water

Table A: Characteristics of the tap water

Parameter	Concentration
pH	8.10 ± 0.05
Conductivity	0.225 ± 0.005 mS/cm
Turbidity	1.10 ± 0.05 NTU
Hardness	94 ± 5 mg/L as $CaCO_3$
Alkalinity (total)	50 ± 10 mg $CaCO_3$/L
Chloride	4.55 ± 0.05 mg Cl-/L
Sulfate	24.75 ± 0.10 mg SO_4^{2-}/L
Solids	-ND-
Iron	0.10 ± 0.01 mg Fe^{2+}/L
Fluoride	0.325 ± 0.05 mg F^-/L
Nitrate	5.50 ± 0.5 mg NO_3^-/L
Ammonia	0.2 ± 0.05 mg NH_4^+/L
Phenol	-ND-
Sodium	4.25 ± 0.01 mg Na^+/L
Potassium	2.00 ± 0.01 mg K^+/L
Calcium	10.75 ± 0.05 mg Ca^{2+}/L
Oil/VFA	-ND-

ND: Not detected

Appendix B: Linear calibration curves

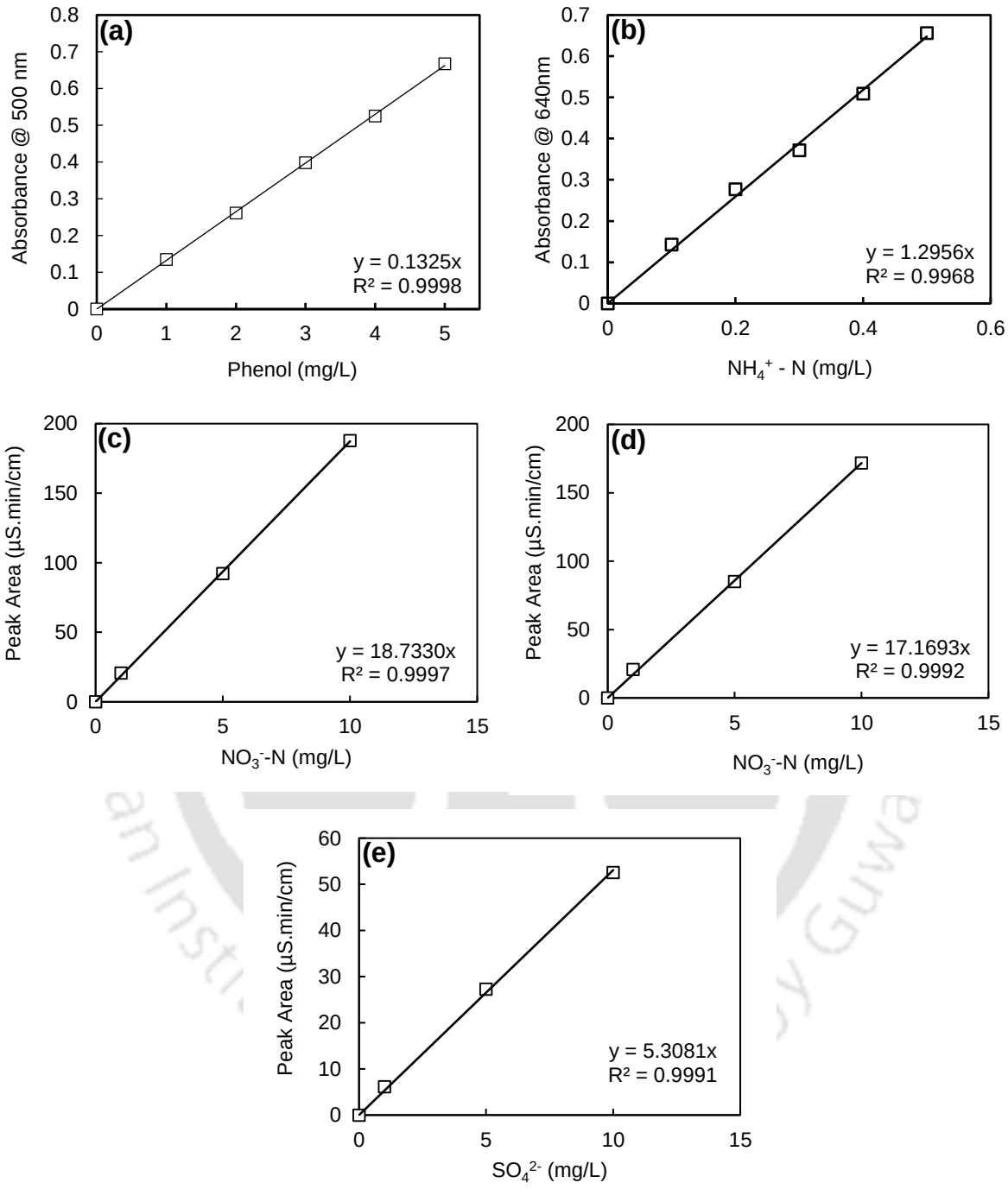

Fig. B: Linear calibration curves for the analysis of (a) phenol, (b) ammonia-N, (c) nitrate-N, (d) nitrite-N, (e) sulfate

Appendix C: Experimental determination of COD of sulfide and thiosulfate solutions

COD was determined for sulfide and thiosulfate by taking five samples of predetermined concentrations. Then average COD was considered to determine the COD/mg of pollutant.

Table C1: Determination of COD of sulfide

Sulfide (mg/L)	COD						
	Sample 1	Sample 2	Sample 3	Sample 4	Sample 5	Average	COD /mg of sulfide
100	384	352	352	320	320	345.6	3.46
200	640	640	640	768	640	665.6	3.33
300	1056	1056	1056	1056	1056	1056.0	3.52
500	1760	1600	1600	1760	1600	1664.0	3.33
750	2400	2880	2880	2400	2400	2592.0	3.46
1000	3840	3200	3200	3840	3200	3456.0	3.46
1200	4000	4000	4800	4000	4000	4160.0	3.47

Taking average of the right most column of the table:

Average COD/mg of sulfide = 3.43 mg O_2/L

Table C2: Determination of COD of thiosulfate

Thiosulfate (mg/L)	COD						
	Sample 1	Sample 2	Sample 3	Sample 4	Sample 5	Average	COD /mg of thiosulfate
100	80.00	80.00	64.00	96.00	80.00	80.00	0.80
150	128.00	112.00	144.00	112.00	144.00	122.72	0.85
200	160.00	176.00	160.00	176.00	160.00	166.40	0.83
250	192.00	208.00	208.00	192.00	192.00	198.40	0.79

Taking average of the right most column of the table:

Average COD/mg of thiosulfate = 0.82 mg O_2/L

Appendix D: List of instruments used during in the present study

Table D: Instruments and equipment used in the present study

Instruments/ equipment	Parameters tested/ measured	Model/Manufacturer specification
Digital pH meter	pH	Systronics 361, India
Conductivity, TDS, Salinity meter	conductivity, TDS and salinity	Labtronics LT-51, India
Electronic balance	Weight	Citizen CX 220
Centrifuge	Separation of suspended solids and oil	REMI CM 8 plus, India
COD digester	COD	Hach DRB 200, India
UV-visible spectrophotometer	Phenol, ammonia-N	Cary 50 Bio, Agilent
Ion chromatograph	Nitrate-N, nitrite-N, sulfate	Metrohm Basic IC, Switzerland
Nephelometric turbidity meter	Turbidity	Systronics 132
Hot air oven	TSS, drying	ICT Kolkata, India
Autoclave	Sterilization	Reico, India
Refrigerator	Store samples and cultures	Labocon, India
Atomic Absorption Spectrophotometer	Metals analysis	SpectrAA 55B, Varian, USA
Shaking incubator	Temperature controlled shaking	LabTech, India
Flame photometer	Sodium, potassium, calcium	Systronics 128
Aquarium pump	Air purging	
Laminar Airflow Hood	To transfer pure culture in aseptic manner	Clean air system, CAH-1800, Chennai, India
Mechanical stirrer	Rotation to A1	REMI 126D, India
Water purification system	MilliQ and Millipore water	Merckmillipore, Germany
Peristaltic pump	Feeding to the reactors	Miclins PP 20x, India
Hot air blower	Maintain temperature	Bajaj, India
Gas chromatograph	Analysis of gaseous samples (N_2, CO_2 and CH_4)	Dhruva, Gujrat, India
FTIR spectroscope	Scanning liquid samples between 400-4000 cm^{-1} wavelength	Model No: IRAffinity-1; M/s Shimadzu, Japan

Appendix E: Photographic and FESEM images of PUF cubes

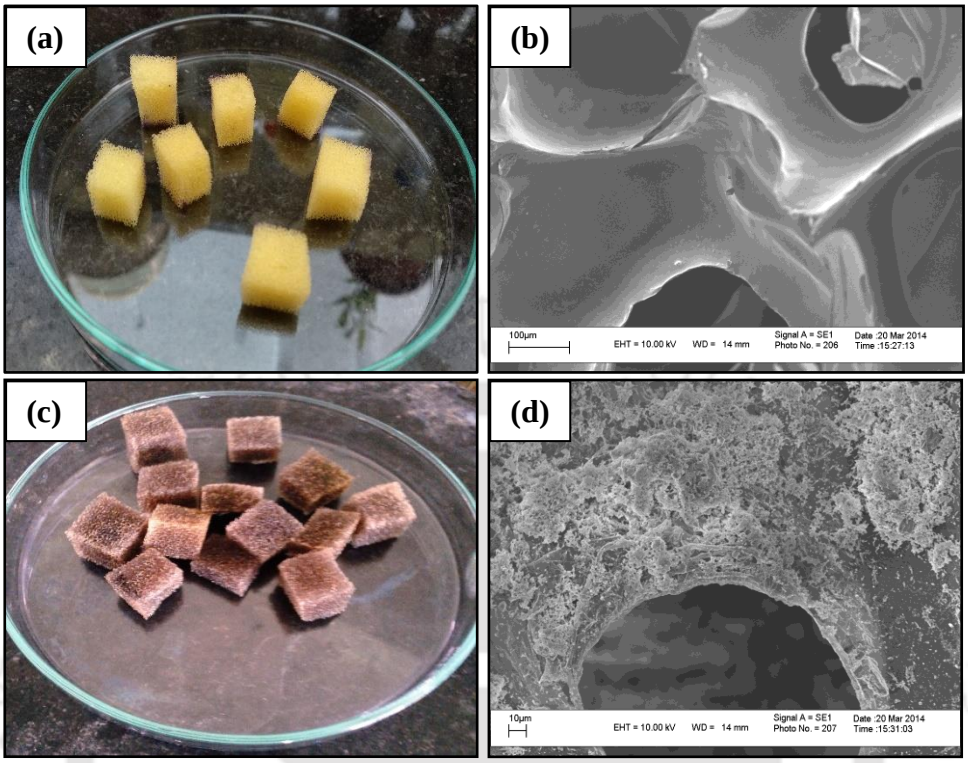

Fig. E: (a) photographic image of virgin PUF cube, (b) FESEM image of virgin PUF cube, (c) photographic image of PUF cube loaded with biomass, (d) FESEM image of PUF cube loaded with biomass

Appendix F: Schematic diagrams of anoxic disc-bed reactor (A1) and aerobic moving bed reactor (A2) with dimensions

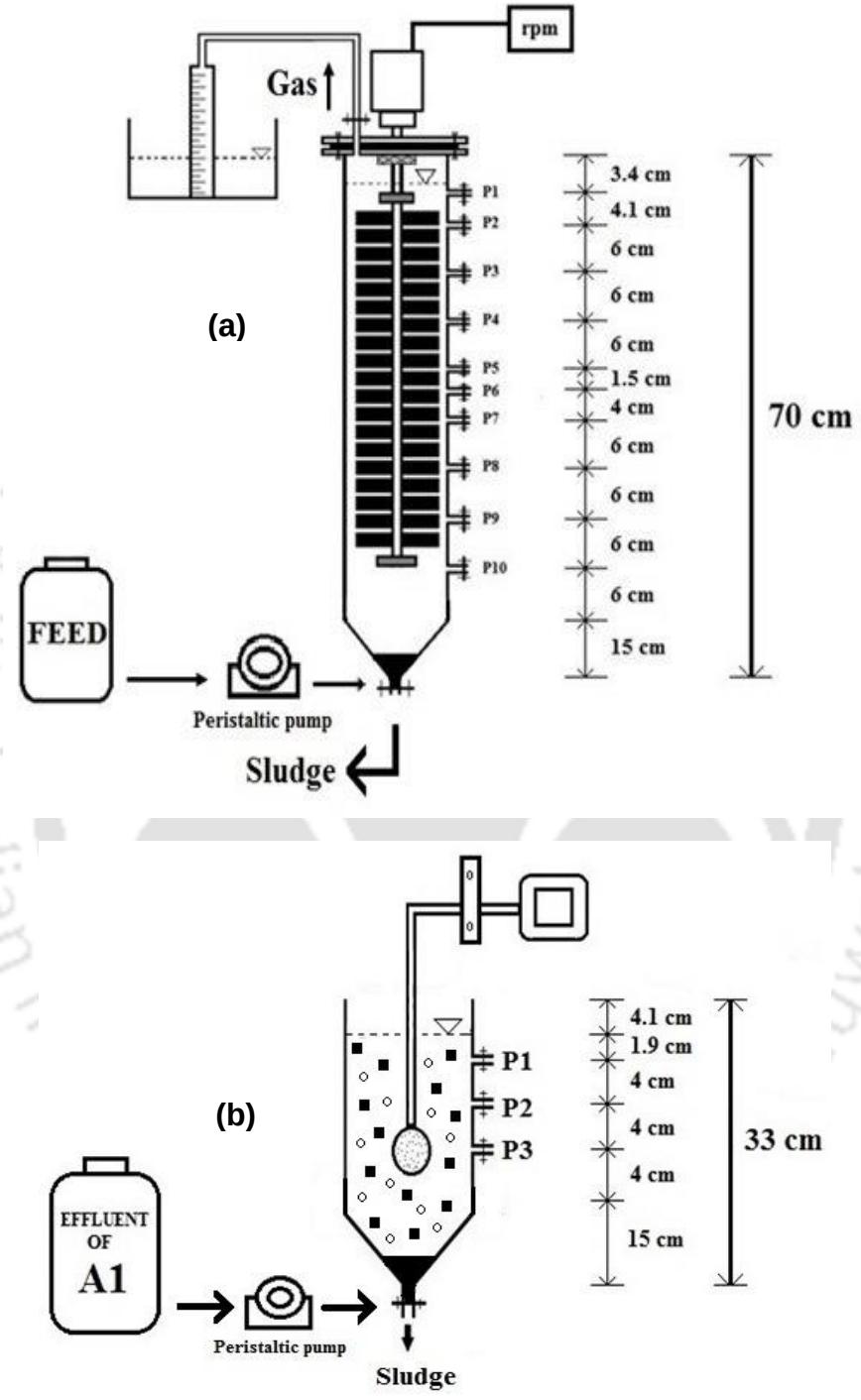

Fig. F: Schematic diagram of anoxic disc-bed reactor (A1) and aerobic moving bed reactor (A2) with dimensions

Appendix G: Characteristics of the seed sludge

Table G: Characteristics of the seed sludge

Parameters	Anoxic sludge	Aerobic sludge
TS (g/L)	7.8 ± 0.2	9.0 ± 0.2
VS (g/L)	5.6 ± 0.2	8.5 ± 0.2
pH	7.6 ± 0.1	7.9 ± 0.1
Conductivity (mS/cm)	62.3 ± 0.3	81.4 ± 0.2
Salinity (g/L)	2.4 ± 0.1	2.5 ± 0.1
Source	Anaerobic storage tank of IOCL, Guwahati, India	Activated sludge reactor of IOCL, Guwahati, India

Appendix H: Effect of digestion time on the COD of different hydrocarbons

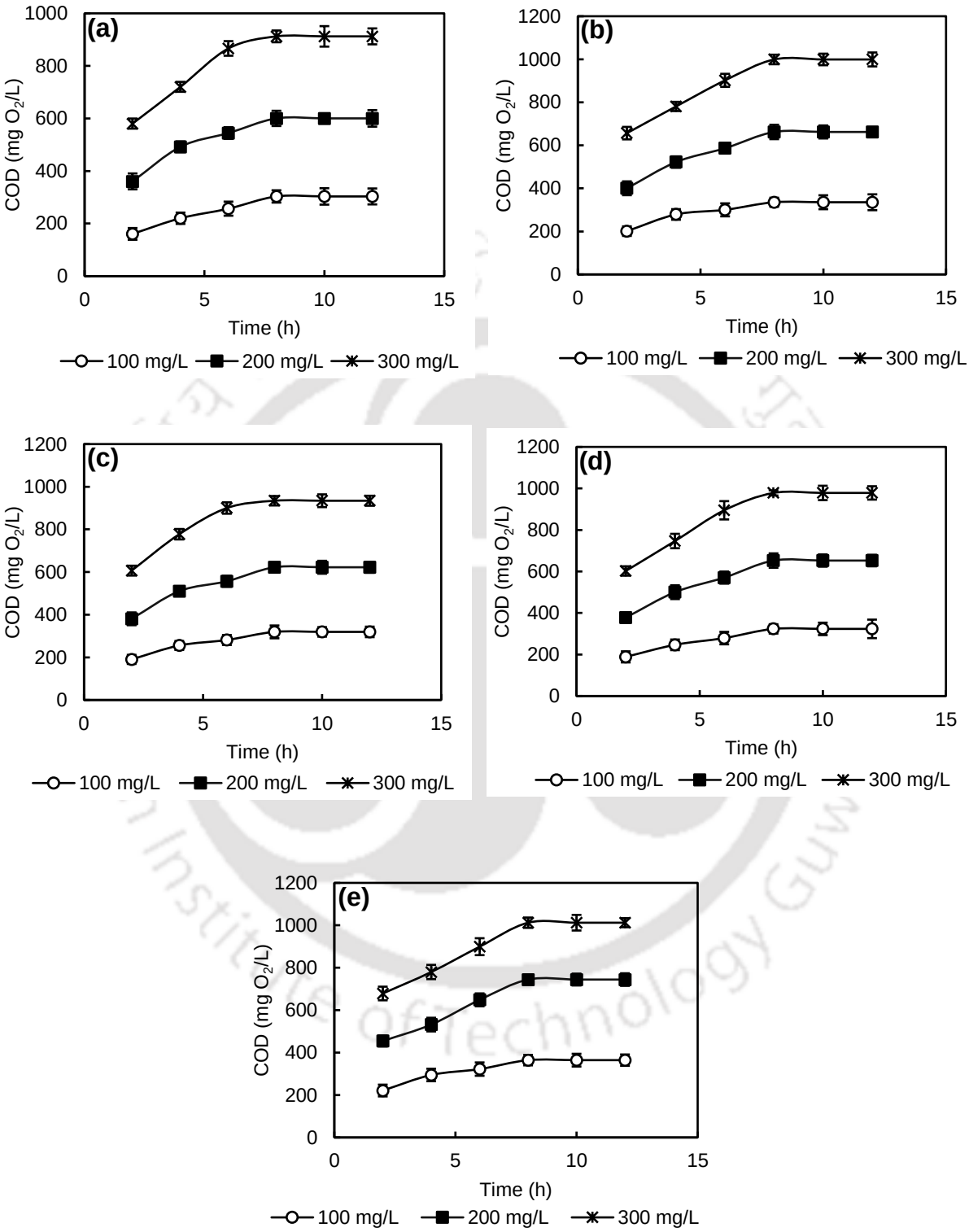

Fig. H: Effect of digestion time on the COD of (a) K, (b) HO, (c) K + HO, (d) K+HO+D, (e) crude oil

Appendix I: Effect of emulsifier concentration on the COD of different hydrocarbons

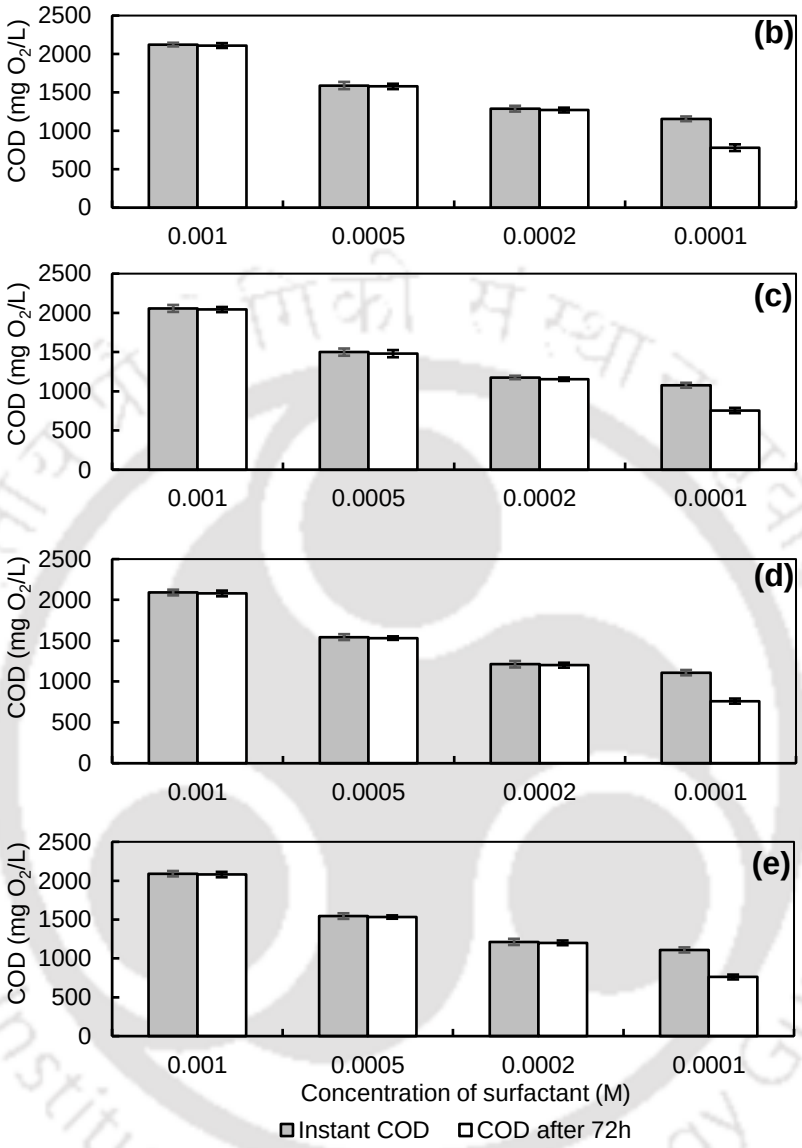

Fig. I: Effect of surfactant concentration on the COD of emulsified (a) K, (b) HO, (c) K + HO, (d) K+HO+D, (e) crude oil

Appendix J: Effect of airflow rate on the COD of emulsified hydrocarbons

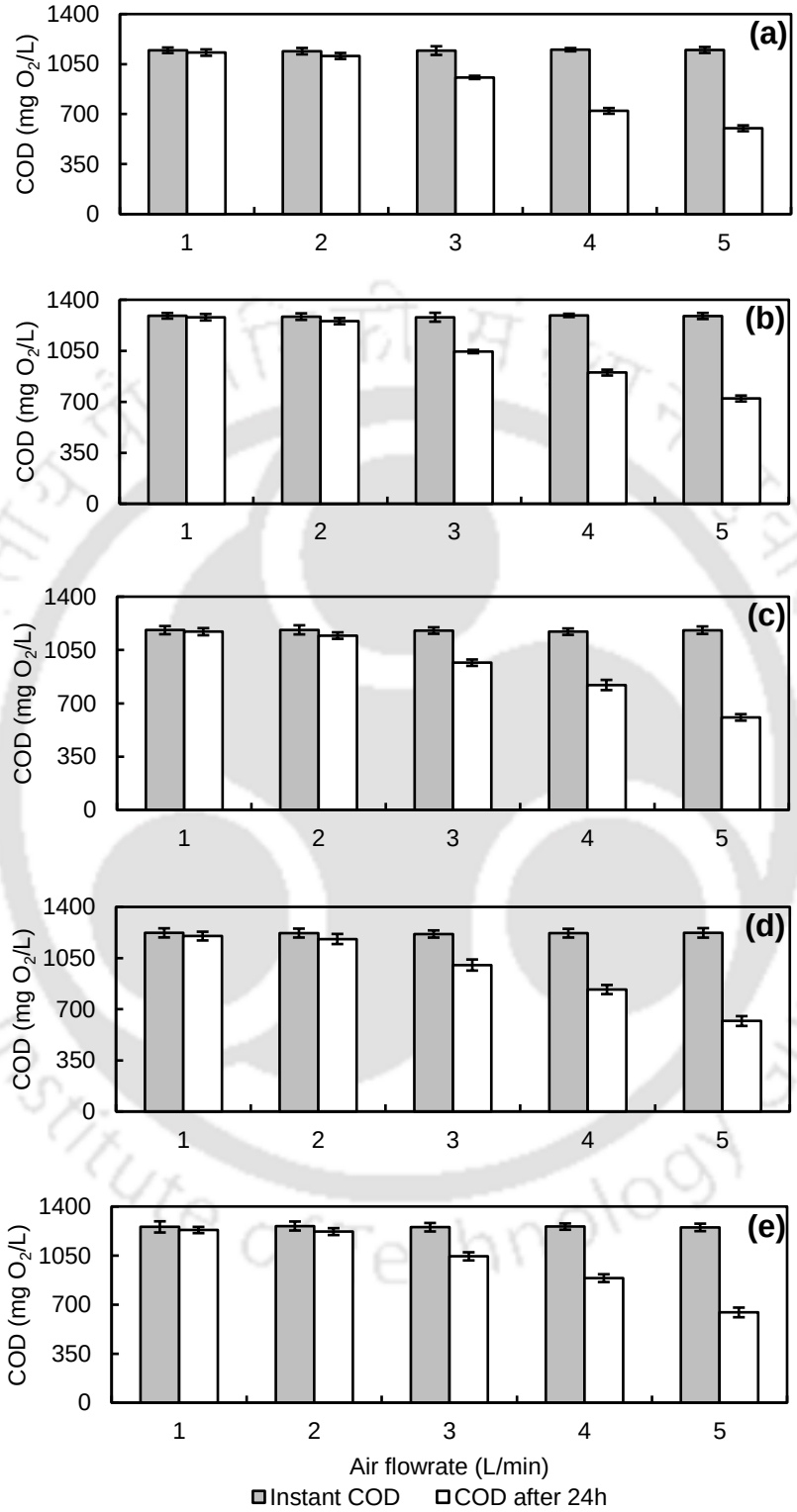

Fig. J: Effect of airflow rate on the COD of emulsified (a) K, (b) HO, (c) K + HO, (d) K+HO+D, (e) Crude oil

Appendix K: Influent and effluent concentrations during abiotic removal study

Table K1: Influent and effluent concentrations during abiotic removal study with kerosene (K), heavy oil (HO) and (K+HO) in feed

Parameters (mg/L)	Kerosene (K)				Heavy oil (HO)				K+HO			
	Anoxic		Aerobic		Anoxic		Aerobic		Anoxic		Aerobic	
	Influent	Effluent[#]	Influent	Effluent[#]	Influent	Effluent[#]	Influent	Effluent[#]	Influent	Effluent[#]	Influent	Effluent[#]
Phenol	751±4	742±5 (9±1)	278±9	269±7 (9±1)	753±4	740±9 (13±2)	453±8	440±10 (13±2)	754±4	742±8 (12±1)	345±9	333±7 (12±1)
TH	1243±25	1218±18 (25±4)	502±13	465±11 (37±3)	1258±14	1224±9 (34±6)	647±6	604±8 (43±4)	1246±14	1211±25 (35±4)	550±8	507±1 (43±4)
Sulfide	755±7	726±8 (29±2)	-	-	755±4	724±4 (31±3)	-	-	756±7	728±6 (28±3)	-	-
COD_T	5434±23	5291±24 (143±11)	1233±16	1167±11 (66±4)	5451±20	5268±26 (183±17)	1872±20	1781±22 (91±5)	5447±27	5292±22 (155±17)	1486±11	1379±18 (107±18)
COD_O	2845±34	2801±19 (44±3)	1088±29	1035±23 (53±3)	2861±19	2785±22 (76±5)	1628±19	1561±21 (67±6)	2854±19	2795±21 (59±3)	1289±19	1200±17 (89±3)
Thiosulfate	-	ND	42±4	28±6 (14±2)	-	ND	49±3	27±2 (22±3)	-	ND	40±3	26±4 (14±3)
Nitrate-N	1009±9	1000±6 (9±1)	-	ND	1002±8	992±9 (10±1)	-	ND	1008±6	1000±9 (8±1)	-	ND
Nitrite-N	-	ND	101±5	99±5 (2±1)	-	ND	185±6	180±3 (5±1)	-	ND	150±6	144±7 (6±1)

Data is represented in xx ± yy format, where 'xx' is the average and 'yy' is the standard deviation

ND: Not detected

Values shown in bracket are abiotic loss in mg/L

Table K2: Influent and effluent concentrations during abiotic removal study with (K+HO+D) and crude oil in feed

Parameters (mg/L)	(K+HO+D)				Crude oil			
	Anoxic		Aerobic		Anoxic		Aerobic	
	Influent	Effluent[#]	Influent	Effluent[#]	Influent	Effluent[#]	Influent	Effluent[#]
Phenol	752±3	744±2 (8±1)	360±2	351±7 (9±1)	755±4	744±6 (11±2)	470±4	456±8 (14±2)
TH	1253±22	1227±13 (26±2)	605±8	565±6 (40±3)	1261±17	1221±6 (40±6)	700±3	659±6 (41±5)
Sulfide	752±7	723±4 (29±2)	-	-	756±4	723±4 (33±3)	-	-
COD_T	5467±13	5371±24 (140±11)	1544±12	1474±9 (70±3)	5540±23	5346±11 (194±17)	1980±23	1879±17 (101±4)
COD_O	2856±24	2809±19 (47±3)	1372±19	1320±19 (52±2)	2967±12	2897±20 (70±5)	1705±13	1641±15 (64±2)
Thiosulfate	-	ND	35±2	21±3 (14±2)	-	ND	48±3	26±2 (22±3)
Nitrate-N	1002±8	994±2 (8±1)	-	ND	1005±7	995±2 (10±1)	-	ND
Nitrite-N	-	ND	145±3	142±3 (3±1)	-	ND	207±3	202±3 (5±1)

Data is represented in xx ± yy format, where 'xx' is the average and 'yy' is the standard deviation
ND: not detected
Values shown in bracket are abiotic loss in mg/L

Appendix L: FTIR analysis of the influent and effluent samples at different hydrocarbons

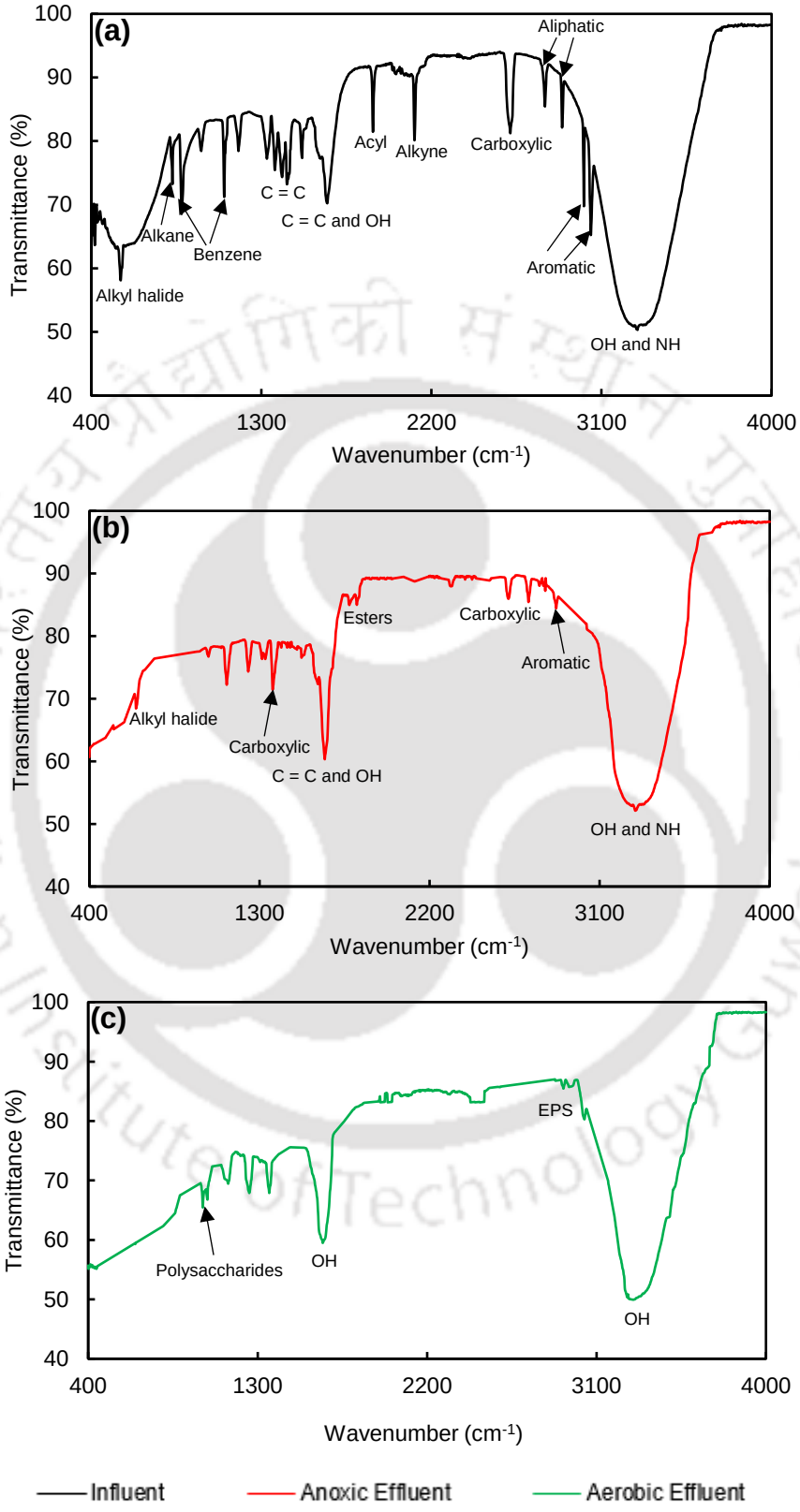

Fig. L1: FTIR absorption spectra of (a) influent, (b) anoxic effluent and (c) aerobic effluent during combined treatment with kerosene (K) in feed

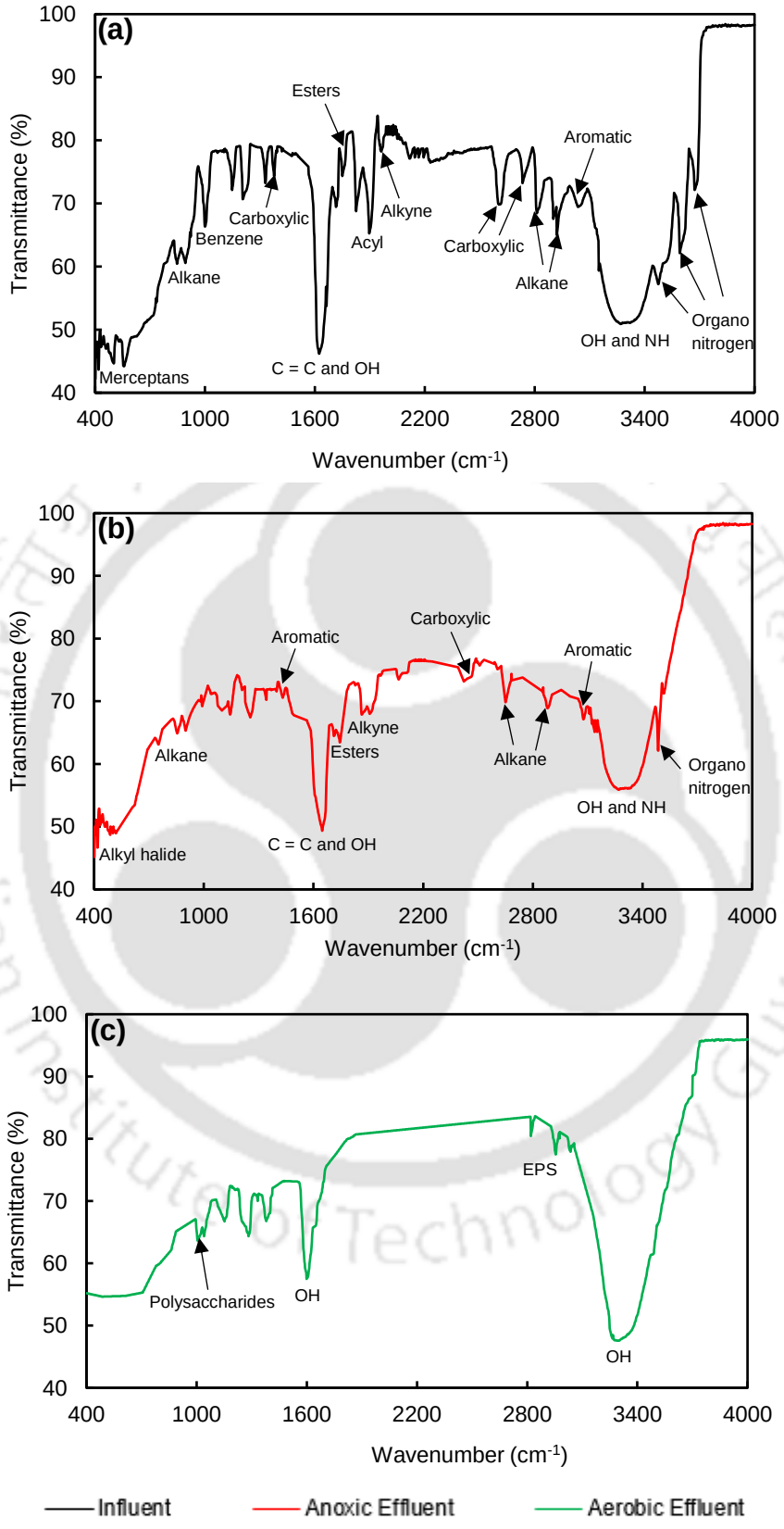

Fig. L2: FTIR absorption spectra of (a) influent, (b) anoxic effluent and (c) aerobic effluent during combined treatment with heavy oil (HO) in feed

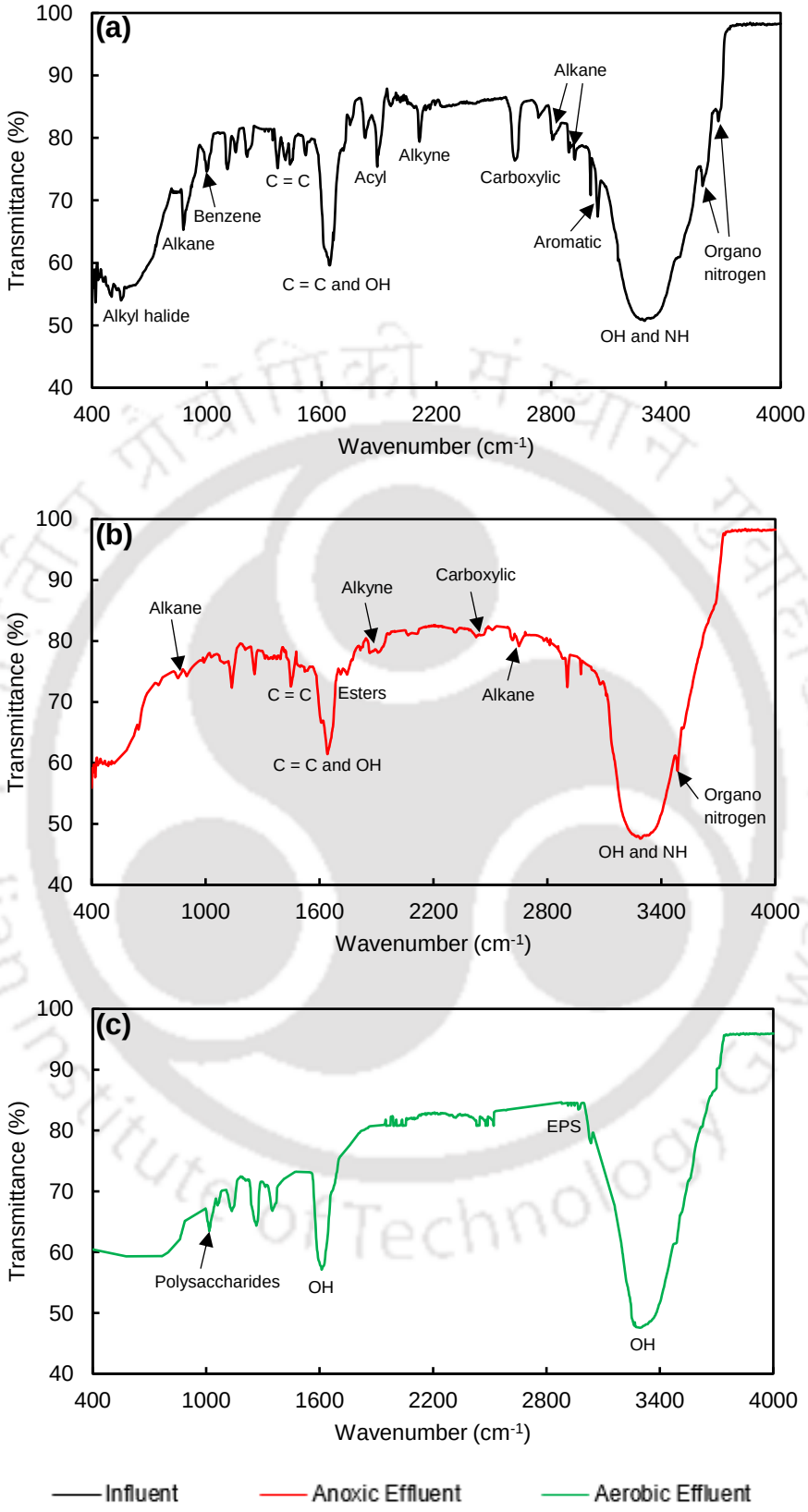

Fig. L3: FTIR absorption spectra of (a) influent, (b) anoxic effluent and (c) aerobic effluent during combined treatment with (K+HO) in feed

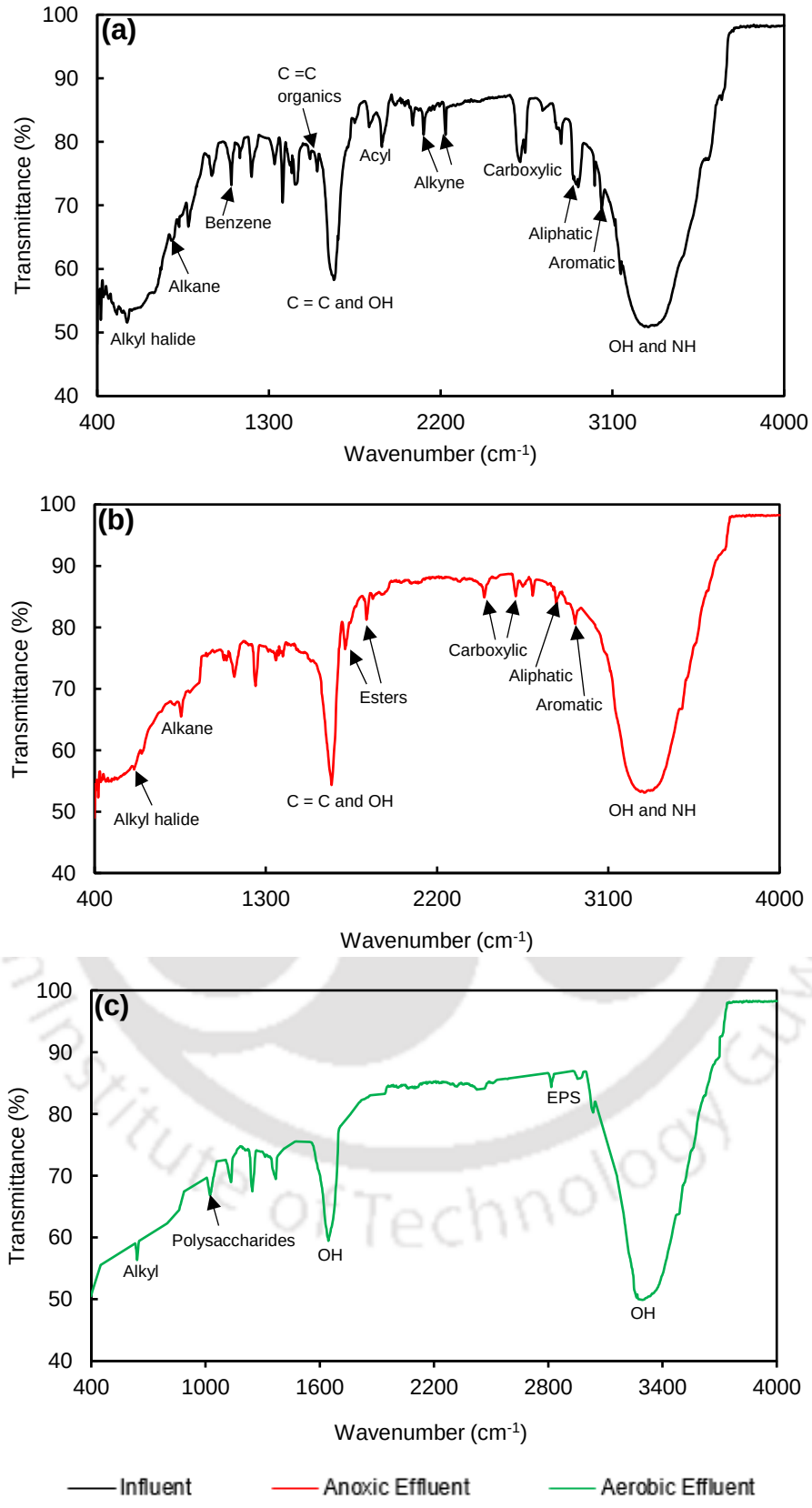

Fig. L4: FTIR absorption spectra of (a) influent, (b) anoxic effluent and (c) aerobic effluent during combined treatment with (K+HO+D) in feed

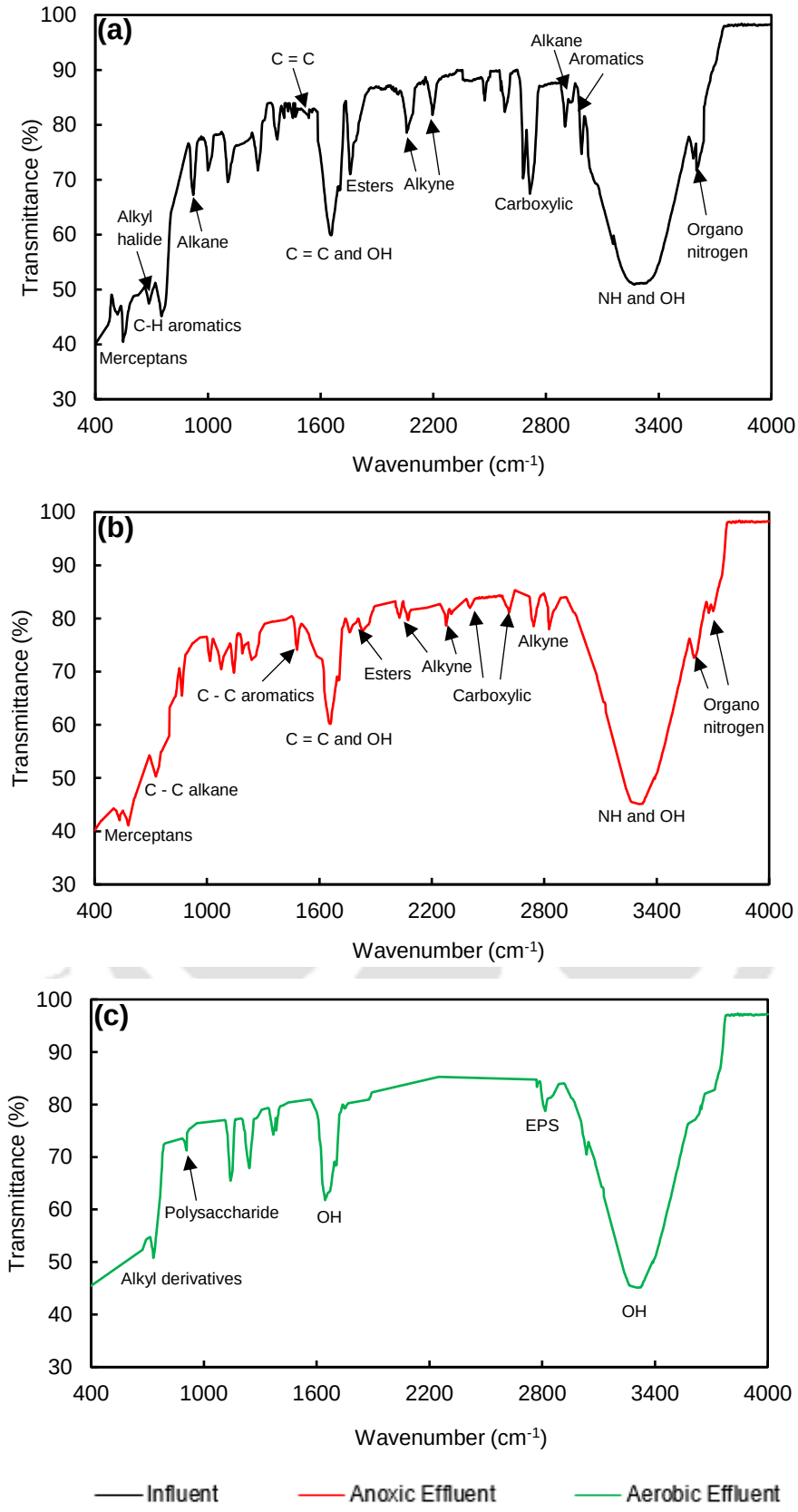

Fig. L5: FTIR absorption spectra of (a) influent, (b) anoxic effluent and (c) aerobic effluent during combined treatment with crude oil in feed

Appendix M: Requirement of surfactant for the emulsification of crude oil during shock load application

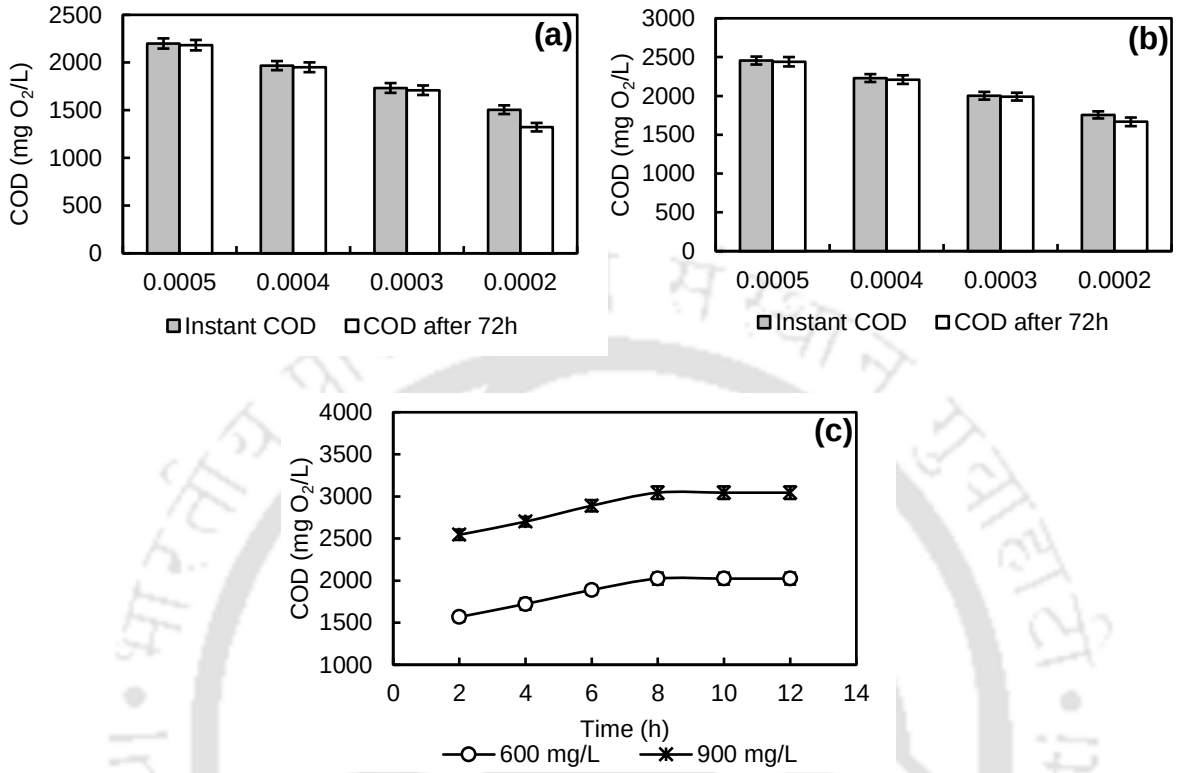

Fig: M: Requirement of surfactant for the emulsification of crude oil (a) 600 mg/L, (b) 900 mg/L, (c) effect of digestion time on the COD of crude oil (600 mg/L and 900 mg/L)